Robert Schönauer, Dipl.-Ing. (FH)

A Microscopic Traffic Flow Model for Shared Space

Doctoral Thesis

to achieve the university degree of

Dr. techn.

Doctoral School: Civil Engineering Sciences

submitted to

Graz University of Technology

Supervisor

Univ.-Prof. Dr. Ing. Martin Fellendorf

Institute of Highway Engineering and Transport Planning

Vienna, July 2017

Affidavit

I declare that I have authored this thesis independently, that I have not used other than the declared sources/resources, and that I have explicitly indicated all material which has been quoted either literally or by content from the sources used. The text document uploaded to TUGRAZonline is identical to the present doctoral thesis.

Date

Signature

Abstract

Where multiple functions of roads interfere, conflict avoidance reaches human and technological limits and constitutes one of the major challenges in transportation engineering. In the last two decades, several concepts of self-explaining roads bring versatile options to urban planning and became valuable tools to manage heterogeneous traffic flows. Shared space and Begegnungszone (“encounter zone”) are the most popular concepts for urban roads and squares. From a scientific and road planning perspective, there are still gaps in the understanding and predicting the complex interaction of different road users.

Microscopic traffic flow models allow dynamic simulation of pedestrians, vehicles, driver behavior and the interaction among each other and with infrastructure. This dissertation structures the problem of simulating traffic flows on shared space and creates new ways of applying agent based microscopic modeling. The underlying multi-agent social-force model describes the impact of social and technical interaction of traffic dynamics by establishing fields of force in analogy to physical models in Newtonian dynamics. The infrastructure is described by a force field keep agents on their path. Agents avoid obstacles and use their individual preferences. With bringing vehicles as non-holonomic objects in the world of social forces, both a single-track model and a bicycle model are introduced. To solve interaction processes on a tactical level, the conflicts are transferred to non-cooperative games with perfect information. This approach offers the novelty to mathematically combine social and rule-based behavior. Finally, the dissertation describes the model calibration approach based on real world trajectories. The model is applied to a shared space layout that is already implemented in Austria to compare the simulated traffic flow to real world data.

The major part of empirical data for calibration is acquired at an intersection in Austria that had been changed from a conventional design to a shared space setting and some years later to a Begegnungszone. The calibrated parameters clearly show a plausible contrast in social and rule-based behavior between shared space and Begegnungszone.

Abstract (German)

Im Straßenverkehr werden ab bestimmten Verkehrsstärken die Konflikte unterschiedlicher Verkehrsmodi meist durch eine weitgehende räumliche und zeitliche Trennung der jeweiligen Verkehrsmodi reduziert und entsch{"a}rft. Die Trennung führt nicht immer zur Erfüllung der gewünschten Verkehrssicherheitsziele oder Leistungsfähigkeit. Europaweit sind daher in den letzten Jahren verstärkt Konzepte zur gemischten Führung des Verkehrs untersucht und umgesetzt worden. Die Planungen solcher neuer Mischverkehrsanlagen kann durch wissenschaftliche Arbeit unterstützt werden, um planerische und politische Entscheidungen zu untermauern. Mikroskopische Verkehrssimulationen - erprobte Werkzeuge von Planern - sind derzeit noch ungenügend auf Mischverkehr eingestellt. Es existieren Modelle entweder für den motorisierten Individualverkehr oder den Fußgängerverkehr oder aber sie weisen eine sehr eingeschränkte Interaktionsmodellierung zwischen unterschiedlichen Modi auf.

Zielsetzung dieser Dissertation ist daher die Untersuchung des Bewegungsverhaltens in heterogenen Mischverkehren und die darauf aufbauende Anwendung von mathematischen Modellen zur Abbildung desselben. Es werden Ansätze entwickelt, die Modelle sozialer Kräfte auch auf den Fahrzeugverkehr auszudehnen. Die Grundidee hierbei ist, die Interaktion zwischen Fußgängern, Kraftfahrzeugen und Radfahrern durch Kraftfelder zu beschreiben, welche die Beschleunigung der Objekte im zeitlichen Ablauf beeinflussen. Speziell die Interaktion zwischen Fußgängern und Fahrzeugen bedarf einer Erweiterung der mathematischen Modelle.

Das Kalibrieren der Modelle erfolgt anhand von umfangreichen Realdaten von Mischverkehr in Österreich. Zum Tracking der verschiedenen Objekte in den Videobildern werden semiautomatische Methoden eingesetzt. Die auf diese Art kalibrierten und validierten mathematischen Modelle können in der Folge verwendet werden, um fundierte quantitative Prognosen der Auswirkungen unterschiedlicher Oberflächenplanungen auf Leistungsfähigkeit, Geschwindigkeit, Gefahrenpotential und Raumnutzung zu erzielen. Im Framework des Modells ist insbesonders das spieltheoretische Interaktionsmodell neuartig. Dieses zeigt den Einfluss von sozialen, regelbasierten (StVO) und physikalischen Aspekten auf das Verkehrsverhalten.

Besonders interessant ist der Umstand, dass während der Arbeit an dieser Dissertation der Sonnenfelsplatz in Graz von einem konventionellen Kreisverkehr im Jahr 2011 zu einem Shared Space umgebaut und 2013 als Begegnungszone verordnet wurde. Der Zusammenhang zwischen sozialem bzw. normativem Verhalten und der "Evolution" der Infrastruktur ist hier empirisch erfasst und wird auch durch das spieltheoretische Modell mathematisch dargestellt.

Acknowledgement

Many people directly contributed to the work on this thesis or supported related projects and I thankfully acknowledge: First of all my supervisor Martin Fellendorf for advising me all those years, sharing enthusiasm for transportation research in general and supporting entrepreneurial activities that appeared together with this dissertation.

I am grateful to Gerd Sammer for supporting the first part of my PhD-studies and for supervising the inital work on this project. I am grateful to Helmut Schrom-Feiertag, Christian Rudloff, Martin Stubenschrott, Weinan Huang and Dietmar Bauer, Thomas Pilz for all the cooperation in scientific work and engineering. I thank Martin Höfner, Katja Schechtner, Walter Wasner, Katharina Zwick, Hans-Jürgen Don and PTV AG, Roman Klementschitz, Iris Buchner, Peter Kalsberger and Bernhard Prendinger for their support in organizational aspects. I thank Erich Grünberger for being appreciative of my absence in the office to finish this thesis. For supporting me in data acquisition issues, I thankfully acknowledge Gottfried Schober, Thomas Fischer, Wolfgang Feigl, Michael Cik, Peter Kollegger and Sabine Porenta.

Considerable shares of this dissertation have been enabled with funding of the project MixME (825227) and MiMiSim (819175) by the Austrian Ministry for Traffic, Innovation and Technology (BMVIT) within the first and second generation of the national funding framework ways2go of IV2Splus. Further, I thankfully acknowledge all project partners of MixME: Mobility Department at the Austrian Institute of Technology (AIT), Institute for Highway Engineering and Transport Planning at the Technical University of Graz, Rosinak & Partner ZT GmbH and SLR Engineering GmbH for their fruitful cooperation.

For the general encouragement of my work I want to thank in particular: Manfred and Theres Schönauer. For both academic inspiration and friendship I acknowledge in gratitude: Christian Schönauer, Clemens Vierthaler and Christoph Buchner.

I would like to thank my fiancé Cathrin Haslinger for her love and for supporting me spiritually throughout writing this dissertation and in my life in general.

Robert Schönauer
Vienna, 2017

Abbreviations

ACC Automatic Cruise Control

AIMSUN Adv. Interactive Microscopic Sim. for Urban and Non-Urban Networks

API Application Programming Interface

BA Behavioral Adaptation

BRT Bus Rapid Transit

CA Cellular Automata

DLL Dynamic Link Library

ICC Intelligent Cruise Control

IDM Intelligent Driver Model

ITS Intelligent Transport Systems

MAS Multi Agent System

MMLOS Multi Modal Level of Service

PID Proportional Integrative Derivative

LOS Level-Of-Service

OD Origin-Destination

ODE Ordinary Differential Equation

PDF Probability Density Function

RHT Risk Homeostasis Theory

ROW Right Of Way

SFM Social Force Model

SPNE Subgame Perfect Nash Equilibrium

TCT Traffic Conflict Technique

TTC Time to Collision

VDM Vehicle Dynamic Model

VISSIM Verkehr In Städten - Simulations Modell

Nomenclature

α Model constant (context: benefit cost cellular model)

α Spatial constant, slightly less than a agent's diameter (context: SFM)

β Slip angle (context: car model)

β_j Set of best answers to S_j (context: tactical model)

χ Pitch angle of a car (context: car model)

$\delta_v(bike)$ Vehicle control parameter (context: steering model)

λ Steering angle (context: car model)

λ_c Flow of vehicles [vehicles/h] (context: flow model)

λ_p Flow of pedestrians [pedestrians/h] (context: flow model)

λ_{df} Discrete Fr*é*chet distance (context: infrastructure model)

λ_{S1}, λ_{S2} Eigenvalues of the oscillation equation (context: bicycle model)

ψ Yaw angle of a car (context: car model)

τ_α Time constant of the SFM for agent α (context: SFM)

θ_E Weight of energy loss disutility (context: tactical model)

Θ_m Certain direction to the target (context: routing)

θ_N Weight of normative related disutility (context: tactical model)

θ_R Weight of the distance related disutility (context: tactical model)

θ_S Weight of social related disutility (context: tactical model)

θ_V Weight of velocity dependent disutility (context: tactical model)

Θ_i, Θ_j Directions of agent i or j (context: tactical model)

Θ_{opt} Optimum walking direction (context: routing)

φ Roll angle, between the vehicle's body and z-axis (context: vehicle model)

φ_d Desired walking direction (context: routing)

$\vec{e}_\alpha^{\,0}(t)$ Directional unit vector for agent α (context: SFM)

$\vec{f}(t)$ Resulting force vector in a certain moment (context: tactical model)

$\vec{f}_\alpha^{\,0}$ Driving force vector of agent α (context: SFM)

$\vec{f}_{Guide}(t)$ Resulting guiding force vector in a certain moment (context: tactical model)

$\vec{f}_{SF}(t)$ Resulting social force vector in a certain moment (context: tactical model)

$\vec{f}_{Tactics}(t)$ Resulting tactical force vector in a certain moment (context: tactical model)

$\vec{x}_\alpha(t)$ Position vector of agent α (context: SFM)

a Shape of Beta distribution $d_{lateral}$ (context: infrastructure model)

$a(t)$ Time-dependent acceleration of an agent or of an observed road-user (context: kinematic models)

$a_f(v)$ Speed-dependent acceleration of an agent or of an observed road-user during free flow (context: car following model)

a_t Constant - the acceleration threshold (context: steering model)

a_{xy}, b_y Parameters of matrices of dynamic vehicle equations (context: steering model)

b Shape of Beta distribution $d_{lateral}$ (context: infrastructure model)

b_r, b_l Boundary of the road's central lane within the road's cross-section (context: infrastructure model)

c Profile center within the road's profile (context: infrastructure model)

c_h, c_v Constants in the model for a specific car characteristic (front and rear) dynamics (context: car model)

$C_{i,j}$ Conflict entity (interaction) between agent i and agent j (context: tactical model)

$C_{x,y}$ Cell grid matrix containing the combination of density and relative speed (context: interaction model)

$crit_p$ Critical gap size for pedestrians [s/pedestrians] (context: flow model)

$d_{conflict}$ Distance, where a driver or pedestrian start to react on a potential conflict [m] (context: tactical model)

D_i, D_j Absolute position vector of decision towards conflict solving of agent i or j (context: tactical model)

$d_{lateral}$ Weight of the center guiding (context: infrastructure model)

e_r, e_l End of the road surface within the road's cross-section (context: infrastructure model)

e_v Desired directional vector (context: steering model)

F_{qh} Lateral force at the rear (context: car model)

F_{qv} Lateral force at the front (context: car model)

$func(X)$ Strength of the influence of a cell within the routing (context: routing)

g Gravity constant (context: bicycle model)

gr_{car}, gl_{car} Right and left boundaries for cars within the road's cross-section (context: infrastructure model)

gr_{cycle}, gl_{cycle} Right and left boundaries for cyclists within the road's cross-section (context: Infrastructure model)

gr_{ped}, gl_{ped} Right and left boundaries for pedestrians within the road's cross-section (context: infrastructure model)

I Integrative control constant (context: steering model)

k_a Constant, describing the controller's proportional factor (context: steering model)

k_c Static control constant vehicle model (context: steering model)

k_v Velocity dependent vehicle control model (context: steering model)

k_x Coupling constant in the cell-based routing (context: routing)

k_{mode} Vector of constants, changing the look-ahead for each mode of transport (context: steering model)

k_{st} Proportional factor in the steering (context: steering model)

k_v Factor in the steering, reducing the steering angle proportional with speed (context: steering model)

kb_c Static parameter in bicycle control (context: steering model)

kb_v Velocity dependent parameter in bicycle control (context: steering model)

L Look-ahead distance [m] (context: steering model)

l Length of the vehicle (context: bicycle model)

$L_i^j(\Theta_m)$ Walking distance (context: routing)

l_{acc1} Desired direction vector of an agent (context: steering model)

l_{gf1} "Error" vector, created of the sum of forces of the guiding force field (context: steering model)

l_{sf1} "Error" vector, created by the agent's percepted sum of social forces (context: steering model)

m Mass of an entity (context: car model)

$n_{sensing}$ Sensing steps (context: steering model)

$n_{simtactical}$ Sub-simulation time-steps (context: steering model)

P Proportional control constant (context: steering model)

$P(i, j)$ Outcome (matrix) of the Stackelberg game (context: tactical model)

$P_L(i)$ Conditional probability of the leader (context: tactical model)

p_x Probability of each cell for a specific agent (context: routing)

$Pr(accept_p)$ Probability of a pedestrian to take a chance to cross a street (context: flow model)

$Pr(gap_c > crit_p)$ Probability that gap_c is longer than $crit_p$ (context: flow model)

r Distance between both axles of the vehicle (context: bicycle model)

S Cost score of a cell k related to agents or objects (context: benefit cost cellular model)

s^* Desired distance in front of agent α (context: car following model)

s_α Actual distance in front of agent α (context: car following model)

s_i^{eq} Sub-game Perfect Nash Equilibrium of agent i (context: tactical model)

s_r, s_l Beginning of the area of the road's side area within the road's cross-section (context: infrastructure model)

S_i, S_j Chosen strategy of agent i or j (context: tactical model)

s_{xy} Spatial vector, describing the position of agent x after choosing strategy y (context: tactical model)

$t_{lookahead}$ Look-ahead time (vehicle model) [s] (context: steering model)

$t_{sensing}$ Time-step duration of the so called sensing run [s] (context: steering model)

$t_{simStep}$ Simulation step duration [s] (context: tactical model)

$u(t)$ Lateral velocity of the vehicle (context: car model)

$u_L(i)$ Expected utility values of the leader (context: tactical model)

$v(t)$ Longitudinal velocity of the vehicle (context: car model)

v_α^0 Speed scalar, desired velocity of agent α (context: SFM)

v_α Speed of an agent α (context: kinematic models)

$v_{bike-center}$ Threshold: Bicycles use center [m/s] (context: infrastructure model)

V_{ij} Velocity dependent disutility matrix of agent i and j (context: tactical model)

V_i, V_j Scalar matrix for all strategy pairs, containing velocities of agent i and j (context: tactical model)

v_n Speed of agent n (context: kinematic models)

w_{gf} Weight of the guiding force (context: steering model)

w_{sf} Weight of the social force (context: steering model)

X_i, X_j Absolute position vector (point), of agent i or j is made (context: tactical model)

y_{ijn} Exponent in the log-likelihood method (value=1 is applied here) (context: interaction model)

Contents

List of Figures

List of Tables

Foreword

When I learned about shared space as concept for designing streetscapes the first time in a lecture held by Prof. Wolfgang Berger in 2004, I became fascinated. Ideas to work on that topic incubated in the following years and finally I have dedicated some years of research to gain insights of human behavior in heterogeneous traffic flow. May this dissertation bring its humble contribution to the understanding of traffic behavior, as it did for me.

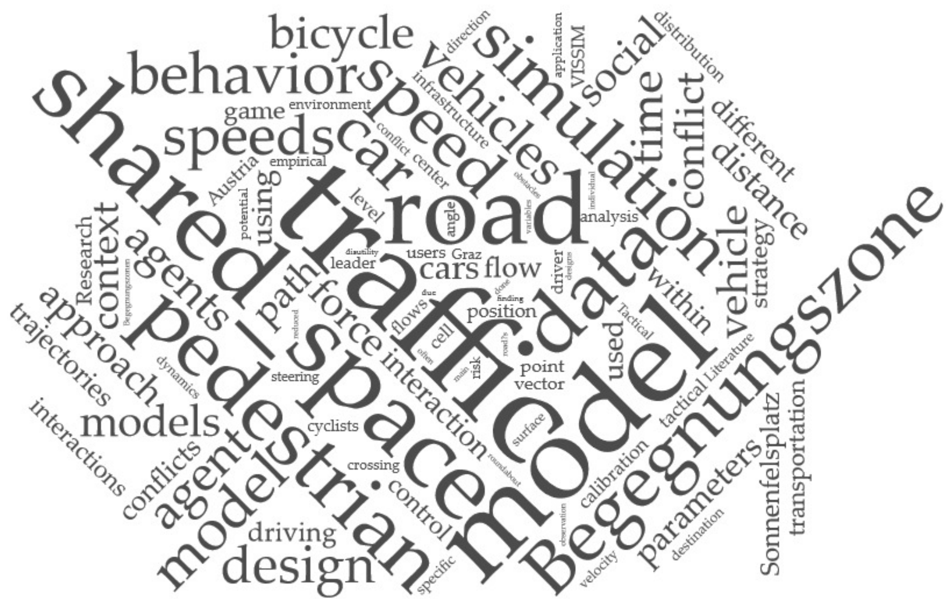

"...you look at traffic, it looks chaotic, but there is a rhythm to it...", Zenga (2012).

"The commuting theater is the Great Wide World, the last bastion of unabstracted human interaction and exposure to limitless potential for happenstance", Weiss (2012).

1 Introduction

1.1 Shared Space Road Design

A shared space is a road segment designed to encourage pedestrians, car-drivers and cyclists to use and share the same surface area with minimized physical segregation. In urban traffic networks, densities at the infrastructure's limits and a diversity of topologies create a high potential for conflicts within and between different modes of transport. Conventionally, these issues have been approached with a separation of modes and flows in time and space with the thoughtful design of roadways and footpaths and the calculated use of traffic control systems.

Shared space as a design philosophy represents an umbrella term for methods aiming on reducing the dominance of vehicles, vehicle speeds, and road casualty rates. This situation further stimulates the ongoing debate between planners, transportation engineers, lawyers and politicians about its practicability, purpose and missing guidelines. However, within the countless traffic-calming road designs, there is a low number of shared space implementations. It is this certain amount of insecurity during planning and furthermore in the daily use of such roads which gives in particular shared space enough weight to be an outstanding object of studying human behavior in traffic flows.

The first implementations of shared space (Monderman et al., 2006) brought the international debate about the design, planning, costs, and their impact to a high public awareness on this topic. Safety issues and worries about the traffic flow were questioned during all of the implementation phases. Due to this lack of legally binding elements, like pedestrian crossings, road–users are said to be more safety-conscious and to pay more attention to the behavior of other people. Especially the high potential of conflicts between different types of road–users is said to be reduced. In conventional designs, the separation of traffic flows by modes is used to avoid these conflicts between cars, buses, pedestrians and cyclists. However, proponents of the philosophy claim that this is an outdated concept leading to unintended consequences (Gerlach et al., 2009; Gerlach and Ortlepp, 2010):

- Attention of road users in one mode of transport towards those in other modes is lessened as they feel safe and privileged on their assigned part of the road.
- As a consequence, not only cars, but also bikes and other motorized traffic, exceed the speed limits and concentrate mainly on their part of the road, leading to a higher risk for pedestrians.

- Current street designs are not flexible enough to adapt to the changes in modes and tend to prioritize PrT, thus hindering the development of active mobility and public transport.

There is a continuous debate about the merits and practicality of shared space (Gerlach et al., 2009; Hamilton-Baillie, 2007). However, across Europe, in particular in Holland, Germany, Austria and the UK, several projects have been planned and implemented. Furthermore, some practical analysis on existing schemes show the effects on reducing maximum speeds and keeping performances high is possible, as observed in through–roads and town centers in Holland and Germany (Füreder and Schwab, 2009; Hamilton-Baillie, 2007; Gerlach and Ortlepp, 2010). Topp (2010) concludes that safety related data in before-and-after analyses shows a neutral tendency in accident statistics of self-organizing zones. Trial demonstrations at three junctions in Bristol (UK) showed that they generally performed better after traffic signals had been voluntarily turned off (Firth, 2011). However, these analyses are carried out as experiments or as before and after studies but do not help traffic planners to judge concrete projects in advance with respect to safety and traffic flow. Adequate planning tools are necessary to help convince the public, as well as local authorities that well-designed areas are advantageous for travelers in all modes (Hamilton-Baillie, 2007; Gerlach, 2015).

1.2 Motivation and Research Objective

Shared space and similar mixed traffic philosophies can be compared to toolboxes themselves, where a flexible and sensitive way of application is necessary. Microscopic traffic simulations allow for the highly detailed modeling of pedestrians, vehicles, driver behavior and the interaction between each other and with the surrounding infrastructure. The state of technology and available simulation software don't provide sufficient degrees of freedom and capabilities to reproduce dynamic and social interaction. One of the most essential phenomena when modeling mixed traffic areas is the social behavior within the interactions between cars, pedestrians and cyclists. This can be observed in situations, where pedestrians want to cross a road not on a crosswalk and cars stop without the normative need but due to social factors. In slightly different situations, the same pedestrian would make a small direction change to walk behind the car instead of waiting for the car to pass. Modeling this and similar behaviors are the main challenges when designing simulations. This thesis shows the first steps towards such a model. To the author's knowledge no available simulation model can yet explicitly handle the requirements that the added social interactions and constraints imply. Such constraints include:

- Compared to conventional road design, finding the way through the infrastructure is more complex because there is no hard separation between different mode of transport. Desired speeds strongly depend on the traffic situation - not only on speed limits and platooning constraints.
- Due to the possible degrees of freedom, vehicles should be able to maneuver in a two dimensional plane - in common microsimulation approaches vehicles have specific one dimensional paths.

- Interaction between different types of road users including pedestrians, bicycles, and cars need to be handled differently from conventional traffic. Instead of modeling technical regulations like traffic lights and priority laws, there is a need to model the social interactions between people in different mode of transport.

1.3 Dissertation Outline

The structure of this document is illustrated in figure 1.1 and defined as follows. This introductory chapter has presented the background of implementation and the motivation of the work, purpose and scope of the dissertation. The state of the art analysis in the following chapter considers the result of the previous studies about mixed traffic, behavior in traffic flows and methodical approaches to model it.
Chapter 3 defines the model's requirements and mathematical definitions. Chapter 4 describes the development of a microscopic simulation framework and the implementation of the novel model components. Chapter 5 shows the application and the work on data acquisition and processing. In Chapter 6, the results of the data analysis, the model calibration and the simulation outcomes are shown. Chapter 7 concludes the dissertation with several new findings and summaries of the results. Open technical and scientific issues are discussed in the context of future research.

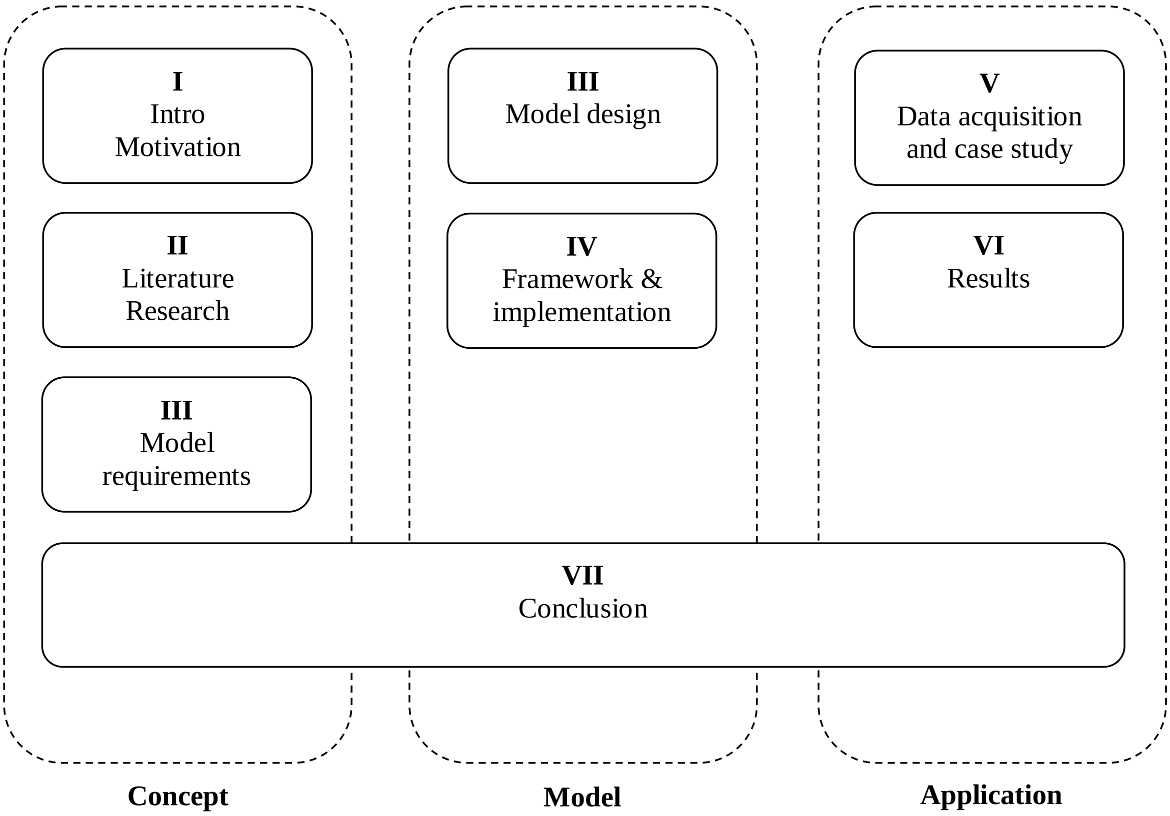

Figure 1.1: Structure of this dissertation.

2 Literature Review

In the first part, this chapter gives some background on urban mixed traffic and its qualities regarding design and traffic behavior. Multiple road surface design concepts are introduced. The research done on *shared space* is under–developed - the experiences and data is still unsatisfying, nevertheless here a wide review on the scientific and practical background of urban mixed traffic is conducted.
The link to the technical part of traffic models is provided with a review on psychological decision and perceptional aspects of road designs. In the second part, theoretical behavioral and social models are described and their applicability towards the presented problem are analyzed. The landscape of traffic models is drafted, the focus on microscopic modeling extends the details on vehicle dynamics and tactical decision models.

2.1 Mixed Traffic and Shared Space

The term *mixed traffic* defines traffic flows on mixed-use urban roads. Motorists, cyclists and pedestrians are using the same segments on the surface of road and squares in towns and cities.

This thesis focuses on urban mixed traffic in its special derivation of shared space in Europe driven by traffic calming and urban design. The term shared space is commonly used to describe:

- A specific design philosophy in traffic engineering.
- The process of planning, including a strong aspect of public participation.
- The real space on the road after the implementation.

In this thesis, especially in the adjacent chapters, shared space describes the actual road space after the construction. There are reduced physical borders and instead of providing a sharp legally binding line (surface marking or curbs), “soft” design elements are used, thus by definition - shared space includes the whole road profile.

2.1.1 History of Shared Space

Shared space as a design philosophy represents an umbrella term for planning methods aiming towards the vision of reducing the dominance of vehicles, vehicle speeds, and road casualty rates. The concept of designing public roads, junctions and spaces as so called shared space became increasingly popular in recent years and is seen as a chance to reduce the car-dominance in cities throughout Europe. The theoretical roots of integrating car traffic and active mobility can be tracked back to the English Professor Colin Buchanan, who published *Traffic in Towns*, an influential report and popular book (Buchanan, 1963). His concluding recommendation was that towns should take care that they are worth living in, which meant more than just the ability to drive into the center: " *... The freedom with which a person can walk about and look around is a very useful guide to the civilized quality of an urban area ... judged against this standard, many of our towns now seem to leave a great deal to be desired ... there must be areas of good environment where people can live, work, shop, look about and move around on foot in reasonable freedom from the hazards of motor traffic...*" (Buchanan, 1963). Other international origins of traffic calming philosophies have been sparked during Europe's grassroots movement and date back to the 1960's (Kjemtrup and Herrstedt, 1992; Schlabbach, 1997). Nevertheless, some years had to pass before any real noteworthy realizations came into being. In 1970, residents of the Dutch city of Delft opposed the high flow of through-traffic by turning their streets into "woonerven", or "living yards" (Schlabbach, 1997). What began with a simple road bump was followed by the redesign of complete roads. Channels for the movement of cars were turned to shared areas, outfitted with tables, benches, sand boxes, and parking bays jutting into the street. The increased road's "friction" aimed to reduce speeds of motor vehicles and comfort residents, extending their home to the public space. In September 1976, a number of new traffic regulations came into effect and minimum design standards for residential precincts (*woonerf*) were published for the first time in Europe by the Netherlands Ministry of Transport and Public Works (Ben-Joseph, 1995). The Delft redesign was a success and its "shared street" concept (*woonerf*) became accepted and established through guidelines and traffic regulations in the Netherlands and then in rapid succession adopted by other countries such as Germany, England, Sweden, Denmark, France, Japan, Israel and Switzerland. Strictly its application was restricted to residential zones and its impact therefore limited. In the recent generation of progressive traffic calming measures, ambitions include collector roads as well. Across Europe different concepts of partial mixing of traffic flows and *self-explaining roads* have been analyzed and established in non-residential roads. The most popular concepts are *shared space* and *Begegnungszone*[1]. While the *Begegnungszone* has a legal basis in the traffic regulation (Bogner and Robatsch, 2013; Salamon, 2013), the shared space concept does not include any additional regulation.

2.1.2 Design Specifics of Shared Space

This thesis aims on traffic flows in roads, where the shared space design paradigm is applied. In addition, on a lower intensity, traffic flows in Begegnungszone will be addressed in this work. Although the customization and participation aspect in the planning process bring in unique elements the following list can be repeatedly found in shared spaces and in Begegnungszonen:

[1]In literature, the German term Begegnungszone is sometimes loosely translated to English with "encounter zone". Its French translation, "Zone de Rencontre" is used in French, Belgian and Swiss traffic regulations. In the context of this thesis, it refers to the exact definition in the road traffic regulations. Therefore, the German word is kept.

- No center lane separator marking.
- Single level of the road surface or low curbs.
- No or reduced parking possibilities along the lanes, parking prohibition is optional.
- No segmentation in physical means and no physical boundaries.
- No traffic control and reduced traffic signs.
- Road furniture and design for guidance and natural segmentation.

In the appendix, an overview of mixed traffic implementations is given (figure 8.3): Only 6 of 24 locations may to some extent be defined as "real" shared space. Gerlach (2015, pp. 5-6) lists implementations of shared space in 2015 together with design-criteria. In shared space designs, the segregation between motorized and non-motorized traffic is removed, creating an integrated space without traffic signs or signals, curbs and road markings. Instead, traffic flows are controlled by social interactions and supported by intelligent infrastructure measures like colored floors or bollards. Due to this lack of legally binding elements like pedestrian crossings, people are said to be more safety-conscious and pay more attention to the behavior of other people. Especially the high potential of conflicts between different types of road users is said to be minimized. In conventional designs the separation of traffic flows by modes was used to avoid these conflicts between cars, buses, pedestrians and bikes. However, proponents of the shared space approach claim that this is an outdated concept leading to unintended consequences (Monderman et al., 2006; Gerlach et al., 2009). The toolbox of optical and/or physical segregations includes multiple possibilities ranging from color markings, change in the surface color, material, marginal changes in levels, as well as the installation of road furniture. The attachment gives a selection of examples taken in the last years within this project. Karndacharuk et al. (2014) finds that there are certain design elements, constituting a shared space. Without them, they claim that it is difficult for a public street to function as a genuine shared space for all road users.

2.1.3 Other Mixed Traffic Concepts

Bogner and Robatsch (2013) claim that shared space stands for a vision of an ideal picture of urban road space. Shared space itself does not include additional traffic regulations. In this section, the Begegnungszone and the residential road are discussed briefly. Figure 2.1 compares maximum driving speeds and the "grade of restrictive regulations for drivers" for shared space, Begegnungszone and residential roads (or zones). The road signs displayed in the diagram, are the official road signs in Austria. The abscissa ("grade of restrictive regulations") has only schematic ordinal quantities - the positions of the three markers in the figure are assigned by the author.

Regardless of the fact that there have been even signs to announce the beginning of a shared space zone in some implementations there is no regulative implication. The design intends for the roads to become self-explaining and to influence drivers in a softer way than normal. It also claims that traffic signs can be widely reduced.

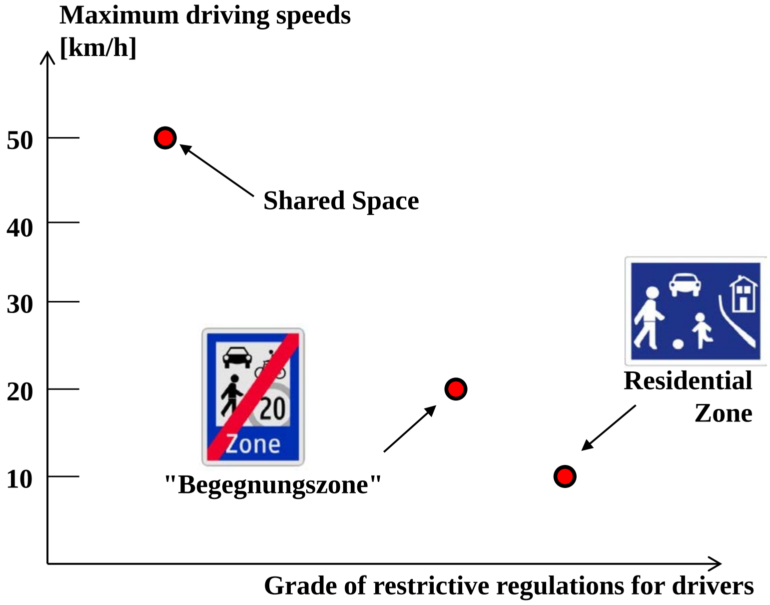

Figure 2.1: Grade of restrictive regulations (especially for motorized traffic) in relation to allowed driving speeds.

Begegnungszone

Thiemann-Linden dates the origin of the Begegnungszone back to 1980, where in the French mid-size town of Chambéry, traffic calming and pedestrian rights have been considered even in main arterial roads (Thiemann-Linden, 2010). In meantime, the Aire Piétonne is a popular traffic regulation measure. The highway codes in France, Switzerland and parts of Belgium include regulations for this traffic zone guaranteeing pedestrians priority to vehicles, driving in walking speeds (Switzerland: 20 km/h) and stopping restrictions. The legislative integration in Austria (§76c in the traffic regulations (Republik Österreich, 1960) came into effect in 2013, based on its relevance for the social/normative section of this work, the text is printed in figure 8.5). The basic traffic rules can be summarized as thus:

- Speed limit is 20 km/h (definition of 30 km/h is optionally allowed under certain circumstances).
- Pedestrians and cyclists are not to be hindered and put at risk.
- Parking is allowed only in marked areas.
- Through traffic is allowed.
- Pedestrians are not allowed to willfully hinder vehicular traffic.

Selections of several international Begegnungszone are shown in figure 8.6 and figure 8.9. In 2013, the formerly shared space at the Sonnenfelsplatz in Graz (Austria) has been changed to a Begegnungszone, defined by decree. This opportunity was taken to conduct a comparative analysis. Schweitzer and Fasciati (2008) analyze accident rates in Begegnungszonen in Switzerland and show a reduction in the number of accidents, quantity of light and heavy injuries and property damage between 10 % and 30 %. A major number of accidents are bagatelles that seem independent of the road traffic regime.

Residential Road

The exact definition of residential or living streets depends on national traffic regulations. Picking the Austrian category (Republik Österreich, 1960), the following set of rules applies:

- Walking is allowed at any place on the road.
- Pedestrians and cyclists should not be put in danger by cars. Car drivers always have to yield to them.
- Motorized through traffic is not allowed.
- Upon exiting the residential street, vehicles have to yield to any other road users.
- Driving speed is limited to walking pace.

The definition of a residential road highly correlates with the original Dutch scheme "woonerf", which is a living street where pedestrians and cyclists have legal priority. Technical measures include a shared road surface, traffic calming, and low speed limits. The article 44 of the Dutch traffic regulations (Dutch Ministry of Infrastructure and the Environment, 2006) restricts motorized traffic in a "woonerf" or "recreation area" to walking pace. In legal literature, quantitative interpretations of the walking speeds of up to 15 km/h are to be found (i.e. in Hentschel et al. (2005)).

2.2 Observed Impacts of Shared Space

In shared space designs, the segregation between motorized and non-motorized traffic is widely reduced, creating an integrated space without or a minimized number of traffic signs, curbs and road markings. Traffic lights are not used. Instead, traffic flows are managing themselves by social interaction that is supported by infrastructure designs like colored road surfaces and the thoughtful placement of road furniture. From a planner's perspective requirements of research on multiple characteristics of shared spaces can be structured in the following manner (Gerlach and Ortlepp, 2010):

- Traffic flows
- Safety and accident aspects
- Impact to driving speeds
- Parking demand
- Change in traffic behavior
- Impact to urban development and land use

This section will be structured according to this list, including normative (legal) issues and design aspects and provides literature review on the topic. The ambition to primarily refer to observations in shared spaces could not be fulfilled in every aspect. To a certain extent, literature related to other design-concepts of mixed traffic is considered.

For the last seven decades, an evolution in the way of using public road space have created rule-based realms, in which insulated users (agents) are free to maximize their own utility. By contrast, adherents to theories of shared space and risk homeostasis claim that streets are socially negotiated spaces, and blame traditional road design for socializing users to drive like Amartya Sen's *rational fools*' (Sen, 1977). This statement leads to the assumption that a road user's risk perception and therefore her or his demand on space and time resources is dependent on the user's social trust and social status. When Monderman attempted to make roads safer, he realized the importance of considering urban design, social science, civil engineering and psychology. He came up with the radically counterintuitive approach: "Build roads that seem dangerous, and they will be safer" (McNichol, 2004).

2.2.1 Impact to Traffic Flows in the Network and Spatial Shifts

Bode (2009) does a quantitative analysis of the impact of the shared space design in Bohmte. Road users have been questioned and the Origin-Destination (OD) relation analyzed. On the main through road the motorized traffic has been reduced by 700 - 800 cars / 24 h (about 6 %) and by 200 trucks / 24 h (about 26 %). The reason is the spatial shift of the flow to a bypass road. Sorenson (2017, pp.34) quantitatively evaluates the contextual characteristics of international shared spaces. He summarizes that shared space can commonly be found in roads of less regional importance but also within a wide range of urban environments.

Yao et al. (2009) analyze the conflicts in the interactions of cars and bicycles in lane based mixed traffic with a CA simulation approach. Their approach focuses on how the modal share of bicyclists affects the general vehicle speeds on the road. They do not measure the interactions between vehicles and bicyclists directly, but rather compare the velocity distribution of disturbed/undisturbed vehicles obtained from practical data and simulation outputs to verify the model. The distribution of vehicle velocities is relatively concentrative when no bicycles exist, as their density is zero. With the increase of the bicycle density, the distribution becomes more scattered and ramified. The cyclists occupy a fifth of the cars cell size - though it is not yet clear how an increasing number of bikes does not induce a higher capacity on a road with a speed limit of 50 km/h. Shared space, has been shown to promote a safer, more vibrant, and multi-modal transportation infrastructure while also improving both pedestrians and vehicle travel times in congested areas (Wargo and Garrick, 2016).

Karndacharuk et al. (2013) provide an extensive data acquisition and analysis of behavior on three streets in New Zealand which have been converted to shared spaces. Their performance indicators include: Dwelling times (residence), activities (eating, chatting etc.), retail occupancy rates in the area, speed reductions for cars and overall crash history. At the time of writing this thesis, however, only the *before* period has been captured and analyzed; the data of the *after* period will only be fully analyzed in late 2012. The conclusion of literature research indicates that there is not a well-defined set of optimization attributes which fits for every shared space. Depending on the surroundings and intention of the shared space, sometimes it could be beneficial to increase the dwelling times of pedestrians, while in other situations the main objective could be the reduction of the travel times of pedestrians. The only recurring objective is, however, that shared spaces should encourage shared usage of the space instead of retaining the old behavior on a newly designed road. This is also the main research objective of this work.

2.2.2 Safety and Accident Aspects

Accident Analysis

Until now, there is still a unsatisfying sample size of accident–data, although trends can be estimated and safety analyses undertaken. The relationship between vehicle speeds and the risk of death or injury is well documented (see table 8.1 in the appendix). At speeds of less than 32 km/h, there are almost no pedestrian deaths - a main reason to limit speeds in traffic calmed areas to 30 km/h. Besides the physical impact, the perceptual abilities and time windows for actual reaction on traffic conflict increase. Edquist et al. (2012) conclude that the limited data available so far on shared spaces in the Netherlands and UK suggests that crash rates are no higher than comparable traditional environments, and in some cases even lower.

Conflict Observations

With the growing number of shared spaces opened to public, more research deals with the effects of the various design elements on the behavior of pedestrians and drivers. Especially in the UK a wide range of reports have been issued on the design of shared spaces (Department for Transport, 2011) which act as guidelines for transportation planners and researchers. The safety effects are based on observations in a handful of converted shared spaces throughout Europe (Reid et al., 2009). The report summarizes the results of an appraisal stage in which available evidence on the performance of shared space has been collated and reviewed. It also includes a literature review by examining the most common characteristics of shared spaces. Among those are: Economic activity and property values, flows of users across the street, opinions of users, use of facilities such as seating and proportion of pedestrians moving freely. Especially the last property is a fundamental idea of shared space, but Reid acknowledges there is little data available. We try to fill this gap by analyzing the pedestrian paths using trajectories obtained from annotated video footage. Many of the other properties are often examined by opinion polls. In example, Kaparias et al. (2012) describe a stated–preference study that links specific elements of a shared space (like pedestrian density, vehicle density, speed of vehicles etc.) to the willingness of drivers to actually share the space with pedestrians in a shared space. Dong (2012) applies a traffic risk analysis tool to data acquired at London' s shared space on Exhibition Road. His work shows a slight decrease in both the frequency and severity of traffic conflict by the conversion to a shared space. The overall risk value decreases by 20 %.

Actual change in behavior by doing video analysis has been researched (Bliek, 2010) by comparing the probability of cars stopping at intersections of conventional roads to the equivalent probability at redesigned shared spaces in Montreal. Two shared space crossings are compared to two reference crossings with similar properties of size and traffic volume. It was observed that drivers are more likely to give way to pedestrians on the shared spaces than on the conventional crossings.

A theoretical classification of interactions between bicyclists and pedestrians applies Butz (2007) to traffic in *Begegnungszonen*. Accidents in *Begegnungszonen* seldom happen, nevertheless conflicts between pedestrians and cyclists can often be observed - especially including elderly and visually impaired people. The authors find that the pedestrians perceive conflicts more critically than cyclists, while no causal explanation is provided. Table 2.1 shows the proposed classification.

Type	**Description**	**Ped. perception**	**Cyclists perception**
Encountering in passive interaction	Pedestrians and Cyclists unconsciously evade, without slowing down or communicating	no issue	no issue
Minor conflict	Both or either the Ped. and the Cyclists clearly have to evade each other by slowing down or communicating	small to medium issue	no issue
Major conflict	Both or either the Ped. and the Cyclists clearly have to act in an emergency manner	medium issue to not acceptable	small to medium issue
Accident	Physical contact between the pedestrian and cyclist	not acceptable	not acceptable

Table 2.1: Classification of interactions between bicyclists and pedestrians in *Begegnungszonen*.

The interaction intensity can be classified in multiple levels and the perceived qualities highly vary. It should be considered that the intensity between pedestrians and cyclists gets higher with the number of conflicts per time unit. Appearing in a high density zone even minor conflicts can get problematic.

Generally, the grade of severity in relation to the frequency of interactions, the accident pyramid is often cited. Figure 2.2 shows such an example. In segregated traffic flows, the green/blueish center segments would appear smaller and the yellow bottom edge would become larger. Applying to shared spaces means to increase the number of interactions and to aim on a smoother slope toward the top segment (collision).

Special Safety Issues

Topp (2010) states that a better social behavior in traffic and the deregulation of traffic spaces are possible and the redesigned areas increase traffic safety. Nevertheless, Topp says that happened to be the case also before the redesign. He claims that there are still some questions concerning children, elderly people, blind and sight impaired people. shared space and Begegnungszonen do not lead automatically to an improved street

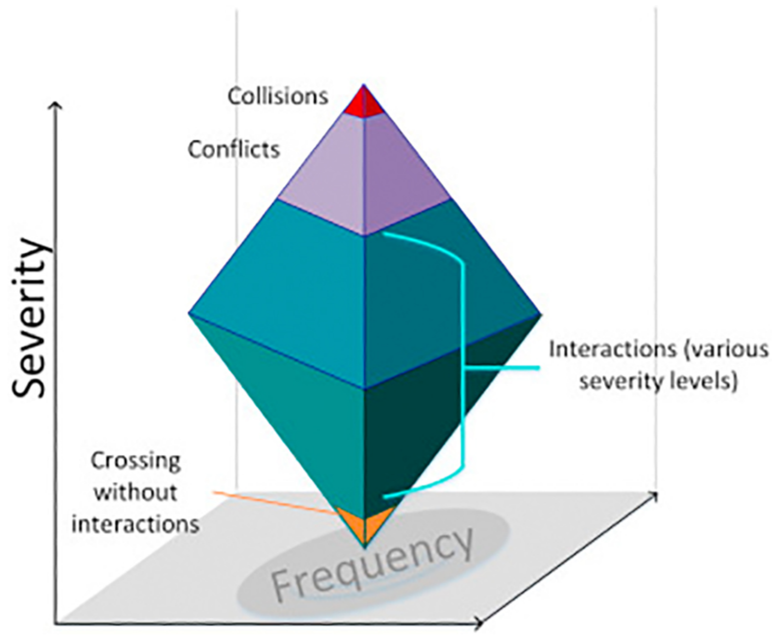

Figure 2.2: Road safety continuum for vehicle / pedestrian interactions, taken from Cloutier et al. (2017).

design. Streetscaping is a high urban design and functional demand, which can be met within the separation principle of street design as well as within the mixed use principle. For a clear distinction from traffic calmed areas, Topp agrees to the proposal of FUSS e.V. (German Pedestrian Association): Spielstraße (playstreet) with a speed limit of 10 km/h and Begegnungszone with a speed limit of 20 km/h, with priority for pedestrians, but no children's play. He critically adds that in urban traffic, more planning creativity is needed, as well as more flexibility of the guidelines and better social behavior for livable urban spaces.

Regarding focus groups there are further aspects worth mentioning. The usability for handicapped and blind people is a major issue regarding shared space. One finding is that in the UK, half of those who had experience on shared surface streets had had an accident (7 %) or a near miss (42 %) on at least one occasion. Of these incidents, only 15 % were reported (Childs et al., 2010). There is no evidence of how many incidents are generally reported in regular urban roads (not shared space).

Childs et al. (2010) present laboratory experiments to estimate the detectability by blind and partially sighted participants of a number of surfaces, as well as the ability of participants with mobility impairments to pass over these surfaces. They conclude that it is difficult to find a surface that is suitable for both detection and ease of passing over, but indicate some possibilities worthy of further research. For example, 0.06 % of the Austrian population is blind and even 5 % is with reduced visual capabilities (Österreichisches Statistisches Zentralamt, 1997) - therefore, the optical contrast seem to be an essential part of the design.

Havik et al. (2012) provides a systematic overview of the appearance of shared spaces in the Netherlands and the consequences that these spaces may have for the independent mobility of visually impaired persons. He finds that none of the selected shared space locations were free of potential problems for visually impaired persons. The level of hindrance that these characteristics could cause visually impaired users of these spaces was judged by a group of experts in the field of orientation and mobility. In addition, the compliance of the selected locations with existing guidelines for accessibility was assessed.

Xin et al. (2008) propose a model aiming to represent "less-than perfect" everyday driving conditions and have reproduced both safe and unsafe driver behavior. The authors' test results indicate that the proposed model is able to replicate both normal, as well as unsafe steering behavior that increases vehicle collision probability.

2.2.3 Impact on Driving Speeds

Looking for a theoretical background, about how drivers choose their driving speeds in relation to shared space, the Risk Homeostasis Theory (RHT) provides reasonable ideas and empirical results. Based on the often cited behavioral theory is Wilde' s RHT (Wilde, 1982), which states that human behavior adopts to the level of risk, intending to keep it constant. Regarding traffic safety issues he presents a decoupling between reduction in the accident loss per unit in distance of mobility and the accident loss per time unit of road-user exposure and per head of population. He assumes a relationship between the accident loss per capita and the road-user behavior in a closed-loop regulation process.

O'Neill and Williams (1998) claim that the risk homeostasis is an unproven hypothesis. He cites multiple case studies of airbag users, with cumulated traffic injury statistics. He concludes that it would be foolish to think people never adjust their behavior in response to perceived risks, but a more productive approach is to try to determine the conditions under which this occurs.

Streff and Geller (1988) conduct the first experimental empirical study examining parameters under which risk compensation in driving can occur following the use of safety belts.

The RHT in the specific situation would hypothesize that if individuals use safety belts, they will drive in a more risky manner than if they do not use safety belts, due to an increased perception of safety. Risk compensation theory was not supported in the between-subject analyses of the research data; however, some within-subject comparisons did demonstrate risk compensation. Subjects who switched from not using the safety belt to using it increased driving speed during the second phase significantly more than subjects who used the safety belt during both driving phases. The study suggested that the occurrence of risk compensation is dependent upon individuals being able to compare the sensations using a safety belt with those of not using a safety belt.

A similar approach in a context closer to infrastructural design develop Edquist et al. (2012) with defining the changed behavior in response to the perceived risk in the driving environment as a form of Behavioral Adaptation (BA). Usually BA occurs in response to an intended road safety improvement (for example, a widened road): In a review of the effects of road environment on speed, Edquist et al. (2012) found that drivers:

- Speed up when guidance (in the form of clear centerlines or edge-lines) improves (negative BA)
- Slow down when the road is narrow, or looks narrow (positive BA)
- Drive at whatever speed they are most comfortable with for that road, which may be higher or lower than the official speed limit, when under high mental workload (may be positive or negative)
- Slow down when sight distance is restricted, but not sufficiently to react in time to a hazard emerging from the unseen area (positive but limited BA).

Evans (1985) develops a generic human behavior feedback formalism in which the actual safety changes in traffic systems is related to the intended or expected change through the introduction of a "human behavior feedback parameter". His formalism includes earlier approaches to describe and understand traffic safety as special cases and, in addition, includes responses outside the range encompassed by the earlier approaches.

Due to this lack of legally binding elements like pedestrian crossings, people are said to be more safety-conscious and to pay more attention to the behavior of other people (Hamilton-Baillie, 2007). There is ongoing debate about the merits and practicality of shared space: Hamilton-Baillie (2007) and Monderman et al. (2006), highlight the positive factors like reduced crash statistics or average speeds. Especially when it comes to opinion-based results, the situation is not as clear anymore. Especially the elderly and disabled people feel less safe in shared spaces (Gerlach et al., 2009). Given this discrepancy between hard facts like crash statistics and public opinion, this thesis wants to research the missing link in between: How has people's actual behavior in a shared space changed after reconstruction of a formerly conventional street into a shared space street.

Up to now, research of shared space concepts has mostly focused on empirical studies showing the impact of shared space, instead of creating simulation models. It is hard to imply a simulation model from these works as the causalities of a measure to an effect is not always clear. Individual aspects were analyzed by Richter and Zierke who show that removing the separation between lanes on a country road effectively reduced speeds of cars (Richter and Zierke, 2010), Davis in turn shows that reducing speeds of cars increases safety of pedestrians (Davis, 1998).

There is empirical evidence that in urban roads of lower speed designs, journey times for vehicles improve at lower steady speeds, due to greater efficiencies at intersections Hamilton-Baillie and Jones (2005). There is evidence for an average reduction of speed: 19-39 % (18-28 to 13-22 km/h). Haas and Herberg (1983) analyzed real driving speeds and the perceived driving speeds in multiple road sections in different towns. He shows that the motorized traffic density (29 % coefficient of determination), the width of the road (18 % coefficient of determination) and the density of parked cars (9 % coefficient of determination) are the strongest variables in drivers' speed choice. Knoflacher and Schopf (1981) show in an empirical study that the presence of vehicular counter flow shifts the path to the right. The strength of the observed phenomenon obviously depends on the speed.

2.2.4 Impact to Urban Development and Land Use

Karndacharuk et al. (2013) present a pedestrian related performance measurement methodology to evaluate the successfulness of shared space schemes. It analyzes pedestrian trajectories, dwelling time and stationary activity. The application of this methodology to three study areas, which have been transformed into shared spaces in the city center in New Zealand, shows three main conclusions:

- With an increase in pedestrian activity and dwelling time, the shared space design highlights the road's functionality of being a public place.
- Shared spaces fundamentally create a road environment where there is enhanced priority for pedestrians (including the visually and mobility impaired) to safely move around and interact with the surrounding environment.
- Mean vehicle speeds decrease as pedestrian density increases in shared space zones.

2.3 Traffic Behavior

Shared space aims to intensify social behavior as well as the perception of road design and infrastructural environment. De Jong (2013) concludes in his research that in traffic flows in shared space zones, there is a distinction between social behavior and normative traffic behavior. To understand this distinction it is necessary to design a plausible traffic flow model.

In this section, the literature is reviewed for models which lead to decision making in interactions, speed choice and risk taking. The background here is wide, compared to conventional traffic flow theory, precisely because shared space traffic emphasizes social behavior.

The reviewed psychological behavioral models of drivers are rooted in the wide field of traffic psychology and address the interdependencies of cognitive, perceptive and emotional entities. A meta-analysis in this field considering multiple cognitive and emotional factors has been undertaken by Vaa (2001). The beginning of this research field was triggered by the upcoming safety issues with automobile road traffic as the greatest threat to human life. Gibson and Crooks (1938) had been one of the first researchers introducing systematic sets of concepts to measure their inferred components. They tried to precisely describe the cognitive process flow when a person drives an automobile and gave it practical, as well as psychological validity. This section gives a structured result of the literature review on the topic of traffic behavior focusing on safety and its perception.

Traffic psychology provides a wide range of contributions on theoretical background, impact analysis and causal research on traffic behavior (i.e. Barjonet (2001)). In this thesis, decision models on priority issues, speed choice and path choice are considered. In the generic literature about human behavior, Fishbein and Ajzen (1975) are often named in relation to human motivation theories. Furthermore, their models consider human values, attitude forming intentions, preparing actions to understand attitudes and to predict behavior.

Traffic behavior is lead by conscious and unconscious actions and reactions, which are an application of learned rules, processes and decisions. Multiple levels influence the microscopic processes of every road user. Human perception and information processing can be structured in a hierarchic approach (Flade, 1994). On a strategic level, planning and attitude dominate the activities. Hence, the underlying motivation is manipulated by multiple aspects as there might be juridical definitions and social norms. Other factors are the perceived costs and utilities of using links, traffic modes and traffic demand. On the operational level, the intended activities are adjusted to the situational requirements. The parameters of the infrastructure and the normative aspects influence the behavior. On the lowest level, the handling of the vehicle is a mostly unconscious and automated action. Physical attributes, driving skills and quality aspects of the road affect the actions.

Speed and visibility deal more with the external conditions, while attentiveness addresses a driver's internal ability to notice and avoid a potential conflict with other road users (Hobson, 2008). The causal effect of inattentiveness in traffic accidents is hard to quantify, since it is an internal state and most drivers involved in a collision do not want to admit to being inattentive. However, research by the National Highway Traffic Safety Administration and Virginia Tech Transportation Institute published in 2006 found that 65 % of near crashes and almost 80 % of crashes involve driver inattention. While attentiveness is an internal state, the environment can encourage attentiveness or subtly suggest that it is unnecessary. The social inventor and street philosopher from Australia, Engwicht (2005), has identified three mental speed bumps: *intrigue*, *uncertainty*, and *humor*. These "speed bumps" engage drivers with the environment around them, by causing them to drive more slowly, attentively, and courteously.

2.3.1 Motorists Behavior

This section reviews and discusses factors influencing the driver's behavior and which mechanisms make them drive slower and encourage them to drive less aggressively. The risk perception seems to be an essential element - based on Vaa's chronology, some of the milestones in the psychological models are reviewed (Vaa, 2001). While Näätänen and Summala (1974) postulate that drivers try to avoid risk by adjusting their behavior according to their perception of zero risk, Wilde (1982) postulates the opposite by stating that drivers seek a certain risk level - a target risk level - a risk level that lies above 0 and defined in the ways risk commonly is defined:

- By exposure, which can be a number of accidents per kilometers driven or accidents per a certain unit of time etc.
- This risk number individually varies; it seems to be partly a regulator in a homeostatic system

- Drivers should not to endanger or interfere with pedestrians
- If the driver is confronted with certain changes in the road environment, she or he will meet the changes by behavioral adjustments to meet her or his certain acceptable level again.

Hamilton-Baillie (2008) concludes that those theories might explain why a lot of traffic safety measures do not provide a sufficient decrease of risk in road traffic. Monderman et al. (2006) claims that increasing the perceived risk goes with an increase of safety. This is what he calls insecurity for safety in shared spaces. Measurable change in the yielding behavior of car drivers increases from 50 to 90 % in interactions with pedestrians. While for cyclists, car drivers are yielding to them to a lesser extent, but still between 35-86 %.

Moody and Melia (2014) found in their empirical study in UK, that in 72 % of the conflicting movements, the pedestrian initially gave way to the vehicle. In 20 % of instances, the drivers subsequently gave way, leaving 52 % of conflicting movements, where the pedestrian waited at the edge of a crossing area (courtesy crossing), until the traffic had moved on. Although most pedestrians treated the courtesy crossings like zebra crossings, most drivers did not treat them in this way; initially giving way in only 37 % of conflicting movements with a pedestrian intending to cross at the courtesy crossing.

Two shared space schemes in Aukland (NZ) have been analyzed in regarding multiple parameters of traffic flow and behavior and compared to measurements at the previous design. Nazla and Williamson (2012) find, that average driving speeds (motorized vehicles) dropped fairly consistently between 2-10 km/h after implementing the shared space.

In another redesign in New Zealand in 2014, Karndacharuk et al. (2015) show an increase in vehicle speeds between 5 and 12 km/h. Karndacharuk postulates that the increase in speed could have been induced with the significant reduction in vehicle volumes. He concludes that speed-reducing-measures are an important instrument to reach the overall goals of shared space.

2.3.2 Pedestrian Behavior

The scientific field of pedestrian modeling and simulation is primarily conducted to obtain design optimization in crowded spaces and evacuation dynamics. In pedestrian traffic flows in urban roads, the major aspect is the *crossing of the roads* profile. Path choice and interactions are topics of interest in transportation planning and road design. This section shows works done in analyzing and modeling pedestrians' behavior in shared spaces.

Moody and Melia (2014) observed and interviewed pedestrians at a shared space scheme in Elwick Square in Ashford, Kent (UK). Their findings show that pedestrians diverted away from their desire lines, gave way to vehicles in most cases and felt safer under the original road layout.

Bell (2008) describes mutual gap acceptance as a conditional probability depending on vehicle and pedestrian flow and gap size. For the probability of a pedestrian expected to take the chance to cross a street is:

$$Pr(accept_p) = Pr(gap_c > crit_p) = e^{-\lambda_c crit_p} \tag{2.1}$$

where λ_c represents the flow of vehicles [veh/s]. $crit_p$ is the critical gap size for pedestrians [s/ped].

On the other hand, the decision making of motorists to not yield to crossing pedestrians can be expressed in the same way using another notation including λ_p [ped/s] respectively. $crit_c$ for the critical gap sizes for vehicles [s/veh]. This "symmetrical" approach considering shared spaces is novel in literature. Deriving the pedestrian flow [ped/s] shows the dependency between the flows:

$$\lambda_p = \lambda_c e^{-\lambda_c crit_p} \tag{2.2}$$

The authors still leave open to what extent the pedestrians affect vehicle speed and how the pedestrian gap acceptance is affected by vehicle speed. Nevertheless, the result of such analysis can show ideal implementation constraints for shared spaces and support the design. Kaparias et al. (2010) fit a binomial multivariate logit model on the willingness of drivers to share space and apply a conflict analysis technique on the same matter (Kaparias et al., 2012).

Kadali and Vedagiri (2013) analyze details in gap size behavior of pedestrians in mixed traffic. An interesting finding is that the mean accepted gap sizes depends on the age of pedestrians. The mean values they find for *elders*, *middle* and *young* age groups in seconds are: 4.75, 3.35 and 3.5 respectively.

Wang et al. (2012) studies the pedestrian–vehicle interaction behavior in the urban street environment by micro–simulation modeling. They propose that the results can be used as a tool to supplement current guidelines for pedestrian related problems.

Daamen et al. (2014) observe and analyze pedestrian interactions and find that individual pedestrians perform movements that are related to interaction in 88 % of all occasions when they meet another pedestrian. These interaction movements consist of lateral and/or longitudinal evasive maneuvers to avoid a collision. A social behavior can be observed what the authors interpreted as some gallantry towards other pedestrians. Another interesting finding is that walking in a hurry increases the probability of passing in front of another pedestrian in crossing situations, as well as meeting a small group of two pedestrians increases the probability of passing from behind.

Teknomo et al. (2001) undertakes simulation experiments of pedestrian crowds crossing a road. He shows that a increasing number of pedestrians linearly reduces the average speed (in a range of 1.1 m/s to 0.9 m/s). The average speed of lane–based segregation is higher than a mixed lane. A higher number of pedestrians tends to increase the average speed difference between the pedestrians in the two distinct types of lanes. Increasing the number of pedestrians in a separated lane has a tendency to lessen the drop in the average speed.

In cities of developing countries, poor quality pedestrian infrastructure and inadequate transit services have led to the continued loss of mode share for walking and public transit trips. Nevertheless some examples show success of Bus Rapid Transit (BRT) systems in cities such as Bogota (Colombia) and Curitiba (Brazil), which have demonstrated that such trends can be reversed. King and Wright (2005) have done research on the nexus of high-quality pedestrian access and BRT systems as a mechanism to preserve the viability of public transport in developing cities. Besides the costs, he states that the aesthetics, comfort, directness, legibility, safety and security are major qualities which pedestrians transit infrastructure should show.

Children and Visual Impaired People

The ongoing debate about sense and risks of shared space always brings in the aspect about how visually impaired people and children are able to navigate, interact and decide in the changed road environment. Childrens' visual perception is limited and they have reduced abilities in estimating velocity and risks. Hüttenmoser (2009) claims that design models with an intended coexistence principles should only be implemented if they are successfully approved regarding their compatibility for children and physically limited individuals. Heinz (2006) offers favorable arguments by stating that in shared spaces, car drivers are aware of the increased danger of children playing in the area who might wish to cross the road. The fear of traffic on normal streets is also a powerful deterrent to allowing children to cycle to school or to play outdoors, especially in deprived neighborhoods, and can be positively influenced with road design measures like shared space. Childs et al. (2010) provide a further interesting aspect with the finding that 6 out of 10 of the interview respondents would go out of their way to avoid shared surface streets (44 %) or were very reluctant to use them (18 %). Havik et al. (2015) show in their survey that navigating in an unfamiliar shared space area is more complicated for visually impaired people than navigating in an unfamiliar, conventionally designed area. Preferred walking speeds of blind probands are consistently lower in shared spaces by approximately 25 %. Melis-Dankers et al. (2015, pp. 124) support the idea of creating "safe zones", "safe spaces" or "comfort spaces" for pedestrians to avoid this potential problem.

2.3.3 Cyclists Behavior

Shared space is thought to support transportation policy's increasing active mobility and to shift the modal share from driving cars to walking and cycling (Hamilton-Baillie, 2008, p. 137). It seems that the presence of cyclists is an important mediator between vehicles and pedestrians. If the design tends to strongly mix pedestrians and cyclists then evidently more frequent conflicts within these two traffic subsystems in Drachten and Haren (NL) can be observed (Gerlach et al., 2009, p. 10). Even in conventional road design, this circumstance is already considered in planning tools like the Multi Modal Level of Service (MMLOS) model methodology. This approach measures the degree to which the urban street design and operations meet the needs of each major mode' s users (automobile, pedestrian, bicycle, and public transit). Transportation research on bicycle safety issues seems to outnumber other aspects of cycling. Summala et al. (1996) empirically investigated cyclists' behavior when changing direction. The outcome shows that drivers develop a visual scanning strategy which concentrates on detection of more frequent and major dangers, but which ignores and may even mask visual information on less frequent dangers. This correlates with other generic traffic perception theories. The analysis and PhD thesis of Duncan (2016) indicates that cyclists rode similarly through both shared and control intersections, and lists a number of infrastructure elements that influence a riders path choice.

2.3.4 Public Transport

Mixed-mode streets are being proposed as a solution to local traffic and land-use problems. In his study, Zacharias (1999) describes a de facto mixed-mode street in Amsterdam with relatively high traffic volume. He determines how the modes and directions are accommodated. Nickel (2009) states in his work that the shared space philosophy might collide with public transport' s need for prioritization and for barrier–free access at the bus–stops.

Neither the effect to public transport, nor the requirements for a microscopic model design for buses and trams are within the focus of this thesis. Nevertheless, a minor empirical study has been done in observing bus–trajectories at the square of Sonnenfelsplatz in Graz (Austria). The results are given in the appendix in figure 8.10 - it shows similar empirical findings as the data analysis of passenger car flows. The following qualitative conclusions might be drawn:

1. Regardless of the slightly lower number of crossing pedestrians, it appears that pedestrians choose their path and timing of crossing in a manner that less disturbs the buses' movements.
2. Length of buses' path decrease in the intersection.
3. Turning radii increase.
4. Path trajectories are optimized according to the origin and destination at the square.
5. A blockage of the traffic in the square is within the new design more unlikely as the size of the center area of movement grew.

A picture taken in 2012 at Sonnenfelsplatz in Graz (2.3) underlines the smaller turning radii and the easier solving of deadlocks between the public buses.

In planning and in modeling, the design of the bus stop has to be considered. The low-level boarding of the buses requires curbs to the side areas in the segment of the bus stop station. An obstacle for all vehicles hereby created and therefore, the profile appears segmented.

2.3.5 Norms and Traffic Regulations

The regulative basis of traffic behavior has been shaped over many decades and is defined in national laws and normative texts. This section is dedicated to the regulations

Figure 2.3: A public bus can use a more direct path at turning left and covering the center design element in the shared space Sonnenfelsplatz (own photo, 2012).

regarding shared space and will briefly discuss the major issues. Even though shared space is not manifested in the traffic regulations it is of course in accordance with the traffic regulations in Austria (Füreder and Schwab, 2009) and Germany (Gerlach and Ortlepp, 2010). In Germany, an even stronger normative protection of pedestrians is given by the regulation of traffic calmed areas ("Verkehrsberuhigter Bereich") according to the essential aspects:

- Pedestrians may use the whole profile of the road
- Drivers have to adapt their driving speeds to the surrounding situation
- Drivers may not endanger or interfere with pedestrians
- Parking is not allowed outside of marked areas

The regulations of these characteristics may not be appropriate to roads outside residential areas; therefore, other concepts have to extend to the range of traffic designs for shared space streets.

One might see the intentions of shared spaces already in the first paragraph of the German traffic regulation: §1 StVO[2] (Thiemann-Linden, 2008). Here, traffic flow definitely follows certain rules, even though to describe their flow the regulative rules do not fully cover specific needs (Keuninginstituut and Senza Communicatie, 2005).

The construction process and its approval by authorities is defined in traffic regulations and other relevant laws. Kettler (2010) describes the juridical path during construction

[2]The German traffic regulations §1 StVO includes the fundamental regulation that 1. The participation in road traffic requires a permanent awareness and mutual respect and 2. That every road user has to act in a way to not harm or endanger any other individual and not to constrain or disturbed them respectively.

of shared spaces. The technical regime is reduced, nevertheless the regulative framework has to be fully considered.

Popitz et al. (2006) defines social norms or regulations as a behavior that one can expect for future actions. It is in accordance with specific behavioral norms and is connected with the risk of being sanctioned in the case of divergence. Behavioral attributes like "normal" or "conform" for instance, are only valid in a specific place or in a specific context. Traffic regulations intends to harmonize the population' s behavior by education, driving training and daily traffic. Still, many variations and aspects can be observed, which will be covered in later chapters.

Ignoring the perceptual, social and physical variations and constraints, the full behavioral processes can be described following the traffic regulations. This section analyzes the relevant paragraphs of the road traffic regulations. The focus lies on the Austrian traffic regulation and in a systematic manner all paragraphs are extracted that seem relevant in the shared space philosophy and its practical implementation. The paragraphs within the law are analyzed using interpretive literature (Grundtner, 2017) regarding their:

1. Relevance within traffic flow
2. Relevance for shared space
3. Distinguishing road user classes

Parsing the law texts provides a list of the relevant generic traffic regulations that address:

- Driving on the right side / lateral safety distance
- A square (intersection) is a virtual extension of the road
- The use of sidewalks is mandatory for pedestrians
- How to evade other road users
- Turning (signs, etc.)
- Behavior when overtaking other vehicles (speeds, keeping distance, left or right)
- To pass other vehicles
- Car following (distance)
- Priority rules
- Driving speeds
- Reducing driving speeds
- Children
- Behavior of cyclists
- Behavior of pedestrians

These major items could form the essentials in a general requirement setup for designing microsimulation models. From a planner's perspective, the guidelines for road design[3] do not explicitly define shared spaces and their varieties. The guidelines recommend road attributes according to the traffic demand and role within the network (Forschungsgesellschaft Strasse, Schiene, Verkehr, 2004, 2001), i.e. the "mixing" of traffic modes is not seen as suitable above a flow of 7000 motorized vehicles/day.

[3] In Austria, these handbooks are covering the planning, construction and maintenance of roads and have no legal status.

When observing real traffic flows, it seems that behavioral studies in literature of social science and normative behavior are relevant as well. The next sections therefore focus on these topics.

2.3.6 Social Strategies

Here the social behavior describes the human factors when making decisions about speed and yielding behavior when moving through shared spaces. Starting from the early days in this scientific field, the first theoretical frameworks regarding social interactions within populations are found - dating back to von Neumann and Morgenstern (1953). Cooperative and competitive paradigms have been discussed further in other game theoretical approaches such as in Luce and Raiffa (2012); Hamilton and Axelrod (1981). A more generic model is developed by Helbing (1998a). He distinguishes between three different kinds of pair interactions:

1. Imitative processes, which describe the tendency to imitate the behavior of another individual.
2. Avoidance processes, causing an individual to change her or his behavior if meeting another individual with the same behavior.
3. Compromising processes, which describe the readiness to change the behavior to a new one when meeting an individual with another behavior.

At first glance, it seems inappropriate in a road traffic conflict process to speak of avoidance processes of social behavior. Nevertheless the imitative and the compromising aspects provide a promising relationship and therefore adopted in a very generous manner. By classifying the observed interactions, Helbing (1998a) proposes the following considerations regarding possible rule sets:

1. Defensive regimes fit to both other defensive and ignorant other behavior.
2. Evasive strategies might fit to all other under specific geometrical circumstances.
3. A pair of ignorant strategies would lead to heavy conflicts or accidents and is empirically hard to observe.

What can be considered, are mixed strategies of all combinations as well as dynamic adaption during the interaction. The idea behind shared space strives to include social considerations in its tactics and decision making. This topic is poorly discussed in modeling research and will be highly prioritized in this work.

Links between group sizes of road user groups (i.e. group of pedestrians or a fleet of cars) seem also to be relevant to traffic flow. In their model, Rinke et al. (2017) already differentiates between single road users and groups of road users on a tactical level.

2.4 Traffic Models

The reasons for traffic simulations lie in the estimation, optimization, prediction and understanding of vehicular or pedestrian traffic. Performance parameters, environmental issues and safety indicators (Archer, 2005) can be calculated to develop and improve road infrastructure design, traffic control or advanced Intelligent Transport Systems (ITS) measures. For instance, impacts to network capacities of events can be predicted by feeding data to traffic management systems. Underlying traffic models are often classified in a hierarchal structure, describing all levels of detail. This categorization can be operationalized by distinguishing traffic entities and the physical or behavioral description levels. Hoogendoorn and Bovy (2001) propose the following classification:

1. Submicroscopic simulation models: High-detail description of vehicles mechanics, drivers' perception, environmental conditions (i.e. weather, road surface)
2. Microscopic simulation models: Distinguished individual behavior and its variance
3. Mesoscopic models: Medium detail
4. Macroscopic models: Cumulated level (low level of detail)

In **submicroscopic models**, vehicle physics, steering and perception issues are described. Dynamic equations describe dependencies between friction, gravity, traction and lateral forces as well as the vehicle, its components and its environmental system. While in common use in Intelligent Cruise Control (ICC), (van Arem et al., 1997) and in combination with traffic simulation (Yannis et al., 2004) in traffic flow research submicroscopic simulation models gain benefits for causal understanding of driving behavior. Samoili et al. (2011) identify significant different headway parameters in a car–following model and claim, the increase to be a consequence of compensating for the lower skid resistance in rainy conditions. Munehiro et al. (2011) even provide equations considering the physical longitudinal skid resistance coefficient. Here, it might not improve the overall simulation quality.

Microscopic simulation of traffic is a modeling technique that operates on an individual vehicle level in a way that enables the user to distinguish the different units and observe their interactions with the infrastructure and with other units. Vehicles are represented by unique identifiers and a set of associated attributes e.g. origins, destinations and operational characteristics. The field of applications is traffic control and optimization, impact analysis of intelligent management technologies and information systems or incident simulations. Recent efforts focus on safety aspects. In particular, studies have confirmed that the reproduction of user behavior by simulation under different conditions can identify the incident hazard potential. Astarita et al. (2011) show possibilities of empirical validation due to comparing non-crash indicators, as there are crash potential indexes, deceleration rates to avoid crashes and maximum available deceleration rate and Time to Collision (TTC).

Mesoscopic models normally describe traffic entities in great detail, but behavior and interaction are described in less detail. There are different approaches to solving this mechanism. Usually several vehicles are grouped into cells which have the properties of all vehicles and their steering behavior. Another possibility is to divide a road into cells which may or may not be occupied by vehicles. The determination of behavior rules is minimal, while only the number of cars crossing the cells is recorded. The main application area of mesoscopic models is where the detail of microscopic simulation might be desirable but infeasible due to a large network, or limited resources available to be spent on the coding and debugging of the network.

Macroscopic traffic models are used to examine whole networks. They describe events in entire regions or countries. Only the traffic flow from one cell to another cell can be observed. The number of vehicles crossing the boundaries is calculated for every time interval. This number depends on how many vehicles the cell of origin can send and the destination cell can receive. The discrete units cannot be accounted for. Because of the aggregation level, macroscopic models do not suffer from high computation requirements; although accuracy is impaired by the already aggregated input data. For these reasons macroscopic traffic models are generally used for research on traffic demand and traffic forecasts. In this aggregation level, distinguishing such systems into static route assignment models, vehicles follow their selected initial route, which is on a fixed course through the network until the destination is reached. Vehicles cannot decide whether to take a shorter or more efficient way or not during their trip, whereas in dynamic models, it is possible to reassign a route during the journey. The decision takes into account changing circumstances during travel time.

Multi Agent Systems

A Multi Agent System (MAS) is used in a wide number of areas and has the ability to cope with a high variety of representing "individuals" ranging from *reactive* agents to *cognitive* agents (Drogoul et al., 2003). Based on the theory, a MAS is an algorithmic system composed of multiple interacting intelligent [4] agents within an environment. A MAS can be used to solve problems that are difficult or impossible for an individual agent or a monolithic system to solve. Like traffic participants, the agents perceive merely small parts of their environment and react according to pre-established rules (Bazzan et al., 1999). Therefore, the infrastructure exists mainly as a perceptual model from an agent's perspective.

Deterministic versus stochastic models

In a deterministic traffic model, the results of every cycle under the same circumstances are identical. On every simulation run, the same vehicles are at the exactly same position in the network at the same time like on previous simulations and also in subsequent ones. In stochastic models, however, each simulation run usually yields different results due to changing variables, which are often generated randomly. Stochastic models are defined by continuously changing variables. These can be the number or properties of vehicles, weather circumstances, incidents, etc.. In discrete models however, variables change excursively if certain events or moments occur.

Many observed phenomena in traffic flows are modeled using physical analogies, statistics and parameterized or non-parameterized functions. Papageorgiou (1998) structures the mathematical approaches as following:

1. Purely deductive approaches - accurate physical laws are applied.

[4] Intelligence may include some methodical, functional, procedural or algorithmic search, find and processing approach.

2. Purely inductive approaches - empirical data from the real world are used to fit mathematical structures.
3. Intermediate approaches, whereby first, the basic mathematical model-structures are developed, after which a specific structure is fitted using real data.

The design of this thesis is shaped in a way that it will merely fit the third approach in this list. Both the empirical data and the model results will deliver trajectory data of the agents. In the next sections, therefore, the microscopic modeling is further reviewed.

Model Building Process

The framework of the modeling building process considers both static and dynamic elements. According to Barceló (2010, p. 4), a model building process can be structured in the following way:

1. Elements of structure describing the physical environment includes the road's structure, buildings, obstacles and their properties.
2. Elements of processes consider activities and all time related changes.
3. Relationships between structure and processes describes the interrelation between the static situation and the dynamic aspects.

The created system relies on inputs and outputs and is defined by boundaries, subsystems and internal processes.

2.5 Microscopic Modeling of Mixed Traffic of Different Types

Multiple approaches have been published in the last decades, even including molecular dynamics (Bando et al., 1995). The most popular microscopic traffic flow models are based on sets of differential equations. Amongst them is Helbing (2001), it includes the stimulus response model (equation 2.3). It is based on the assumption that the net distance is given by the velocity influenced safe distance $s^*(v_\alpha = s' + Tv_\alpha)$. T means a head up clearance safe time:

$$\frac{dv_\alpha(t + \Delta t)}{dt} = \frac{1}{T}[v_{\alpha-1}(t) - v_\alpha(t)]. \tag{2.3}$$

The left term side represents an agent' s (α) response to the stimulus trigged by the speed difference to the leading agent $\alpha - 1$. To include non-perfect driving behavior (and therefore showing observed density waves on highways), a delay time of $\Delta t \approx 1.3s$ reduces the response' s agility.

Other techniques are coupled maps (Gipps, 1981), extended in Krajzewicz et al. (2002) and Gloor et al. (2004), Cellular Automata (CA), classical queue models and approaches where vehicles are moved according to fluid-dynamic equations (Flötteröd and Nagel, 2005). Microsimulation of traffic offers an agent based modeling of pedestrians, vehicles, driver behavior and the interaction between each other and with the surrounding infrastructure. Teknomo (2002) divides the microscopic traffic modeling approaches into three categories: cell based, physics-related analogies (solid state physics, from fluid dynamics to mechanic forces) and network graph orientated. By modeling pedestrians, Helbing (2001) presents an overview of the most important research in the field.

2.5.1 Car Following Models

In one-dimensional models, the network is represented as a closed graph including vertices and nodes where multiple links connect and intersect. The traffic flow functions are car-following, lane changing and deterministic rule sets at intersections. The history of those techniques dates back to Reuschel (1950) and Pipes (1953). Pipes assumed that the follower wishes to maintain a certain safe time headway from the leading vehicle. Using Laplace transformations, he developed theoretical expressions for the subject's acceleration.

Chandler et al. (1958) publishes the General Motors - model framework by introducing the stimulus-response principle. According to this framework drivers react to stimuli from the environment. The response they apply is delayed to account for reaction time:

$$response_n(t) = sensitivity_n(t) * stimulus_n(t - T_n) \tag{2.4}$$

In terms of vehicle control, the response is represented by the acceleration $a(t)$ of the following vehicle:

$$a(t) = \alpha * \Delta V_n(t - T_n) \tag{2.5}$$

where the following vehicle is delayed by the reaction time T_n and the relative speed ΔV_n. With respect to the vehicle ahead, α is the driver's sensitivity towards the perceived stimulus. The model was later modified to a nonlinear form after incorporating spacing and speed into a sensitivity term.

Today's research tools (van Arem et al., 1997) and commercial microscopic multi–modal traffic flow simulation software packages like VISSIM[5], AIMSUN[6], and Quadstone Paramics[7] use extended psycho-physical dynamic models. The most famous theoretical base for car-following was introduced by Wiedemann (1974), followed by many more in the recent centuries, i.e. Fritzsche (1994).

In 2002, Treiber and Helbing (2002) introduce the Intelligent Driver Model (IDM), which includes a term of free flow driving $a_f(v) := a[1 - (v/v_0)^\delta]$ and another term for controlling the following of another car $a_{int}(v, s, \Delta v) = -a[s^*(v, \Delta v)/s]^2$. v_0 is the

[5] Verkehr In Städten - Simulations Modell (VISSIM) is a product of PTV Planung Transport Verkehr AG, Karlsruhe, Germany (developed since 1992), i.e. in Fellendorf and Vortisch (2001).

[6] Adv. Interactive Microscopic Sim. for Urban and Non-Urban Networks (AIMSUN) is developed and marketed by TSS - Transport Simulation Systems, Barcelona, Spain (first prototype in 1989), i.e. in (Barceló and Casas, 2005).

[7] Quadstone Paramics is a product of Quadstone Paramics, UK (since the early 1990s), i.e. in (Cameron and Duncan, 1996).

desired free flow speed and s_0 is the minimal distance to the leading vehicle. The full IDM equation is:

$$\dot{v}_\alpha^{IDM}(v_\alpha, s_\alpha, \Delta v_\alpha) = a[1 - (\frac{v_\alpha}{v_0}) - (\frac{s^*(v_\alpha, \Delta v_\alpha)}{s_\alpha})^2]. \tag{2.6}$$

The interaction to the leading vehicle is given with s_α and an effective desired distance $s^*(v, \Delta v) = s_0 + Tv + \frac{v\Delta v}{2\sqrt{ab}}$, where T is the temporal safety distance and a/b is the maximum acceleration / deceleration. The authors claim that the continuous acceleration function of a reasonable number of parameters and the high driving stability make the IDM suitable for driving assistance systems and control. Applying IDM on Automatic Cruise Control (ACC), Kesting et al. (2010) show a realistic generic behavior. Limitations arise at the simulation of lane changing in dense traffic situations and other incidents, which can cause irregularities in traffic flow.

Public Transport and Car Following

Microsimulation of public transport is a widely used approach for optimizing priority configurations using VISSIM (Ngan et al., 2004; Fellendorf and Vortisch, 2010; Ahuja et al., 2003) and other software packages (Currie et al., 2007; Barceló et al., 1999) or to predict delays in real time (Abdelfattah and Khan, 1998; Lee et al., 2005) to feed to online traffic management services. Effects on modal travel speeds, environmental issues (Wegener, 1996) and reliability can adequately be estimated. Recently, the interaction in transit processes and the interaction of pedestrian flows and buses, trams or metros grew. Commercial packages like VISSIM have some options to simulate transit systems (Galiza et al., 2009) in order to evaluate and maintain a desirable pedestrian related Level-Of-Service (LOS), idle times at loading procedures and even evacuation dynamics. Other teams develop similar techniques using PARAMICS' Application Programming Interface (API) (Cortés et al., 2007) to simulate the different aspects of a realistic public transport system.

2.5.2 Cellular Automata

CA discretize the space into a grid and describe the agent's movements through explicit models of the transitions between the cells. The transitions depend on the actual states of the cell, which can be occupied or free (Helbing, 2001). Mallikarjuna and Rao (2009) give an excellent introduction to CA and literature in the application for heterogeneous traffic modeling. In Nagel and Schreckenberg' s approach (Nagel and Schreckenberg, 1992), interactions between vehicles, road and drivers were considered implicitly and applied on two lane, directional highway traffic. Even though their model could not reproduce all the empirical traffic characteristics, it was able to reproduce the trends observed in real traffic. Meanwhile, multiple evolutions of the model extended its applicability to network traffic flows (Simon and Nagel, 1998). Blue and Adler (1999) show both realistic microscopic behavior and reasonable aggregate simulation outcomes in modeling bi-directional pedestrian walkways. Keeping the basic structure of CA intact, an attempt has been made to utilize its efficiency in modeling complex systems, for heterogeneous traffic. Burstedde et al. (2001) gives examples, while Lan and Chang (2005) demonstrate CA' s capability to model heterogeneous traffic of cars and motorcycles. The aspect of heterogeneity is considered by using different numbers of cells and stochastic CA rule sets. Yi et al. (2007) model the stochastic and deterministic behavior on a cross walk using CA. An interaction model represents pedestrians that are ignoring the red light during situations of low traffic-densities.

Zhang and Chang (2011) propose a simulation model integrating the strengths of the CA method with some probabilistic functions, offering a realistic mechanism to reflect the competition and conflict interactions between vehicle and pedestrian flows. Their experimental results clearly indicate that failing to account for the impact of mixed flow interactions in a congested traffic system could result in a gross underestimation of the delay, travel time, and system throughput. Lee (2007, p. 52) discusses the model constraints regarding interaction and lateral behavior.

2.5.3 Benefit Cost Cellular Models

The area of movement is divided into a square grid and the agents are simulated as a particle in a cell (Teknomo, 2002). Gipps and Marksjö (1985) came up with this approach for pedestrians. Each cell can be occupied by only one agent and a score value is assigned to each cell based on other agents' proximity. This score represents the repulsive effect of the nearby agent and has to be balanced against the gain made by the agent in moving toward his destination. An initial score value is given to each cell occupied by a pedestrian and an adequately lower value is assigned to cells with a side in common (edges are rated even lower). The score of the surrounding cell of an agent is approximately inversely proportional to the square of the separation of pedestrians in two cells as shown:

$$S = \frac{1}{(\Delta - \alpha)^2 + \beta} \tag{2.7}$$

where S represents the cost score of a cell k related to agents or objects. Δ is the distance between cell i and the agent. α is a spatial constant, slightly less than an agent's diameter. Parameter β strengthen the effect of closer agents.

2.5.4 Continuous two Dimensional Models

Arasan (2005) uses a continuous model space including heterogeneous vehicle parameters. For every vehicle, all interactions with other agents affect their acceleration and direction of movement. Vehicle dynamics are simplified. The interactions are constrained to straight sections while interactions on junctions are not modeled. Later, Arasan' s model HETEROSIM for simulating heterogeneous traffic flow could be positively applied to study effects of bus lanes (Arasan and Vedagiri, 2008).

Similarly, Oketch (2001) introduce a new modeling approach that was suitable for a heterogeneous road traffic. Furthermore, they developed a detailed lateral movement model including both longitudinal and lateral movements of vehicles. Using this model, Oketch (2003) later propose theoretical performance characteristics for heterogeneous traffic and observed that the traffic flow behavior in heterogeneous flow might not be consistent with the fundamental relationships on which the macroscopic analysis is based.

Focused on motorbikes, Lee (2007) develops a package of models to describe motorcycle movements:

1. A longitudinal headway model focus on describing the phenomenon that a motorcycle will maintain a shorter headway when aligning to the edge of the preceding vehicle.
2. An oblique & lateral headway model describes the headway distribution of motorcycles when they are following the preceding vehicles obliquely.
3. A path choice model represents the dynamic virtual lane-based movements of motorcycles using a multinomial logit model.

Within a simulation framework, Lee shows that the model fulfills the requirements and represents the main characteristic behavior patterns of motorcycles. Many attempts were made in the 80's (Raghava Chari and Badarinath, 1983; Ramamayya, 1988) to develop a modeling approach for heterogeneous traffic.

Another approach has been published in the field of control and autonomous driving. Widyotriatmo and Hong (2011) transform the position and orientation information of individual vehicles to navigation variables. This includes the remaining distance to the target coordinates, the angle made by the orientation of the vehicle at the goal position, the vehicle-to-target (v-to-t) vector, and the angle made by the heading direction of the vehicle and the v–to–t vector. Similarly, Makarem and Gillet (2012) apply the technique to one–dimensional paths and show the capability of solving interactions using vehicle to vehicle communication.

2.5.5 Force-Based Models

The modeling of motion in road traffic through "force fields" was first brought up by Henderson (1971). He simulated pedestrian flows based on fluid dynamics. The characteristics of this model are the lack of individual choices and an external force field. The following analogies can be identified:

- Motion patterns are similar to flow lines
- At border lines of counterflows, "fringing" is observed, called "vicious fingering"
- With pedestrians of equal walking direction, the forming of bulks can be observed, similar to stratification phenomena in granular materials
- In "bottlenecks", the flow oscillations in regions of equal densities can be observed, which show homogeneous internal characteristics

This model of low complexity cannot explain the following human behavior: Individual background and parameters of pedestrians as groups, desired speeds and desired distances. Therefore, they are not considered.

Helbing's and Molnar's Social Force Model (SFM) (1995) describes the impact of social and technical interaction of traffic dynamics by establishing fields of force in road spaces similar to physical models in Newtonian dynamics. This approach allows the detailed modeling of interactions between road users and infrastructure. Social force models are using analogies to Newtonian mechanics and let the infrastructure and the agents emit individual force fields. An agent's acceleration is modeled as a function of the inbound force vector in the simulation environment. Since then, this approach was enriched with anisotropy orientation, velocity components and performance increasing algorithm designs. It is popular for simulating pedestrians, although the application for vehicle flows dates back to 1998 (Helbing, 1998b).

The energy to allow pedestrians (and vehicles) to move is defined as the driving force $\vec{f}_\alpha^{\,0}$ which motivates the agents to maneuver to a target in the road network at the desired velocity v_α^0:

$$\vec{f}_\alpha^{\,0} = \frac{v_\alpha^0 * \vec{e}_\alpha^{\,0}(t)}{\tau_\alpha} - \frac{\vec{v}_{\alpha(t)}}{\tau_\alpha} \tag{2.8}$$

where $\vec{e}_\alpha^{\,0}(t)$ represents the desired direction and $\vec{v}_\alpha(t)$ is the actual speed of agent α. In equation 2.9, the desired direction is given by the actual position of the agent $\vec{x}_\alpha$ and the destination position $\vec{p}$.

$$\vec{e}_\alpha^{\,0}(t) = \frac{\vec{p} - \vec{x}_\alpha}{\|\vec{p} - \vec{x}_\alpha\|} \tag{2.9}$$

Based on this work, many papers have been published. For instance, Delpiano et al. (2015) derive a five-parameter social force car-following model that converges to the "kinematic wave model" with a triangular fundamental diagram.

2.5.6 Route and Path Choice

The route choice describes the strategic choice of finding the way through the road network, while the path choice addresses the tactical decisions within the actual road section. Especially in the field of pedestrian evacuation dynamics, the methods have been developed and validated. Multi-objective routing can combine the quickest and shortest path alternatives. Kretz (2009) manipulates the flood fill dynamic potential field method with decreasing cell values which are presently occupied by other pedestrians to demonstrate the effect of a quickest path choice. With every pedestrian's move, a probability is assigned to each cell he or her could reach and then a destination cell is selected according to these probabilities. Most influences on an agent's motion are modeled as partial probabilities. A common way to describe the influences on the agent's motion follows an exponential function:

$$p_X = e^{k_X * func(X)} \tag{2.10}$$

using k_X as a coupling constant, denoting the strength of the influence $func(X)$.

Pedestrian route choice is a complex-, situational- and population-dependent issue: Gräßle and Kretz (2008) observe seemingly irrational, or at least unexplainable behavior in non-daily life situations.

Asano et al. (2007) have developed a perception based approach with maximizing the walking distance of pedestrian i toward the direction Θ_m, which is denoted by $L_i^j(\Theta_m)$ and is calculated subject to this constraint. Figure 8.11 (in appendix) shows the setup for this calculation, which is made for every direction $\Theta_m \varepsilon \Omega$. The optimum direction Θ_{opt} is determined in a way to maximize the walking direction toward the desired direction φ_d as follows:

$$\Theta_{opt} = argmax_{\Theta_m \varepsilon \Omega}(L_i^j(\Theta_m)cos(\Theta_m - \varphi_d)) \tag{2.11}$$

2.5.7 Bicycles in Traffic Flow Models

As a matter of fact, traffic flows in bicycle traffic (at common traffic densities) depend not as critical on travel speed as in motorized traffic. Although case studies including bicycle flows using VISSIM exist (Mosseri et al., 2004), little research has been done on behavioral analysis of cyclists. At the physical level, linear and nonlinear approaches to modeling bicycles and their steering has been done for a long time (i.e. in Whipple (1899); Limebeer and Sharp (2006)). Research about bicycle path–following using an adequate control algorithm can be found in (Sharp, 2007) or (Åström et al., 2005). Raksuntorn (2002) develops a microscopic bicycle model and introduces a generalized linear modeling framework. He develops a set of equations that represent the initial acceleration and deceleration of bicyclists, bicycle following and the turning speed of bicycles.

2.5.8 Visualization Issues

Visualization is able to provide essential insights during the model design and implementation processes. Agents' perception, internal processes and actions can be viewed and its dynamic observed. On the other hand, a highly sophisticated visualization is often used to overcome technical shortcomings. Traffic simulation can support the planning process from its strategic level to the planning of detail. While for the visionary part, a mere animation can be quite useful, because for the estimation of speeds and impact to the network, a valid model is necessary. Tonndorf and Vorotovic (2007) describe functionality and design options based on projects developed in VISSIM. In a practical approach they demonstrate the methods and functionality applied in micro simulation in two London, UK regeneration schemes, being "Borough High Street" and "Exhibition Road". However, the application provides state of the art visualization (figure 8.7 in the appendix), which is useful in the planning process because there is no generic continuous model available to properly model the behavior. Instead, the VISSIM' s priority functionalities are used. Nevertheless, it might have fulfilled its purpose of pure visualization for the shared space implementation.

2.6 Conclusion on the Background

Shared space is a road design concept that is being implemented in increasing numbers. Examples of shared space differ from each other because of the big variety of local conditions, design elements and traffic mixes. The philosophy inherits a high experimental potential. This makes it extremely difficult to show the effects of a planned shared space with the currently available tools. Different topography, complex traffic situations and a wide variety of design elements are a great challenges for planners. Behavior analyses in case studies confirm that the intended goal of remixing the traffic at a specific area is reached (i.e. in Schönauer et al. (2012c)). However, it is still hard to conclude which specific elements helped to achieve the effects, which makes it difficult to assess the impact of potential future shared space projects. Therefore, a realistic shared space simulation is proposed, which could help in the planning phase for future projects. A simulation model allows the planners to test the effects of different design elements during the concept phase - before they are implemented:

- Addressing capacity concerns
- Determining potential bottlenecks
- Improving safety and comfort

It also is suitable to illustrate the traffic flow in a planned shared space to citizens, politicians and stakeholders. A clear quantifiable visualization about how the new road design would work can be provided. While there is no combined simulation tool for shared space, many applications of microscopic simulation for a single mode exist in scientific literature. These are useful starting points for a shared space simulation model. Physics-related analogies like social force models exist for pedestrian flows and cars (Helbing and Tilch, 1998). These models provide a good foundation for handling basic interactions between agents from the same mode of transport. Therefore, the work in this thesis is largely based on the model suggested by Schönauer and Schrom-Feiertag (2010).

Less research has been performed on the interaction between individuals using different modes. Most current publications dealing with conflicts between pedestrians and cars concentrate on a rule based approach, where the Right Of Way (ROW) is given by the infrastructure, e.g. a pedestrian crosswalk (Bönisch and Kretz, 2009). Cars give way to pedestrians within a certain area close to the crosswalk. Kaparias et al. (2010) are one of the few references which explicitly researches social interaction by fitting a discrete choice model on the willingness of drivers to share space with pedestrians according to different input factors. Other examples of interactions between different modes include the merging behavior of cars and motorcycles that relies on the fact that motorcycles can fill the spaces left by cars. However, there are still missing pieces in linking specific design elements to the behavior of people. Therefore, a new infrastructure model is incorporated into a microscopic traffic simulation. Furthermore, this thesis presents a vehicle model and an underlying game theoretic tactical model that can deal with the social interactions happening in a shared space environment.

3 Model Definitions

The first part of this chapter (section 3.1) expands upon the literature and defines the requirements of the model. The structure of the required framework and sub-models are defined in the second section (section 3.2 to 3.5).

3.1 Model Requirements

Due to the complexity of infrastructural topologies, traffic demand, and characteristics of the interaction processes, a traffic flow model for shared spaces has numerous requirements that must be defined and fulfilled. The technical setup (editor, models, and graphics) requires additional aspects in the design of the model and architecture of its implementation. This chapter first describes the extended form of the social force approach and its application to mixed traffic. An infrastructure model, an interaction model, and vehicle mechanics models are then implemented and discussed. Finally, both the external and intrinsic (technical) model requirements are described. From the perspective of a potential user, an overview of relevant aspects and a rating of each of this aspects is given in the appendix (table 8.4 in the appendix).

3.1.1 Requirements towards the Infrastructure Model

This section lists the elements that matter in the shared space paradigm. The list includes all elements necessary to define the design and shape of a shared space site as well as the role and its impact in the surrounding network.

Road network

A review of shared space designs that have already been implemented shows that they have been applied in through-roads, residential areas and town centers. Table 8.3 in the appendix shows a selection of the first shared space designs in Europe. Aside from the distinct intent to calm vehicular traffic and improve aesthetic appearance, road topologies cover a wide range of possible needs. Shared spaces are implemented at roads and squares of different scale and capacity. A simulation model must therefore be capable to consider any possible arrangement of road sections, junctions and associated side areas. Since shared space includes the presence of pedestrians and cyclists by definition, the area of application can be restricted to roads in urban or residential areas. Bidirectional highways are excluded in the model. It is worth noting that mixed road traffic in Asia might include multi-lane bidirectional roads. Nonetheless, they are not considered in the model.

Design elements

Different design elements affect traffic behavior and flow in many ways. For instance, road users maintain a distance from poles, hedges, and trees. Benches are not only obstacles, but also a point of interest. Curbs, grassy areas, and trees, all serve to separate and guide traffic. Different sidewalk colors influence traffic behavior in a more subtle manner. All these elements of road topography influence the route chosen through an area and towards a destination. Points of interest like shops and benches attract road users. Given the vast number of the different design elements - such as those outlined above - an accurate analysis of the effects of the elements on the traffic behavior and on the interaction between road users is called for. In physical terms, the objects are described by their shape and attributes, and their influence on driving and walking. It should also be considered that objects below a certain size cannot simply be represented in the model by their base area because the spatial resolution is constrained to maintain a certain level of processing performance during the simulation. For example, common steel pipe bollards have diameters of approximately 0.1 m, but have an enormous leading effect on vehicular traffic.

Origin and destination points

The most common origin and destination points for all road users are at the borders of the planning area where they enter and exit the shared space (and the simulation). Within that area, different road users are attracted to different points of interest. For instance, important points of interest for vehicles are parking facilities. Cyclists not only use cycle stands but also poles for parking. Public transport stations and stops are origin and destination points for both vehicles and for pedestrians. Building entrances are the primary origins and destination of residents. Shops and restaurants are origin and destination points for pedestrians and cyclists. Some elements such as shop windows attract people. They are also origin and destination points and invite people to stay for a while.

Prioritization

The vast number of design elements and heterogeneous traffic makes it necessary to identify the most relevant factors that should be included in the simulation. The assessment criteria used here include occurrence, relevance, and data availability:

- **Occurrence** describes the frequency of certain road users and design elements in existing shared space areas. If a certain type appears often, it is important that it is represented in the simulation. Elements seldom found in shared spaces are excluded.

- **Relevance** refers to the impact of elements and its diversity. Some different elements may influence traffic flow in a similar way, and can thus be simulated as one.
- **Data availability** is included for a pragmatic reasons: Even if an element occurs often and affects the traffic flow, it cannot be simulated if there is not enough available data.

These criteria are applied to road users, to design elements, and to origin-destination relations. The criteria are aggregated to the criterion of **priority**. This priority indicates the importance for the element to be represented in the simulation model and can show "cultural peculiarities". For the area analyzed in Austria, based on the above criteria, the priorities of road users are cars, bicycles and pedestrians. The most important design elements in the Sonnenfelsplatz are obstacles like bollards, benches, green areas and side areas where pedestrians feel safe. The origin-destination relations used in the simulation should be based on empirical observations.

3.1.2 Requirements towards the Infrastructure's Perception

This section is about human factors in vehicle steering and control and addresses lateral behavior on the tactical and operational level as well as speed choice.

Distance to the road boundaries

While the chosen distance to the right edge of roadway depends on actual speed, drivers tend to keep a minimal distance. Case et al. (1953) report the findings of a study on effect of a roadside structure (a barrier) on the lateral position of the driver. The authors major conclusions are:

1. Driverss reactions to the distance of the barrier to the vehicle are greater than their reaction to the size of the barrier; however, it is expected that drivers give a higher priority to collision avoidance with other road users.
2. Maximum driver reaction occurs farther from a barrier when the barrier is placed closer to the road.
3. Even under minimum size and distance conditions, drivers pulled over an average of 0.13 m.

Knoflacher and Schopf (1981) analyzed the results of a controlled experiment with three different drivers and found a squared interdependency, demonstrating the interdependency of speed and lateral position. In numerical terms they found (values rounded):

$$v = -0.005 * R^2 + 1.5 * R + 7 \tag{3.1}$$

This is valid for $0.1m < R < 1.2m$, where R is the remaining width in cm and v the vehicle speed in km/h. This relation brings to mind previous research in basic force models where actual velocity affects the repulsive force in squared terms.

Stratil-Sauer (1996) observes the distance cyclists maintain to physical road boundaries. The distributions obtained from the study show that the chosen distance depends on the type of road boundary. Cyclists maintain a greater distance to parked cars than to road curbs. The study also shows that cyclists diverge from their ideal path when overtaken by cars and the distance from the road boundary decreases from 0.55 % to 0.8 %.

Results show that the human steering control loop generates a control error that results in an oscillating lateral movement, even when the driver or rider is on straight road stretches. Later, Schopf (1985) calibrates a regression model to estimate the error in dependency of the sum of the left and the right margin of the road (the lateral distance of the vehicle to both physical road boundaries). The outcome shows, that the minimal amplitude of oscillation is given at approximately 1 m (sum of both sides). The empirical description of this human factor seems relevant for this thesis because it influences both the infrastructural model and the single-agent behavior model.

Qualitatively, these results are confirmed by Zwielich et al. (2001), who measured driving speed on rural roads. The authors found that a higher permitted speed limit leads to correspondingly higher average car speeds, and straight road stretches lead to a decrease in distance from the side of the road. Guiding elements on straight stretches such as guideposts, trees on the right-hand side, and external markings seem to have only a minor effects on speed. This is particularly the case, when guiding elements serve to clearly delimit the side environment and are not part of the road. However, Zwielicht et al. show that guiding elements that are only applicable to oncoming traffic (such as central markings or rows of trees on the left) reduce speed.

When cyclists are overtaken by motorized vehicles, they choose a path significantly closer to the road boundary. A study conducted in Switzerland (Metron Verkehrsplanung und Ingenieurbüro AG, 1999) concludes that cyclists move more closer by an average of between 0.09 m to 0.29 m to the edge of the road when overtaken by cars.

Pedestrians

As long as there is a designated space for pedestrians, then - according to traffic regulation (Republik Österreich, 1960) - all pedestrians can use both sides of the road. In terms of the model this means that the agents can freely choose what side to walk on. This is also true when the pedestrians enter a new section of road, or after they cross a road. It should be considered in designing paths and positions that the minimum width of a pedestrian is about 0.75 m (Schopf, 1985). The minimum distance of pedestrians to objects and boundaries does not seem to be dependent on their own speed.

Cars and motorbikes

Studies show that the space between vehicles and road boundaries depends on infrastructural characteristics, including Klebelsberg (1982); Zwielich et al. (2001):

- Lane markings on the surface
- Radius of the road segment

- Direction of the curve (left/right)

The studies' results show that drivers orientate themselves towards road markings; a lane at the roads axis appears to "pull" drivers towards the center. The distance can nevertheless be seen as a variable, influenced by the drivers steering. For instance, the width of a vehicle might be considered in drivers planning of their paths, or the "repulsive" force of a boundary may cause drivers to keep a certain distance.

Bicycles

The lateral positioning of cyclists is based on the perception of the lateral boundary (Stratil-Sauer, 1996, p. 57ff). In roads with mixed traffic or a "soft" separation, the path of cyclists depends on multiple aspects. Bode (2009) observes strong variances in the usage of the shared space in Bohmte (Germany). Depending on their subjective perception of personal safety, cyclists use either the left or right side of the "soft" separation elements. Based on this observation, cyclists seem to use either the side similar to pedestrians or the central area of the road as car drivers do.

Individual Interpretation

It is obvious in the literature and through observation that pedestrians and drivers do not choose the same lateral position, even when they experience similar conditions (speed, other road users etc.). A stochastic term structure has to be applied in the model to shift the chosen lateral positions within the certain statistical distribution. Schopf (1985) shows that the lateral shift is velocity dependent and this phenomenon could therefore be considered in the placement of guiding lines.

The authors own empirical research in Gleinstätten and Graz aimed to estimate the lateral distribution of the vehicles from the road boundaries. The distribution from the tracked data is shown in figure 8.12. In the calibration of the simulation model, the mean of the real speed and its distribution is used to set up the stochastic parameters of the agent-chosen free flow speed.

Obstacles

Surface design is plays a part in many traffic calming initiatives; street furniture can help reduce driving speed, accentuate risk areas, channel traffic flows and indicate the *function of a road*. This is part of holistic traffic planning, which includes urban design and social requirements and considers village gateways, reduced clutter, paving and road surfaces, street furniture, traffic management, and street life (Carson and Hickman, 2006). Figure 8.3 illustrates some examples of street furniture in shared spaces. In addition to serving an aesthetic and revitalizing function, the objects positions can clearly serve to channel traffic flow. Street furniture has an impact on the effective width of the profile segments by controlling speed, crossing position, and separation of modes of transport. The main issues to consider in regards to obstacles for the model requirements are:

- Handling in the model
- Constrains to the ground plane: edges, width, etc.
- Impact of height and material (can it stepped over etc.)

Street furniture can often have a filtering effect. Bollards, for example, are used to block cars from entering an area, but they do not usually affect pedestrians and can be carefully placed in cycling areas.

Network

Most shared spaces have been implemented in city centers. Urban road networks have been shaped to a wide variety of topologies over history. Figure 8.4 shows some different examples of shared space zones in Europe, including through roads and squares. The dimensions are limited, however: most roads are bidirectional with only one lane for each direction. So far, intersections of up to five entrances have been redesigned into a shared space. The network model should therefore consider squares, road sections and intersections with multiple entrances/exits.

3.1.3 Requirements towards Single-Agent Model

Beuck et al. (2007) distinguish between a mental and a physical layer in microscopic multi-agent models. The definition of the physical layer essentially includes everything that can be observed and measured. The mental layer contains the background of the decision and the decision process that cannot be observed. Social interaction is the precondition of mixed traffic in giving way processes, road crossing, and lateral evasion. At low speeds and holonomic dynamics (pedestrians) the social force model ensures a good fit with empirical data even in high traffic densities. When vehicular traffic is included in the simulation, greater foresight is exceeds social force abilities. In the strategic level no other agents are considered. The routing and path finding algorithms include only static objects and geometries.

Free Walking Speeds

The desired speeds of pedestrian crowds are Gaussian distributed with a mean value of approximately 1.34 m/s with a standard deviation of about 0.26 m/s (Henderson, 1971). Knoflacher (1995) presented a study in Austria on walking speed. The mean walking speed of 1.45 m/s lies above the European mean value of 1.41 m/s (Hoogendoorn and Daamen, 2006). It should also be noted that the free speeds found in Hoogendoorn and Daamen (2006) are higher than those found in other literature. This is to be expected since the literature discusses observed speeds, whereas this author considers free speeds, namely the preferred walking speed of pedestrians. The difference can be accounted by the facts pedestrian free speeds cannot directly be observed, since the observer cannot know if the pedestrian is actually walking with his free speed. Free speeds based on observation tend therefore to be underestimated.

Free Driving Speeds

Road speed on tree-lined sections of road is affected by a number of road features. Typical features are, for example, road markings, maximum speed limits, or road quality. The distance cars drive from the side of the road is influenced far more by the structural design of roads (for example the width) but is also influenced by the impression aroused by the environment (such as the distance of trees at the side of the road or visual restriction due to vegetation). The distance maintained by drivers from the side of the road is more impacted by traffic situation or the state of the roads (such as if there are on-coming vehicles, day- or night-driving, or weather conditions) than by the structure of the road itself. Road markings, whether in the middle or at the side of the road, are a major exception. Like the crowns of trees, guideposts, protective planks or sign boards, they play a very influential role on road speed. The correlation between measured speeds and speed limit signs is especially high. Higher permitted speeds led to correspondingly higher average speeds by drivers and straight road stretches also led to a reduced distance from the side of the road.

In the simple definition model agents choose their free driving or walking speeds when they are not influenced by other vehicles or pedestrians. In the extended definition special local road characteristics are also considered as well. The characteristics considered include:

- Sharp curves
- Steep grades
- Narrow structures (bridges, tunnels....).

Within the shared space context, physical perception and speed are significantly related. A relatively old work of Volmuller (1976) proposes and explains a separation: Speed-choice of a driver in free flows is an interdependent function of speed and multiple stress factors. Volmuller structures these stress factors into the following three categories:

1. Destination stress, caused by the desire to reach the destination.
2. Physical stress, relying on noise, vibrations, vertical and lateral accelerations and jerks. This stress quadratically increases with speed and dependents on the road's surface and alignment.
3. Psychological stress due to the driving task. The rate of driving relevant information increases with speed. Since human perception and processing is limited, this stress function increases steeply at certain speeds.

Figure 3.1 presents an example of the multiple functions and the cumulative result. The numerical example is related to rural roads.

An approach to implicitly set speed on the operational level is the friction force given by all obstacles and other agents. Keller' s (1983) regression model on speeds show

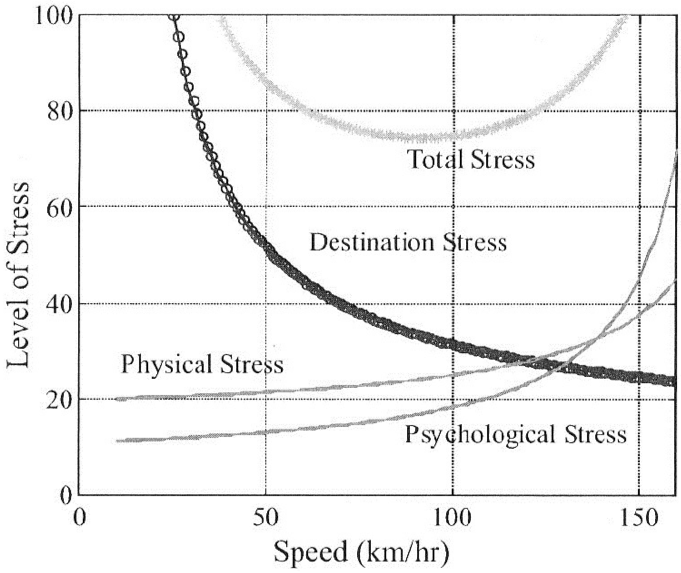

Figure 3.1: Three components of driver stress and its sum as a function of speed - which may prove to be of particular relevance for shared spaces and other roads with a high level of interaction, taken from Volmuller (1976). It has to be remarked, that the figure is related to rural roads.

that chosen speeds are mainly influenced by objects and parking and driving cars. This approach makes it possible to define free flow speeds as dependent on infrastructure.

This model explains the reduction of speeds within shared spaces based on the friction of interaction and design.

Path and Route Choice

Pedestrians' behavior is often classified hierarchically into three levels, i.e. according to Hoogendoorn et al. (2001):

- Strategic level (minutes): The agent plans her route. She generates a list of destinations.
- Tactical level (seconds): The pedestrian decides on the route between the destinations, making a rough decision on route and solving conflicts with vehicles.
- Operational level (milliseconds to seconds): The actual movement is performed including evading other agents and obstacles (pure pedestrian conflicts are solved on this level).

At the tactical level, road users must decide what is the ideal path for them to take. This includes the position within the sidewalkhow far from the curb they will walkconsidering the design of the route. Major obstacles like trees, bollards and road furniture influence the path and therefore are important at both the operational and tactical levels.

The operational level is defined by the actions taken to remain on the chosen path, the choice of speed, and the reactions to other road users and objects. Basically, it will be implemented by social force features for all agents.

3.1.4 Requirements towards the Multi-Agent Model

Modes of Transport

The foremost question when simulating a shared space model is to decide what type of road users will be present: motorized vehicles, pedestrians and cyclists are widespread in shared spaces. Private motorized vehicles should be treated separately in three classes: passenger cars, motorbikes and heavy vehicles. Public transport is not present all shared space areas; but if it is present it is very important that it be included in the simulation. This is particularly the case when stations are located close to the investigated area and congestion caused by the stations affect the shared space area. Persons in wheelchairs and the visually-impaired are representing minorities, but call for a special approach not only in the simulation but in planning generally. Other road users were found to be less important in the simulation. For instance, emergency vehicles appear rarely and they are not included in the simulation.

Observed Behavior

Observations of shared spaces and the interaction processes within the traffic flow (Schönauer et al., 2012b,c) or (Kaparias et al., 2010, 2013, 2015) conclude that the number of processes can be reduced to a few behavioral patterns:

1. Ignorant behavior (continue on path with $a_i \geq 0$)
2. Defensive (gallant) behavior: $a_i < 0$
3. Evasive behavior $a_i = 0$, walking direction or drivers heading $\gamma \dot{\neq} 0$.

Where a_i is the agent's acceleration between the point of decision D_i an the point of conflict $C_{i,j}$. Accelerations during conflicts $a_i > 0$ can hardly be empirically observed - it is not considered in further practical classifications and implementation.

Normative considerations

Norms would usually be the leading consideration to understand how interactions are handled and conflicts are solved or avoided. Traffic laws contain a hierarchic structure of rules that organize right-of-way at intersections. The following rule-set is an excerpt from Austrian traffic regulations §19 (Republik Österreich, 1960).

1. If no other rule applies, all vehicles approaching from the right have priority.
2. Railed vehicles always hold ROW.
3. Emergency vehicles always have priority.
4. Vehicles on a main road (with permanent right-of-way) have priority.

5. Traffic signs "Give way" or "Stop" accordingly set the right-of-way.
6. Vehicles maintaining their direction have right-of-way over the left turning vehicle.
7. Vehicles in moving traffic flows have right-of-way over vehicles approaching from frontage roads, pedestrian areas, residential roads, entrances, parking suits etc..
8. Cyclists on bicycle lanes must yield to vehicles in moving traffic when leaving the bicycle lanes.
9. Vehicles coming from frontage roads have right-of-way over vehicles approaching from pedestrian areas, residential roads, entrances, parking suits etc..
10. Vehicles that must yield are not allowed to force other vehicles to yield by intersecting, turning or queuing.
11. Every driver can waive his or her right-of-way, but such a waiver must be clearly observable. Stopping the vehicle is considered as waiving right-of-way.

Road safety and traffic rules differ even within Europe - but the system of the rule-set listed above is widely used in most countries.

3.1.5 Social considerations

Socially motivated interaction is an inherent phenomena in mixed traffic. This affects the following interaction processes:

- Crossing a road by pedestrians (interaction with vehicles)
- Lateral evading at passing by or overtaking maneuvers (pedestrians and drivers)
- Give way procedures at intersections (both pedestrians and drivers)
- Speed choice of drivers that closely pass other, non-motorized road-users

At low speeds (which are typical for pedestrians), the social force model ensures a good fit with empirical data even in high traffic densities. When vehicular traffic is included in the simulation, however, advanced foresight would be needed but this exceeds the usual capabilities of social force models. Furthermore, voluntary actions like stopping to allow a pedestrian to pass seem to be more common in shared spaces and therefore need to be addressed separately.

"Uncertainty creates safety" is the underlying hypothesis of Hans Monderman, the inventor of the concept of shared space (Grassmuck, 2009). In order to promote social interaction, shared spaces aim to have as little as possible measures that control traffic. Priority rules are replaced by interpersonal communication and understanding. If it is no longer obvious who has the right-of-way, the social rules of human politeness will come into effect. In this manner, shared space design deliberately strengthens uncertainty, intending to increase actual safety (Gerlach et al., 2009).

3.2 Modeling Framework

Based on the model requirements of the last section, multiple sub-models are defined and designed. Figure 3.2 gives an overview about the structure and interaction of models used in this thesis. The modeling approach can be split into three sections:

- Strategic Models
- Tactical Models
- Operational Models

The infrastructure model is mapped in all three sections - it provides context for the route and path as well as objects and moving areas.

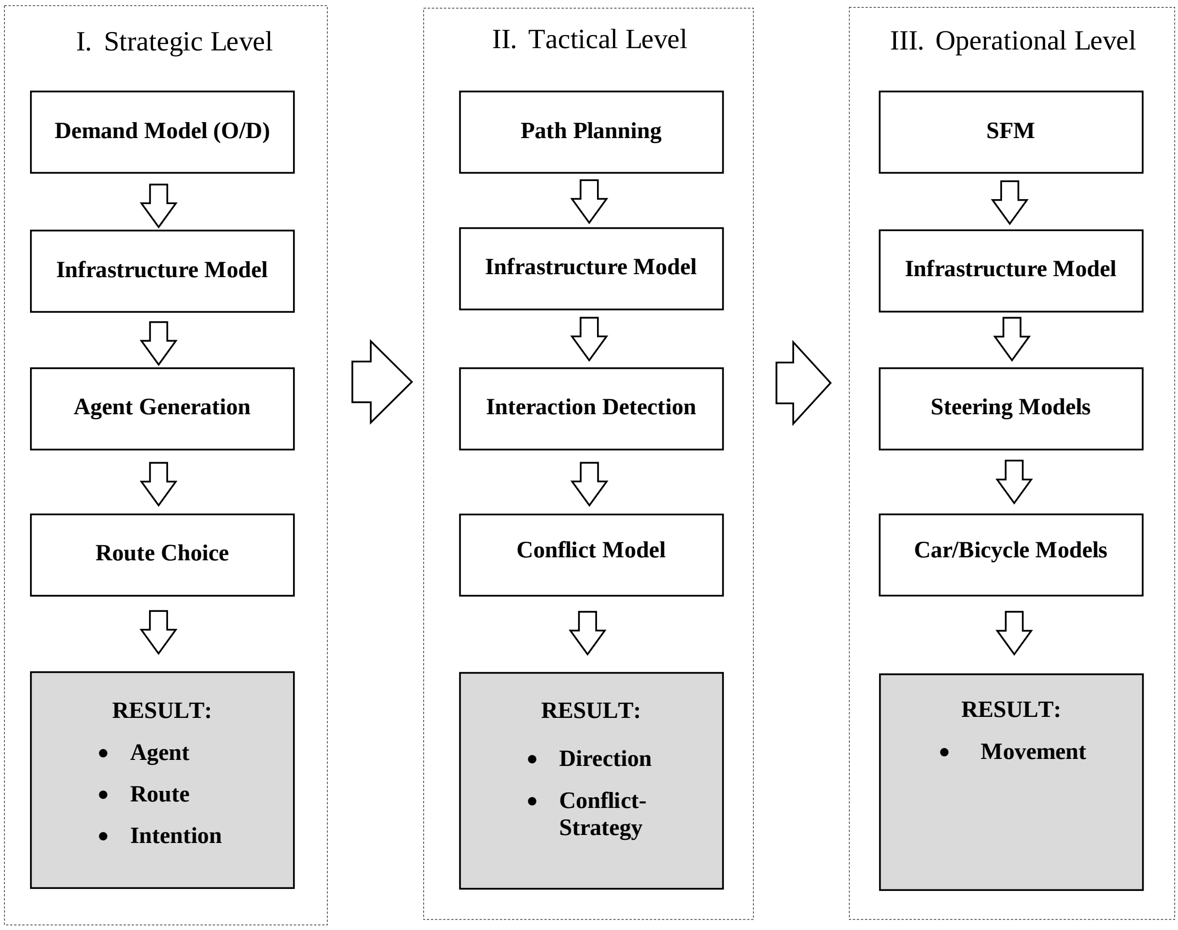

Figure 3.2: Structure and interaction of models - divided in three sections/levels.

Figure 3.2 summarizes the results of each modeling section and drafts the full process from an agent with intentions and characterization to actual movements in the digital road. The full modeling process is covered in this thesis. The model design in this very chapter 3, implemented in chapter 4, applied to a certain topological setup and compared to real world data in chapter 5 and chapter 6.

The structure of this framework is comparable to those, recently published by Anvari (2014); Anvari et al. (2015) and Pascucci et al. (2015); Pascucci and Friedrich (2017), whose research and PhD projects both aimed/aim on similar intentions.

3.3 Infrastructure Model

Three layers can be identified to describe the road's topology, structure, and static objects in the environment:

- Area of movement where agents find their route and can interact with each other
- Guiding fields that motivates the agents to use particular lateral paths
- Obstacles that keep agents at a distance

Schönauer and Schrom-Feiertag (2010) propose to describe infrastructure as a force-field that keeps agents on track, avoiding obstacles and accommodating their individual preferences. An example is given in the appendix (figure 8.41).

To model the topology and static objects, an infrastructural guiding field structures the network into two types of sections: junctions and non-junctions. A measurement algorithm generates the mean of an ideal lateral position within the areas that represents the maxima of the guiding fields. It is shown in the next section how the controlling elements attempt to keep agents on their paths.

A guiding force can be established for any point within a two-dimensional space. The force pulls towards a polygon, describing one agents' "ideal" path within the road. The literature in the field shows that the positions of vehicles (bikes and cars) are speed-dependent and profile-dependent. It seems appropriate that different modes have different sets of parameters.

In addition, a stochastic term describes the distribution around an ideal path. Every agent chooses its own position within the profile. A solution has to be found to stochastically interpret the road in the most simple manner. Since a force base approach is used it is obvious to extend the force model with additional forces which add an intention to follow an ideal path. This methodology is described now.

Measuring the profile

In straight sections, the polygons have a set of designated entrance and exit vertices. Connecting the central points of two of these vertices, we gain a line segment describing the shortest path from entrance to exit. It is assumed that the road profile is normal to this line. This concept is illustrated in figure 3.3. If the road section includes a curve, the central line is replaced by a polyline. The vertices of this polyline could be placed manually or automatically.

When thinking of numerical values for the distance between two profile measurements, there are multiple aspects to be considered:

- The "sampling" should detect the obstacle of the smallest relevant diameter in the road (i.e. steel bollards - yellow circles in figure 3.3)
- In curves, the measurement lines are no longer parallel: the angles splay the lines
- Performance of the calculation

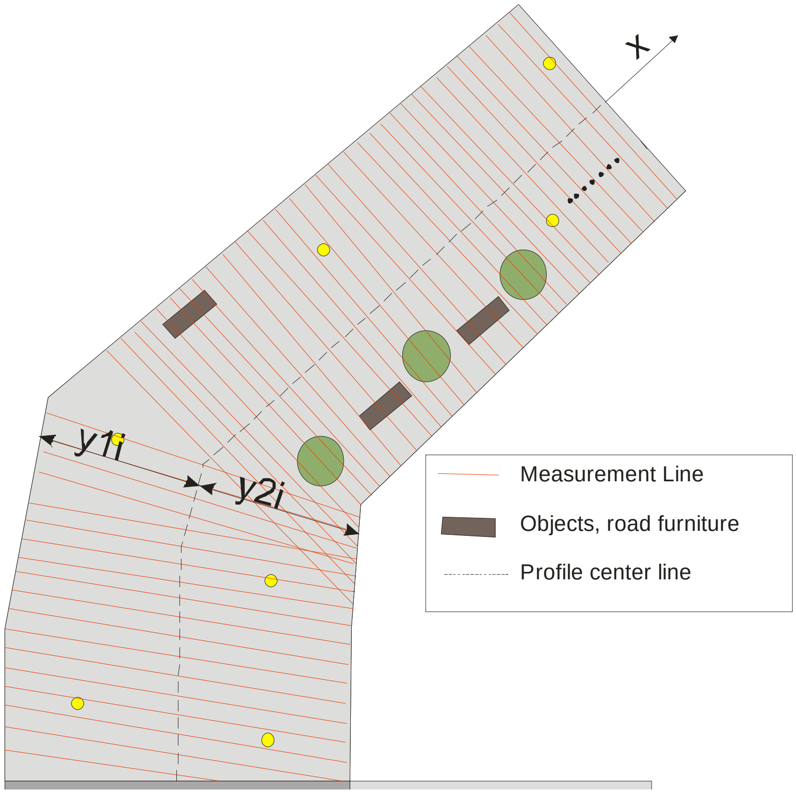

Figure 3.3: Method of obtaining profile measurements in a curve. The measurement lines show how the profile is captured. All the profile's parameters are taken along those lines.

The definition of the measurement resolution within a single profile raises similar issues.

Splitting the profile

After establishing the road profile, it is segmented for each mode of transport and four points are extracted for each side:

- Profile center c
- Boundary of the road's central lane b_r, b_l
- Beginning of the area of the road's side area s_r, s_l
- End of the road surface e_r, e_l

The boundary can be given by road surface markings, and physical boundaries can be defined by surface level or differences in the materials structure / design. Based on this characteristics, for each profile a guiding line for each of the three modes is derived. The result can be compared as an enveloping function: In figure 3.3, the y-axis' zero lies at the road's center.

In the next sections, all relevant variables are defined. The estimation of the actual function and its parameters has to be calibrated in order to fit the real world observations.

3.3.1 Cars and Infrastructure

In Austria and most other countries, motorized vehicles are required to use the right side of the available and designated space of the road. The path therefore does depend on the direction of driving, as well as the measurement algorithm does. Furthermore, drivers orientate themselves using both the center line and the road's boundary. In a one-way road segment, c is replaced with b_r or b_l. Figure 3.4 is an example of how both boundaries are considered equally - the example is valid for motorized vehicles.

Figure 3.4: Photo of a one-way (for motorized vehicles) road segment leading to the shared space at Sonnenfelsplatz . It illustrates that in the absence of road markings, the boundary of the vehicle's space is constrained by road furniture and bollards.

The boundary can be defined by road markings on the surface, curbs, parked cars and road furniture or other obstacles.

$$gr_{car} = f(c, b_r) \tag{3.2}$$

$$gl_{car} = f(c, b_l) \tag{3.3}$$

The actual position of the desired path lies between the centerline and the road boundary and depends on the total width of the road.

3.3.2 Pedestrians and Infrastructure

Based on the author's own observations and literature, it is concluded that pedestrians commonly use the space between e_r and s_r respectively e_l and s_l. If there is a boundary of marginal dimension, then $s_r \approx b_r$ and $s_l \approx b_l$ respectively. Within this span, the distribution functions are defined as:

$$gr_{ped} = f(e_r, s_r) \tag{3.4}$$

$$gl_{ped} = f(e_l, s_l) \tag{3.5}$$

where gx_{ped} (x for left or right) is the distribution defined by the variables e_x and s_x, and the distribution's skewness γ_{ped} can be assumed to be $\gamma_{ped} \neq 0$. In the empirical outcome, the results of such a figure are described. It should be noted: This definition is a simplification that does not model multiple parallel paths for pedestrians through a "grid" of street furniture. In these situations, $f(e_x, s_x)$ would represent the outer borders, and obstacles can therefore block the chosen track. The avoidance of the obstacle must also be addressed on the tactical level.

3.3.3 Bicycles and Infrastructure

The measurement and the desired track depends on the direction of driving. Cyclists orient themselves on the road's boundary and the space available. In a one-way road segment, c is replaced with b_r or b_l . Alternatively, bicyclists are often observed to use the side area of the profile: In that case, the behavior is similar to the path choice of pedestrians.

$$gr_{cycle} = f(c, b_r) \ or \ f(e_r, s_r) \tag{3.6}$$

$$gl_{cycle} = f(c, b_l) \ or \ f(e_l, s_l) \tag{3.7}$$

The choice of the type of path chosen (such as cars in the center lane or pedestrians in the side area) is influenced by the profile's dimensions as well by the riders' individual preferences. No literature was found that covers this type of choice.

3.4 Dynamic Vehicle Models

Two types of dynamic vehicle models are introduced as non-holonomic objects in the modeling framework: First, the discrete form of the single-track model equations, based on Kramer (2008), is implemented to model motorized vehicles. Second, a bicycle model based on Whipple (1899) completes the agents' mechanics. The use of the bicycle model is relatively rare in the area of traffic flow research; most approaches represent bicycles with the same single track models as used for cars, trucks and buses.

3.4.1 Car Model

In this model, all motorized vehicles are considered, including buses, trucks, motorbikes and motor-scooters. In figure 3.6, the variables used are visualized in the mechanical scheme:

- Front or back movements along the x axis.
- Lateral shifts at the y axis.
- Vertical lift.
- Roll angle φ.
- Yaw angle ψ.
- Pitch angle χ.

Only ψ and lateral and longitudinal movement are considered to be relevant for the model (Kramer, 2008). The lateral dynamics of a vehicle includes properties such as steering and curvature behavior and influences the driver's perception of position (Heissing and Brandl, 2002). The design of the lateral dynamics used in the model is shown below, and its based on Kramer (2008).

The linear single track model can be described as:

$$\begin{bmatrix} \dot{\beta}(t) \\ \ddot{\psi}(t) \end{bmatrix} = \begin{bmatrix} -\frac{c_h+c_v}{mV} & \frac{c_h b - c_v a}{mV^2} - 1 \\ \frac{c_h b - c_v a}{J_z} & \frac{c_h b^2 + c_v a^2}{J_z V} \end{bmatrix} * \begin{bmatrix} \beta(t) \\ \dot{\psi}(t) \end{bmatrix} + \begin{bmatrix} \frac{c_v}{mV} \\ \frac{c_v a}{J_z} \end{bmatrix} * \delta(t) \tag{3.8}$$

The next equations will briefly introduce the derivation of this linear equation. The first assumption: The lateral forces F_{qv} and F_{qh} linearly depend on the tilt angle α_v and α_h:

$$F_{qv} = -c_v \alpha_v \tag{3.9}$$

$$F_{qh} = -c_h \alpha_h \tag{3.10}$$

For small angles α_v and α_h, we can assume that:

$$\alpha_v \approx \frac{v + \dot{\psi} * a}{u} - \delta \tag{3.11}$$

$$\alpha_h \approx \frac{v + \dot{\psi} b}{u} \tag{3.12}$$

where a and b are shown in figure 3.6. The momentum theorem allows us to define the model as:

$$\dot{u} = f_1(v, \dot{\psi}, \delta, F_{qv}(u, v, \dot{\psi}, \delta), F_{lv}, F_{lh}, F_W(u)) \tag{3.13}$$

$$\dot{v} = f_2(u, \dot{\psi}, \delta, F_{qv}(u, v, \dot{\psi}, \delta), F_{qh}(u, v, \dot{\psi}), F_{lv}, F_W(v)) \tag{3.14}$$

$$\ddot{\psi} = f_3(\delta, F_{qv}(u, v, \dot{\psi}, \delta), F_{qh}(u, v, \dot{\psi}), F_{lv}) \tag{3.15}$$

Linearizing this model with the input variables δ, F_{lv} and F_{lh} for $\delta = 0$ (straight driving) allows for further simplifications (Kramer, 2008):

$$u = u_0, v = 0, \dot{\psi} = 0, F_{qv} = F_{qh} = 0 \tag{3.16}$$

Replacing the lateral and longitudinal velocity $u(t)$ and $v(t)$ by the absolute value of velocity $V(t)$ as well as the slip angle $\beta(t)$ yields:

$$u(t) = V(t)cos(\beta(t)), v(t) = V(t)sin(\beta(t)) \tag{3.17}$$

This approximations can be found close to the idle state: $u = u_0 \approx V$ and $v \approx V\beta$. For $F_{lv} = 0$ and $\partial F_W / \delta_v = 0$ at constant velocity, we gain a "common model for lateral dynamics" (equation 3.8), which was first introduced by Riekert and Schunck (1940).

3.4.2 Bicycle Model

Cyclists demonstrate a behavior that is distinct from that of motorbike drivers. According to Hong-bo and Hui-ling (2009), the most important differences are:

1. Bicycles have rapid start-up speed; they start more easily than motorbikes and the time lost during starting a bicycle is minimal.
2. Bicycles demonstrate slower clearance speed in intersections (lower acceleration).
3. Cyclists risk severe conflicts with motor vehicles when they cue on the right side of the road or lane.
4. Bicycles demonstrate an unstable driving trajectory during the acceleration process and in very dense traffic situations.

Although Hong-bo and Hui-ling (2009) focus their study on urban Asian mixed-traffic conditions, an application of some of their findings to shared space design might be fitting. Meschik (2008, p. 45-49) summarizes additional relevant cyclist-related considerations, including average free flow speeds, turning radii, dimensions and foresight distances.

Klein and Sommerfeld (1910) postulated more than 100 years ago that: "*A bicycle is a doubly non-holonomic system; it has five degrees of freedom in finite motion, but only three such degrees of infinitesimal motion (rotation of the rear wheel in its instantaneous plane, to which the rotation of the front wheel is coupled by the condition of pure rolling; rotation about the handle bar axis; and common rotation of front and rear wheel about the line connecting their points of contact with the ground), as long as we do not consider the degrees of freedom of the cyclist himself*".

The tilt aspect can be described as an inverted pendulum (Åström et al., 2005); the right hand side configuration in figure 3.5 shows this as a bottom-up pendulum. The roll angle φ is the angle that the rear frame makes with the inertial z-axis. Assuming a rigid $\varphi = 0$, the steering angle is the input and linearizing for small tilt angles we find the equation:

$$J\frac{d^2\varphi}{dt^2} = m\,g\,l\,\varphi + l\,F \tag{3.18}$$

where l and m are the pendulum's length and mass.

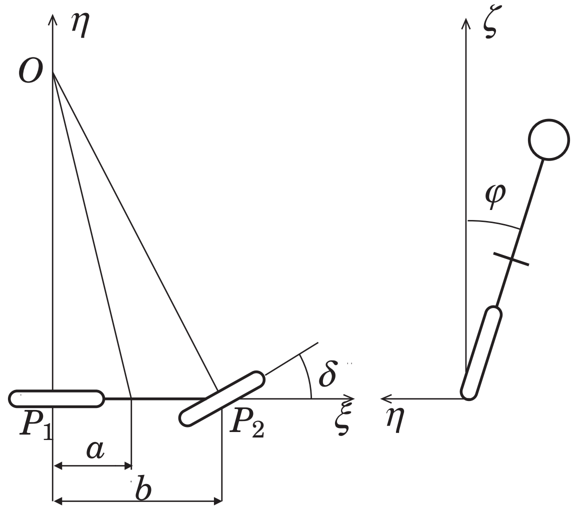

Figure 3.5: LEFT: Kinematics generate the lateral force component, RIGHT: Pendulum substitute.

Considering lateral forces in the kinematics, the forces acting on the center of mass are:

$$F = m(\frac{V_0^2}{r} + \frac{dV_y}{dt}) = (\frac{V_0^2}{b}\delta + \frac{aV_0}{b}\frac{d\delta}{dt}) \tag{3.19}$$

Figure 8.14 gives the graphical reference to equation 3.20 that shows the dynamic equation of a bicycle:

$$M\ddot{q} + vC_1\dot{q} + [gK_0 + v^2K_2]q = f \tag{3.20}$$

where:

$$q = \begin{bmatrix} \varphi \\ \delta \end{bmatrix} and f = \begin{bmatrix} T_\varphi \\ T_\delta \end{bmatrix} \tag{3.21}$$

The cyclist controls the bicycle via the steering torque T_δ, and via the tilt torque T_φ. The system is linear with a constant coefficient matrix. Meijaard et al. (2007) shows the stability of the model by analyzing the Eigenvalue λ_{S1}, λ_{S2}. These findings - shown in figure 8.13 - identify two important modes: the weave and capsize modes (Limebeer and Sharp, 2006). The weave mode begins at zero speed with two real and positive eigenvalues. When its real part Re is negative, the system is bounded, the imaginary part Im of λ_{S1}, λ_{S2} will introduce a weave mode into the system, but will not affect the bounded feature. This is to say, when the bicycle is at a suitable speed (at λ_{S1}, λ_{S2} with a negative Re) it is in an "auto stable" state, it is not necessary to modify input torque T_δ to prevent the bicycle from falling over. However, if $v < v_w$ or $v > v_c$, the system is in an "unstable" state, because a real positive λ_{S1}, λ_{S2} introduce an unbounded term into the final solution. Under those conditions, a control loop is needed for the bicycle to keep running. In other words, the rider has to continually adjust the handlebar to avoid falling over. The nature of bicycle steering was already discussed over a hundred years ago. Archibald Sharp noted that in order "*to avoid an object it is often necessary to steer for a small fraction of a second towards it, then steer away from it; this is probably the most difficult operation the beginner has to master...*" (Sharp, 1886, p. 222). This historical observation does not distinguish between steering torque control and steering angle control. Whipple (1899) later surmised, the riders main control input is the steering torque T_δ . This control input is considered in the model described in this thesis.

Full sets of reasonable default parameters can be found in the literature, such as in Limebeer and Sharp (2006); Defoort and Murakami (2009).

3.4.3 Controller

The movement and control processes of vehicles introduce non-holonomic kinematics, linear dynamic models for both motorized vehicles and bicycles, and a need for a controller (driver) to guarantee realistic driving in the model. Keeping the vehicle on its chosen path is a task for a driver-vehicle-road combination. The simulation initiates so called *sensing–runs* to simulate the preview error vectors that occur during driving. Figure 3.6 illustrates the preview during the simulation and the generation of the error vector.

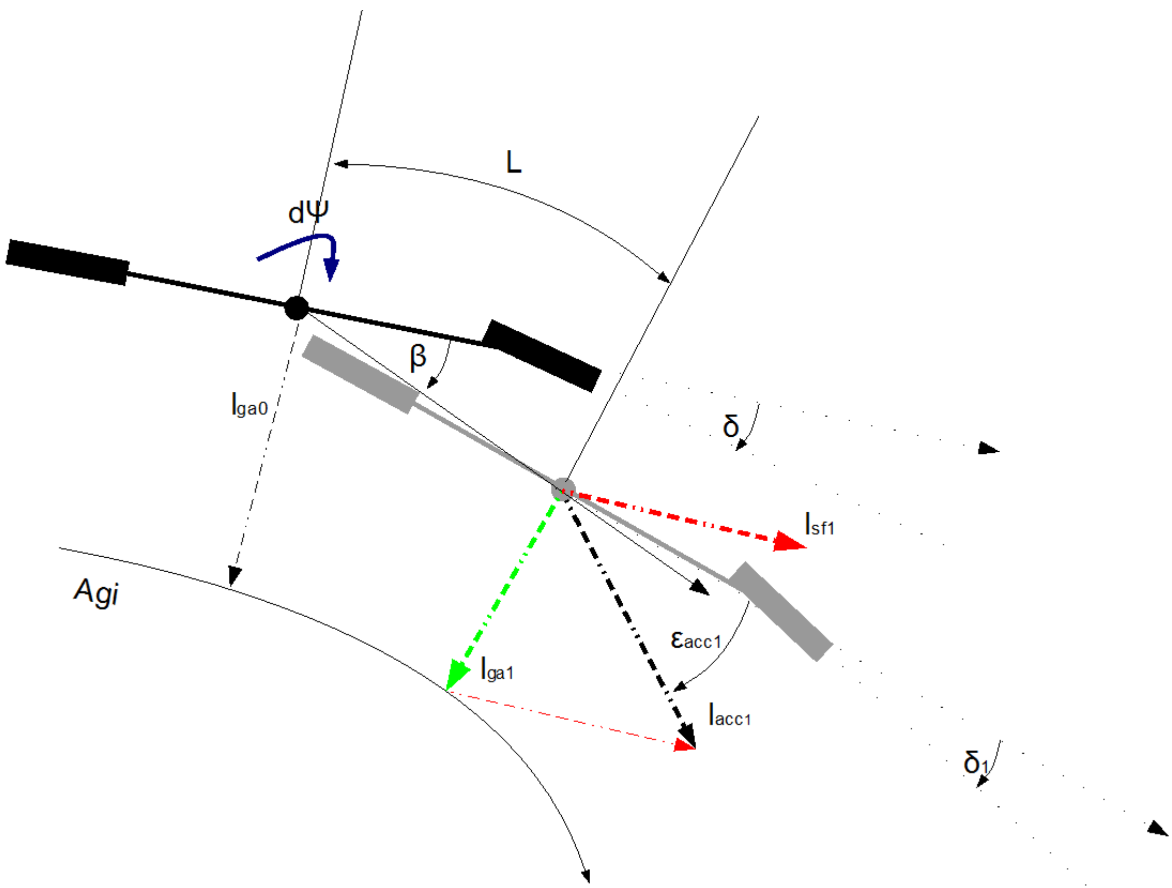

Figure 3.6: Each so-called *sensing–run* generates a new preview of the vehicles position. The gray–colored structure is the projection of the vehicle's position within the next discretization step.

On the one hand, the lateral component of force is the main input of the steering model, while on the other hand the longitudinal part of force controls acceleration and braking of the vehicle model. Since the vehicles are guided by social and infrastructural forces (characteristics), a control system has to stabilize the driving on an appropriate path during the simulation. The input forces are given by social interaction with other agents, by obstacles, the target vector plus the guiding field of the infrastructure. The control system (figure 3.7) represents a part of the driver of the vehicle; the agent senses its own position and the position of other agents in the environment, plans the desired path, and estimates the steering. The second driver output in this model is the acceleration (positive and negative) in order to adjust the speed-to-curve radii and conflict avoidance.

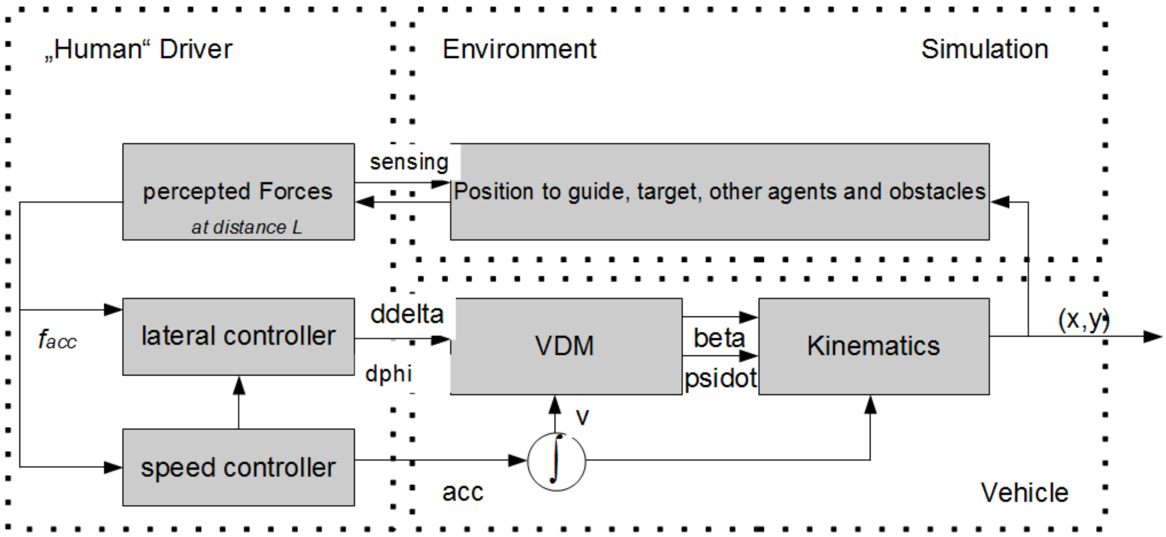

Figure 3.7: Simplified control loop in the driver - machine - environment. The "sensing" is a bidirectional flow in order to represent the perceiving and emitting force.

Kraus (2011) shows the design of a non-linear vehicle model, a simplified tire model, and a driver model to provide a model capable of microscopic simulation. Huang et al. (2012) show that in speeds up to 45 km/h, the linear single-track model is sufficient to simulate realistic driving. Nevertheless, the non-linear calculation approach causes a much higher processing effort due to solving.

The Vehicle Dynamic Model (VDM) assumes acceleration to be minimal in lateral dynamics for simplicity. This assumption is based on the generally low speed in daily traffic and its low impact on lateral forces, and therefore dynamics. A function $T_1 = [\delta\ \alpha]$ maps the force vector into the δ and acceleration:

$$\overrightarrow{F} \rightarrow \begin{bmatrix} \delta \\ \alpha \end{bmatrix} \rightarrow \begin{bmatrix} Deltax \\ \Delta y \end{bmatrix} \tag{3.22}$$

where T_1 represents the mapping of target force $\overrightarrow{F}$ to the response of driver, represented by the steering angle δ and acceleration a. T_2 represents the mapping of driver response to vehicle motion ($Deltax\ \Delta y$). The function T_1 will be defined in this chapter, and mapping T_2 is described by the VDM.

l_acc1 is the actual error angle, derived from the desired directional vector l_{acc1}, which is the result of accumulating social force and the guiding vectors:

$$l_{acc1} = w_{gf} * l_{gf1} + w_{sf} * l_{sf1} \tag{3.23}$$

where w_{gf} is the weight of the guiding force and w_{sf} is the corresponding weight of the social force vector (in figure 3.6, both weights are assumed to be 1 for simplified drafting). The measurement of the sensing is done in distance L where L for small β, $d\psi$ and δ can be estimated as:

$$L = V * t_{sensing} \tag{3.24}$$

The time step width $t_{sensing}$ is the simulation time in which the agents predict forces of the infrastructure or other objects and agents.

The l_{acc1} , received in the sensing mode, is the lateral controller input. To calculate the actual steering δ using proportional control and a linear speed dependency we get:

$$\dot{\delta} = \epsilon_{acc} / (k_{st} + k_v * v) \tag{3.25}$$

where k_{st} is the proportional factor and k_v is the factor controlling the steering reduction at increasing speeds. $|\delta|$ is kept within constraints to achieve adequate steering moves. The single track model is based on the assumption that accelerations (positive and negative) do not affect the lateral forces and the vehicles dynamic behavior significantly.

$$e_v = \begin{bmatrix} cosy \\ siny \end{bmatrix} \tag{3.26}$$

A generic Proportional Integrative Derivative (PID) controller is a typical algorithm used in a wide range of control systems (Åström et al., 2005; Abdullah et al., 2006). In a generic configuration, the control signal $u(t)$ is the sum of three terms. Each of these terms is a function of the tracking error $e(t)$. The term K_P indicates that this term is proportional to the error. The term k_I is an integral term, and the term k_D is a derivative term. Each of the terms works 'independently' of the other. Figure 3.8 shows the arrangement in a signal flow diagram.

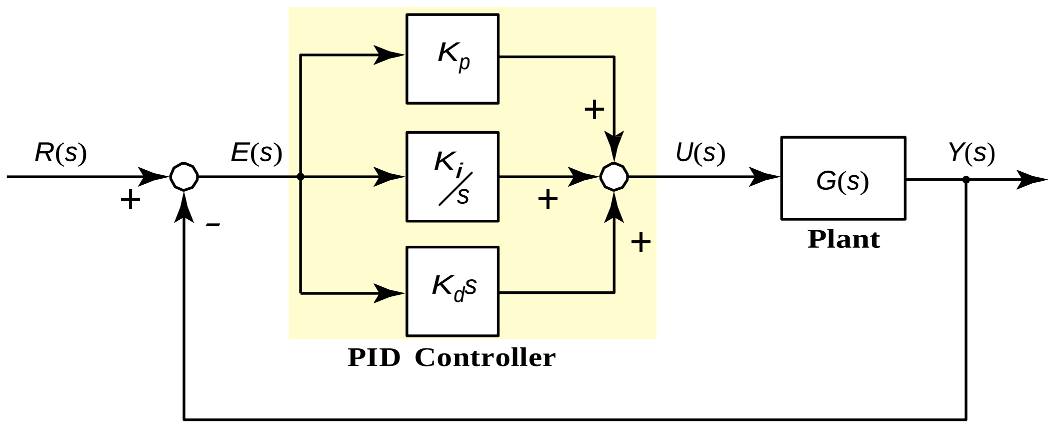

Figure 3.8: PID Controlled System is primarily defined by three parameters k_P, k_I and k_D.

In the present study, the PID controller is used to transfer the lateral angular error to the steering angle. Huang and Fellendorf (2012; 2012) have conducted similar work. The authors have transfer the lateral component of the resulting social force to the controller input:

$$F_s(t) = A * [\overrightarrow{F}_t(t) + \sum_{p=1}^{n} \overrightarrow{F}_p(t)] \tag{3.27}$$

where $A = [0 \ \ 0]$, $\overrightarrow{F}_t(t)$ represents the target force and $\overrightarrow{F}_p(t)$ is the repulsive force vector of an obstacle p.

In the present research, a different approach is used - the angular error *epsilon* is derived as previously shown and transferred to the steering angle δ_v:

$$\dot{\delta_v} = (k_P * \epsilon + k_I * \Delta t * \int \epsilon + k_D * (\Delta\epsilon)/\Delta t)/(k_{st} + v * k_v) \tag{3.28}$$

The steering and the driving angle depend on the velocity v and the error e_v. An auxiliary simulation is done to show the effect using a single - track model and approximate discretization (Euler). The slip angle can be written as equation 3.29 shows, where for every time interval Δt the former state and the actual δ leads to an updated system state.

$$\beta_{k+1} = (1 + a_{11} * \Delta t) * \beta_k + a_{12} * \Delta t * \dot{\psi}_k + b_1 * \Delta t * \delta_v \tag{3.29}$$

Theoretical approaches to the PID controller

$$\dot{\psi}_{k+1} = a_{21} * \Delta t * \beta(k) + (1 + a_{22} * \Delta t) * \dot{\psi}_k + b_2 * \Delta t * \delta_v \tag{3.30}$$

The matrices are calculated as: $a_{11} = -(c_h + c_v)/(m * V)$, $a_{12} = (c_h * b - c_v * a)/(m * V^2) - 1$, $a_{21} = (c_h * b - c_v * a)/J_z$, $a_{22} = -(c_h * b^2 + c_v * a^2)/(J_z * V)$, $b_1 = c_v/(m * V)$ and $b_2 = c_v * a/J_z$. In Figure 3.9 the black curves describe the end of the path dependent on the path error e_v and the blue curves indicates the path driven to this position within a time period of t_{sim} = 1 s and a set of parameters given in the appendix in table 8.2. The simulation parameters chosen are T =1 s, D_t = 10 ms. Speeds vary between v =1 to 10 m/s. Control parameters are k_{st} = 15 and k_v = 30 and k_P = 2.4. The error scalar is constant during the simulation: ϵ = $\pm$ 0.5 ($\approx$ 30 degrees).

Figure 3.10 shows the vehicle' s direction and the yaw angle at the end of the path. At v = 20 m/s, the maximum change in direction after T = 1 s is $\Psi' \approx$ 11 degrees.

The constraints have values of 0.4 rad (23 degrees) to 0.3 rad (17 degrees). In literature, empirical observations of Anvari (2014) state speed dependent numerical results between 15 to 45 degrees. The author uses a heuristic approach and defines a constrained $v_{\gamma\ empirical}(\psi_{car})$, where $\psi = arctan(\frac{v_{\gamma 2}}{v_{\gamma 1}})$ is called the *steering angle*. It is assumed that ψ is the yaw angle.

In calculating the dynamics, a = 0 is chosen (assuming a constant velocity). Even in free traffic flow the vehicle's speeds varies, for example during a turn. In our model, the acceleration describes the directional fitting of the movement vector e_v and the desired

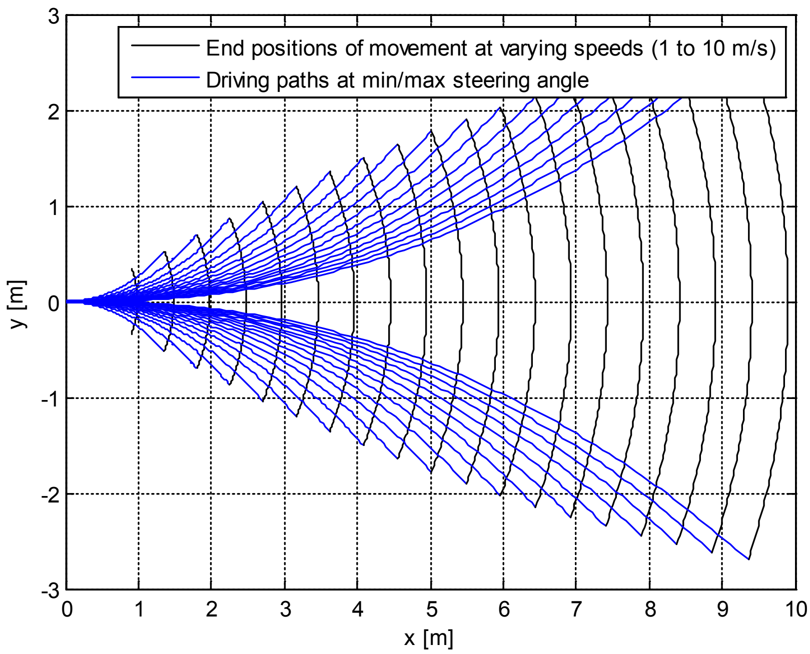

Figure 3.9: End positions of movement at varying speeds (1 to 10 m/s) and the driving paths at min/max steering angle.

directional vector e_d (both unit vectors) in the sensing: The fitting is calculated by the dot product and an proportional element.

$$a = (e_v * e_d - a_t) * k_a \tag{3.31}$$

where a_t describes the acceleration threshold; where the acceleration ends and braking begins. k_a is a constant describing the controller′ s proportional factor. Observing real world data, appropriate values for a_t lie around 0.5. This means that at an inclusive angle of 45 degrees, the vehicle will brake. Looking at the desired accelerations of VISSIMs fleet of passenger cars and the numerical range of $(-1 < e_v * e_d < 1)$, k_a can be found to be between 4 and 7. To reflect the stochastic distribution of acceleration and deceleration values, each graph consists of three different curves showing the minimum, mean and maximum values.

The acceleration parameters are speed-dependent in VISSIM. $|a|$ is thereby limited, but runs to its maximum with free driving. So, $a = 0$ when v_{max} is reached - the values are individually assigned to the agents.

The look-ahead distance, L should also be adjusted according to the longitudinal velocity for a better performance (Abdullah et al., 2006).

$$L = k_{mode} * n_{sensing} * t_{step} * v \quad [m] \tag{3.32}$$

This implies that the foresight linearly increases with actual driving speed.

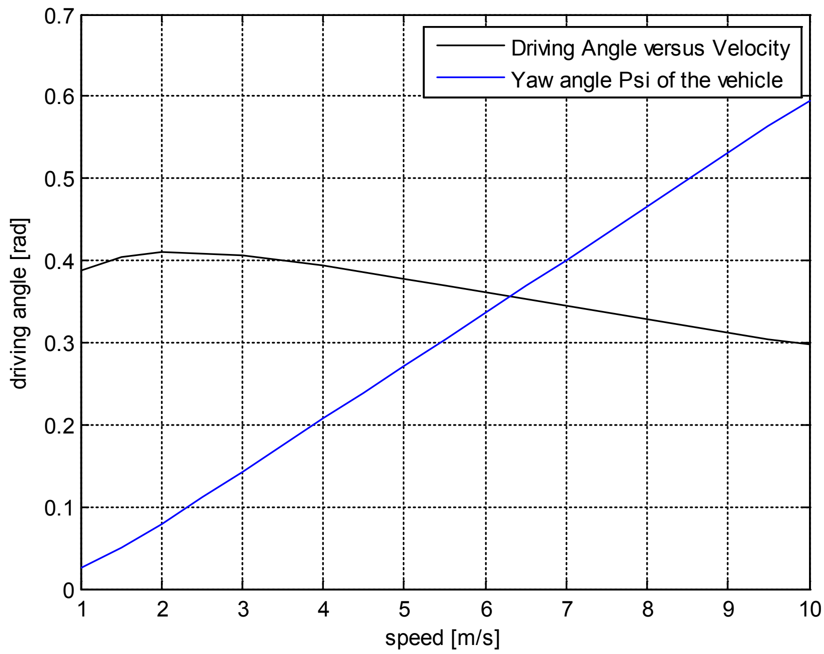

Figure 3.10: Driving angle and the yaw angle ψ versus velocity of the vehicle.

3.5 Interaction model

The interaction model is relevant on a time-horizon of a few seconds, depending on the actual road segment or square. Therefore, this study implements two layers of interaction models:

- Tactical layer: Conflict resolution
- Operational layer: Extended social force, distance keeping, small corrections

This hierarchical approach should guarantee interaction between road-users when there is multiple seconds of foresight and a continuous reaction to environment and road users at the tactical level. Other agents and therefore interactions are not handled at the strategic level. The tactical interaction model is in charge of maintaining distance to other agents in non-conflicting interactions, and of making corrective movements in the conflict situations.

In chapter 3.1.4, item 1 and 6 are the most important in the estimation of the normative situation. The agents must gain the information about the position of the conflicting agent and its intention. That requires a spatial analysis of the agent's position and direction. From an algorithmic perspective, both aspects (of right of way) can be covered by determining whether a point lies to the left or right of a line. The line is the trajectory of the first agent i where the point is the position of the second approaching agent j. Due to the terms *left* and *right*, an orientation for the line is needed: Two points on the first agent's (i) trajectory are assigned to be $A(x_1, y_1)$ and $B(x_2, y_2)$, where it is moving from A to B. $M(x_0, y_0)$ is a point in the trajectory of the approaching agent j. Let there be

$m = (x_2 - x_1) * (y_2 - y_1)$ a rectangular, $p_1 = (x_0 - x_1) * (y_0 - y_1)$ a second rectangular, $p_2 = (x_2 - x_0) * (y_2 - y_0)$ another rectangular and $p_3 = (x_2 - x_0) * (y_0 - y_1) * 2$ then two rectangulars.

- $m = p_1 + p_2 + p_3$: the point is on the line (no clear result possible)
- $m < p_1 + p_2 + p_3$: the point is left, agent i has $N_i = 1$ and $N_j = 0$
- $m > p_1 + p_2 + p_3$: the point is right, agent j has $N_i = 0$ and $N_j = 1$

In addition, for pedestrians the relevant regulations are extracted from §76 (Republik Österreich, 1960).

- Pedestrians must use sidewalks. If there are no sidewalks, they have to use the outermost area of the road.
- If there is no designated pedestrian crossing or traffic control systems, pedestrians are allowed to enter the main lane only when they do not endanger other road users.
- Pedestrians must cross in adequate speed and in a direct path.

Applying this rule–set, an pedestrian-agent i has N_i = 0, if agent j represents a vehicle (regardless if car or bicycle). An agent i owning ROW N_i = 1 is always allowed to waive its ROW N_i = 0. This possibility offers space for social-minded behavior.

3.5.1 Moving as tactically intended

To put the tactical strategy into action, an additional force $\vec{f}_{Tactics}(t)$ is added to the existing forces. Hence, the resulting force vector $\vec{f}_{(}t)$ of each agent is the vectorial sum of the forces of the infrastructure guiding field $\vec{f}_{Guide}(t)$), of the adapted SFM related force $\vec{f}_{SF}(t)$ and the new tactical force $\vec{f}_{Tactics}(t)$:

$$\vec{f}(t) = \vec{f}_{Guide}(t) + \vec{f}_{SF}(t) + \vec{f}_{Tactics}(t) \tag{3.33}$$

The following sections describe this tactical conflict solving system. First, it is needed to explicitly detect situations where a possible conflict between agents occurs that, cannot be handled by the standard operational model. Each conflict has potential solutions such as stopping or dodging/evading to the side. A Stackelberg game (von Stackelberg, 1952) is run to decide what strategy has the highest pay off.

3.5.2 Defining tactical conflicts

In transportation engineering, a standard definition of a road traffic conflict is that "*a conflict consists of an interaction between two road-users (or between one road-user and the road environment) that would shortly lead to a collision unless at least one of the road-users involved performed an evasive action*" (Muhlrad, 1993, p. 53). In order to transfer this definition from the the field of Traffic Conflict Technique (TCT) into simulation models, three point have to be specified on each trajectory:

- Point of recognizing the conflict
- Point of initializing any reaction
- Estimated point of conflict

Here, the definition of conflict is extended to non-emergency situations, while keeping the TCT's definitions of objective measures and the conflict decision point.

3.5.3 Conflict detection

Conflict detection is done in regular intervals. Intervals between 1-5 second seems to be a reasonable trade-off between detection and processing effort - the final value will be derived from empirical observation. Each agent is simulated individually without taking any other agents into account. The resulting trajectories indicate the exact path that would be taken, if no other agents were involved in the scene. All these trajectories are then compared to find pairs of agents that are conflicting in time and distance. Other agents within a certain radius are considered to be relevant for interaction.

Two steps are applied:

- **Step 1:** Trajectories intersect at a point $\hat{C}$ at a proximity below $t_{C,min}$
- **Step 2:** Trajectories do not intersect, but positions of $r_i - r_j$ gain proximity below $d_{C\,min}$ AND $t_{C,min}$

Step 1: Identify the point of intersection: State vector of agent i X_i contains a set of coordinates $P_{i(t)}$ and agent j X_j contains a set of m coordinates $P_{j(t)}$. Method 1 looks for any intersections between the section $\overline{P_{i(n)}\ P_{i(n+1)}}$ and $\overline{P_{j(m)}\ P_{j(m+1)}}$. To do the geometrical test, let's pick P_1 out of $P_{i(n)}$ and P_3 out of $P_{j(m)}$ (P_2 and P_4 analogously). The equations $P_a = P_1 + u_a(P_2 - P_1)$ and $P_b = P_3 + u_b(P_4 - P_3)$ introduce the two unknowns u_a and u_b. P_a and P_b meet in $\hat{C}$ under the following condition:

$$x_1 + u_a(x_2 - x_1) = x_3 + u_b(x_4 - x_3) \tag{3.34}$$

and

$$y1 + u_b(y2 - y1) = y3 + u_b(y4 - y3) \tag{3.35}$$

Solving the equation for u_a and u_b yields:

$$u_a = \frac{(x_4 - x_3)(y1 - y3) - (y_4 - y_3)(x_1 - x_3)}{y_4 - y_3)(x_2 - x_1) - (x_4 - x_3)(y_2 - y_1)} \tag{3.36}$$

and (with the same denominator as in equation 3.37)

$$u_b = \frac{(x_2 - x_1)(y1 - y3) - (y_2 - y_1)(x_1 - x_3)}{y_4 - y_3)(x_2 - x_1) - (x_4 - x_3)(y_2 - y_1)} \tag{3.37}$$

respectively. Since the target is to find the intersection $\hat{C}$ of line segments (not lines) the values of u_a and u_b must lie between 0 and 1. Whichever one lies within that range then the corresponding line segment contains the intersection point. If both lie within the range of 0 to 1 then the intersection point is within both line segments. In addition, the estimated arrival time has to fulfill: $t_{i\hat{C}} - t_{j\hat{C}} < t_{C\,min}$. It is obvious that this approach is not able to detect all conflicts.

Step 2: Identify proximity of positions: In the second (alternative) step, both the "critical" spatial distance $d_{C\,min}$ and the time interval have to be met. The following pseudo-code explains the procedure:

```
procedure DetectConflict(X_i, X_j)          ▷ Returns the conflicting agent's id
    for all agents i do
        C_i = 0
        for all agents j ≠ i do
            if ||r_i − r_j|| < d_C min then
                if C_j = 0 then
                    C_i = j
                end if
            end if
        end for
    end for
end procedure
```

Its not a straightforward calculation of the Frèchet distance[1], but also includes temporal considerations. Based on simple geometrical and kinetic thoughts, the combination of adequate spatial distances and time windows are important.

Once a conflict has been predictively identified, the conflict is parameterized with the agents' state vectors, path, and the normative situation. The angular classification is the first estimation before further processing is done. Three types of conflicts are distinguished: **Perpendicular**, **Head–On** and **Rear**. For each type, a different method is created to fill the game matrix .

3.5.4 Conflict strategies

Simplification of Strategies

Due to simplification issues, the possible conflict-resolution strategies are reduced to a number of five. Figure 3.12 drafts the spatial conflict situation and its strategy alternatives.

Without reacting, proximity of two agents i and j would drop below $d_{C\,min}$ when reaching point s_{i1} and s_{j1}, respectively. In the moment, the conflict is identified, agent i is located at s_{i0} and agent j at s_{j0}. In a spatial context, the five strategies of agent i are s_{i1} to s_{i5}. The alternatives of agent j are not shown in order to keep the overview as simple as possible. Besides the strategy to continue along its path (s_{i1}), the strategies

[1] In mathematics, the Frèchet distance is a measure of similarity between curves that takes into account the location and ordering of the points along the curves. It is named after Maurice Frèchet.

Figure 3.11: For two situations, the "continue" strategy S_{CONT} paths (blue) and the observed paths (yellow marked) are drawn. The red ring marks the detected conflict point. LEFT: A cyclist evades and lets the pedestrian cross. RIGHT: A crossing pedestrian evades, while the car continues.

of decelerating, accelerating and evade left or right are considered. The pay-off values are given by exogenous variables, which includes speed, type of agent, time to the theoretical collision, the ideal path and rule-sets in the traffic regulations.

For all strategies S_i and S_j, the spatial vector matrix-pair R_i, R_j and the velocity matrix-pair V_i, V_j has to be estimated based on the strategies' predicted trajectories. This could very well be the most challenging and sensitive part in the tactical interaction model.

The point D_i and D_j are obtained from $X_i(t_d)$ and $X_j(t_d)$ where $t_d = t_c - t_{preview}$. The preview distance is estimated by observing the empirical $t_{preview}$ in evading scenarios of vehicles.

The mean time in own observations is 2.7 s. This value is the time between the observable reaction and the estimated TOC, it does not include information processing and reaction time. In addition, an experiment shows the fit of the calibrated model using values between 1 s to 3 s, the sensitivity of this parameter within this range is low. Table 3.1 shows the compatibility of traffic modes with strategies. In most situations, constrained by infrastructure or situation, car drivers are only able continue or brake. In an urban

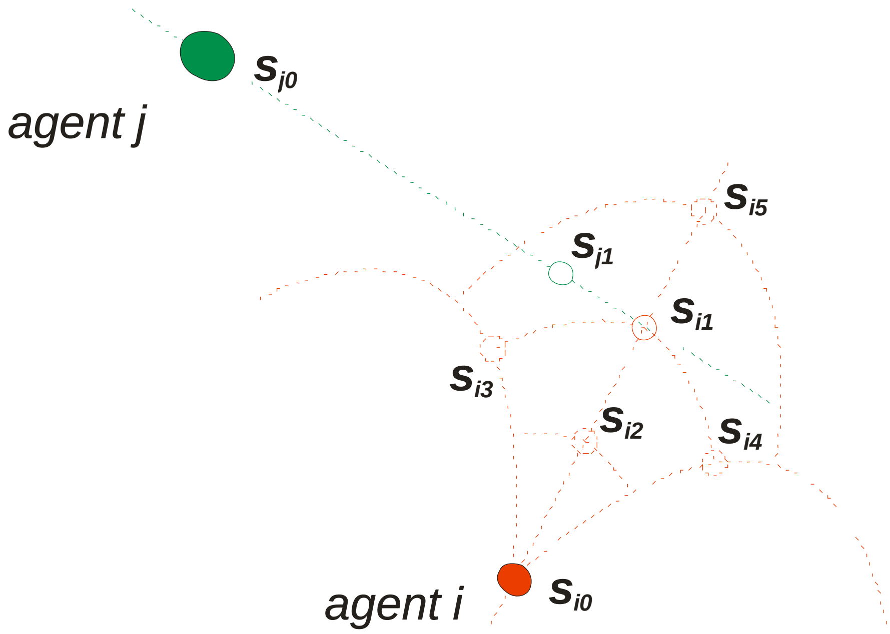

Figure 3.12: Simplified drawing of the possible strategy paths of agent i. The scheme illustrates the alternative S_{i5} (*accelerating*) as well, which was not observed in real shared space traffic flows.

context, car drivers usually do not accelerate to avoid conflict. Cyclists usually have more available strategies, depending on the circumstances. Pedestrians have the full set of alternatives and also choose more freely.

	car	**bicycle**	**pedestrian**
car	only continue + braking	continue + braking	continue + braking
bicycle	+ evading left (right)	all strategies	all strategies
pedestrian	all strategies	all strategies	all strategies

Table 3.1: Possible strategy pairs of mode combination.

The acceleration strategy was not further applied as it was not observed in the field. To illustrate the constraints in the available set of strategies, figure 3.13 demonstrates the conflict detection in the left picture and the available set of strategies is shown in the right scheme.

In figure 3.13, each agent can choose from different strategies: a pedestrian can continue, walk left or right or stop. Cars can only continue or stop in this game. In this particular example, the car stops and the pedestrian continues.

Strategy CONTINUE

When picking strategy $s_{i,CONT}$ and $s_{j,CONT}$, the agent does not change its reaction to solve the conflict; either the empirical path is used or a hypothetical path is estimated

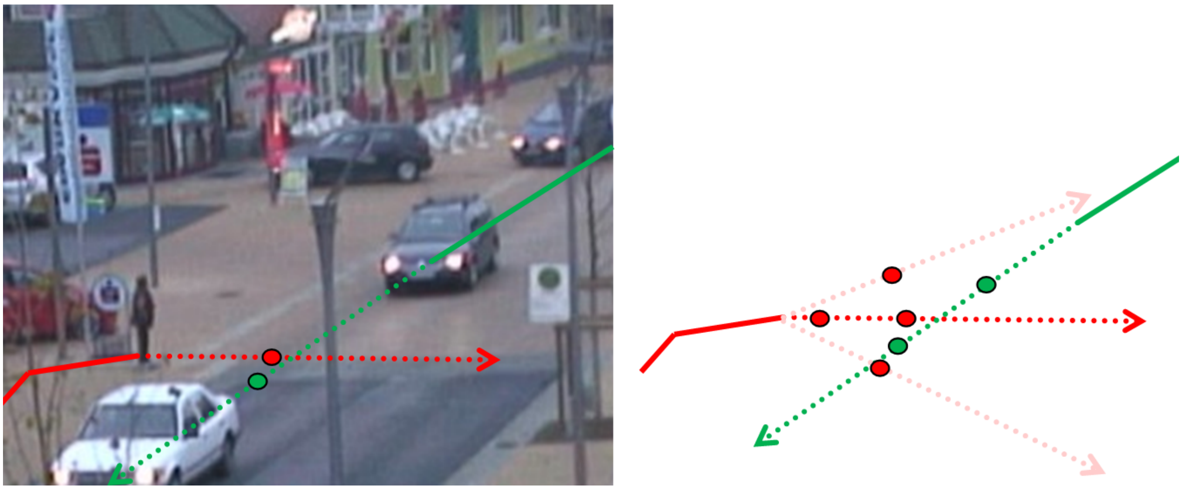

Figure 3.13: A conflict is detected whenever two agents want to occupy the same area within a similar time interval in the near future. Solid lines indicate past trajectory data of the agents, dotted lines simulated future positions. The circles indicate the projected position at the same time.

considering $v_i d$ or $v_j d$ respectively and the destinations' position and direction:

$$\overrightarrow{S_{i,CONT}} = C_{ij} \;\; and \;\; \overrightarrow{S_{j,CONT}} = C_{ij} \tag{3.38}$$

$$\overrightarrow{v(S_{i,CONT})} = X_i(t_c) - X_i(t_c - 1) \;\; and \;\; \overrightarrow{v(S_{i,CONT})} = X_j(t_c) - X_j(t_c - 1) \tag{3.39}$$

Strategy STOP

The agent yields to the other agent. Here, $s_{i,BRAKE}$ and $s_{j,BRAKE}$ describe the agents' path upon deciding to decelerate at $a_{brake} < 0$, where a_{brake} depends on the agent' s speed. The agent does not alter his course to solve the conflict.

Directions Θ_i or Θ_j are maintained, which leads to $a_{brake} = k_b * v_{i,mean}$. For bicycles k_b is replaced by $k_{b,bicycles}$.

$vi, mean, vj, mean$ are scalar variables gained in a time window of 1 s around the $C_i j$. The spatial vector from D_i is: $R_{i,BRAKE} = a_{brake} * t^2_{preview}/2$[2].

$$\overrightarrow{S_{i,BRAKE}} = D_i + R_{i,BRAKE} \;\; and \;\; \overrightarrow{S_{j,BRAKE}} = D_j + R_{j,BRAKE} \tag{3.40}$$

$$\overrightarrow{v(S_{i,BRAKE})} = X_i(t_c) - X_i(t_c - 1) \;\; and \;\; \overrightarrow{v(S_{j,BRAKE})} = X_j(t_c) - X_j(t_c - 1) \tag{3.41}$$

Breaking is a suitable strategy for all modes (both drivers and pedestrians).

[2]Generic equation for length of brake path: $x = a * t^2/2$.

Strategy LEFT

$s_{i,LEFT}$ and $s_{j,LEFT}$ describe the agents' path upon deciding to laterally evade at an angle α_{LEFT}. This angle is the key-parameter in this heuristic. The agent is he changing the speed due to obstacles or to follow a particular. It is continuing on $v_i d$ or $v_j d$ respectively. The rotation matrix for the evading movement vector of angle k_α is:

$$R_\alpha = \begin{bmatrix} \cos(k_\alpha) & \sin(k_\alpha) \\ \sin(k_\alpha) & \cos(k_\alpha) \end{bmatrix} \tag{3.42}$$

The spatial vectors and speed vectors are:

$$\overrightarrow{S_{i,LEFT}} = R_\alpha * (C_{ij} - D_i) \ \ and \ \ \overrightarrow{S_{j,LEFT}} = R_\alpha * (C_{ij} - D_j) \tag{3.43}$$

$$\overrightarrow{v(S_{i,LEFT})} = \overrightarrow{S_{i,LEFT}}/t_{preview} \ \ and \ \ \overrightarrow{v(S_{j,LEFT})} = \overrightarrow{S_{j,LEFT}}/t_{preview} \tag{3.44}$$

Strategy RIGHT

$s_{i,RIGHT}$ and $s_{j,RIGHT}$ describe the agents' path upon deciding to laterally evade at an angle α_{RIGHT} reaction. The agent does not alter her course to solve the conflict nor is he changing the speed and direction due to obstacles or to follow a particular. She is continuing on $v_i d$ or $v_j d$ respectively. Directions Θ_i or Θ_j are maintained. The rotation matrix for the evading movement vector is the same as for the left side (equation 3.42), but used inversely. The spatial vectors and speed vectors are:

$$\overrightarrow{S_{i,RIGHT}} = R_\alpha^{-1} * (C_{ij} - D_i) \ \ and \ \ \overrightarrow{S_{j,RIGHT}} = R_\alpha^{-1} * (C_{ij} - D_j) \tag{3.45}$$

$$\overrightarrow{v(S_{i,RIGHT})} = \overrightarrow{S_{i,RIGHT}}/t_{preview} \ \ and \ \ \overrightarrow{v(S_{j,RIGHT})} = \overrightarrow{S_{j,RIGHT}}/t_{preview} \tag{3.46}$$

In both strategies s_{LEFT} and s_{RIGHT}, for cyclists, another parameter α is set. Usually, evading is a suitable strategy for non-motorized agents (pedestrians and cyclists).

Strategy ACCELERATE

The agent accelerates to avoid the conflict with the other agent. Here, $s_{i,ACC}$ and $s_{j,ACC}$ describe the agents' path upon deciding to accelerate at $a_{acc} > 0$. The agent does not alter his course to solve the conflict.

Directions Θ_i or Θ_j are maintained, which leads to $a_{acc} = k_a * v_{i,mean}$. For bicycles k_a is replaced by $k_{a,bicycles}$.

$v_{i,mean}$, $v_{j,mean}$ are scalar variables, gained in a time window of 1.0 s at $C_i j$. The spatial vector from D_i is: $R_{i,ACC} = a_{acc} * t_{preview}^2/2$.

$$\overrightarrow{S_{i,ACC}} = D_i + R_{i,ACC} \ \ and \ \ \overrightarrow{S_{j,ACC}} = D_j + R_{j,ACC} \tag{3.47}$$

$$\overrightarrow{v(S_{i,ACC})} = X_i(t_c) - X_i(t_c - 1) \ \ and \ \ \overrightarrow{v(S_{j,ACC})} = X_j(t_c) - X_j(t_c - 1) \tag{3.48}$$

Remark: ACCELERATE is a theoretical strategy that could not be observed in the field.

Generation of a Proper Path

Previously, $\overrightarrow{S_{i,x}}$ and $\overrightarrow{v(S_{i,x})}$ have been presented. In order to smooth the path and to extend it to the target, a shape - preserving piecewise cubic interpolation is applied to the drafted paths. The three input coordinates are D_i, $\overrightarrow{S_{i,x}}$, $X_i(end)$ and D_j for agent i as well as $\overrightarrow{S_{j,x}}$ and $X_j(end)$ for agent j.

3.5.5 Choice of Strategy

Thoughts and Background

From a system-wide perspective, the optimum lies within one common goal. Distributed planning, task sharing (Gasser and Huhns, 1989) and distributed planning algorithms (Yokoo, 2012; Doniec et al., 2005) follow a cooperative approach to optimize the interactions, i.e. at a traffic intersection. Few of these studies are available in the more recent field of multi-agent simulation, where every driver tries to achieve his or her own goal. Champion et al. (2001) and Doniec et al. (2006) present a competitive coordination mechanism dedicated to road traffic simulation.

Doniec et al. (2008) state that studies of driving psychology could enrich multi-agent models for traffic simulation. It could provide a better understanding of the underlying reasons in real driver decision-making by revealing specific facets and characteristics of driver behavior (Björklund, 2005). For instance, they show that drivers tend to:

- Maintain their desired speed and their lateral position in the road
- Act differently depending on the region in the world (Summala, 2005)
- Show varying respect for traffic regulations depending on the road's design, etc.

Doniec et al. (2008) propose a multi-agent behavioral model for microscopic traffic simulations. This model has its roots in the authors' work in 2006 where algorithms consider drivers' anticipation of traffic situation at intersections. The aim of the research was to examine: How to avoid deadlocks within pairs of drivers.

Conflict resolution at traffic-light controlled road intersections is a very deterministic process. Violations of traffic regulations are quite rare and hardly affect the traffic flow. At junctions without road lights and conventional designs the road signs and traffic regulations clearly control the right-of-way behavior. However, shared space and Begegnungszonen aim to increase the cooperation of pedestrians and drivers, supported by road design. By observing road conflicts and outcomes, both social and a competitive behavior can be identified (Schönauer et al., 2012b).

Interaction processes on the tactical level are modeled based on game theory. Game theory has previously been applied to road traffic interaction in urban contexts by Zhen-long and Liquan (2008); Zhen-long and De-wang (2003), where gap acceptance behavior on highways was modeled. While both publications aim for optimization on a strategic level from an operators' point of view, Kita (1999) formulated a game for car conflicts.

Application in Heterogeneous Traffic Situations

Applying such a game here, it must first be amended for handling multi-modal conflicts. To describe this situation as a game, the following aspects need to be specified:

- Number of players (agents)
- Number of repetitions until the conflict is settled
- Information (transparency of decisions)
- Type of cooperation
- Symmetry of the game

First, the number of players is considered. The behavior of a pair of agents *i,j* in conflicts influences both partners as well as the traffic participants surrounding them. Both original partners are in turn influenced themselves by the reaction of the surrounding agents, and consequently all the agents in the vicinity of the conflicting partners can be recognized as interacting players. For the objective purposes, the number of games is assumed to be one for each of the agent pairs in conflict, and the games are assumed to be independent from one another. In a scene every agent can be in a game and each game is restricted to only two partners. This is because the amount of time that the agent has to make a decision is long enough to make multiple decisions, and because each decision is not affected by preceding or following decisions, but is rather made independently.

The second characteristic to be specified is the number of games to be repeated. For our purposes it is assumed that there is only a single game for each of the agent pairs in conflict, and the games are independent from one another. This is because the amount of time that the agent has to make a decision is not so long that it can make multiple decisions, and because each decision is not affected by preceding or following decisions, but rather is made independently.

Thirdly, the transparency of pay-off matrices has to be defined. On the background of the "principle of reliance", an agent can assume that every other agent has the same mutual interest to settle the conflict at a similar set of perception. Both agents can understand the situation that the other agent is facing. The game can therefor be defined as a game of perfect information, the drivers or pedestrians know the strategies of each other.

Finally, the possibility of receiving information about the other agent suggests the potential of cooperation. The agents, however, have no way to exchange their decisions on strategies, and consequently the game is characterized as a non-cooperative game. Observing traffic situations, it often can be seen that one of the road users initializes the reaction - the other agent follows. But in most scenarios, it is not obvious who might be the agent that starts. To bring answers to this very question, a non-symmetric hierarchical game with leader and follower players is used. The initial leader, who holds the powerful position, announces her strategy, and followers react to the leader's announced strategy.

Summarized, the game is specified as:
Non-cooperative, **leadership** game, **2 agents**, **perfect information**, and **no repetition**.

Pure Strategy

Kita (1999) formulated a game for car conflicts. Here, such a game is extended for handling multi-modal conflicts. The presented approach to resolve conflicts is based on rational game play. The available strategies are continue (without physical reaction to the interaction), brake (or stop), avoid left side, avoid right side. For each strategy pair, both players obtain a certain utility - the game matrix. The game is based on random utility maximization. For the game, it is assumed that both players have full information about the deterministic part of the utility of the other player. As a result, the leader knows the expected outcome of any of their actions and decides on their strategy by maximizing that expected utility. The follower reacts to the leader by choosing the strategy that offers the highest available utility. The leader's decision is triggered by maximizing the random expected utility that is defined as:

$$v_L(i) := E_F[u_l(i)] + \epsilon_{Li} := \sum_j u_L(i,j) P_F(j|i) + \epsilon_L(i) \tag{3.49}$$

where $u_L(i,j)$ is the utility of the leader if it chooses strategy i and as a reaction the follower chooses strategy j, $P_F(j|i)$ is the conditional probability that the follower conditionally chooses j when the leader chooses i and $\epsilon_L(i)$ is the unexplained, random part of the utility of the leader. At a game of pure strategies $\epsilon_L(i) = 0$.

Note: The indices i and j have been used to address the agents in the previous sections. In the game-theory context, i and j are used as the strategies' indices.

Mixed Strategy and its Setup

It is obvious that in identical situations different drivers or pedestrians will act differently, or even the same driver might choose differently at another time. This stochastic is considered in the game by introducing so-called mixed strategies. The strategies of the leader and follower are then drawn using the probabilities above.

The utility of the follower when choosing j is given as $u_F(j|i)$ as the utility of the decision for j conditional on the leader choosing i. Again, there is a random part ϵ_{Fj} contained in the utility. To guarantee the applicability of the Logit model, the random parts of the utilities $\epsilon_L i$ and $\epsilon_F j$ are assumed to be distributed according to an extreme value distribution. Accordingly, the conditional probability $P_F(j|i)$ can be calculated as:

$$P_F(j|i) = \frac{exp(u_F(j|i))}{\sum_k exp(u_F(k|i))} \tag{3.50}$$

Similarly, the probability of the leader choosing i is given as

$$P_L(i) = \frac{exp(u_L(i))}{\sum_k exp(u_L(k))} \tag{3.51}$$

The pure strategy defines a specific move or action that a player will follow in every possible attainable situation in a game. Here, that means:

- The moves may not be random, or influenced by a random variable
- The moves are not drawn from a (probability) distribution

The leader picks a single strategy to gain its highest utility $u_L(i)$ at the highest $P_L(i)$. Accordingly, the follower picks a single strategy of its highest utility $u_F(i)$ at the highest $P_F(i)$.

Setup of Utilities and the Game Matrices

Each utility is defined as a weighted sum of the following thematic utilities and disutilities:

- V_{ij}: Velocity dependent disutility based on the relative speed vectors of all pairs of strategies of the leader and follower. This disutility does not consider the spatial distance of the agents trajectories and positions respectively. The disutility is calculated as $-exp(v_{ij}^{rel} - max_{nm}(v_{nm}^{rel}))$, where v_{ij}^{rel} is the relative speed after following the strategy pair S_{ij}. The cell value is 0 when the agents are moving away from each other ($v_{ij}^{rel} < 0$). The background is the intention of both agents to minimize risk and and danger. Remark: The kinetic energy - that would be transformed to deformation energy in collisions - is proportional to v_{ij}^2.
- R_{ij}: Distance related disutility, calculated as, length of the spatial relative vector of collision probability disutility coming from distance, utility calculated as $-exp(r_{ij}^{rel} - max_{nm}(r_{nm}^{rel}))$, where r_{ij} is the closest distance between the agents after following the strategy pair S_{ij}.
- SU_{ij}^L, SU_{ij}^F: Social utility for agents i, j given as $SU_l(i,j) = 1$ when the decision (i,j) is supported by social convention and 0 otherwise. Social convention means the defensive strategy towards a road–user of a lighter mode of transport. The weights are - in descending order - the following: Car - Cyclist - Pedestrian. This assumption is simply based on the average physical weight.
  In example, for a car it is socially preferable to let the pedestrian cross the street. At conflict of road-users of identical mode of transport, the defensive strategy (STOP) is considered to be social. At the strategies left, right the positions of the agents is included into the calculation. If the position and direction of movement allows a dodging maneuver behind the other agent (less disturbing) the equivalent s_{ij} is set 1. The social utility is included in the this way: $exp(s_{nm}^P - max_{nm}(s_{nm}^P)$.
- E_{ij}^l, E_{ij}^f: Energy loss disutility (zero-strategy = 0) of the agents i, given as the negative absolute value of the velocity change. Average weights of vehicles are

not considered here. It seems more relevant to This component is equivalent to the square root of the kinetic energy loss $-exp(|v^P_{nm}| - |v^P_{11}|)$.

- N^l_{ij}, N^f_{ij}: Normative utility according to traffic regulations (give way etc.).
  Shared Space: Within this component, the pedestrians crossing the road always gain 0 except the vehicles having to stop to let them cross. If the strategies left or right allow a crossing of the road without disturbing vehicular traffic the corresponding n^P_{nm} is set to 1.
  Begegnungszonen: Pedestrians gain 1 for all strategies in all conflicts. Bicycles gain 1 for all strategies in conflicts with cars. Cars gain 1 only for defensive strategies. The normative utility is considered as: $exp(n^P_{nm} - max_{nm}(n_{nm}P))$.

It is assumed, that not all aspects count in similar relevance during conflict solving. Therefore, a set of weights $[\theta_V, \theta_R, \theta_S, \theta_E, \theta_N]$ is introduced. For agents at decision S_{ij}, the utilities are now:

$$u_L(i,j) = \theta_V V_{ij} + \theta_R R_{ij} + \theta_S SU^L_{ij} + \theta_E E^L_{ij} + \theta_N N^L_{ij} \tag{3.52}$$

and similarly for $u_F(i|j)$.

The components above are calculated by simulating the decisions using path estimators, described in the previous section. Parameters such as speeds are then derived from the resulting trajectories. The weights require calibration. The estimation methodology and the data used for calibration are described in the next chapter.

Solving the Game

In the first step, a pure deterministic model is described that will later on be extended with stochastic choice in mixed strategies. The presented conflict solving approach is based on a rational game play. This means, for the same input variables, the game has a deterministic outcome. The Stackelberg game, originally introduced to model unbalanced markets, is a non-symmetric hierarchical game with leader and follower players (von Stackelberg, 1952). The leader holds the powerful position and announces her strategy, and followers react to the leader's announced strategy. Due to the perfect information, the leader knows a-priori that followers answer to his own strategy. Below is a simplified illustration of a crossing conflict in road traffic: The car driver knows that the pedestrian will stop if possible should the driver continue with full speed. In the proposed model, a lower car speed, and normative and social aspects can shift the leader's optimum towards stopping.

Solving the Stackelberg model is done by finding the Subgame Perfect Nash Equilibrium (SPNE), after calculating the best response functions of the follower. The SPNE can be deduced by backward induction. The sets of options the two players can choose from is denoted as S_i for the leader and for the S_j follower. Let $u_i(s_i, s_j)$ be the utility of the leader when the option $s_i \epsilon S_i$ is chosen and the follower reacts by the move $s_j \epsilon S_j$ and similarly $u_j(\acute{s}_j|s_i)$ the utility of the follower is dependent on the choice of the leader. Let β_j be the set of best answers to S_j.

$$\beta_j(s) := \{\acute{s}_j \epsilon S_j | u_j(\acute{s}_j|s_i) = max_k u_j(s_k|s_i)\}, \tag{3.53}$$

Then the SPNE S_i^{eq} is stable for both players, providing that player i chooses the maximum of the utilities dependent on the choice set $\beta_j(s)$ of the follower j:

$$s_i^{eq} = max_{s_i \epsilon S_i}(u_i(s_i, \beta_j(s))) \tag{3.54}$$

It's likely that within the same situation different individuals would act differently and a stochastic component could include this random behavior. Both s_i and β_j can be replaced with probability vectors $P_L(i)$ and $P_F(j|i)$. In game theory this approach is called mixed strategies, the international encyclopedia of social sciences describes the mixed strategy as following (Saenz et al., 2007): "In game theory a player is said to use a mixed strategy whenever he or she chooses to randomize over the set of possible strategies." Formally, a mixed strategy is a probability distribution that assigns a likelihood to each available action. If only one action has a positive probability of being selected, the player is said to use a pure strategy. A mixed strategy profile is a list of strategies, one for each player in the game. A mixed strategy profile induces a probability distribution or lottery over the possible outcomes of the game. Nash (1951) contributed a definition of a mixed strategy Nash Equilibrium for any game with a finite set of actions. He proved that at least one mixed strategy Nash Equilibrium must exist in such a game. The outcome of the game can be described as:

$$P(i, j) = P_L(i) * P_F(j|i). \tag{3.55}$$

The simulation then draws a random number r_j to chooses the multiple strategy vectors for the follower $P_F(j|i)$ then r_i chooses within the single probability vector $P_L(i)$.

The importance of using mixed strategies for modeling interactions in road traffic can be described by the two following stochastic phenomena:

- Different individuals do not act or react in the same way in similar situations
- Individuals' behavior varies dependent on external and intrinsic influences (trip purpose, mood, etc.).

Those reasons outline the importance to generate full probability vectors for each the leader and the follower agent. Examples about the dynamic within the 2 strategy vectors are shown in the results.

Definition of Leader and Follower

The definition of follower and leader is assumed to be dependent on the situation of the conflict. Based on available parameters, following aspects or any combination of them could influence the way how the leader is defined:

- Speed: The faster agent is representing the leader (higher speed dominating).
- ROW: According to the traffic regulations.
- Distance: The agent who is closer to the conflict point - in terms of time.
- Weight: Either the "heavier" or the "lighter" agent (its mode) who leads.

The most suitable definition is expected to be found during the calibration using empirical data.

4 Model Implementation

This chapter drafts the integration of software into the VISSIM based framework and shows the essential elements of the written code. The alternatives to implement the model and simulation algorithms range from prototyping in MATLAB combined with simplified two-dimensional graphics to developing own of-the-scratch frameworks including editors and visualization features. For this work, the decision has been made towards VISSIM and its proprietary interfaces to run the model's code. There are multiple strategic intentions to use a major simulation toolkit :

- Use of calibrated SF models
- GUI to edit and visualize the infrastructure and parameters
- Features to visualize the simulation (2D and 3D)
- Faster prototyping

From a software engineering perspective, this approach does not represent the trivial path. Even though rudimentary specifications exist, a lot of effort is invested in understanding and wrapping the *DLL* interfaces. Debugging abilities are widely lost due to the use of the external *DLL*. On the other hand, the visual performance of VISSIMs editor and three-dimensional models make them useful tools in observing the simulation experiments and offer valuable features for presenting the results.

4.1 System architecture

Within the system framework, the new model libraries are positioned in the proprietary data flow between VISSIM and the program library *pedestrianmodel.dll* (both PTV AG). The interface, the simulation process and specific parts of the model functions are used, extended or replaced with own modules. In figure 4.1, the implemented architecture is drafted. Usually, VISSIM interacts with its *pedestrianmodel.dll* (red flow-arrows). Here, VISSIM interacts via the green arrows with own code of *pedestrianmodel.dll*, which again interacts with PTV's *pedestrianmodel.dll*.

Two parts of VISSIM are utilized: The editor and simulation framework is used to generate the infrastructure model, the demand, and other behavioral parameters (desired velocity, acceleration, weight etc.), while the pedestrian model provides social force implementation, path finding and certain parameters related to pedestrian behavior. This chapter shows the implementation of the two-level tactical planner for pedestrians and vehicles in the mixed traffic plane with obstacles. The first level applies social force, implementing the Ordinary Differential Equation (ODE) approach by using a "sensing-mode" (simulation runs) to predict all agents' positions over n time-steps. The

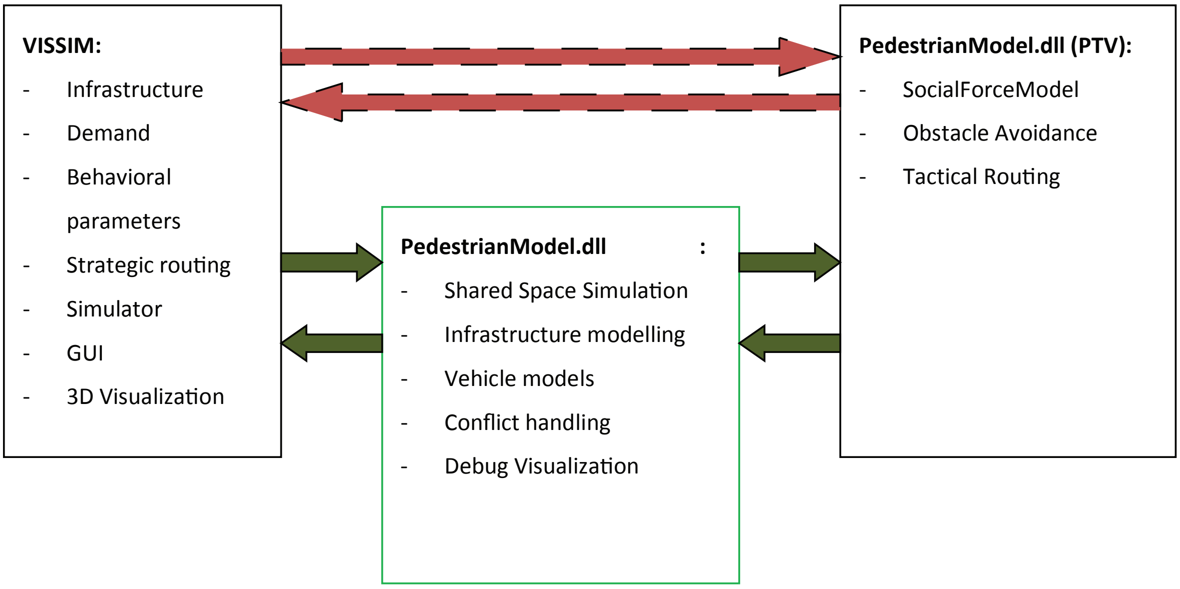

Figure 4.1: System architecture of the implementation using VISSIM. The pedestrianModell.dll from PTV is wrapped and included into the own library architecture.

second level introduces a set of tactical methods to estimate the best conflict avoidance strategy.

In order for the social force model to work well for pedestrian simulations, a mixed traffic model must include projections to model traffic behavior at high speeds (up to 50 km/h). The simulation process is a sequence of both logical decisions and continuously connected elements. Unlike the pure SF model in our approach, the sensing simulations prepare the choice of conflict resolution strategy and according actions.

The core of the simulation is the extended, continuously triggered SF sensing. Sub-frequent cycles, the so called "sole sensing" identify conflicts in agents' trajectories. If this check is positive, the conflict is analyzed and a tactical game-matrix is set up. The game decides what actions to be set for each agent and the agents' movement is controlled accordingly.

4.2 Interfaces and Processes

The object-orientated design includes an interface to VISSIM, a wrapper to the *pedestrianmodel.dll* and about 200 new functions that are distributed in four main classes and more than ten auxiliary classes. The main classes are *Agent*, *Object*, *SensingRun* and *Conflict*. In figure 8.26 (appendix), the full class-model is illustrated, as automatically created by the tool Doxygen[1].

The infrastructure is defined with the *Object* class, which fully describe the geometrical and qualitative outline of the roads' surface, obstacles and zones. The editor of VISSIM

[1]Doxygen is a tool for generating documentation from annotated C++ sources.

is used to design the polygonal objects; project-specific parameters are encoded in the object's name. In the own software, a parser reads this tags and assigns it accordingly.

The central module is the class *Agent*, member of the *AgentContainer*. This class contains all the individual parameters, either the car or the bicycle physics and some interactive behavior. The overall simulation engine is provided by VISSIM: the self- made sub-simulation engines *SensingSim* and the *InteractionAnalyser* do sub-frequent simulation steps during single simulation cycles.

Based on the VISSIM manual (PTV AG, 2010) and code templates for a third party Dynamic Link Library (DLL) for the VISSIM release 5.20, there are several requirements for an external DLL and for the wrapping of the existing *pedestrianmodel.dll*. VISSIM requires a whole set of handshakes and acknowledgments during the initialization and the entire simulation run. The next section roughly describes the simulation process, which consists of an initializing phase and a simulation phase.

4.2.1 Pedestrian Simulation Run in VISSIM

The generic pedestrian simulation initialization phase in VISSIM transfers the whole static simulation data to the external DLL. In the following sequence all static objects and simulation parameters are included:

- Simulation: Status, type, path, parameter file, time step, time, random seed
- Static objects: Name, obstacle, source, intermediate, destination, waiting time, all vertex coordinates

At the generation of a new agent (this emerges also at any move onto a new polygon), all static parameters and initial dynamic parameters are transferred.

- Agent's static parameters: ID, length, width, height, weight, desired velocity, maximum acceleration, type, color
- The route of the agent is described by the origin polygon id, next destination polygon id, idle time at the next most polygon
- Agent's dynamic parameters: front 3-dimensional coordinates, rear 3-dimensional coordinates, wants to leave network

4.2.2 Single Pedestrian Object

In the new model, all agents from VISSIM point of view are considered as pedestrians. The visual vehicular appearance is achieved with larger dimensions for the three dimensional models of bikes or automobiles.

Static Agent data: The agents are defined by a set of static parameters which affect the model and its visual appearance:

- Type (numerical Code)
- Length (on the surface plane)
- Weight (relevant for SF parameterization)
- Height (not relevant in the models used)
- Color (for visual purposes only)

Further parameters regarding dynamic constraints include:

- Maximum acceleration
- Desired acceleration
- Desired velocity

These parameters are initialized for every agent at its generation in the network. The parameters are used in both the PTV's DLL and in the now developed algorithms. An explanation of the SF parameters of PTV is given in the appendix (chapter 8.5).

Global social force parameter set:

- a, b in the (see table 6.4)
- Desired acceleration
- Desired velocity.

Destination and route information Path finding is managed by the PTVs *pedestrian-model.dll*. As an agent enters the next polygon of the ground plane, a new path is generated. The path is defined as a sequence of polygons. During the simulation a agent always aims for the closest vertex of the actual destination polygon.

4.2.3 Path Choice in VISSIM

During the simulation run, the agents positions are only calculated in the *pedestrian-model.dll*. If the agent reaches a polygon border an according flag is submitted to VISSIM and then VISSIMs request to re–initialize this agent in the next polygon is submitted to the DLL. This sequence affects and constrains the handling of the sensing mode. However, the agents position is not simply transferred to VISSIM but wrapped and manipulated forward.

Another feature is the *waiting time*, which is activated for an agent when it is re–initialized in the new polygon. In our application this could be used for watching shop windows etc. The destination polygons id is transferred at every re–initialization. If no strategic route information is set, the agent leaves the network.

The tactical path finding is done using a utility maximization on a spatial floor filling potential field. It should be considered that this is a static field, which can be cached in temporarily assigned files but does not include other agents positions or other dynamic aspects (PTV AG, 2010, p. 318). In further VISSIM releases, PTV includes dynamic path finding through travel time estimations and choice models (PTV AG, 2010, p. 365).

VISSIM is capable of using multiple floors and connecting ramps, however in this thesis these features are not needed and therefore not considered.

4.2.4 Social Force in VISSIM

In the operative level, the movements of the pedestrians are calculated in the external DLL which uses an extended type (Helbing et al., 2000, 2001; Werner and Helbing, 2003) of Helbings SF model (Helbing and Molnár, 1995).

Johansson et al. (2007) give the generalized form of the repulsive potential and its stated here to demonstrate its behavioral effects.

$$V_{\alpha\beta}(b) = ABe^{b_{\alpha\beta}/B} \tag{4.1}$$

where b is the distance that exponentially controls V (generating elliptical equipotential lines V). Johansson et al. specify a reduction of the repulsive gap with approaching velocity $\vec{v_\beta}$:

$$2b_{\alpha\beta} = \sqrt{(||\vec{d}_{\alpha\beta}|| + ||\vec{d}_{\alpha\beta} - v_\beta \Delta t \vec{e}_\beta||)^2 - (v_\beta \Delta t)^2} \tag{4.2}$$

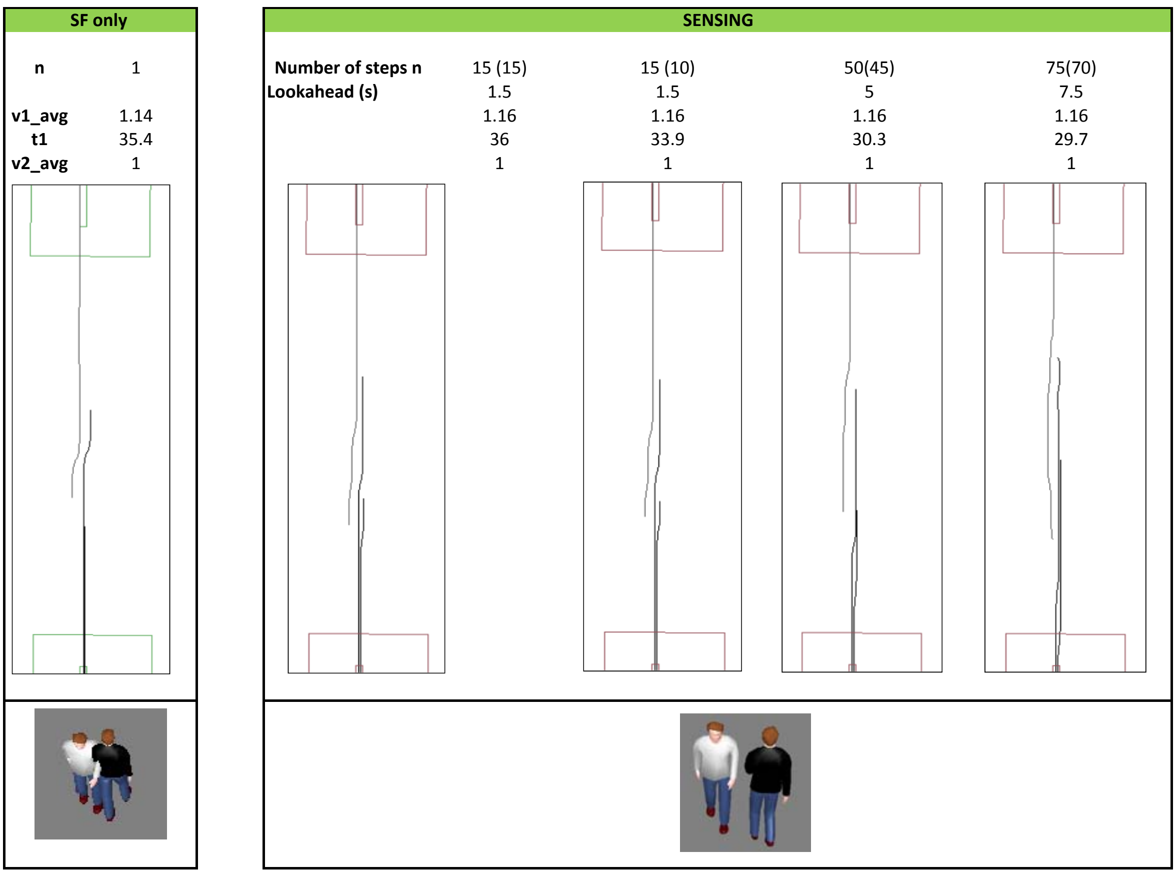

Figure 4.2: Demo of the effect of the sensing mode to pure pedestrian interaction.

These extended models ensure some kind of foresight, the elliptical shape of the "field" aims mainly to influence interaction in the walking/driving direction. To demonstrate the need for longer foresight at higher speeds, figure 4.2 shows agents trajectories at avoiding each other in the counter–movement. This visualization is done by simulation runs with the implementation of the proposed system architecture.

The column on the left gives the movement at generic SF principle. On the right, the effect of the foresight parameter is shown using the sensing mode to extend the foresight. The trajectories get smoother at larger foresight time intervals - the angles in the trajectories get lower. However, walking speed is not affected. In this example, the control parameter for the repulsive force is set low to better visualize the foresight–effect.

4.3 Editor Simulation Scenario

VISSIM's GUI is used to edit the infrastructures topology and parameters. Like in any commercial drawing software the polygons are drafted (by overlaying it on a map, technical scheme or aerial photo) and names and parameters adopted. In the prototypical approach centerlines and side areas have to be drawn to enable the calculation of the guiding field. The scheme in figure 4.3 shows the topological setup. The thin GREEN lateral lines indicate the longitudinal positions of the "measurements' profiles". the and the guiding field centers in GREEN, ORANGE and BLUE). The square is built with sections and intersections based on an aerial overlay.

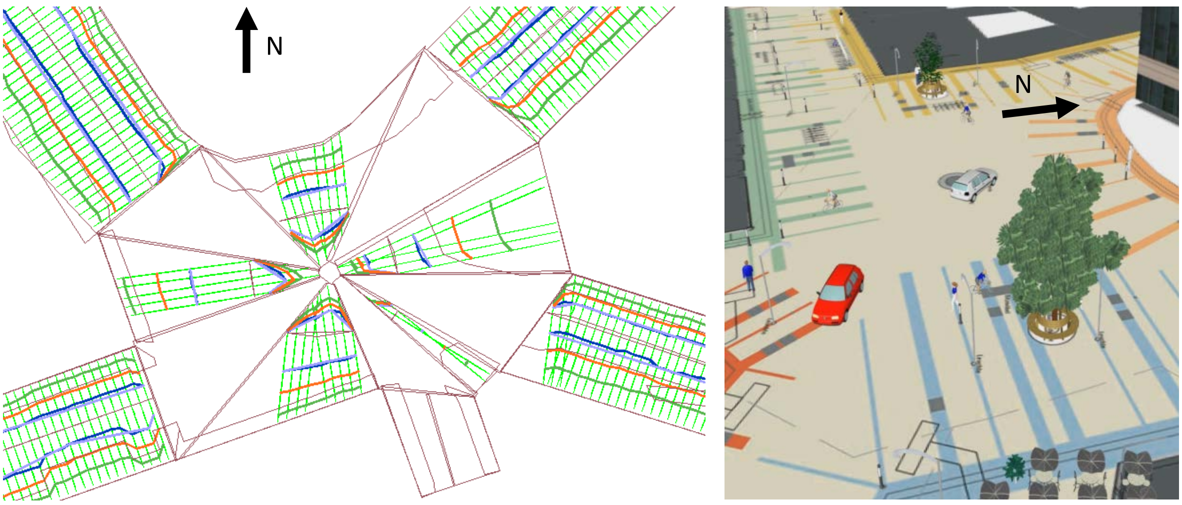

Figure 4.3: LEFT: The narrow RED lines outline the topology of the Sonnenfelsplatz by a combination of polygons. The polygons represent both sections (2 entrances) and intersections (n entrances). RIGHT: 3D-Visualization of the same site.

The demand is related to origin polygons and can be flexibly configured in open time intervals, as random or uniform agent generations. Agents' class and destination can be edited here as well as their static parameters and visualization properties.

4.4 Intrinsic Requirements

The use of VISSIM implicates several intrinsic constrains and requirements, some of which have to be overcome with tricky workarounds.

Parameters

In VISSIM, all modes of agents (pedestrian, bicycle, car) are handled as pedestrians. The velocity of pedestrians is constrained at 6 m/s - therefore the speeds in the editor are entered as a tenth and handled in the own implementation accordingly higher. Applying this scaling in speed, some parameters used in non-linear speed-dependent equations may require an adoption. Another issue is the extension of lookahead with the sensing mode. VISSIM triggers the PedestrianModel once while the own modeling framework launches several sensing modes during each main simulation step.

Path Finding Constrains

The path finding is calculated in VISSIM - it influences both the agent sequence of polygons as well as the actual path within each segment. In the editor the route is described by marking the road segments according to the desired sequence. There can be multiple routes for each origin–destination pair. Since the roads design should be influenced by establishing the force field, the agents path will be manipulated. Route planning should be taken into consideration, when designing the road topology, including the structure and shape of the segments. Equation 3.33 shows the sum of the cumulated forces, which are steering inputs for the agent. $\vec{f}_{SF}(t)$ includes the force that leads the agent to its destination. The possible interference between contrary forces $\vec{f}_{Guide}(t)$ and $\vec{f}_{SF}(t)$ can be avoided with the careful arrangement of neighboring road segments.

Performance Issues

The demonstration of the full simulation has been processed on an Intel i7/3400 machine with 8 GB RAM and SSD drive. The processing time is around 15000 seconds (4.2 hours). The simulation time is around 400 seconds with about 40 agents. The reason behind the enormous processing time: The number of calculation steps increase with n^2 (if $n > 1$) with n as the number of agents that are simultaneously in the arena. For a single agent: simulation time $\equiv$ processing time.

4.5 Calibration and Validation Framework

The calibration methods of the interaction model and the kinetic vehicle model are based on different approaches. While the calibration of the interaction model is purely handled in MATLAB, the calibration of steering, control, and vehicular parameters requires the full simulation framework, including VISSIM. Figure 4.4 illustrates the tools that are used in the calibration methods.

4.5.1 Steering and Vehicular - Calibration Setup

VISSIM's generation of agents is done accordingly to an editable distribution. It can be set to be random or uniform within certain periods. During the calibration, a certain generation time step is required to let the agent start its movement in the network at a certain place. The calibration is trajectory–based and optimizes the fit between the simulated and observed trajectories. The setup of the simulation requires:

- Origin and destination setup
- Demand and distribution
- Mode and agent parameters (speed, acceleration, weight, etc.)
- Start time and path

The fit of the simulated and observed trajectory can be obtained using the discrete Fréchet distance between the two "curves". This approach does not consider the differences in time due to different speeds and paths. The second approach would minimize the sum of the spatial distance of the two trajectories for each simulation time step. The actual calibration methods and results are documented in chapter 6.1.

4.5.2 Interaction Model - Calibration Setup

The tactical interaction model is based on identifying and solving the agents conflicts and in reacting according to the strategy found. Each conflict is described as a set of parameters which is derived from the agents positions, the agents static parameters (weight, mode), and the dynamic variables (speed, direction). These values are derived from the observation and the calibration and can be handled purely in MATLAB - a simulation run in VISSIM is not required. In validating the fit of the resulting trajectories, a full simulation would be the appropriate approach.

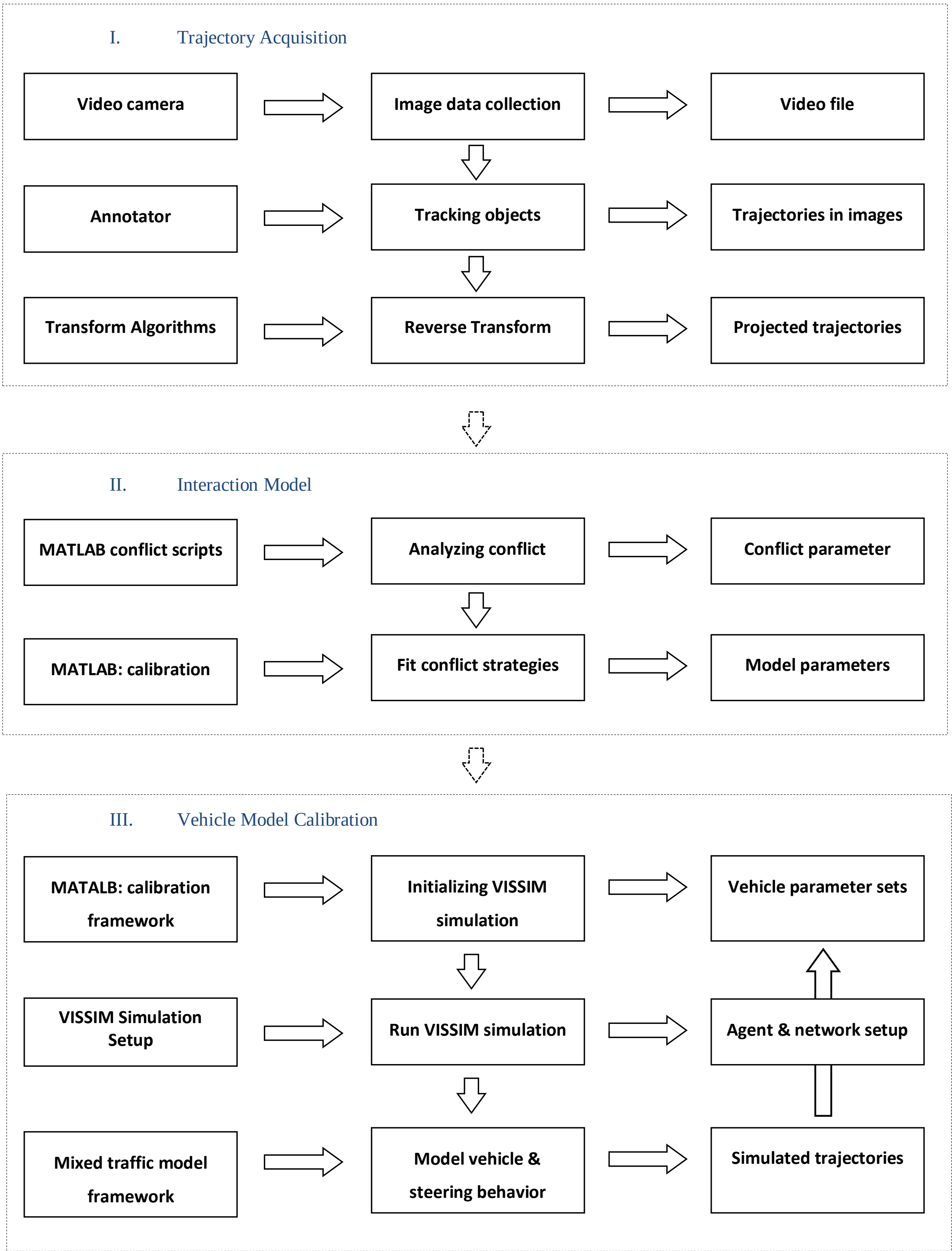

Figure 4.4: Calibration: Used tools, processes, output and work flow in the generation of trajectories and the calibration of the vehicle and interaction model.

5 Application

5.1 Design Summary

During the initialization phase of this thesis, the planning processes of two shared spaces in quite different locations in Austria were launched. Both sites offer the opportunity to study the impact of shared space as well as record before-and-after footage. In this chapter, the data characteristic is presented as well as the simulation setup of one of the two sites. To validate and calibrate the model, video footage has been recorded in *Gleinstätten* after the shared space implementation, and - more important - at the Sonnenfelsplatz in Graz, Austria. At Sonnenfelsplatz, it was possible to record footage before and after the reconstruction of a complex roundabout using shared space principles (see figure 5.8) in 2010, 2011, 2012, and 2016 respectively. Both, the geometrical model and the demand of sites is generated in the VISSIM setup.

5.2 Data Acquisition

The acquisition of data was a part of an associated research project but is not a immediate aspect of this thesis, although it is an essential component of the research on the topic - particularly the ways in which data acquisition is tailored to the model calibration procedure. An AXIS Network Camera, type P1346 (MJPEG, 3 MP/HDTV, 1080p) was used to record the footage.

5.2.1 Notes about Privacy

In general, privacy issues significantly affect and constrain data acquisition in public places. For this thesis, video footage has only be acquired in Austria. The Austrian Federal Constitutional Law does not explicitly recognize the right of privacy. But some sections of the Austrian Data Protection Act have even constitutional status. The right to the data protection is a fundamental right in Austria, laid down explicitly in a constitutional provision (sect. 1 of the Austrian Data Protection Act 2000 (Republik Österreich, 1999)). The acquisition of the video recording complied with data privacy regulations because:

- The individuals in the video footage cannot be identified.
- The data was not given to any other individuals or organizations.

In addition, the footage has been stored with a color filter to invert the pixel colors. Without inverse filtering measures, even at high picture-resolutions, it would be almost impossible that persons can be identified, or vehicle number plates can be read.

5.2.2 Annotating the Path of Movement

This section shows the application and outcome of object detection and tracking for calibration of the microscopic traffic model. To cover a large and versatile amount of real world data for calibration and validation processes, this thesis uses semi–automated data acquisition in video analysis. This work concentrates mainly on the aspects of a semi–automatic annotation tool applied to create trajectories of traffic participants over space and time. The acquired data is analyzed with a view towards calibrating vehicle models that navigate through a road' s surface and interact with the environment. The applied vehicle tracking algorithms for automated data extraction provide many trajectories not applicable for model calibration. Therefore, an additional automated processing step was applied to remove faulty trajectories. With this process chain, the trajectory data can be extracted from videos semi-automatically in a quality that is sufficient for the calibration of speeds, lateral positioning, and vehicle interactions in a mixed traffic environment.

Trajectories of moving pedestrians, cyclists and cars are required, with and without interactions ("conflicts"). The empirical data is generated out of video footage. Because these videos were recorded in public spaces, privacy protections have been considered (see chapter 5.2.1).

The tracking of agents in video footage is time–intensive, in each frame each relevant agent' s position has to be marked by mouse clicking. Experience has shown that dense scenes of several minutes of footage can require whole working days to manually track all road-users. A tool has been developed and adopted in order to acquire data more economically (Schönauer et al., 2012a). The automatic tracking algorithm is manually initialized by marking a pedestrian or vehicle. The tracker attempts to follow the objects based on trained shapes for that class of vehicles or specific so-called "omega shapes" (head-shoulder) for pedestrians. The second support for tracking is the real-time extrapolation of positions based on world coordinate projections, shown in figure 5.1.

The perspective-transformation H between two planes is applied using:

$$s_i \begin{bmatrix} x_i' \\ y_i' \\ 1 \end{bmatrix} \sim H \begin{bmatrix} x_i \\ y_i \\ 1 \end{bmatrix} \tag{5.1}$$

The goal is to minimize the back-projection error, which is:

$$\sum_i (x_i' - \frac{h_{11}x_i + h_{12}y_i + h_{13}}{h_{31}x_i + h_{32}y_i + h_{33}})^2 + (y_i' - \frac{h_{21}x_i + h_{22}y_i + h_{23}}{h_{31}x_i + h_{32}y_i + h_{33}})^2 \tag{5.2}$$

A calibration target is used to define a representative amount of points within the visible camera area. The positions of these points are annotated in both picture and

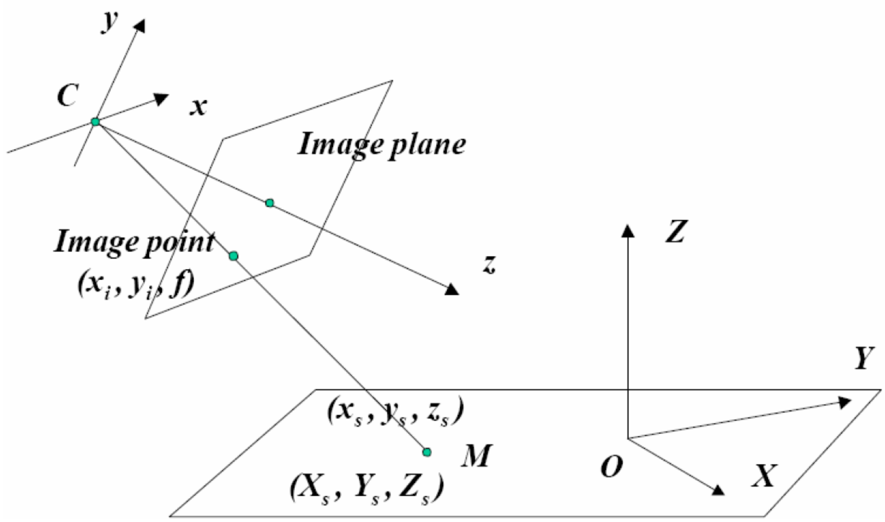

Figure 5.1: Principe of picture coordinate to world coordinate, taken from Zhang et al. (2006, p. 22).

in world coordinates. A method, based on RANSAC[1], is used to remove possible outliers. The remaining inliers are used in the error function and optimized by the Levenberg-Marquardt[2] approach to further reduce any re-projection errors.

During the tracking, projections between the video coordinates and the world coordinates are made in both directions each time step. The algorithm proposes the next position by a projection in the video, the operator then has "only" to eventually adjust the proposed flags. Figure 5.2 shows an editing example, which demonstrates the tracking GUI of both pedestrians and vehicles.

Later, the trajectories are transformed into world coordinates and smoothed before further processing.

Lateral Distribution

In the scene of interest, most boundaries are optically integrated in the road' s surface. The automatic gained trajectories are analyzed against validated reference data. Based on the formulation of the *Fréchetdistance* [3], the discrete *Fréchetdistance* (Eiter and Mannila, 1994) method (equation 5.3) is applied to yield minimum distances between the automatic tracked data set D and the reference data R for the destinations:

$$\delta_{df} = min||L|| \tag{5.3}$$

[1] An iterative method to estimate parameters of a mathematical model from a set of observed data that contains outliers.

[2] Usually used to solve non-linear least squares problems

[3] For all points on A, the distance to the closest point on B may be small, but if we walk forward along curves A and B simultaneously, and measure the distance between corresponding points, the maximum of these distances may be larger. This is called the *Fréchetdistance* δ_{df} (Veltkamp and Hagedoorn, 2000, page 472).

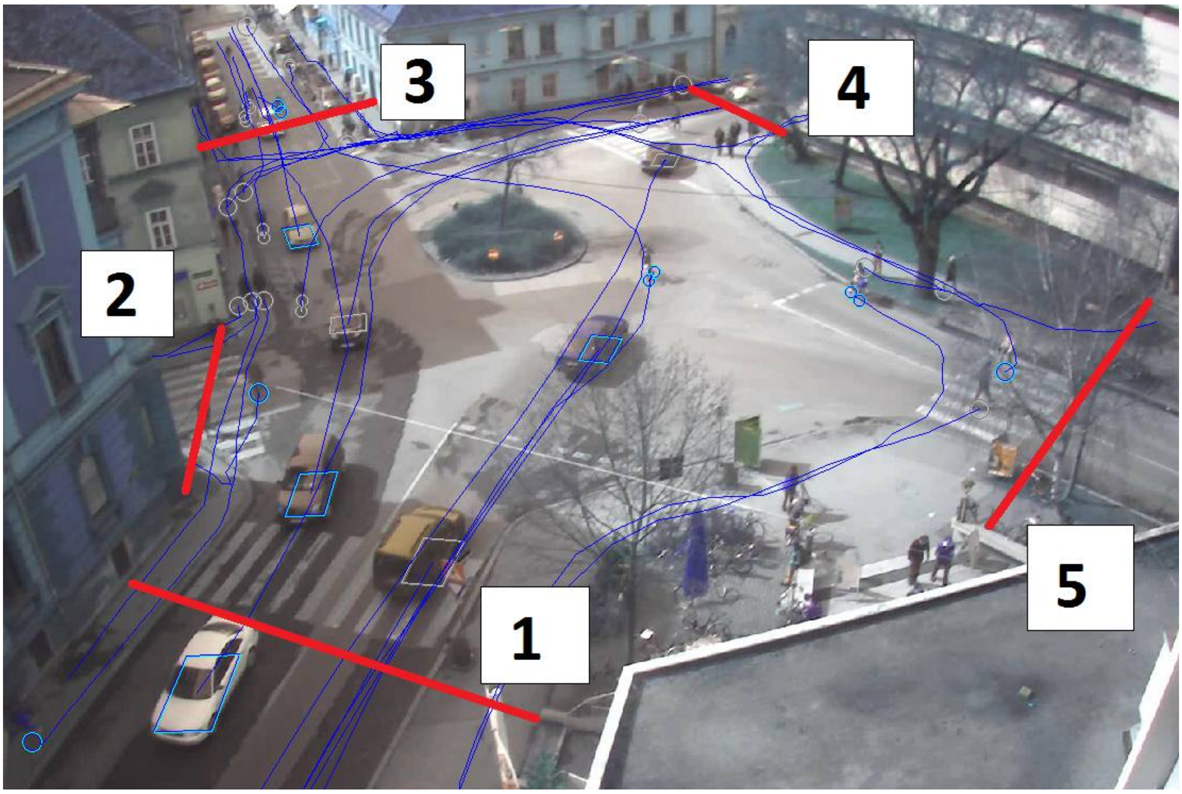

Figure 5.2: Tracking of pedestrians and vehicles and cars at the Sonnenfelsplatz in Graz, Austria.

where L is the coupling between D and R. Both the reference trajectories R and the automatic gained trajectories D for straight relations are shown in figure 8.15 (appendix). The absolute histogram of δ_{df} is given in figure 8.15. For the whole sample, the mean is 0.42 m in $OD = 3/1$ and 0.67 m for $OD = 1/3$. The shift of the projected vehicles' centers to the ground plane increases with the dominance of side view. To minimize the lateral error, the cameras' positions should be close in line with the driving vehicles. Since speed is not relevant in determining the lateral position, the distance to the area of observation should be as high as possible (constrained by the minimum pixel size of the moving objects).

In figure 8.16, the trajectory of a single vehicle is shown to demonstrate the effect of projection to ground plan due to the angular shift in perspective. An imaginary line from the camera through the center of the car (its center in the image) obviously hits the ground plane behind the car. This projection-error increases with lower heights of the camera.

5.2.3 Conflict Data

To observe and understand tactical behavior as well as to provide a solid basis for calibrating the tactical model, the trajectories of selected conflicts have been acquired (see table 8.5 and 8.6 in the appendix).

Observed Strategies

To get a deeper understanding of the data used, some descriptive statistics are calculated first. Figure 5.3 and figure 5.4 show the spatial location of the sets of conflicts C_{ij}, observed in 2011, 2012, and 2016 respectively. The color of the outer ring indicates S_i, the leaders i choice (according to the color bar). The color of the filling represents the followers j choice S_j. For this section - only for this very purpose of visualization - it is anticipated that the definition of leader and follower is done according to priority rule sets of the traffic regulations ("definition nr. 6" in sub-chapter 6.1.3).

1. $S_x = 1$: Continue
2. $S_x = 2$: Decelerate or stop
3. $S_x = 3$: Evade left
4. $S_x = 4$: Evade right

Figure 5.3 shows the street at the primary school in the through–road in Gleinstätten. The road - including sidewalks - is the white center area with a total width of approximately 15 m. Only conflicts of pedestrians were observed that cross from the north to south of the road. Figure 5.4 shows the topology of the Sonnenfelsplatz in Graz - buildings are

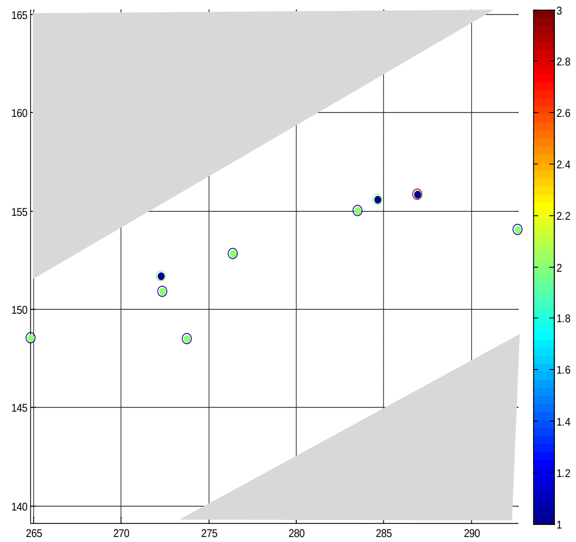

Figure 5.3: Location of the conflicts at the school in Gleinstätten.

indicated with filled gray polygons. The samples show an obvious behavioral change in the chosen strategies: 2012 in the shared space, drivers or pedestrians did chose to evade left or right more often than they did in 2016.

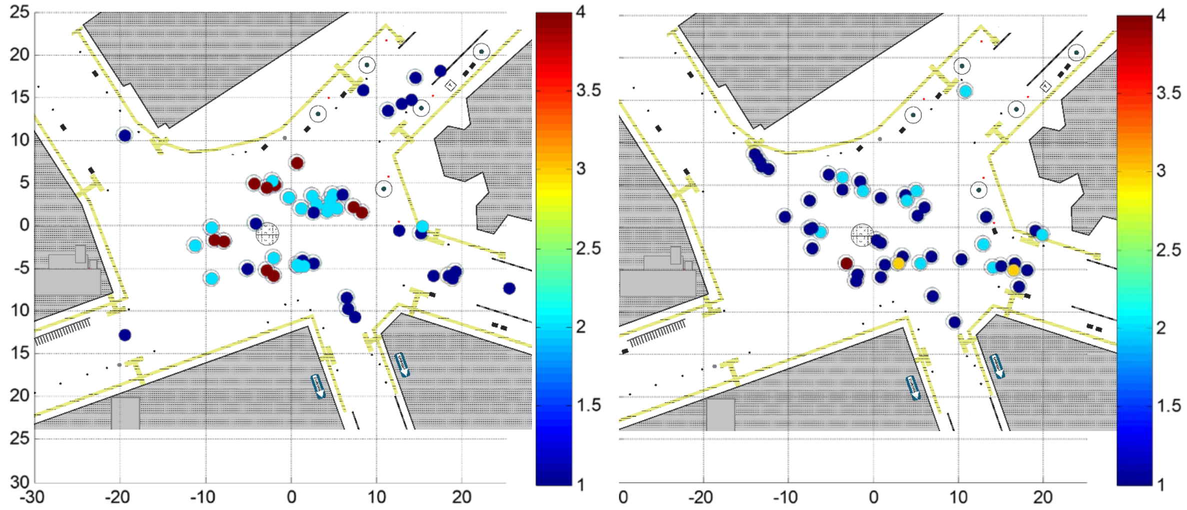

Figure 5.4: Location of the conflicts at the Sonnenfelsplatz with indication of the **strategy** chosen. LEFT: 2012, Shared space. RIGHT: 2016, Begegnungszone.

In figure 5.5, the involved transportation modes m_i and m_j are shown. The color-code represents pedestrians as $m_x = 3$, cyclists as $m_x = 2$ and cars as $m_x = 1$. The plot clearly indicates the concentration of pedestrian conflicts at the crossing area to the side while vehicular conflicts cluster in the center.

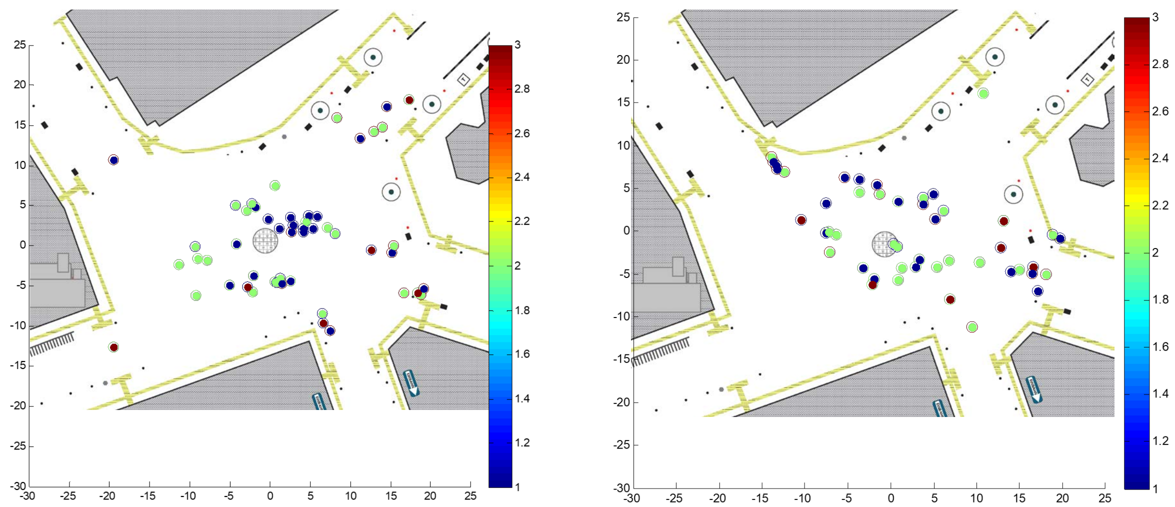

Figure 5.5: Location of the conflicts, colors indicate **traffic modes**, Sonnenfelsplatz. Outer circle: Leader. Filling: Follower. LEFT: 2012, Shared space. RIGHT: 2016, Begegnungszone.

To demonstrate the involved walking and driving speeds, figure 5.6 indicates the values in [m/s].

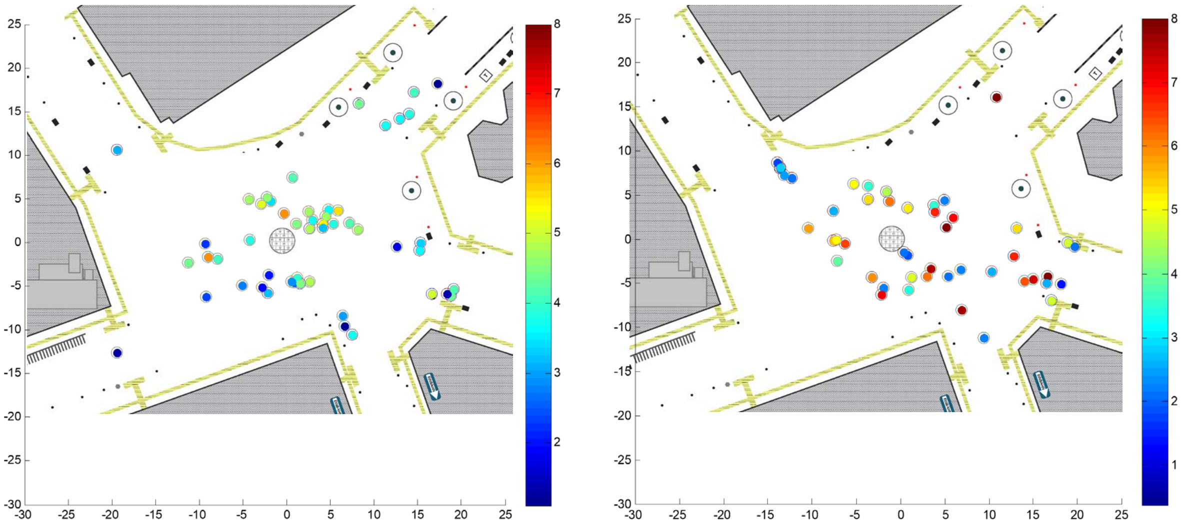

Figure 5.6: Speeds at the pairwise conflicts at the Sonnenfelsplatz. Filling: Leader. Outer circle: Follower. LEFT: 2012, Shared space. RIGHT: 2016, Begegnungszone.

5.3 Trajectory Data Processing

5.3.1 Origin-Destination Filter

Filtering trajectories based on the origin and destination of the vehicles is applied as well as spatial low–pass filtering. Smoothing by applying a local regression method (weighted linear least squares and a 1st degree polynomial model with a vector size of 10) is used for preprocessing.

The following tests were conducted to assess the capability of the tracked trajectories

1. Verifying the OD flows,where a single trajectory has to pass a pair of predefined origin and destination polygons.
2. Checking the tracking failures. this test can easily filter out all trajectories that are too short and not applicable and provides an estimation of the reliability of the tracking algorithms.

The OD relation is relevant for the clustering of trajectories for further analysis. The OD matrix is given in table 5.1. The number of observed vehicles in the reference data set is smaller than the number of vehicles tracked automatically. The count is done using 3 detector-like regions, plotted in figure 5.7.

Given the values in table 5.1, only the relevant relations are considered in further analysis. This selection is shaded grey in table 5.1. 82 objects are detected and tracked in the footage of 15 minutes. 11 vehicles can be excluded, because their origin or destination lies within the observing area. After OD processing, 56 vehicles are correctly classified, leading to a detection miss of 23 vehicles and a detection rate of 71 %, for further details, please refer to Schönauer et al. (2012a).

Format: Q_r / Q_d [number of observed vehicles]		Destination		
		1	2	3
Origin	1	-	4 / 2	33 / 26
	2	1 / 3	-	2 / 1
	3	38 / 24	1 / 0	-

Table 5.1: Origin-Destination matrix of the reference scenario.

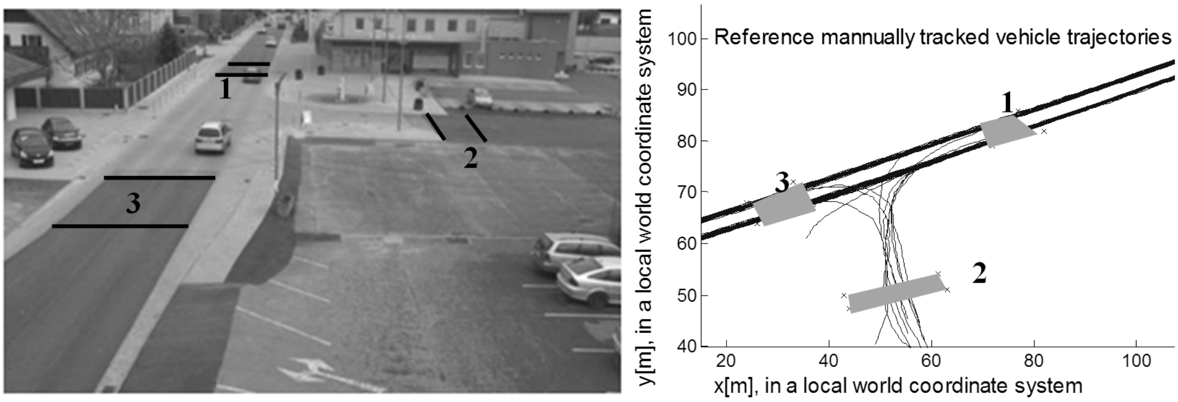

Figure 5.7: LEFT: Area of acquisition is the through-road in Gleinstätten (Austria), its design is made according to the shared space concept. Numbers show the origin and destination segments; RIGHT: Reference Trajectories in the world coordinate system.

Figure 8.19 gives the plot of all detected vehicles in the footage and demonstrates the application of the OD filter for OD = [2, 1]. "Hot–spots" of false detection are mainly based on poles of the road lighting have to be filtered in further steps.

5.4 Characteristics of the Data

Only external-external traffic demand has been considered. In motorized traffic, only demand through traffic could be observed. Within the observation area, there are two designated parking spots and some other objects attracting bikers to park and lock their bicycles. During the observed time window, 4 cyclists are at their destination and lock their bicycles.

In this sub-chapter, multiple separately acquired data sets are used to analyze traffic flow characteristics as well as interactions:

- **Data Set 1**: Trajectory data of all road users within time windows $t_{Sonne2010}$, $t_{Sonne2011}$ and $t_{Sonne2012}$
- **Data Set 2a**: Conflict trajectories from Gleinstätten in 2011 (Shared Space)
- **Data Set 2b**: Conflict trajectories from Sonnenfelsplatz in 2012 (Shared Space)
- **Data Set 2c**: Conflict trajectories from Sonnenfelsplatz in 2016 (Begegnungszone)

Figure 5.8 shows an example frame of footage for each Data Set. The choice of the recording–periods considered similar daytime, atmospheric conditions (no precipitation and mild temperature) and day of the week (Thursday or Tuesday) have been the same in all 4 measurement campaigns. At Sonnenfelsplatz, there is only a single position to install the camera. In a additions to the weather conditions, the foliation of the birch tree in the front constrains the possible month to the following: October, November, February, March and April. Recording daytimes have been around noon, where also the peak in the traffic flows for all modes of transport can be observed (Kleboth Lindinger Dollnig and Komobile Gmunden and Michael Sammer, 2009). Table 8.31 (appendix) shows relevant meta-data of the 4 measurement campaigns.

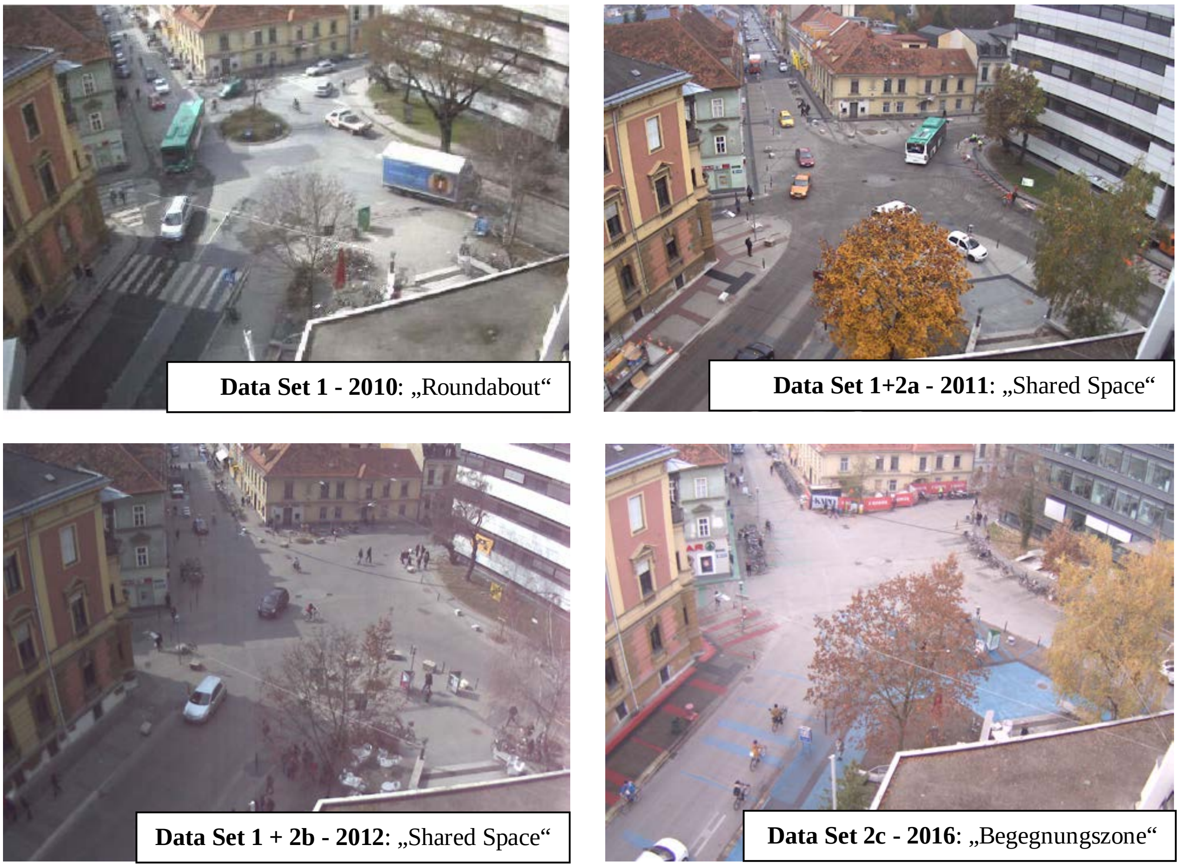

Figure 5.8: Sonnenfelsplatz. TOP LEFT: Before the reconstruction. TOP RIGHT: 1 month after the reconstruction as a shared space. BOTTOM LEFT: 6 month after the reconstruction as a shared space. BOTTOM RIGHT: 3 years after it became a Begegnungszone.

5.4.1 Behavioral Analysis - Data Set 1

Figures of simultaneously tracked traffic participants in the observation area are shown in figure 5.2. The minimum sample size is 50 trajectories for each mode. In all further qualitative conclusions, the limited number of trajectories should therefore be considered. The observed demand is used to generate the demand in the simulation case study. No more than 21 agents are observed in the network at the same time.

The willingness to share the available road space between traffic modes is a major aim of the shared space concept. This section is about the spatial distribution and chosen paths for each mode of transport. Before the reconstruction, the individual path–choice was narrowly constrained. The left side of figure 5.9 shows that pedestrians (red) crossed the road exclusively in the area of the crosswalks. Bicycles (green) and cars (black) followed the regulations to circle the central traffic island. Overtaking maneuvers of bicycles can be observed within the roundabout. After the reconstruction, several changes in walking

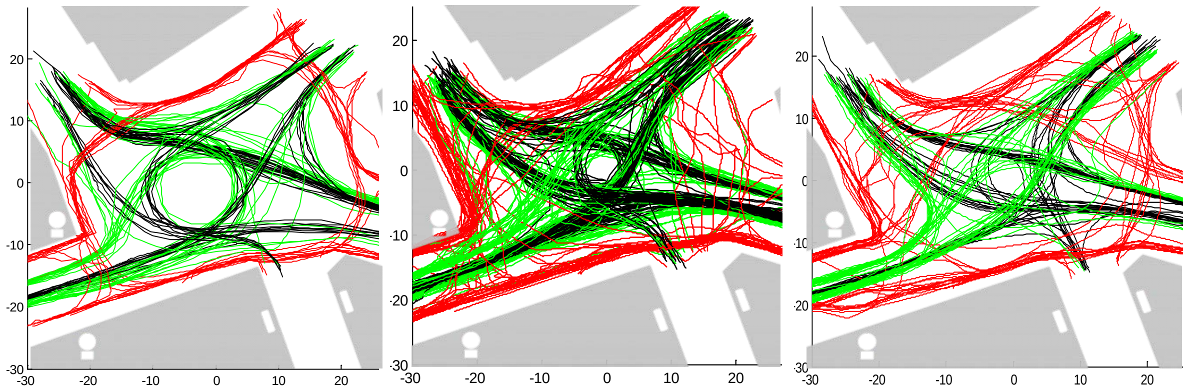

Figure 5.9: Trajectories of pedestrians and vehicles. LEFT: Roundabout in March 2010. MIDDLE: Shared space in October 2011. RIGHT: Shared space in March 2012.

behavior can be observed. Many pedestrians cross the place using shorter paths closer to the center of the square, (figure 5.9, right hand side) and a higher variation in the crossing locations can be observed. In the new design, a slightly elevated island forms the center of the square, causing a white spot in the trajectories (figure 5.9, right hand side). However, the island' s dimension was reduced from 8 m x 11 m to about 3 m x 3 m. Due to the smaller island, the driving radii did also change: At low turning angles ("straight" relations) the radii increased, while for high turning angles and U-turns, the radii for cars and bicycles decreased. The trajectories in figure 5.9 imply two phenomena, created by the redesign that reduce both path length and the travel time:

- A shift of the pedestrian crossings towards the square' s center.
- Changes in the turning radii of vehicles.

Travel time, average speeds, and path lengths were calculated for each cell in the OD matrix. The empirical weight (number of samples in this mode and OD relation) was considered by cumulating the results for each mode. The classification into OD relations generates small groups of trajectories for most of the links and the statistical significance shows that the standard deviation error is refusing the tests. Higher sample sizes could provide a better statistical validity. To overcome the lack of data, the next approaches do not split the trajectory sample into OD relations.

5.4.2 Speed Distribution - Data Set 1

Assessing speed requires accurate time stamps for each frame (in addition to the path in world coordinates). Therefore, the camera encodes the time stamps in each single video frame in real-time, and errors caused by frame drops and deviating frame rates can be identified and taken into account. For a better comparison, the entire trajectories were re-sampled to 0.1 second (10 frames per second), a linear interpolation algorithm is used. The speeds were calculated for each segment in a trajectory using two neighboring points and time stamps. For the computation of the speed distributions, the speed values were smoothed using moving averages over the last two values. This was necessary to reduce jitter resulting from the annotation of discrete pixel positions in the video frames due to transforming to real world coordinates. In figure 5.10, the speed distributions are shown separately for each mode of transport and of both roundabout and shared space. The estimated mean speeds are shown in table 5.2.

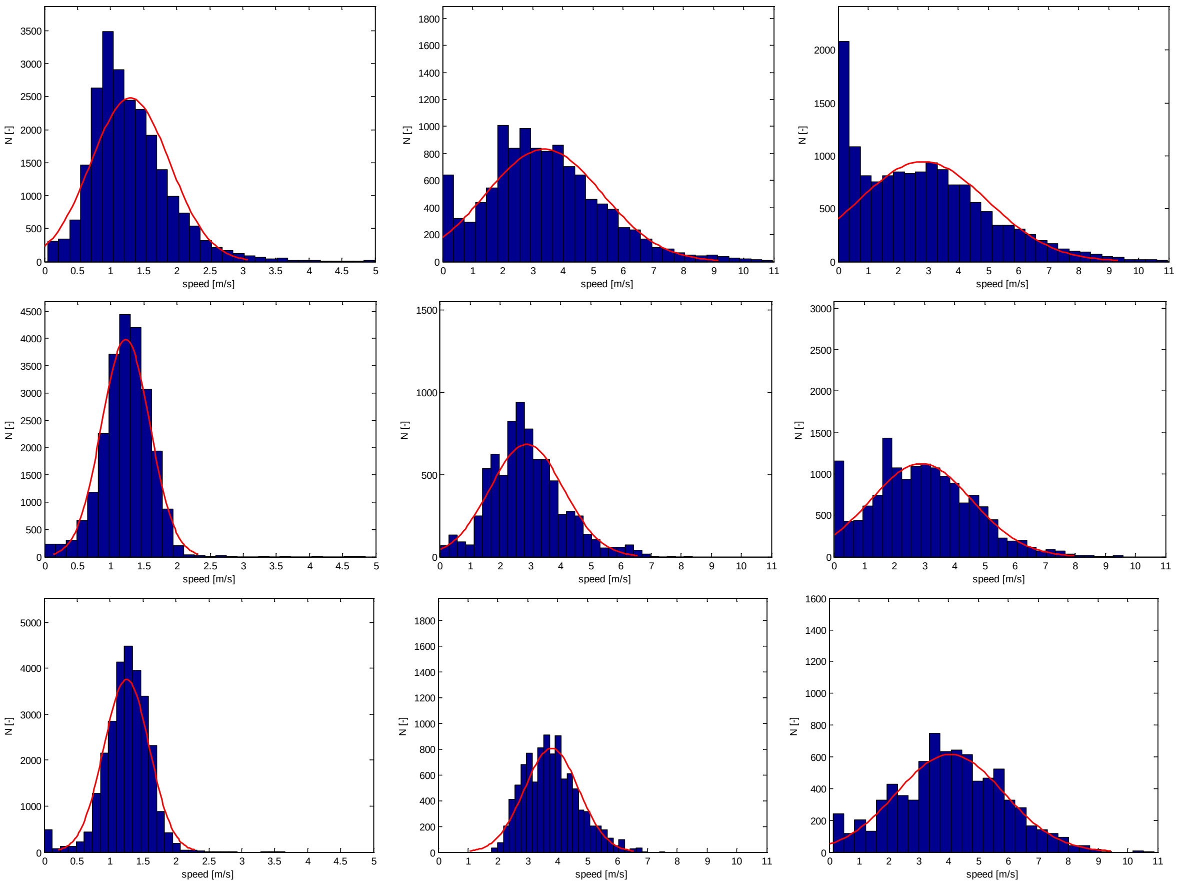

Figure 5.10: Histograms of estimated speeds, based on cell grid speeds, all speeds in m/s (Sonnenfelsplatz). TOP: Roundabout 2010. MIDDLE: Shared space 2011, BOTTOM: Shared space 2012. LEFT: Pedestrians, MIDDLE: Bicycles, RIGHT: Cars.

Figure 5.10 shows speed histograms of the roundabout (first row) and the shared space two weeks (second row) and six months (third row) after opening.

Year/mode	Pedestrians	Bicycles	Cars
2010	1.30	3.38	2.83
2011	1.23	2.88	2.89
2012	1.25	3.80	4.06

Table 5.2: Comparison of mean speeds, cells are in accordance to the sub-plots in figure 5.10.

5.4.3 Short-term Impact - Data Set 1

Inspecting the shape of the shared space configuration two weeks after its opening in 2011, (figure 5.10, second row) yields a smaller variance in speed-distributions for all modes of transport and indicates constant speeds and less stop-and-go behavior compared to the roundabout. Both the mean speeds and maximum speeds decreased. Slower movement speeds might have been caused by insecurities and curiosity about the new design. This could be an indication that people in the roundabout make short runs to pass the street before the vehicles arrive. The generic desired speeds within pedestrian crowds are said to be Gaussian distributed with a mean value of approximately 1.34 m/s and a standard deviation of about 0.26 m/s (Henderson, 1971). Literature' s mean speed positively correlates with the observed speed of observed pedestrians in 2010. The distributions in the observations, however, show standard deviations of 0.79 (2010) and 0.37 (2011). One qualitative explanation may be the multiple sampling of each pedestrian while Henderson uses an interpersonal approach - one single mean value of each person. The walking speeds in the shared space are lower but due to the shorter routes total travel time also decreases. The difference between car speeds is shown in much lower peaks in 2011 at lower speeds, indicating less waiting times and a more continuous flow. After the redesign, the mean bicycle speeds dropped from 3.38 m/s to 2.88 m/s. A bias due to a higher vehicle density in the time window between 100 and 200 seconds has to be considered.

5.4.4 Habitual Change after 6 Month - Data Set 1

Six months after the implementation of the new design, the speed distribution curve got more narrow in the shared space for all modes of transport and decreased with time. One hypothetical explanation is that the people got used to the redesign and its impact on traffic behavior. Homogeneity, absolute values, and speed rose especially for vehicles. It can also be observed that car waiting and stop times further decreased. There is no indication that the redesign lowered maximum speeds in the observed traffic density. This conclusion is in accordance with observations of Österreichische Forschungsgesellschaft Straße-Schiene-Verkehr (2016). The authors claim that the main reason is the higher rate of driving time, compared to waiting time at cross-walks.

Observed Speeds:

In this sub–section, the spatial distribution of the speeds is presented. Traffic behavior includes both normative and social aspects. Perception, communication and other psychological phenomena influence velocity. At a certain speed, technical norms dominate social behavior. Literature (i.e. Topp (2010)) defines this critical speed to 30 km/h. At the Sonnenfelsplatz, the speed limit was 30 km/h during all four measurement–campaigns. Car speeds over 30 km/h (8.33 m/s) were reached in 1.7 % of segments in car tracks at the roundabout in 2010. In the shared space, 30 km/h was exceeded in 0.2 % (2011) and 0.8 % (2012) of the sample track segments. Cyclists reached 30 km/h in 1.8 % of their tracks in 2010. This number dropped to zero by 2012.

Driving and walking speeds are major traffic performance and safety indicators. The speeds for the three modes of transport are calculated and discretized using a cell grid with cell size of 1 m x 1 m to show their spatial distribution. Finally for each cell, the mean speeds for each mode of transport are computed and low pass filtered. The result is shown in figure 5.10.

The main impact of shared space for pedestrian is the shift to a more homogeneous speed level. The crossings of the roads were done at a slower and steady speed, which correlates with expectations. Figure 6.9 shows that the crossings closer to the square's center were done at higher speeds. At the three bidirectional entrance roads (NW, NE, SE), the crossing speed using shortcuts is in a range of 1.5 m/s. Bicycle speed levels dropped immediately after the reconstruction in 2011. This could have been caused by an increased risk awareness, reduced space, or the increased number of obstacles for bicyclists. Hypothetically, adoption and habituation have allowed the speeds to rise again after 6 months. Compared to the roundabout, the shared space reaches a higher spatial homogeneity, shown in figure 6.9.

The spatial distribution in the plots for bicycle data clearly shows that more homogeneous driving speeds. Most peaks are close to the center of the square. A reduction in car speeds, however, can be observed in the very center of the square, while not at the entrances. Car speeds stay high at the two straight east roads. In the square's center, bicycle speeds now clearly dominate the speeds of motorized vehicles.

Thoughts regarding Capacity Optimization:

Looking at the speed diagrams during observation, the flow hardly reaches the capacity limits of the square. Helbing' s work on the analytical optimization of operation regimens at a controlled intersection (Helbing and Mazloumian, 2009) shows different interesting outcomes, some of them involving a "slower–is–faster effect". A possible interpretation is that a delayed switching of the traffic signals reduces the average travel times. This counter-intuitive effect has formerly been observed in pedestrian crowds rushing through a bottleneck (Helbing et al., 2000). The slower–is–faster effect in minimizing total travel time occurs when the utilization of a road section is small enough to require extra time to collect more vehicles for an efficient service during the green phase, taking into account the efficiency losses by switching traffic lights. This analytical technique and optimization approach could be extended to evaluate the optimal flows for shared space paradigms. Helbing' s $\gamma_j(t')$ would have to be replaced with a function describing the priority behavior of the drivers.

5.4.5 Interaction Aspects - all Data Sets

In this section, multiple separately acquired data sets are used to analyze interactions:

- **Data Set 1**: Trajectory data of all road users within time windows $t_{Sonne2010}$, $t_{Sonne2011}$ and $t_{Sonne2012}$
- **Data Set 2a**: Conflict data and trajectories from Gleinstätten in 2011 (shared space).
- **Data Set 2b**: Conflict data and trajectories from Sonnenfelsplatz in 2012 (shared space).
- **Data Set 2c**: Conflict data and trajectories from Sonnenfelsplatz in 2016 (Begegnungszone).

During the work on this thesis, in 2013, the Sonnenfelsplatz had been designated as a "Begegnungszone" (further details about the concept in chapter 2.1.3). A photo that shows the street-scape is given in the appendix (figure 8.23).

Data Set 1

Data set 1 is used here to estimate safety issues. Safety studies often focus on the interaction between and within motorized and non-motorized traffic, as well as the conformity to traffic control regulations. Traffic safety analysis has traditionally relied on historical collision data. However, the shortcomings of this approach are the rare and random occurrences of collisions and the poor availability of data. Of course, traffic conflicts are more frequent than traffic collisions. The first concept of TCT for roads was proposed by Perkins and Harris (1967) and involves observing and evaluating the frequency and severity of traffic conflicts at an intersection by a team of trained observers. Ismail et al. (2010) use indicators of time as objective and quantitative measurements of the severity of conflicts. Here, the intention is to outline the combination of speed and distance between traffic participants. A new indicator has been defined, which includes relative speed, and distance in time and space of a pair consisting of a non-motorized road user and a car. It is calculated as the quotient of the squared relative speed and the distance between the objects. A trajectory is a vector of agent's i or j position X_i in a 100 milliseconds-interval. m, n are the numbers of the segment (vector index). Agent i can either be a pedestrian or a cyclist, j always is a car. For each segment of the bicycle track and a single segment of a car track, we calculate:

$$v_{i,n_j} = \sum_{m=1}^{number\,of\,car\,track\,segments\,(1\,m\,each)} \frac{|\overrightarrow{v_{i,n}} - \overrightarrow{v_{j,n}}|^2}{m * d_{X(i,n),X(j,m)}} \; if d_{X(i,n),\,X(j,m)} < 1\,m\,,\, AND\;\Delta t_{X(i,n),X(j,m)} < 0.5\,s \tag{5.4}$$

We calculate this for all pedestrians and bicycles i to all cars j:

$$v_{i,n} = \frac{1}{number\,of\,cars} \sum_{j=1}^{number\,of\,cars} v_{i,n(j)} \tag{5.5}$$

For all cyclists and pedestrians i, there is a component of vector v_n at the position X_n. A cell grid matrix C is generated, describing the space of the Sonnenfelsplatz in a 1 m x 1 m grid. $v_{i,n}$ is then assigned to the cell grid:

$$C_{x,y} = \frac{1}{number\,of\,vector\,components\,v_{i,n}\,in\,C_{x,y}} \sum_{i=1}^{number\,of\,pedestrians\,and\,cyclists} v_{i,n(j)} \tag{5.6}$$

$$if\ |Xi,n - cellcenter_{C_{x-1,y}}| < |X_{i,n} - cellcenter_{Cx,y}| < |X(i,n) - cellcenter_{C_{x+1,y}}| \tag{5.7}$$

$$and\ if\ |Xi,n - cellcenter_{Cx,y-1}| < |X_{i,n} - cellcenter_{Cx,y}| < |X(i,n) - cellcenter_{C_{x,y+1}}| \tag{5.8}$$

The result is a 60 x 60 matrix, representing a simplified approach to identify the spatial distribution of interactions' intensities. Figure 8.43 shows the indicator C calculated for 2010, 2011 and 2012, for pedestrians/cars and bikes/cars in the appendix.

The higher values represent spots where pairs of non–motorized road users and cars meet at higher speeds and lower distances. The comparison of before-and-after data shows that the critical areas moved and that in particular bicycle conflicts shifted to the center. Sums of the matrices C are listed in figure 5.3. The analysis of the 2012 samples shows larger hot–spots and a higher total sum of C for pedestrians. A possible explanation is that the stop-and-go behavior of cars was replaced by homogenious speeds or lateral evasion. Pedestrians are more flexible in their path–finding. Table 5.3 shows the sums of the matrices C for the three periods.

Scenario	Cyclists vs. Cars	Pedestrians vs. Cars
Roundabout 2010	195	58
Shared space 2011	141	76
Shared space 2012	149	116

Table 5.3: Sums of the matrices C, scenario Sonnenfelsplatz.

There is no scientific evidence to directly conclude conflicts to accident probabilities. Nevertheless, in the plotted heat-map in figure 8.43, the registered accidents in which bicyclists were injured between 2006 and 2008 in (Kleboth Lindinger Dollnig and Komobile Gmunden and Michael Sammer, 2009) are marked by a red cross in a black filled circle. A clear spatial correlation between the accidents' location and the hot spots of high speed cannot be found.

Accidents in the road accident database show a decreasing trend in numbers of accidents with personal injury during the last decade (figure 5.11). Nonetheless, sample numbers are too small to statistically back up a clear trend. The official numbers are gratefully provided by the municipality of Graz - data of 2016 is not yet available.

Comparing the heat-map of figure 8.43 to similar visualization of classical crossing-designs in the literature confirms the findings of a clear shift of conflicts to the crossings' centers. An example: Tageldin and Sayed (2016) analyze an intersection in Shanghai (China) and derive spatial conflict distribution of road-users (see figure 8.42). The conflict density increases at the edge-areas of the cross–walks - similar to the conflict density patterns of Sonnenfelsplatz in 2010 (figure 8.43).

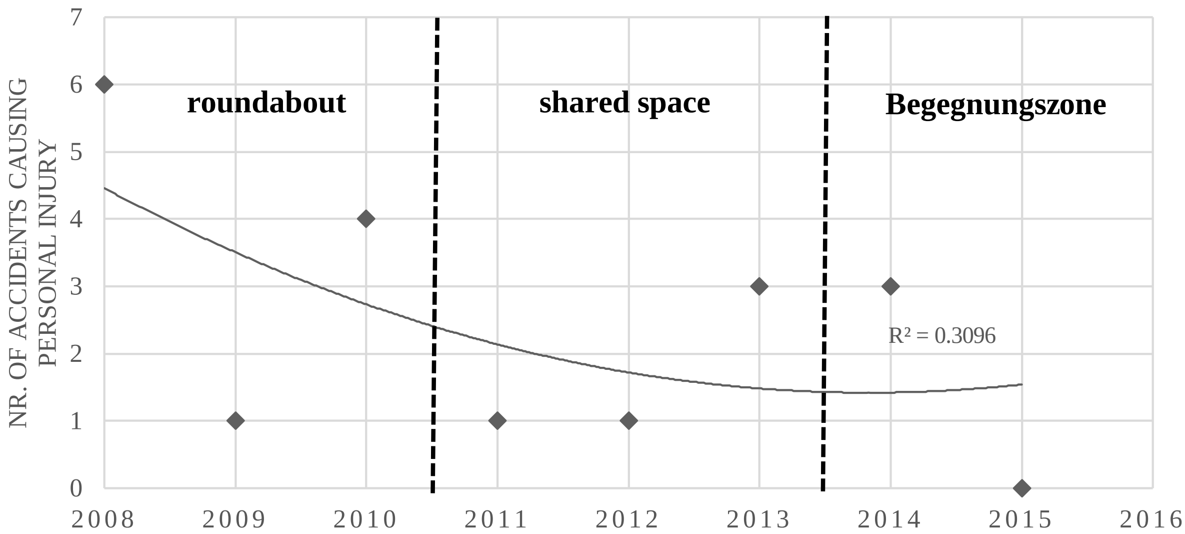

Figure 5.11: Number of accidents causing personal injury. A polynomial function is fitted (n=2). The curve is purely a simplified indication of a trend - no statistical significance.

Data set 2

Data set 2 is the basis for calibrating the tactical model. The conflict data sets 2a (Gleinstätten) in 2011 - and the data set 2b (Sonnenfelsplatz, 2012) are used to calibrate the parameters for a shared space scenario. To calibrate the reference scenario for Begegnungszonen, data set 2c is used. Lists of conflicts: table 8.6, table 8.5. Due to the difficult process of finding relevant video scenes and the labor intensive manual annotation of the scenes, only a relatively small amount of data is available (see table 5.4). In figure 5.12, trajectories of pedestrians, cyclists and cars are shown of both data sets 2b and 2c.

Scenario	Pedestrians	Cyclists	Cars	Sum
Gleinstätten 2011 (data set 2a)	9	0	9	18
Shared Space 2012 (data set 2b)	22	42	42	106
Begegnungszone 2016 (data set 2c)	26	26	48	100

Table 5.4: Sample sizes of the data sets that are used for calibrating the tactical game.

Speeds in conflicts' Data Set 1 versus Data Set 2

Since the legal concept has been changed from shared space to Begegnungszone in 2013, also the driving speed limit is reduced from 30 km/h to 20 km/h. The comparison is done separately for each mode of transport - figure 5.13 shows histograms and mean values. The following differences seem obvious:

- In both scenarios, pedestrians and cyclist usually don' t stop
- In the shares space, speed distributions are more narrow

- In the Begegnungszone, pedestrians walk faster ($\Delta > 0.5$ km/h)
- Cycling mean speeds are higher in the Begegnungszone ($\Delta > 1$ km/h)
- Driving mean speeds of cars positively correlate in both scenarios

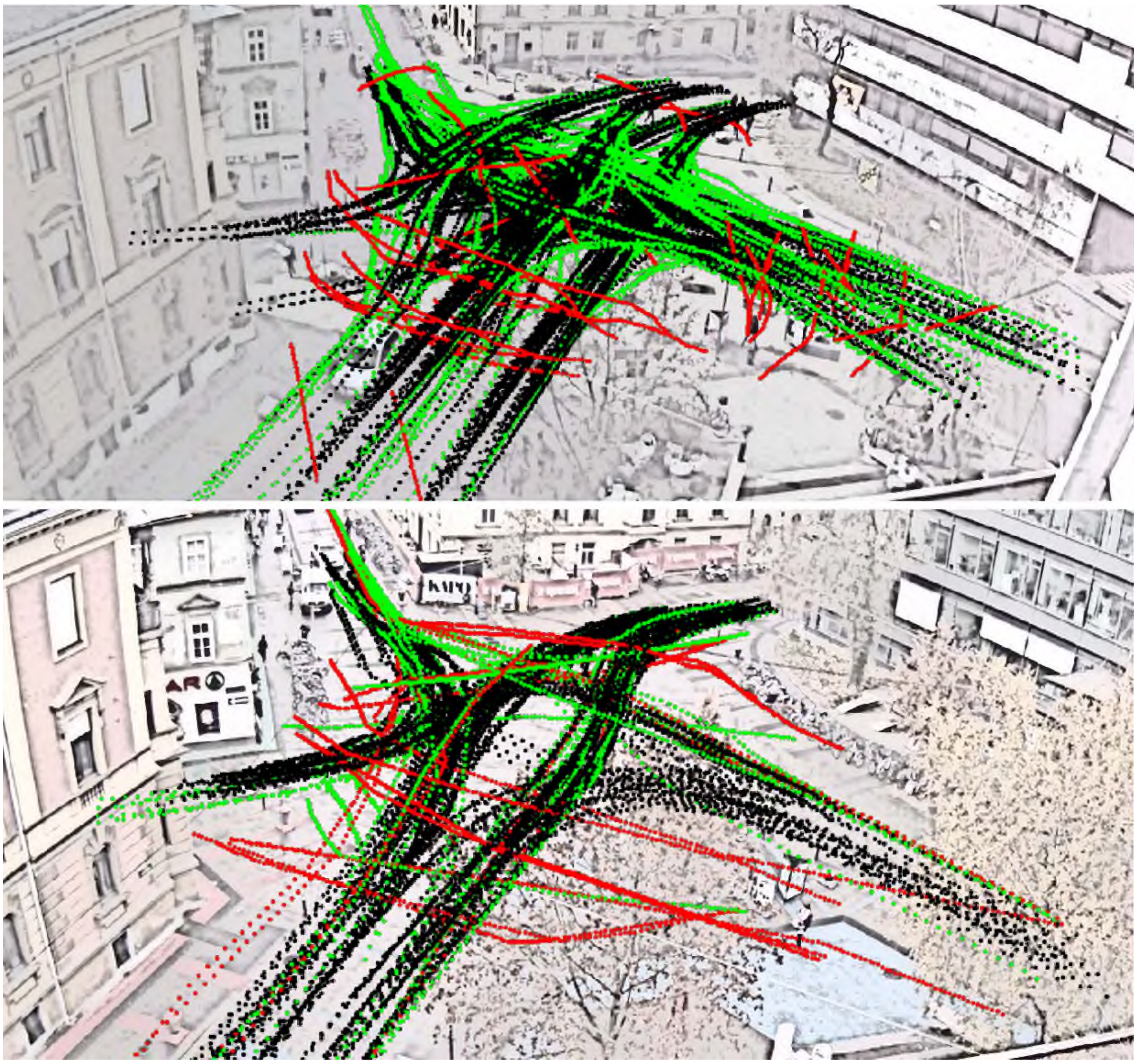

Figure 5.12: Empirical trajectories of pedestrians (red), cyclists (green) and cars (black) - re–transformed into video frames. TOP: Shared space in 2012, Data Set 2b. BOTTOM: Begegnungszone in 2016, Data Set 2c.

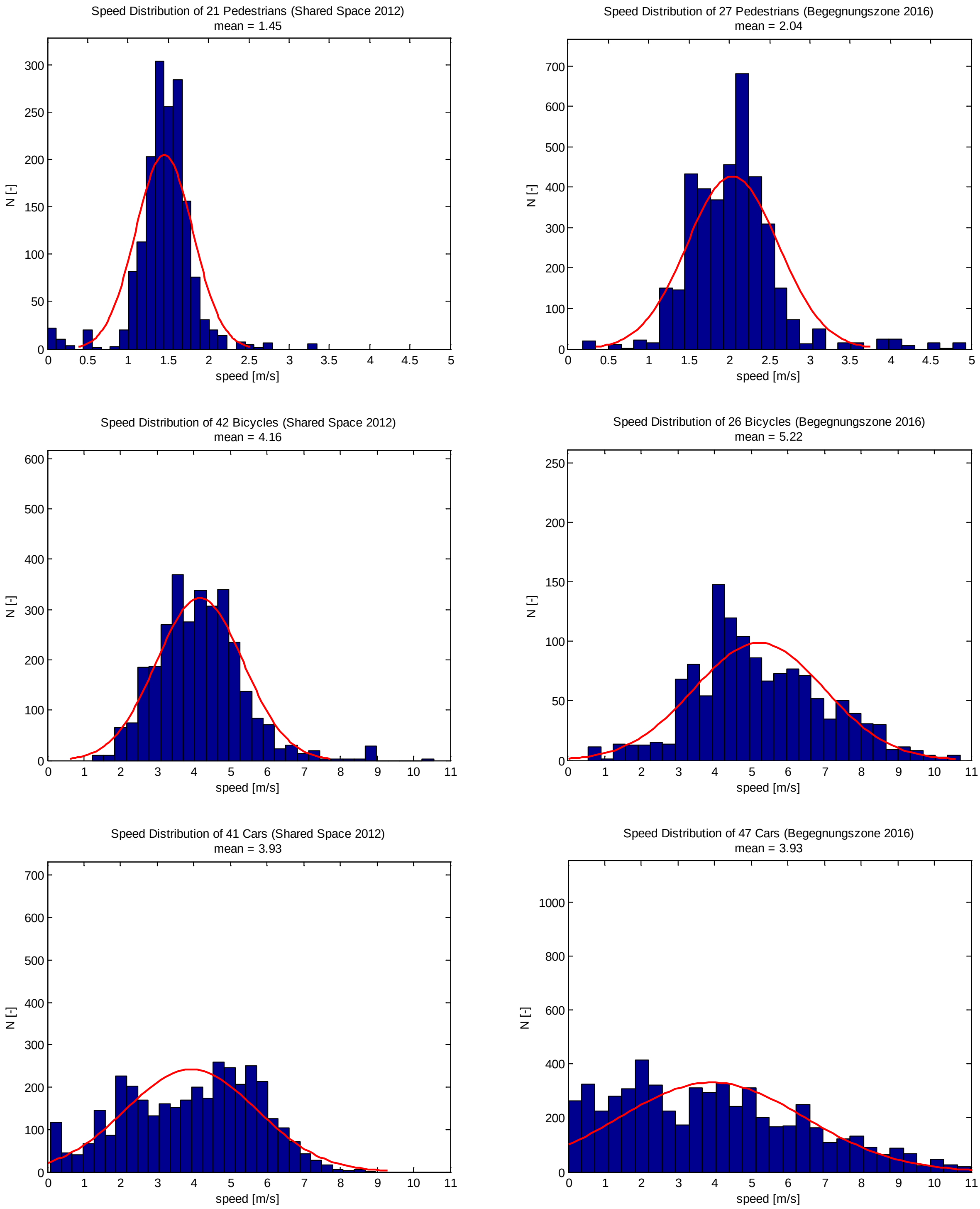

Figure 5.13: Walking and driving speed histograms of the trajectories in the conflict data set 2b and 2c. TOP: Pedestrians. MIDDLE: Cyclists, BOTTOM: Cars. LEFT: Shared space 2012, RIGHT: Begegnungszone 2016, all data: Sonnenfelsplatz, Graz, Austria.

5.5 Simulation Setup

This section describes the setup of the simulation, including the traffic-demand (agent generation), network and topology, and agents' setup (distribution of parameters).

5.5.1 Network

The resulting movement trajectories of pedestrians and vehicles form the base for further traffic flow analysis, spatial distribution of speed, and interaction characteristics. The analysis of the spatial distribution of the data after reconstruction yields empirical information for civil engineers and can be used as the basis for reliable traffic simulations. A before–and–after comparison can identify potential benefits and drawbacks of the new road design. The spatial distribution is especially interesting, because it explores the changed use of the new space.

Infrastructure Setup

In the topology based editor, the square of Sonnenfelsplatz is a combination of 5 straight entrance sections, 5 turning spaces and 5 short sections that are combined to create a circle-like structure in the square. The guiding field is therefore defined as a round shape surrounding the design object in the square's center. Vehicles and pedestrians are free to move across the central element. The roads physical boundaries are provided by road furniture, the curbs at the bus station and the designated road surface design characteristics. The agents in the simulation are not physically hindered to move through objects or surface design elements. However, the force field tends to keep them from traveling into these areas.

Once this information has been entered using VISSIMs 3D rendering capabilities, the output can be written to video files. The frame in figure 6.1 shows a scene in the simulation.

5.5.2 Demand

In the following sections, the data samples are analyzed and differences are discussed. While a large amount of data is the basis for any meaningful analysis, the high extraction effort of about 8 minutes for one trajectory limits the amount of traffic participants that can be observed. Comparable weekdays and daytimes were chosen for the data samples. In the appendix, figure 8.20, figure 8.21 and figure 8.22 show the distribution of extracted trajectories and the traffic demand in the simulation for a given time span. In the simulation, 51 pedestrians, 44 bicycles and 35 cars are generated based on the values of the empirical OD matrix. The generation of agents at the origins stops after 400 seconds and the simulation fades out - in accordance to the real world trajectories.

6 Results

This chapter presents the results of the work on calibration of all implemented models with empirical data, acquired at two sites during a time period between 2011 and 2016. Finally, a practical scenario is simulated and its findings analyzed.

Different data sets are used that have been acquired during 5 measurement–campaigns. The calibration data involves a high level of detail (10 samples/s, continuous tracking) but the available quantity is kept at a minimum. The complexity in the link between empirical data and model calibration in flow models is often underrated (i.e. in Benner et al. (2017)). Therefore, the calibration work has been conducted by continuously observing plausibility and transferability.

6.1 Calibration

The results presented in the thesis primarily aim to prove the feasibility of the concept and its implementation. Pre-verification of the uncalibrated model proves the feasibility of representing mixed traffic on a flat plane. Vehicles and pedestrians follow their chosen path while collisions are detected. Compared to data samples (figure 6.1), the vehicle model and its control is capable of generating plausible trajectories.

A demonstration of a possible visualization is given in figure 6.1 - it shows some single frames from different perspectives in a simulation run of the shared space scheme at Sonnenfelsplatz. Pedestrians, cars and cyclists have been generated according to traffic demand measurements.

To determine the force field for a vehicle, the position of the guiding line within a road's profile is drawn from an empirical distribution. This distribution needs to be calibrated in shape and position. Observed data trajectories from straight road sections have been used for calibration.

The models defined and applied in the previous chapters need to be calibrated using real data to be able to reproduce real life behavior of all modes (pedestrians, bicycles and cars). Data for the calibration process was acquired at two shared space sites in Austria. The first one is a through road in Gleinstätten, Austria. The second one is a redesigned urban roundabout in Graz, Austria. In both cases, video data was recorded for several hours on a weekday. The videos were visually analyzed to find relevant scenes. In the Gleinstätten data, two kinds of scenarios were collected. The first included scenes with only one vehicle present to focus on free flow to be used for the calibration of the force field. The second included scenes with conflicts, i.e. scenes where two vehicles would come closer than a certain distance within a three second interval if they were

Figure 6.1: Simulation frames in a mixed traffic environment at medium traffic demand (Sonnenfelsplatz, Graz, Austria). MixMe is the name of the research project, where parts of this dissertation were embedded.

to continue at their current speeds. At the Graz site, only conflict data was collected. In all of the 60 conflict samples the (hypothetical) closest distance was obtained, the mean found to be 1.7 m - the 90 % quartile at 3.95. Accordingly, the distance threshold was set to 4 m. The latter data was used for the calibration of the tactical game. For the relevant scenes, trajectory data was collected by semi-manual annotation (Schönauer et al., 2012a).

6.1.1 Calibration of the Force Field

Observed trajectory data taken in straight road sections have been used for the calibration. For each of the 10 vehicles in free-flow, the best possible guiding line was found by minimizing the mean distance between the real trajectory and the trajectory estimated in the simulation model. This was possible as there were no conflicts or interactions between agents in the data that would have made it necessary to calibrate the game first, but it was possible to simulate the vehicles and pedestrians solely using the precalibrated SFM in VISSIM. Finally, the distribution was estimated by fitting a beta distribution to the calibrated points. The two shape parameters were fitted as a=15.78 and b=6.09 using MATLAB (Rudloff et al., 2013). The mean of this beta distribution is around 0.72. In the implementation of the model for each agent, one value is picked from the distribution randomly.

6.1.2 Calibration of the Tactical Game

The well-known theory from the area of discrete choice models can be applied. As the two random parts $u_L(i)$ and $u_F(j|i)$ are independent, the probability $P(i,j)$ of the pair (i,j) being chosen by the leader and the follower is given by:

$$P(i,j) = P_L(i)P_F(j|i) \tag{6.1}$$

Given the chosen strategies in the collected data, a log-likelihood approach can be used to estimate the parameter values in the following way:

$$L(\theta|y_{in}) = \prod_n \prod_i \prod_j P(i,j)^{(y_{ijn})} \tag{6.2}$$

where $y_{in} = 1$ if i is chosen by n and 0 otherwise. For estimation, logarithm is applied:

$$L(\theta|y_{in}) = \prod_n \prod_i \prod_j P(i,j)^{(y_{ijn})} = \sum_n \sum_i \sum_j y_{ijn} log(P(i,j)) \tag{6.3}$$

Shared Space on two sites: The calibration data was acquired at two sites (data sets 2a, 2b and 2c). Since the data was recorded from two separate sites, it was necessary to statistically test if the data was actually from a single population before it could be combined for the game' s final estimation of parameters. To do so, both the data set 2a (Gleinstätten) and the data set 2b (Graz) has been analyzed by the Wald test. Due to the small amount of data, the test gives only an indication as not all the parameters are significant. However, the Wald test returns a value of 7.967 (p-value = 0.151) showing that the null hypothesis of the two models being from the same data cannot be rejected. As a consequence, the data is combined and the parameters are estimated, see table 6.1. The parameters are estimated by minimizing the log-likelihood above using numerical optimization in MATLAB. One can see that all parameters are significant. This is especially interesting as it reaffirms that the social component is important in choosing a conflict resolution strategy in a shared space environment (compared to normal environments, where it is expected that conflicts are resolved using normative behavior).

Parameter	Value	Standard deviation
θ_V	1.3538	0.6598
θ_R	1.1458	0.3730
θ_S	2.0249	0.5787
θ_N	1.1258	0.5679
θ_E	1.9803	0.4612

Table 6.1: Shared space, data sets 2a and 2b: Parameters found and theirs standard deviation.

Comparing Shared Space with Begegnungszone: It appears that this is one of the most interesting parts of this thesis. Conflict data of the Sonnenfelsplatz data sets 2b (2012, shared space) and 2c (2016, Begegnungszone) is analyzed, and for both sets, the tactical model is calibrated in a equivalent setup. The normative situation and therefore the model is different in the two scenarios (see section 5.4.5).

Parameter	Shared Space 2012		Begegnungszone 2016	
	μ	σ	μ	σ
θ_V	0.92	0.48	0.11	0.45
θ_R	0.96	0.41	0.9	0.46
θ_S	**2.16**	0.62	**1.7**	0.54
θ_N	**1.47**	0.68	**5.15**	1.52
θ_E	1.62	0.47	1.79	0.39

Table 6.2: Comparison between shared space and Begegnungszonen: Values for the utility models and their standard deviation.

The maximum likely-hood method provides a mean value μ and a standard deviation σ for each theta. In order to visualize the relation between shared space and Begegnungszone, for each θ, a Probability Density Function (PDF) is plotted in figure 6.2. This PDF is defined as:

$$y = f(x|\mu,\sigma) = \frac{1}{\sigma\sqrt{2\pi}}e^{\frac{(-x-\mu)^2}{2\sigma^2}} \tag{6.4}$$

Velocity: In both data sets (shared space (2b) and Begegnungszone (2c)), the relative velocity of the road users' choice of strategies plays a minor role ($\theta_V < 2\sigma_V$).

Relative Distance: In both data sets, the effect of the relative distance on the road users' choices is low ($\theta_R > 2\sigma_R$). When using data set 2a and data set 2b, this aspect seems relevant. This leads to the hypothesis, that in simple crossing scenarios, the spatial distance plays a certain role in decision making.

Social Aspect: In both data sets, the effect of a specific social behavior on the road users' choice is strong ($\theta_S > 2\sigma_S$). In the data set taken in the shared space scenario, the social aspect dominates the rest (weighted by θ_S). This is in accordance to the theory of shared space and plausible when comparing it to qualitative findings in international literature on shared space.

Normative Aspect: The largest difference of μ at all θ_x between the data sets of shared space and Begegnungszone is clearly the normative aspect: In the data of the shared space scenario, the normative aspect (weighted by θ_N) is relevant, but is clearly

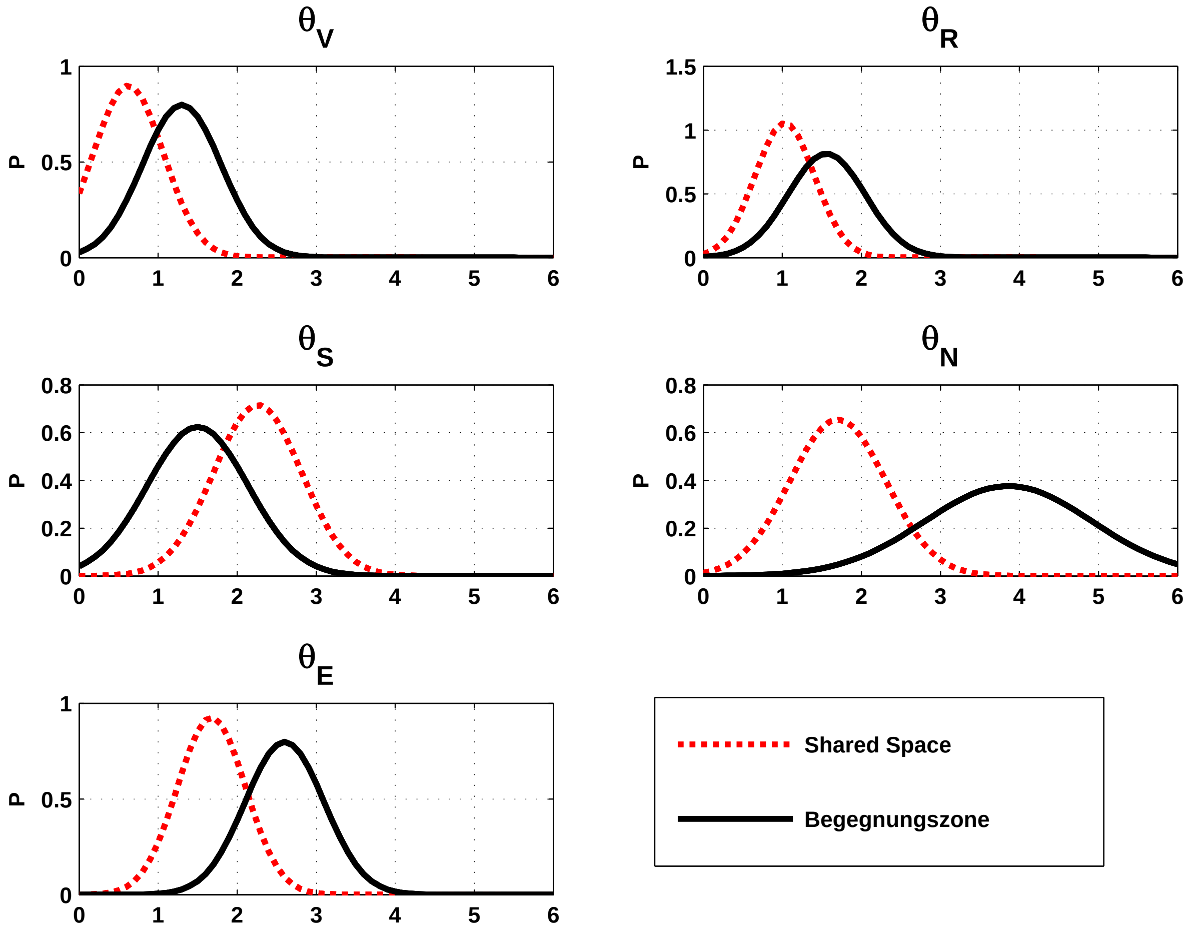

Figure 6.2: Comparing probability density functions of θ_x in the tactical model.

dominated by the social aspect (weighted by θ_S). In the Begegnungszone, it is vice versa: The θ_S is one of the low values, and the whole model is clearly dominated by θ_N.

Important remark: The traffic regulations for Begegnungszone already consider a high level of social behavior (give way to a non-motorized road user). Therefore, the calibration result doesn' t mean that motorized road–users in Begegnungszonen act less social or less defensive. In other words: In Begegnungszonen, voluntarily defensive strategies ("social behavior") are considered as normative behavior.

Aspect of Energy Loss: In both data sets, the effect of energy saving of the road users' choice is low ($\theta_E > 2\sigma_E$). Interestingly, this aspect plays a larger role in the outcome of the conflicts than the relative velocity. Basically, the kinetic energy loss is proportional to the square loss of moving speed. Interestingly, when using data set 2a and data set 2b, this aspect is very strong. It is remarked, that in data set 2a, the speeds (and therefore the kinetic energy) is much higher (up to 50 km/h).

Varying Θ_N and Θ_S: To demonstrate the sensitivity of both Θ_N and Θ_S, both parameters are varied and the result of the game is compared to the empirical data. The result of the game is defined by (similar to equation 6.3):

$$f(\Theta_{V,R,S,N,E}) = -\sum_{i=1}^{n}(log(P_{Leader}(\Theta_{V,R,S,N,E})xP_{Follower}(\Theta_{V,R,S,N,E}))) \qquad (6.5)$$

where n is the number of conflicts. The result of that function $f(\Theta_{V,R,S,N,E})$ is then optimized, results are shown in figure 6.3.

The surface in figure 6.3 for the shared space data set 2b shows a very homogeneous curvature for both the varied ranges for Θ_N and Θ_S. The second surface plot in figure 6.3 for Begegnungszonen shows the difference of level and curvature of Θ_N and Θ_S. The shapes are similar to those, shown in figure 6.2. Two other visualizations of varying Θ_V, Θ_E and Θ_R are shown in the appendix:

- Varying Θ_V and Θ_E: Figure 8.33 (appendix) shows a strong influence of both parameters for the shared space data set 2c. The equivalent surface plot for Begegnungszone (data set 2c) visualizes the low impact of Θ_V.
- Varying Θ_V and Θ_E: Figure 8.34 (appendix) shows a strong and homogeneous influence of both parameters for the shared space data set 2c. The equivalent surface plot for Begegnungszone (data set 2c) visualizes - as expected - a plain curvature.

All the surface plots in figure 6.3, figure 8.33 (appendix) and figure 8.34 (appendix) show continuous curvatures with a single maximum. This provides an indication that the log-likelihood maximization is able to find absolute minimum values for each Θ_x (not only regional minimums).

Behavior in Begegnungszone and Shared Space: Regarding the social and normative behavior in Begegnungszone and shared spaces, the social aspects from a perspective of agent i are:

- Cars (i) choose a defensive strategy if j is a pedestrian or cyclist
- Cyclists (i) choose a defensive strategy if j is a pedestrian

SU^L_{ij}, SU^F_{ij} social utility for agents i, j given as $SU_l(i,j) = 1$ when the decision (i,j) is supported by social convention and 0 otherwise. Social convention means the defensive strategy towards a road - user of a lighter mode of transport. The weights are - in descending order - the following: car - cyclist - pedestrian. In example, for a car it is socially preferable to let the pedestrian cross the street. At conflict of road-users of identical mode of transport, the defensive strategy (STOP) is considered to be social. At the strategies LEFT and RIGHT, the geometry of the agents is included into the calculation. If the position and direction of movement allows a dodging maneuver behind the other agent (not hindering or stressing the other agent), utilities of 1 are gained.

6.1.3 Estimating: Who is the leader?

In an exploratory manner, the best method of defining the leader and the follower in the proposed game is estimated. Following approaches are evaluated:

- The faster agent represents the leader (higher speed dominates).
- The agent who is in the right-of-way according to the traffic regulations represents the leader.
- The agent who is closer to the conflict point - in terms of time - represents the leader.
- The agents weight decides, it could be the "heavier" or the "lighter" agent who leads.

If there is no clear difference in weight between two agent of the same mode, combinations of two criteria above are considered as well.

The comparison was done by comparing the log-likelihoods of the different model parameters. The result can be seen in table 6.3. It shows the values of the objective function in both scenarios. While the log-likelihoods show that the first three selection processes produce models of very similar fit, the one with the best fit has been chosen. It appears that - independently from whether shared space or Begegnungszone - the best fit is gained with **"time to conflict point"**.

In the simulation, therefore, the leader is the player that is closer (in terms of time) to the conflict point at the time of the decision.

Leader selection method	**Log-Likelihood data set shared space**	**Log-Likelihood data set Begegnungszone**
Time to conflict point	115.26	73.94
Higher speed	115.83	77.87
Right of way	115.50	74.03
Weight then time to conflict	117.11	82.4
Weight then speed	117.72	83.63
Weight then right of way (right before left)	116.64	83.24

Table 6.3: Log-likelihood values for the different ways to select the leader in the two models / two data sets.

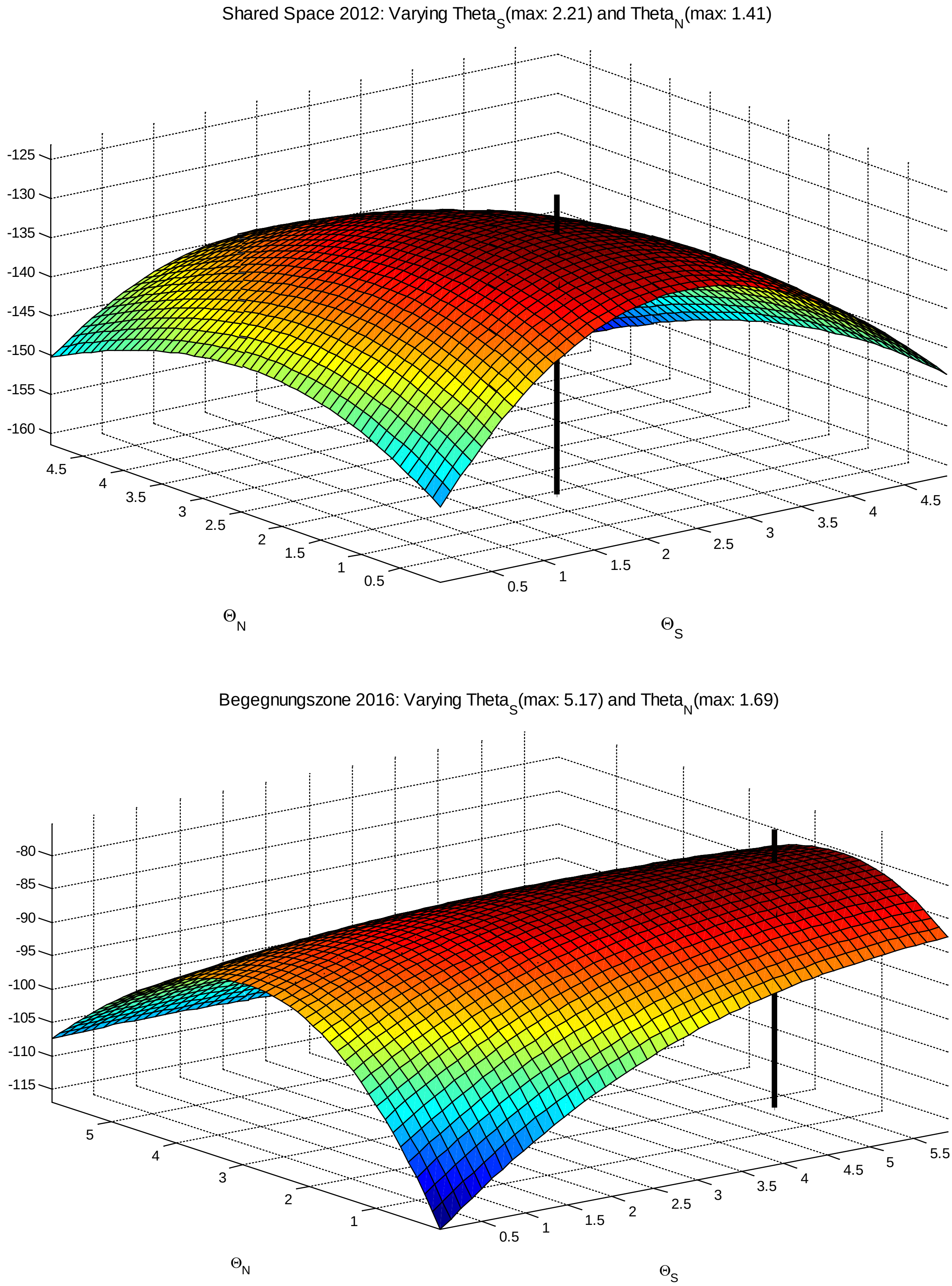

Figure 6.3: Varying Θ_N and Θ_S. leaving other Θ_x as shown in table 6.2. TOP: Based on shared space, data set 2b (2012). BOTTOM: Based on Begegnungszone, data set 2c (2016).

6.2 Validation on Specific Examples

To further explain the model's characteristics, it has been applied to a real world scenario with varying parameters. Two scenarios have been taken from the data at Sonnenfelsplatz (2012).

Cyclist and Pedestrian

An example of an interaction between a pedestrian and a cyclist is shown in figure 8.35 (appendix), conflict 51 has been picked (see table 8.5). While the pedestrian continues on his desired path, the bicycle turns left to avoid the person. To demonstrate the models reaction to variances in the scenario (spatial constellation) of the interacting pair, the approaching time of the bicycle has been shifted back and forth (for each by one second). The results in figure 6.4 show $P(i,j) = P_L(i)P_F(j|i)$ where i represents the bicycle and j the pedestrian. When the cyclists earlier comes to the point of the hypothetical conflict, she or he is the leader in the conflict and gains almost equal results in all strategies. For the pedestrians, the strategy with the highest utility is to turn left which would bring him closer to the bicycle.

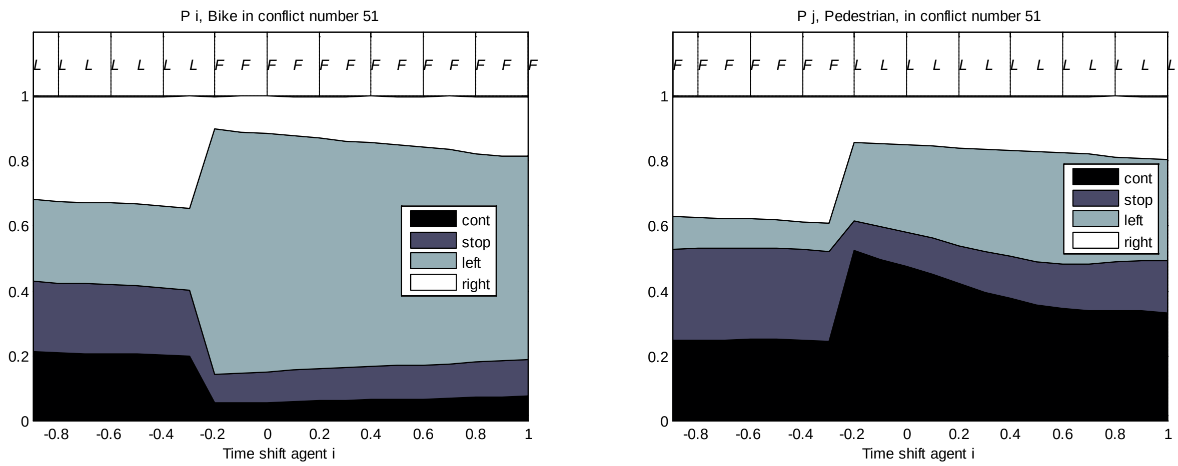

Figure 6.4: Probabilities for choosing specific strategies at varying the approaching time of the cyclist. Assignment of leadership alternates. LEFT: P_i for the cyclist. RIGHT: P_j of the pedestrian.

When the leader assignment shifts to the pedestrian (indicated with L and F in figure 6.4), she or he is able to obtain a higher utility by simply continuing on the same path. Using the given leaders' strategies the followers' behavior can be visualized. Figure 8.36 shows that if the pedestrian stops, the advantage of the avoiding strategy LEFT decreases. If the pedestrian i would turn right (time shift ¡ -0.2), it is obvious that the bicycle would gain a higher distance by turning right, too.

Car and Pedestrian

Figure 8.37 (appendix) shows the interaction between a pedestrian and a car (conflict 41 in table 8.5, appendix). While the pedestrian stops at the island-like central place in the square, the driver continues without any obvious reaction. To demonstrate the model's reaction on varying the geometrical constellation of the interaction pair, the approaching time of the bicycle is shifted 1 second back and forth. The results in figure 6.5 show $P(i,j) = P_L(i)P_F(j|i)$, where i represents the bicycle and j the pedestrian. When the cyclists arrives earlier at the point of the hypothetic conflict, she or he is the leader in the conflict and gains almost equal results in all strategies while the pedestrians' strategy of highest utility is to turn left that would bring him closer to the bicycle.

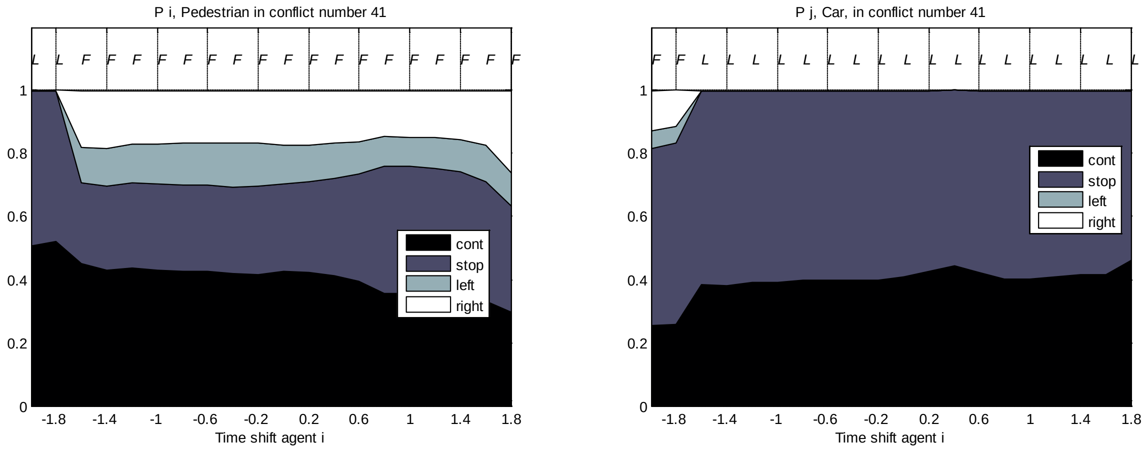

Figure 6.5: Probabilities for choosing specific strategies at varying the approaching time of a pedestrian. Assignment of leadership alternates. LEFT: P_i: pedestrian. RIGHT: P_j: car.

When the pedestrian takes over the role of the leader (indicated with L and F in figure 6.5), she or he is able to obtain a higher utility by simply continuing on the path. In figure 8.38 (appendix), the follower' s response to an assumed leaders choice is shown. In the real scenario, the pedestrian slightly turns right (at a very small turning angle). In the model, turning right shows only a low probability. Hypothetically, the reason lies in the very defensive behavior of the pedestrian since she or he is exposed in the square' s center. Remark: It is the only situation in the data set 2b, where a pedestrian crosses the squares through the center.

6.2.1 List of all Parameters Found

The estimation and calibration of parameters represent the primary base for future research of this thesis. Table 6.4 gives an overview of the model parameters found. The values for Θ_x are those, valid for the shared space scenario.

Variable	Model	Value	Std. Dev.	Description
$d_{lateral}$	Force Field	0.72	0.0918	Weight of the center guiding
a	Force Field	15.78	-	Shape of Beta dist. $d_{lateral}$
b	Force Field	6.09	-	Shape of Beta dist.$d_{lateral}$
$v_{bike\,center}$	Force Field	4	0.4	Threshold: Bicycles use center [m/s]
$t_{simStep}$	Conflict	0.1	-	Sim. step in the conflict detection [s]
$d_{conflict}$	Conflict	4	-	Distance where vehicles [m]
θ_V	Tactical	0.92	0.48	Weight of velocity dependent disutility
θ_R	Tactical	0.96	0.41	Weight of the distance related disutility
θ_S	Tactical	2.16	0.62	Weight of social related disutility
θ_N	Tactical	1.47	0.68	Weight of normative related disutility
θ_E	Tactical	1.62	0.47	Weight of energy loss disutility
$n_{sim\,tactical}$	Tactical	5	-	Sub-simulation time steps
P	Vehicle	24.2	-	Proportional control constant
I	Vehicle	1.0	-	Integrative control constant
$\delta_v(bike)$	Vehicle	0.3	-	Vehicle control parameter
$t_{look\,ahead}$	Vehicle	7.5	-	Lookahead time (vehicle model)
k_c	Vehicle	15	-	Static control constant vehicle model
k_v	Vehicle	30.0	-	Velocity dependent vehicle control model
kb_c	Bicycle	0.5	-	Static cycle control model
kb_v	Bicycle	0.5	-	Velocity dependent cycle control model

Table 6.4: Essential parameter values for the various sub models found by calibration.

6.2.2 Experimental Fun: Crazy Cyclist and Van

This demonstration is not part of the scientific study, but a theoretical piece of work enjoying the model' s capabilities. It is not situated in the shared space context. Figure 8.39 (appendix) shows the interaction between a cyclist and a white van. The footage was taken from a helmet camera (Zenga, 2012) during an unofficial bicycle race in New York City. It should be noted that the trajectories used here are more of a rough estimation than a measurement and the real van' s trajectory and the hypothetical bicyclist' s trajectory are shown in the bottom left of figure 8.39. The scene has been rebuilt in a calibrated straight road section. The estimation of the path and speed was done manually by comparing the vehicles position to the lane markings. The data has been validated by checking reasonable speeds and velocities.

Figure 6.6 shows $P(i,j) = P_L(i)P_F(j|i)$, where i represents the white van and j the racing cyclist. The experiment was conducted without changing any parameters in strategy calculation or conflict resolution. The model clearly presents that turning right yields the best utility and therefore positively correlates with the empirical data. It should be mentioned that the dynamic parameters might be shifted to a higher a_{brake} and a higher α_{evade} due to the extreme situations, excellent driver skills, and an immense readiness to take risk.

If the cyclists arrives at the point of conflict earlier than the van, he is more likely to continue, while the van might consider using an emergency brake to avoid a collision. It can be assumed that if the bicyclist were to know that the van driver would stop, then he

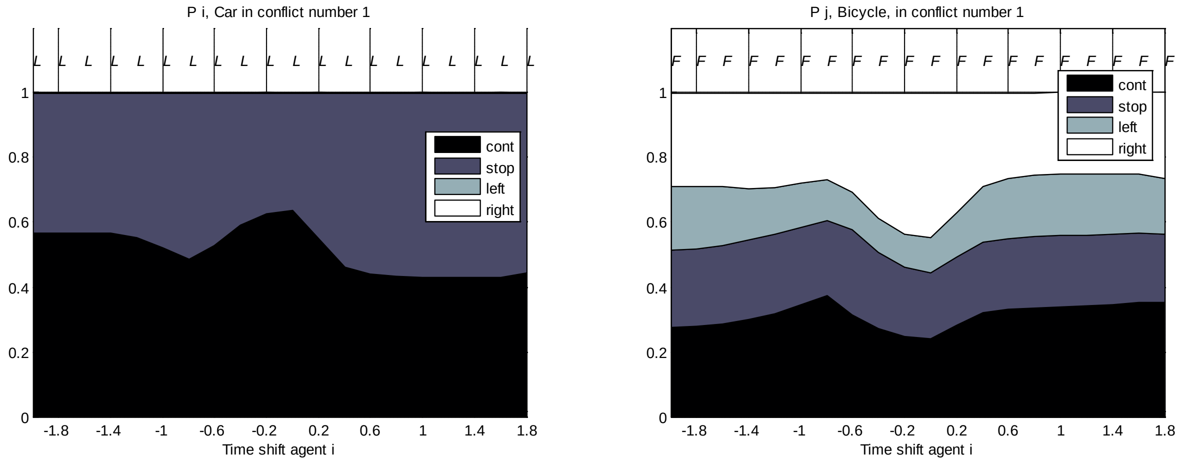

Figure 6.6: Probabilities for choosing specific strategies at varying the approaching time of the cyclist. LEFT: P_i for the van. RIGHT: P_j for the cyclist.

would most likely simply continue on his path (figure 8.40, TOP RIGHT). Considering that this assessment was not based in a shared space and that the bicyclist ignores the red traffic light, the van is assumed to be the leader (indicated with *L* and *F* in figure 6.6). When the van turns left or right, the cyclist seeks to gain distance by driving to the left side. As it was impossible to observe a car' s lateral evasion, this purely hypothetical scenario is not included in the tactical game.

6.3 Simulation Results

The willingness to share the available road space between modes of traffic is a major aim of the shared space concept. This effect was successfully reproduced within the simulation. This section qualitatively shows the spatial distribution change of the chosen paths for each traffic mode.

After the reconstruction of the roundabout in Graz, several changes in the walking behavior of pedestrians could be observed. Many pedestrians (red) cross the place using shorter paths closer to the center of the square (figure 6.7, left hand side). A higher variation in the crossing locations can also be observed. In the new design, a slightly elevated island forms the center of the square, causing a white spot in the trajectories (figure 6.7, left hand side) of bicycles (green) and cars (black). The trajectories of the simulation run (figure 6.8, right hand side) show higher channeling effects through the square. This channeling effect is also shown in simulation studies of shared space in the literature (i.e. in (Anvari et al., 2016, p.20)). The central element is not avoided by all agents since it is not modeled as an obstacle or any higher friction. The pedestrians' crossing trajectories are less curved than the real world trajectories and show higher curvature radii. The reasons lie in the path finding of the agents: Segmentation automatically leads to an orientation system similar to the way points - this can generate angular trajectories after reaching such a point.

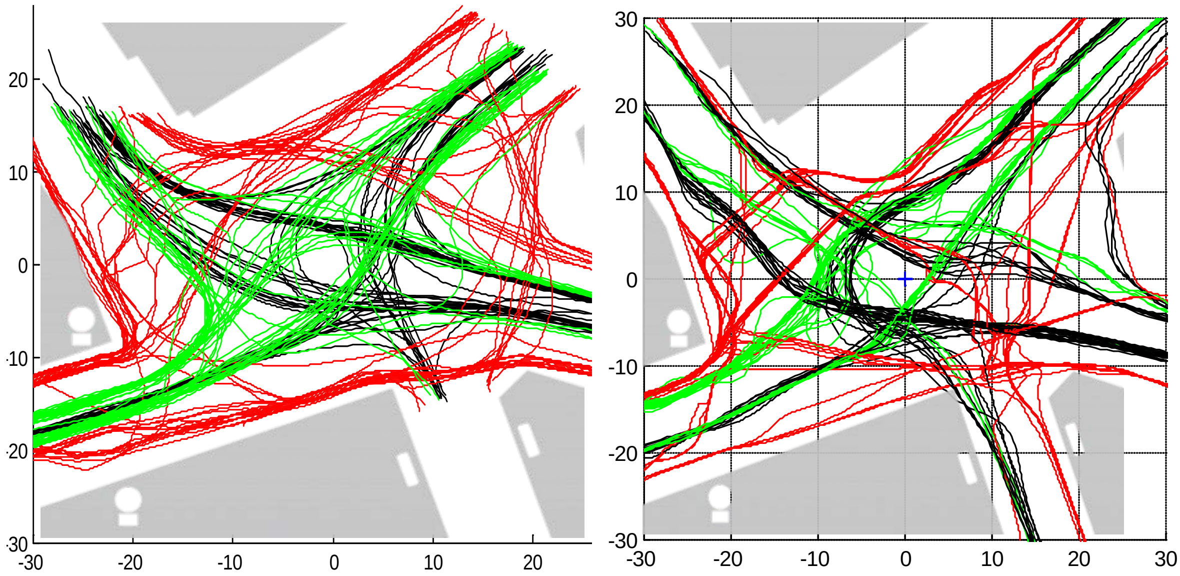

Figure 6.7: Trajectories of pedestrians and vehicles. LEFT: Shared space in March 2012. RIGHT: Simulated trajectories.

6.3.1 Comparing Speeds

The pedestrians' speed distribution is very narrow - both in the simulation and in the real world data. The probability that a pedestrian "brakes" or stops is marginal. Eigenvalue analysis of the bicylce model (see chapter 3.4.2) shows that the transition speeds in which the cycle changes from capsize mode to weaving mode is 4.2 m/s. Cycling speeds in the simulation are constrained to a minimum of 4.2 m/s - the characteristics of the bicycle stability transforms at this speed and would require a different vehicle controller. Therefore, the mean cycling speed is quite high. The dynamic vehicle model for cars is a linear single track model with continuous stability.

Driving and walking speeds are major traffic performance and safety indicators. To show the spatial distribution, the speeds for the three traffic modes have been calculated and discretized using a cell grid with cell size of 1 m x 1 m. Finally, for each cell the mean speeds for the three modes are computed and low pass filtered. The result is shown in figure 6.9.

In the empirical trajectories, the pedestrians in the shared space design move at a more homogeneous speed level. They also cross the roads at a slower and steadier speed. Looking at the car speeds in the very center of the square, a reduction can be observed that does not apply for the speed at the entrances. Car speeds stay high at the two straight east entrances to the square. In the square's center, bicycle speeds clearly dominate the speeds of motorized vehicles, which also occurs in the simulation. Interaction solving might be one of the reasons. Considering the simulated trajectories, the pedestrians' higher speeds are within the areas where pedestrians directly cross the square. The pedestrians in the simulation choose more direct paths than in the empirical

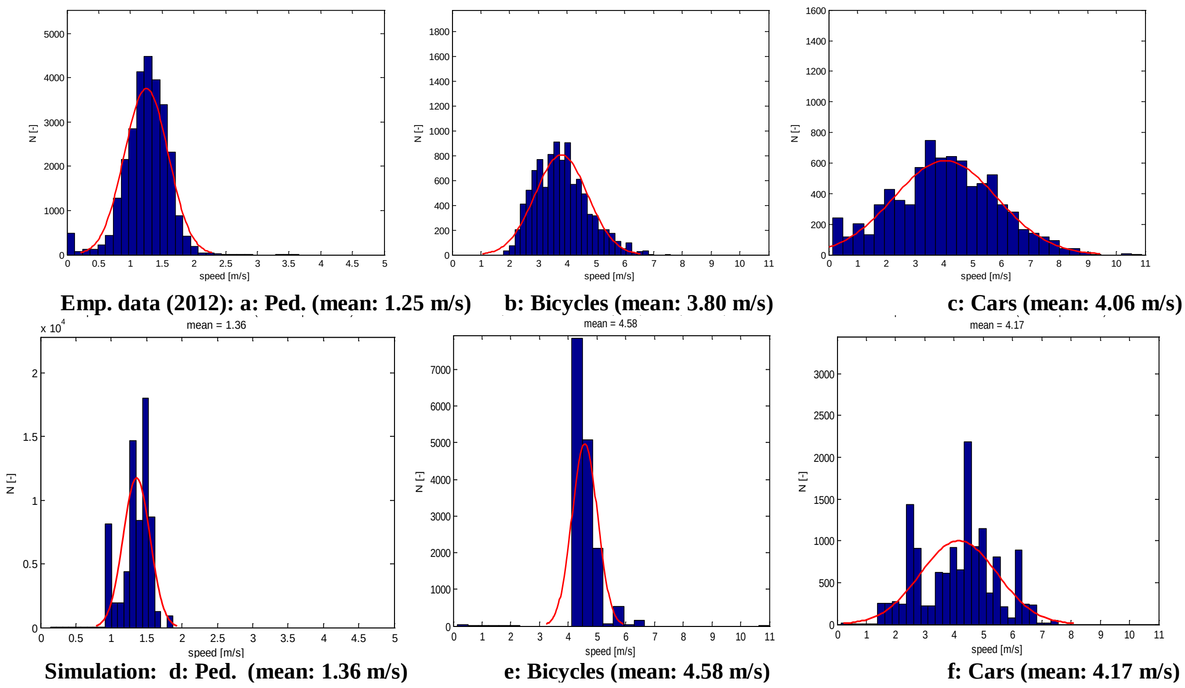

Figure 6.8: Speed histograms of the shared space (first row: a, b, c) and the data, gained from the simulation. TOP: Empirical data (2012). BOTTOM: Simulation results (d, e, f).

set and cross the square' s center more frequently. The reasons lie in the path finding methods of the agents (and probably in the infrastructural setup in the model).

In the simulation, cars and bicycles show lower speeds when leaving the square. In the real world, the drivers' speed choice show the tendency that they approach faster and leave slower. This might indicate that the total "friction" in the simulated system is too high. In some situations, social forces can influence each other at some level and reduce the speeds more than real interactions and conflict-resolution do.

The crossing of pedestrians in the simulation shows a higher spatial concentration at certain crossing spots. The reality shows that pedestrians often adjust their path of crossing to correspond to the actual vehicular traffic flow. An approaching car may shift the spot of crossing for several meters. It seems that the infrastructure force field in many situations visibly dominates the tactical force.

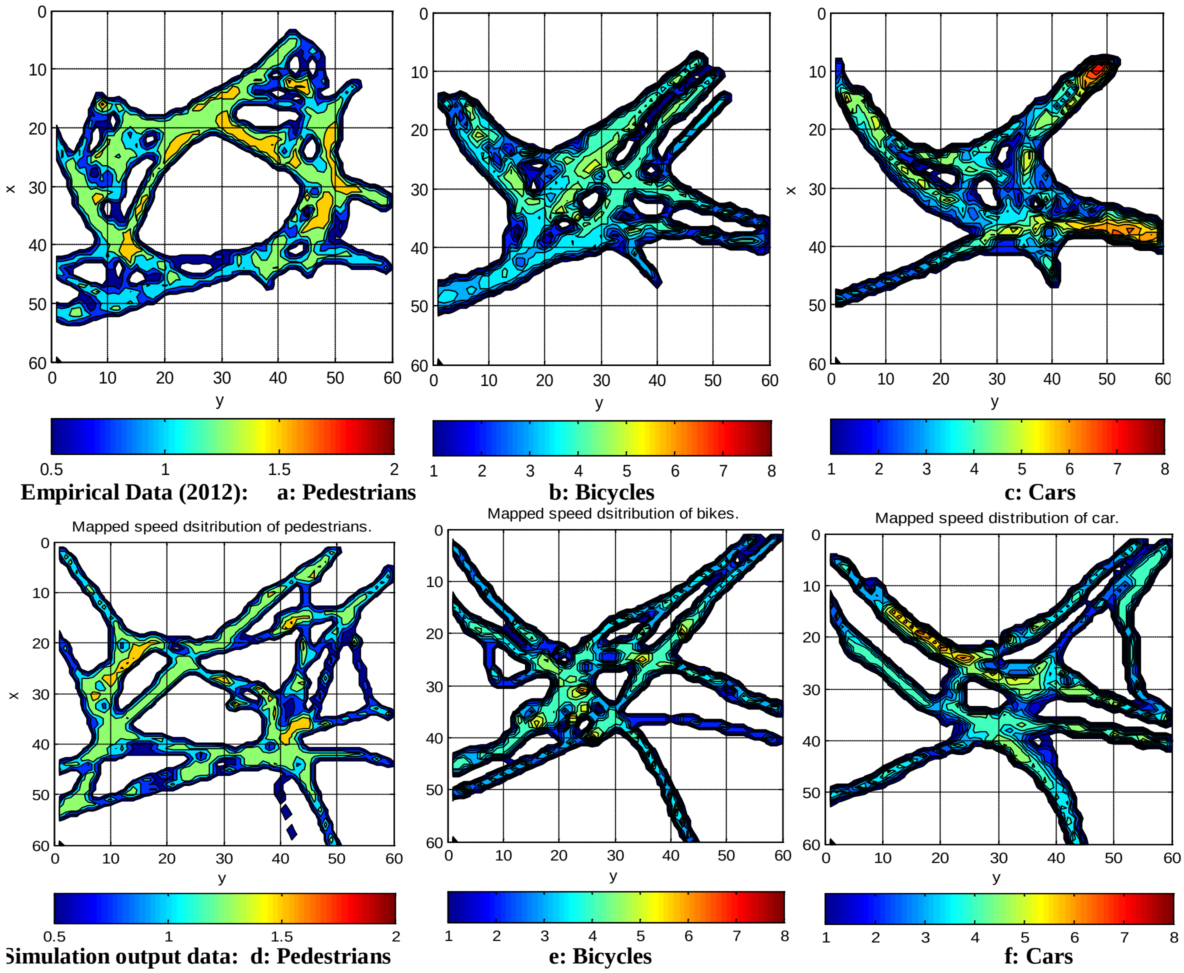

Figure 6.9: Modal map of estimated speeds, based on cell grid speeds, all speeds in m/s. TOP: Shared space 2012. BOTTOM: Simulation.

7 Conclusion

The purpose of this closing chapter is to summarize the main findings of the dissertation and to give an outlook for future research. The initializing content of this document is the analysis of microscopic traffic flow models suitable for mixed traffic flows like shared spaces. A combination of multiple sub-models has been utilized to overcome the special circumstances of the heterogeneous flows. The model has been implemented in a framework together with VISSIM and data has been acquired for calibration and validation. Furthermore, the application of the model is shown as a kind of use case in a specific topology.

7.1 Summary

Intro

Shared space and similar mixed traffic philosophies can be compared to toolboxes. Their application requires a flexible and sensitive approach. Microscopic traffic simulations allow for the highly detailed modeling of pedestrians, vehicles, and driver behavior, as well as their interactions with each other and infrastructure. The state of technology and available simulation software does not provide sufficient freedom and capabilities to reproduce the required dynamics and social interaction. One of the most essential element when modeling mixed traffic areas is the social behavior within the interactions between car drivers, pedestrians and cyclists. This can be observed in situations, where pedestrians want to cross a road at a point other than a crosswalk and cars yield because of social factors. In a slightly different situation, the same pedestrian might make a small directional change to walk behind the car instead of waiting for the car to pass. Modeling this and similar behavior is one of the main challenges in designing shared space simulations.

- Finding the way through the infrastructure is more complex because there is no hard separation between different traffic modes.
- Due to the possible degrees of freedom, vehicles should be capable of maneuvering in a two dimensional plane - not on one–dimensional paths.
- The interaction between different types of road users including pedestrians, cyclists, and car drivers has to show social considerations.

To the author's knowledge, no available simulation model can explicitly handle the requirements that the added social interactions and constraints imply, yet. This dissertation provides a prove–of–concept, lessons learned and technical methods towards such a model.

Background

Shared space and similar road design concepts are implemented more and more frequently. Examples of shared space can differ greatly from each other because of the variety of local conditions, design elements, and traffic demand and therefore, the philosophy exhibits a high potential for experimentation. This makes it extremely difficult to show the effects of a planned shared space with the presently available tools. Different topography, complex traffic situations, and a wide variety of design elements present great challenges for planners. Behavior analysis has confirmed that intended goal of traffic calming, increased road safety and urban street–scape qualities have been reached in the past. However, it is still hard to conclude, which specific elements helped to achieve the effects, making it difficult to assess the impact of potential future shared space projects. Therefore, a realistic shared space simulation was proposed that could help in the planning phase for future projects. A simulation model allows planners to test effects of different design elements before they are built. The simulation could help during the concept phase by:

- Addressing capacity concerns
- Determining potential bottlenecks
- Improving safety and comfort

While there is no combined simulation tool for shared space, many approaches to microscopic simulation of segregated modes of transport exist in the scientific literature. These are useful starting points for a shared space simulation model. Physics-related analogies such as social force models exist for pedestrian flows and cars (Helbing and Tilch, 1998). These models provide a good foundation for handling basic interactions between agents from the same mode.

Some research has been performed so far on the interaction between individuals using different modes, especially in the last 5 years. Most current publications dealing with conflicts between pedestrians and cars concentrate on a rule based approach, where the right of way is given by the infrastructure, e.g. a pedestrian crosswalk where cars give way to pedestrians within a certain area close to the crosswalk. However, there are still some missing pieces in linking specific design elements and traffic concepts to the behavior of people. Amongst those missing pieces the following seem especially relevant:

- Path choice in a street–scape without physically constraining side-areas and the road's center
- Decisions for right-of-way in conflicts
- Speed choice in free flow (affected by the road' s design)

This may necessitate an infrastructure model incorporated into a microscopic traffic simulation. Furthermore, this thesis presents a vehicle model and an underlying game theoretic tactical model that can deal with the social interactions taking place in a shared space environment.

Model Design

Modeling shared spaces induces numerous requirements on the complexity of infrastructural topologies, demand, and characteristics of interaction processes. The technical setup requires additional aspects be considered in the model and architecture design. The extended form of the social force approach and its application to mixed traffic has been described above. An infrastructure model, an interaction model, and vehicle mechanics models have also been implemented and discussed. The design has to be flexible and has to consider versatile topologies, designs and traffic modes. An approach is introduced showing how the agent based model can offer physical plausibility in a 2D environment and consider social interactions with other agents as well.

To reflect the road's topology, structure and static objects in the environment, the concept describes three layers:

- Area of movement, where the agents decides on their path and can interact with each other.
- Guiding field, which motivates the agents to use certain lateral paths.
- Obstacles, which keep agents at distance.

The model design proposes a force field of the infrastructure which overlays the general path finding with design based directions in the operative movement. It is shown how the force field is generated on sections of squares and lanes. A representation of the physical models are separately defined for cars and bicycles. A control unit acts as an interface between the vehicle models and the perception of forces. A novel method to describe interactions between agents even allows the inclusion of social considerations. The tactical interaction model is based on identifying and solving the agents' conflicts and in reacting according to the strategy found. Each conflict is described as a set of parameters which is derived from the agents' positions, the agents' static parameters (weight, mode) and the dynamic variables (speed, direction). Those values are derived from observation and the calibration respectively.

Implementation

Two parts of VISSIM are utilized:

- The editor and simulation framework is used to generate the infrastructure model, the demand, and other behavioral parameters (desired velocity, acceleration, weight etc.)
- The pedestrian model provides social force implementation, path finding and parameter sets.

The implementation of the two level tactical planner for pedestrians and vehicles in the mixed traffic plane with obstacles is shown. The first approach extends the social force - coupled ODE approach by using a "sensing mode" (simulation runs) to predict all agents' positions over n time-steps. The second level introduces a set of tactical methods to evaluate the best conflict avoidance strategy. To transfer the social force model road users at high speeds (up to 50 km/h), requires a higher look-ahead distance and path planning. Research on robotics, autonomous driving and driver assisting systems show different approaches of algorithms. Mechanical models and control systems are applied to theoretical models on tactical path decisions and following. The simulation process is a sequence of both logical decisions and continuously interacting agents. Unlike the pure SF model in our approach, the sensing simulations prepare the choice of conflict resolution strategy and its actions.

Results

The data characteristics have been presented along with the simulation setup of the *Sonnenfelsplatz* scenario. To validate and calibrate the model, video footage has been recorded in Gleinstätten after the shared space implementation and at the Sonnenfelsplatz in Graz, Austria, both before and after reconstruction of a complex roundabout using shared space principles (see figure 5.8). Both, the geometric model and the traffic demand model of both sites have been generated in VISSIM.

Calibration procedures are also applied to finding parameters in the conflict model, the tactical model, the force model, and in the vehicle kinematics. The simulation is able to reproduce conflict resolution as well as realistic trajectories. It is shown on a macroscopic level how the spatial distribution and speed choice fit with real data.

In the presented approach, the square in the case study was used by vehicles counter–clockwise, similar to a conventional roundabout. This was due to the limited possibility to combine the static route choice with the dynamic traffic situations.

7.2 Conclusion

Summary

The dissertation gives a vast literature review about mixed traffic concepts and all of their aspects to design valid microscopic models. The thesis shows possibilities for modeling infrastructural design specifics and the impacts on traffic flows in mixed traffic. It shows the potential of this approach to mathematically describe social interactions in heterogeneous traffic flows. The presented simulation framework is based on continuous interaction between pedestrians, cars, cyclists and the road infrastructure. The core elements of the SFM and two different mechanical models are presented. Furthermore, this thesis demonstrates an approach of game theory–based handling of traffic conflicts. The methods used to acquire data have also been outlined, and finally the expectations on calibration and the perspective for science and civil engineering have been drafted. Such a model offers civil engineers the chance to evaluate their design for a new shared space project before implementation. Planning tools could therefore benefit from further development.

Tactical Game

This work presents the calibration and evaluation of a shared space simulation model using real data. The calibration of tactical game theoretic conflict handling confirms the assumption that in a shared space purely normative behavior does not dominate the variety of behavioral strategies during interactions. In shared spaces, socially acceptable behavior is an important part of the utility that the players maximize during the described game. In contrast to that, in Begegnungszonen, the rule-based behavior dominates the social aspect. However, in Begegnungszonen, the rule-based (normative) behavior includes some of the factors that are here considered to be "social". Furthermore, in both shared space and Begegnungszonen it can be seen that it is not the heavier, faster vehicle that decides the strategy as the leader. It is rather the case that the person closer to the conflict point is the leader and can choose the best strategy. For the guiding field, a very simple approach was used. This is quite restrictive for path finding, especially for pedestrians. Despite this easy approach, space usage is already quite realistic.

Comparing Simulation and Real World

It is shown that the simulation performs in a comparable way to the behavior observed in the real world data, despite the complex setting of the shared space at Sonnenfelsplatz which includes a relatively large square. In particular, it can be seen that both in real life and simulation, all three modes of transport have a larger space usage compared with data from the time before refurbishment. In addition, for pedestrian and cars, the speed profiles for real and simulated data both follow similar distributions. In particular, it can be seen that the cars in the simulation decelerate quite strongly to avoid conflict situations. For bikes, the bicycle model used does not yet support low speeds well enough, so the speed distribution is not similar. However, bikes tend to avoid conflicts by riding around an obstacle instead of braking; therefore, the fact that there are no very low speeds is not unrealistic. From the maps of estimated speeds, it can be seen that in both the real data and the simulation, pedestrians cut across the square much more than they had on the roundabout. In both cases, speeds are higher during the crossing process than they are while the pedestrians are at the edge of the road. This is not the case for cars, which have areas in the square where they decelerate to give right of way to other traffic participants in both real life and the simulation. The combination of VISSIM' s DLL and the vehicle model and control model could not be implemented in a satisfactory way. Issues at a stable vehicle control are observed that could not be solved here.

Potential for Safety Studies

As shown in chapter 5.4.5, trajectories can be utilized to estimate safety indicators. The simulation framework, therefore, would be a valuable tool to evaluate road safety issues in infrastructure designs. It would also be suitable for illustrating the traffic flow in a planned shared space to citizens, politicians and other stakeholders. The persons concerned would be able to get a clear visualization and quantities in order to better understand how the new road design would work.

Alternative Model Approaches

Considering the high complexity of the linear steering model and its relatively low share on the validity in the modeling system, a heuristic approach would be a promising alternative. One possibility would be a dependency function of yaw–angle ψ and v as introduced by Anvari (2014); Anvari et al. (2014). Higher steering stability and a lower number of calibration parameters could be gained. Independent of the modeling approach, the combination of target vectors and tactical maneuvers seem to be one of the biggest challenges.

Technical Aspects

The implementation of the simulation models in a framework including VISSIM as major simulation and visualization engine had some implications on both work and findings:

- Debugging is limited and constrained using the DLL that was provided by PTV. Simple data exchange requires a certain overhead.
- The simulation performance of VISSIM is high, the models developed here are as well. To combine both via a constraining interface showed critical bottlenecks and turned out not to be the perfect choice for research work in this phase of developing software and methods.

The framework's computing requirements are immense. Two agents can be simulated in real time, higher numbers increase with n^2 and the case study with 40 agents requires a processing time of around 4 hours (at 400 seconds simulation time). This is caused by the complex wrapping structure and the "sensing methods" to gain higher lookahead.

7.3 Future Research

7.3.1 Model Design and Architecture

Technical Framework

If the SF model could run on its own code, most of the performance and debugging issues can be solved. The earlier mentioned combination of guiding and path finding would possibly gain a higher efficiency and further reduce processing time.

Model Design

Future work should address the remaining problems in the model design and implementation. This includes in particular a more realistic bicycle model and vehicle control. Public transportation, which is not currently included in the simulation model, may also be addressed in future research. A guiding field that already considers aspects of tactical routing would also make the pedestrians' routes more realistic. The check on transferability of the model to different shared space settings is an important aspect of future research. In particular, it would be interesting to see if it is enough to adjust desired speeds or even behavioral parameters to transfer the model to a shared space in a different country.

The results showed that the overlay of guiding forces and target forces can interfere and therefore reduce the agents' speeds. An approach that includes all infrastructural objects in path finding could solve this issue and create more realistic results. The experiments showed that parameters within the control unit have a strong influence on the trajectory and the path in conflict situations and in curves. Simplified heuristic methods might be more stable for all modes of transport and suitable for the purpose of shared space simulations.

7.3.2 Model Application and Transferability

Simulation of Traffic

The data on driving speed shows a lower number of very slow and waiting cars due to the shared space implementation. This implies that stop stations of public transport could affect the total flow more than in conventional road design. The impact of the stop positions could be evaluated in simulations. Loading procedures would therefore have to be modeled and parameterized, as well. This issue could be addressed with the agent generator and random or periodic bus schedules.

The deviation between the observed and simulated trajectories is based on the constraints of the vehicle model and the limited steering capabilities. A heuristic control method could simplify the computations as well as the oscillation behavior in the control loops and bicycle kinematics. Future research may verify this through the assessment of more diverse data sources and different environmental conditions. Even though the complexity of the topologies is quite high, the impact of design elements should be isolated and observed separately.

The model's transferability might be one of the most important aims of future research. All the following aspects could play key role in determining the traffic behavior:

- Traffic demand / traffic densities (group behavior, "gap-acceptance",...)
- Grade of urbanity (city, village...)
- Traffic culture (different countries, different traffic regulations)
- Modal mix (relation between motorized vehicles, pedestrians and cyclists)
- Topology (size, complexity)

- Relevance within the road network (through–road, shopping–area, residential area)

Autonomous Driving

Autonomous driving and driver assisting systems show different approaches of algorithms. While most papers in the field of autonomous driving address the social dilemma about prioritizing lives during critical decision making in conflict avoidance (Bonnefon et al., 2016), there is low research on how and if autonomous agents integrate "social" considerations into their decision making. The presented tactical model could be a valuable base for future research on that issue.

7.3.3 Data Acquisition

Automation

To isolate certain aspects, a lot of trajectories of various sites would have to be acquired and analyzed. To conduct such studies with a reasonable effort, the annotation process should be done on a higher level of automation. Current state of technology in the field of pattern recognition in general and tracking of vehicles and pedestrians offer a higher grade of reliability every year. Future research should revise the semi-automated methods and technology used.

Aerial Cameras

The acquisition of trajectories is labor–intensive task. The quality of the output depends on the quality of tracking road-users and transformation of the image–coordinates to world–coordinates. Both processes are influenced by the angle of view. Recently, unmanned aerial vehicles / drones have been used to generate video footage of roads (Liu et al., 2013) - future research could benefit from the technical evolution and the potential to use static unmanned aerial vehicles with a camera.

8 Appendix

8.1 Literature

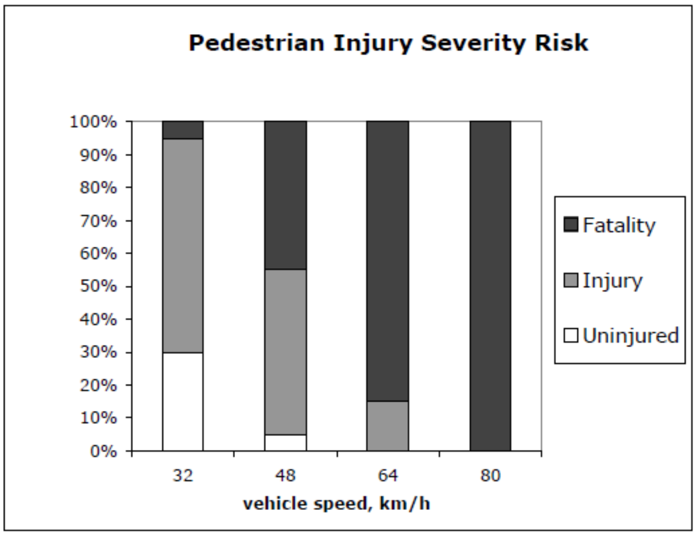

Figure 8.1: Relation between involved vehicle speeds in pedestrian accidents and the degree of injury (United Kingdom Department of Transport, 1993, in King and Wright (2005).

Number of Causal Variable	Causal Variable	Determinacy [%]	Residual Average
1	11	19.6	
1	7	16.9	
2	6/7	38.3	27.7
2	7/8	35.0	
3	6/7/8	55.1	
3	6/7/11	51.1	22.7
4	6/7/8/11	60.7	18.9
4	6/7/8/10	55.2	
5	6/7/8/10/11	60.9	19.6
5	6/7/8/9/11	60.8	19.8
6	6/7/8/9/10/11	61.1	20.2

Table 8.1: Factors of free speed choice in a regression model (Haas and Herberg, 1983). Description of variables: 6 = Traffic signs, 7 = Number or parked cars, 8 = Height of vegetation, 9 = Height of buildings, 10 = Number of pedestrians, 11 = Grade of familiarity.

Figure 8.2: Examples of soft segregation of lateral modal designation. Captions from TOP to BOTTOM. LEFT SIDE: Haren (Schönauer, 2009), Drachten (Schönauer, 2009), Haren (Schönauer, 2009). RIGHT SIDE: Bohmte in Germany, (Schönauer, 2009), Gleinstätten in Austria (derstandard.at/blei, 2011), Gleinstätten in Austria (Schönauer, 2009).

Figure 8.3: Examples of soft segregation of lateral modal designation. Captions from TOP to BOTTOM. LEFT SIDE: Gleinstätten in Austria (Schönauer, 2009), Graz in Austria (Jürgen Fuchs, 2011). RIGHT SIDE: Gleinstätten in Austria (Schönauer, 2009), Graz in Austria (Schrom-Feiertag, 2011).

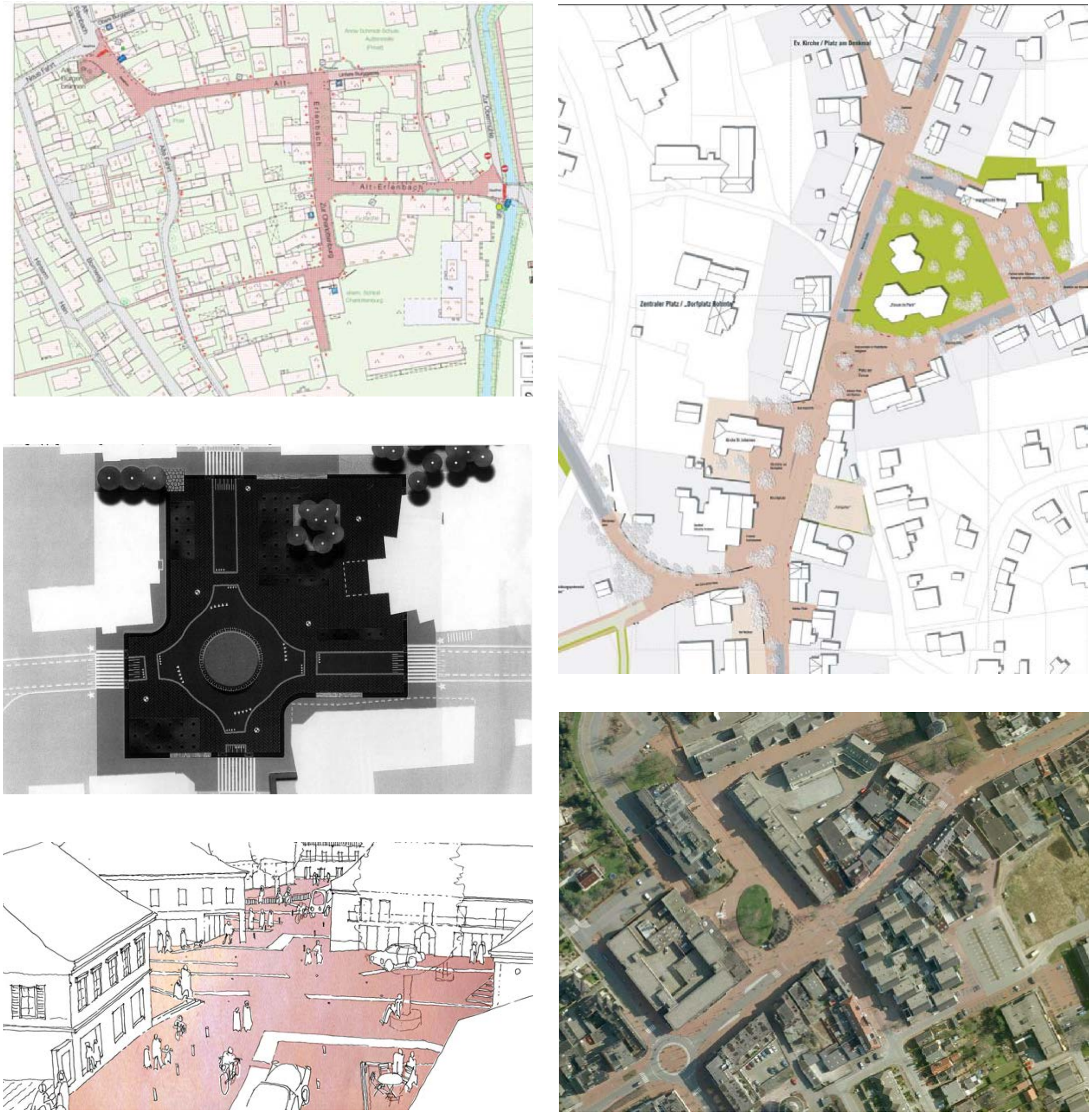

Figure 8.4: Examples of shared space topologies. Captions from TOP to BOTTOM. LEFT SIDE: Nieder-Erlenbach in Frankfurt, model of the Laweiplan in Drachten (NL) Hamilton-Baillie (2007), Velden (Austria), (copyright: Thomas Pilz, Forschungsgesellschaft Mobilität - Austrian Mobility Research). RIGHT SIDE: Bohmte (D), GfL Planungs- und Ingenieursgesellschaft GmbH (2006), Haren (NL) (copyright google maps).

Kurztitel

Straßenverkehrsordnung 1960

Kundmachungsorgan

BGBl. Nr. 159/1960 zuletzt geändert durch BGBl. I Nr. 39/2013

Typ

BG

§/Artikel/Anlage

§ 76c

Inkrafttretensdatum

31.03.2013

Abkürzung

StVO 1960

Index

90/01 Straßenverkehrsrecht

Text

Begegnungszonen

§ 76c. (1) Die Behörde kann, wenn es der Sicherheit, Leichtigkeit oder Flüssigkeit des Verkehrs, insbesondere des Fußgängerverkehrs, dient, oder aufgrund der Lage, Widmung oder Beschaffenheit eines Gebäudes oder Gebietes angebracht erscheint, durch Verordnung Straßen, Straßenstellen oder Gebiete dauernd oder zeitweilig zu Begegnungszonen erklären.

(2) In Begegnungszonen dürfen die Lenker von Fahrzeugen Fußgänger weder gefährden noch behindern, haben von ortsgebundenen Gegenständen oder Einrichtungen einen der Verkehrssicherheit entsprechenden seitlichen Abstand einzuhalten und dürfen nur mit einer Geschwindigkeit von höchstens 20 km/h fahren. Lenker von Kraftfahrzeugen dürfen auch Radfahrer weder gefährden noch behindern.

(3) In Begegnungszonen dürfen Fußgänger die gesamte Fahrbahn benützen. Sie dürfen den Fahrzeugverkehr jedoch nicht mutwillig behindern.

(4) Die Anbringung von Schwellen, Rillen, Bordsteinen und dergleichen sowie von horizontalen baulichen Einrichtungen ist in verkehrsgerechter Gestaltung zulässig, wenn dadurch die Verkehrssicherheit gefördert oder die Einhaltung der erlaubten Höchstgeschwindigkeit unterstützt wird.

(5) Für die Kundmachung einer Verordnung nach Abs. 1 gelten die Bestimmungen des § 44 Abs. 1 mit der Maßgabe, dass am Anfang und am Ende einer Begegnungszone die betreffenden Hinweiszeichen (§ 53 Abs. 1 Z 9e bzw. 9f) anzubringen sind.

(6) Wenn es der Leichtigkeit und Flüssigkeit des Verkehrs dient und aus Gründen der Sicherheit des Verkehrs keine Bedenken dagegen bestehen, kann die Behörde in der Verordnung nach Abs. 1 die erlaubte Höchstgeschwindigkeit auf 30 km/h erhöhen.

Zuletzt aktualisiert am

14.06.2017

Gesetzesnummer

10011336

Dokumentnummer

NOR40147695

Figure 8.5: Print (”law gazette”) of the version 2017-06-14 of §76c of the Austrian traffic regulation (Republik Österreich, 1960), put into effect in March, 2013. There is no official translation to English - its printed here based on its extraordinary relevance.

Figure 8.6: International examples of Begegnungszonen. Captions from TOP to BOTTOM. LEFT SIDE: Biel in Switzerland (Rosinak & Partner, 2009), Burgdorf in Switzerland (Fussverkehr Schweiz, 2004). RIGHT SIDE: Turnweg, 3000 Bern (Switzerland) (Fussverkehr Schweitz, 2010), (Schönauer, 2009), Traffic sign for *Begegnungszonen* according to (Bundesbehörden der Schweizerischen Eidgenossenschaft, 2002).

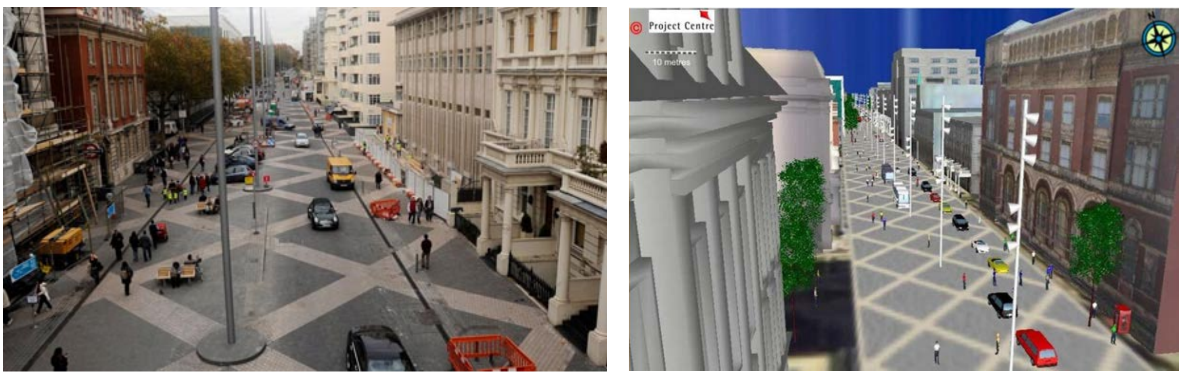

Figure 8.7: LEFT: "Cultural criss-cross" in the Exhibition Road, London. (Photograph: The Royal Borough of Kensington and Chelsea). RIGHT: Demonstration of pedestrians - vehicle give way behavior, (Tonndorf and Vorotovic (2007)).

Figure 8.8: Photos of the redesigned Exhibition road in London (Landscape architecture blog, 2012.)).

Figure 8.9: Austrian examples of Begegnungszonen (all photographs from www.begegnungszonen.or.at). Captions from TOP to BOTTOM. LEFT SIDE: Pöchlarn, Lower Austria; Bregenz in Vorarlberg; Linz, Upper Austria. RIGHT SIDE: Bischofshofen, Salzburg; Kufstein, Tyrol; Velden, Carinthia. CENTER: Tags are representing all Begegnungszonen in Austria (2017).

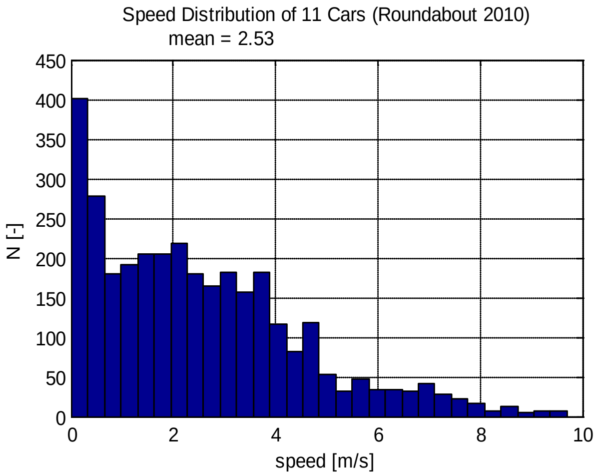

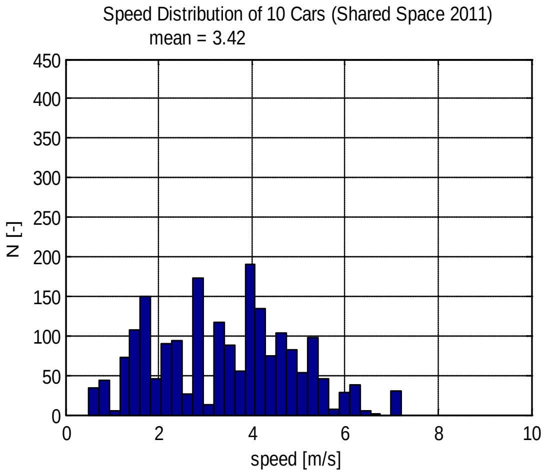

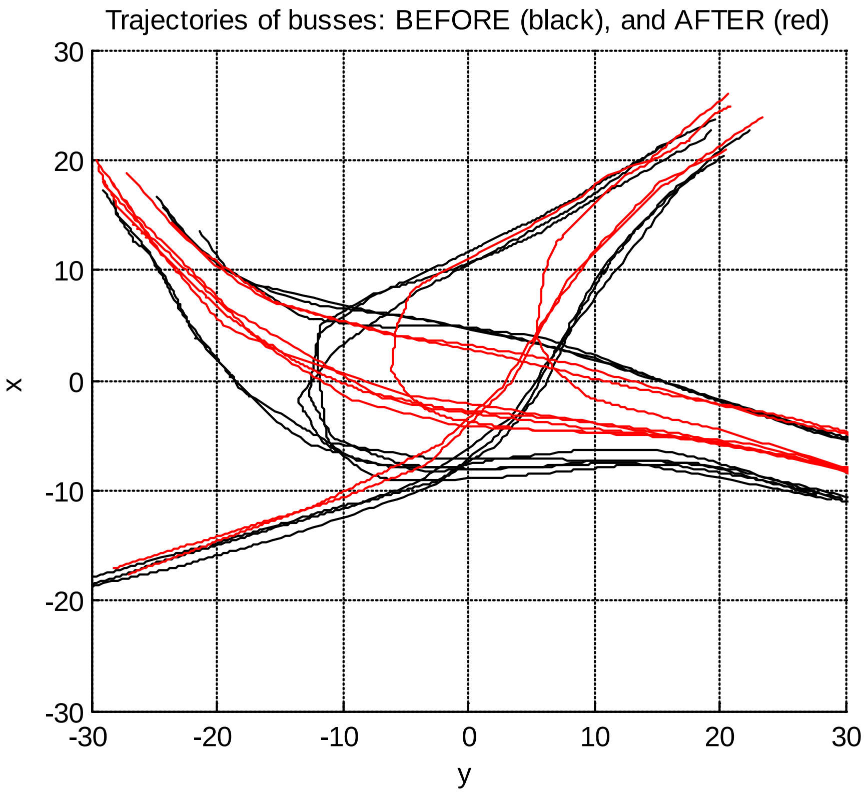

Figure 8.10: LEFT: Speed histogram of 11 buses on the roundabout at the Sonnenfelsplatz in 2010. MIDDLE: Trajectories from busses at the Sonnenfelsplatz. At the roundabout in 2010 (BLACK) and in the shared space in 2011 (RED). RIGHT: Speed histogram of 10 buses on the shared space at the Sonnenfelsplatz in 2011.

Parameter	Value	Description
ch	60000.0	lateral force coefficient back [N/rad]
cv	47000.0	lateral force coefficient front [N/rad]
m	867.7	mass [kg]
Jz	1146.0	masse inertial along vertical axis [kg m2]
a	0.88	distance gravity center S - front axle
b	1.52	distance gravity center S - back axle

Table 8.2: Parameter values for the linear vehicle lateral dynamics on basis of two–wheeler model by approximatively discretization according to Euler Kramer (2008).

8.2 Model Design

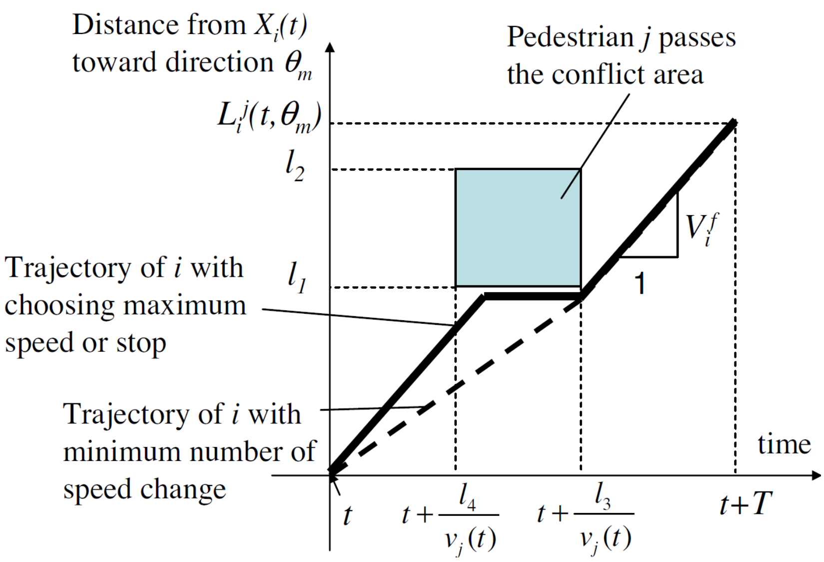

Figure 8.11: Scheme of a simplified trajectory of a pedestrian to avoid a collision, taken from Asano et al. (2007)

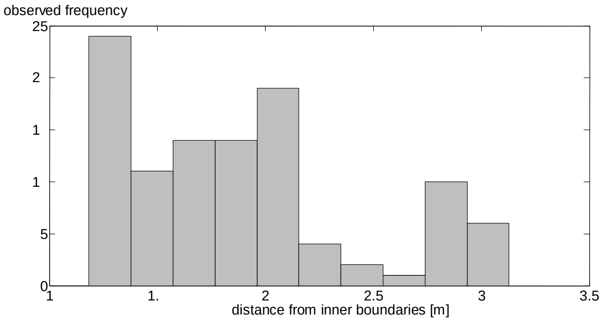

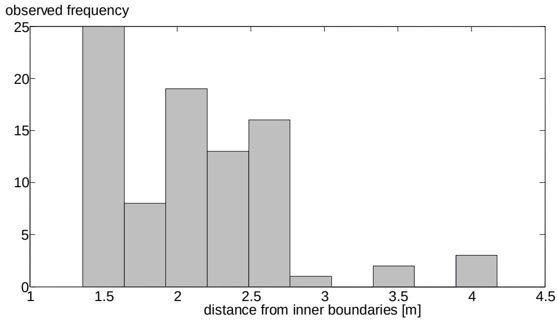

Figure 8.12: Lateral distance to the boundaries of the road. RIGHT: Tracked data. LEFT: Reference data.

Country	Town/City, Location	Target of the shared space design	Traffic demand			Road's function			
			Motorized	non-motorized	PTr	Within the network	Stay	Traffic	POI
Netherlands	Drachten, Laweiplan	Increasing urban quality	high	high	low	regional	no	yes	yes
	Drachten, De Drift	Increasing urban quality	high	high	low	local main aterial	yes	yes	yes
	Oudehaske	Calming of traffic	low	low	low	through-road	no	yes	no
	Donkerbroek	Calming of traffic	medium	low	low	through-road	no	yes	no
	Makkinga	Calming of traffic	low	low	low	through-road	no	yes	no
	Wolvega	Calming of traffic	low	medium	low	through-road	no	yes	no
	Njenga	Increasing urban quality	high	low	low	through-road	no	yes	no
	Oosterwolde	Calming of traffic	high	low	low	main arterial	yes	yes	no
Switzerland	Biel	Increasing urban quality, Calming of traffic	high	high	high	through-road	yes	yes	yes
	Burgdorf	Calming of traffic	medium	medium	low	town center	yes	yes	yes
	Köniz	Increasing traffic quality for pedestrians	high	high	high	through-road	no	yes	yes
Germany	Bohmte	Increasing urban quality	high	high	low	through-road	no	yes	yes
	Kevelear	Increasing urban quality	high	high	low	main arterial	yes	yes	yes
Austria	Ottensheim	Increasing urban quality	low	low	low	town center	yes	yes	yes
	Vöcklabruck, Dürnau	Increasing urban quality, Calming of traffic	medium	medium	low	through-road	yes	yes	yes
	Grieskirchen	Increasing urban quality	high	high	low	town center	yes	yes	yes
	Gleinstätten	Increasing urban quality, Calming of traffic	high	low	low	through-road	yes	yes	yes
	Graz, Sonnenfelsplatz	Increasing urban quality, Calming of traffic	high	high	high	local main aterial, square	yes	yes	yes
	Wien, Mariahilfer Straße	Increasing urban quality, Calming of traffic	medium	high	medium	local main aterial	yes	yes	yes

Table 8.3: Selection of shared spaces and relevant attributes (German), widely based on an assessment within the project MixME (Schönauer and Schrom-Feiertag, 2010), copyright: Rosinak & Partner.

Area	Topic	Aspect	Priority
INPUT	Degree of automation	Scripting tasks	2
		COM-Interface	3
	Design Elements	Compatibility with CAD-software	1
		Import of vector graphs and maps	1
		Geo-referencing	2
		Compatibility with 3D-software tools	3
		Using internet services	3
		Chosing attributes of design elements	3
		Impact and effect	1
	Behavioral diversity	Validity of default values	1
		Coverage by default-data	3
		Manual control	1
		Exchange demand- or other data with other sim.-tools	3
		Road user's parameters	1
RESULTS		Traffic safety	1
		Speeds	1
		Driving speed distribution	1
		Speed distribution	3
		Travel Times	1
		Path length	1
		Number of Stops	2
VISUALIZATION		Visualization	1
		Comparability	1
		Exchange / export to other simulation tools	3

Table 8.4: Assessment of the relevant aspects of a simulation model for shared space, widely based on an evaluation of the project MixME (Schönauer and Schrom-Feiertag, 2010). Priority: 1 = highest relevance, 3 = lowest relevance.

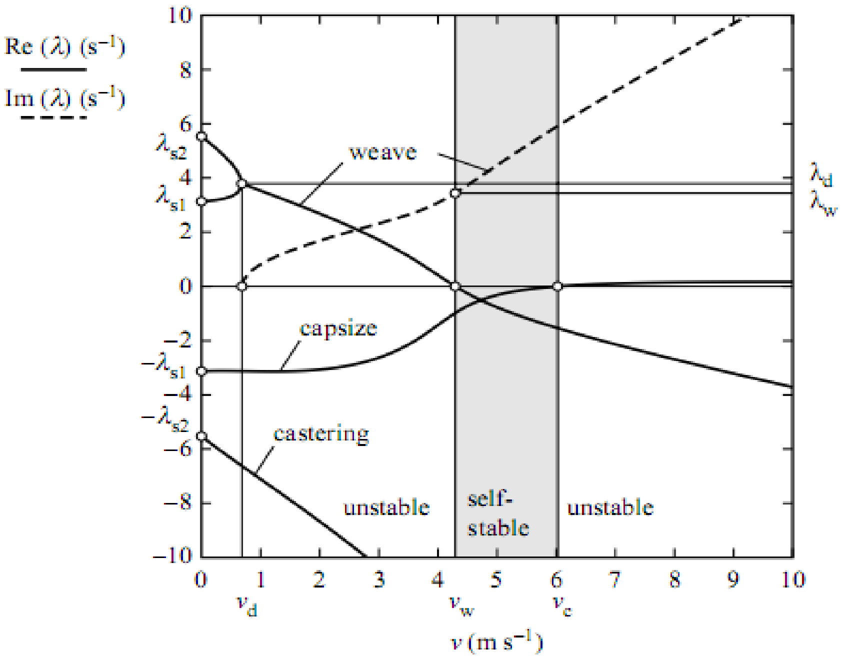

Figure 8.13: Stability issues of the bicycle model analyzing eigenvalues.

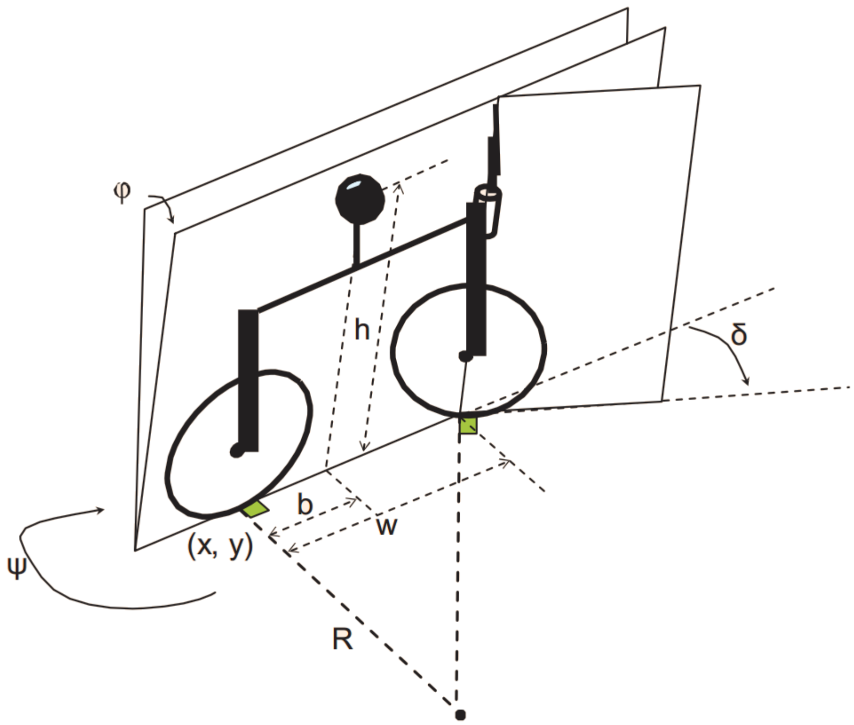

Figure 8.14: Inverted pendulum bicycle model. Schematic diagram of an elementary non-holonomic bicycle with steer δ, roll ϕ, and yaw γ degrees of freedom. The machines mass is located at a single point h above the ground and b in front of the rear-wheel groundcontact point. The wheelbase is denoted w. Both wheels are assumed to be massless and to make point contact with the ground. Both ground-contact points remain stationary during maneuvering as seen from the rear frame. The path curvature is $\delta(t) = 1/R(t)$. Taken from Limebeer and Sharp (2006).

8.3 Application

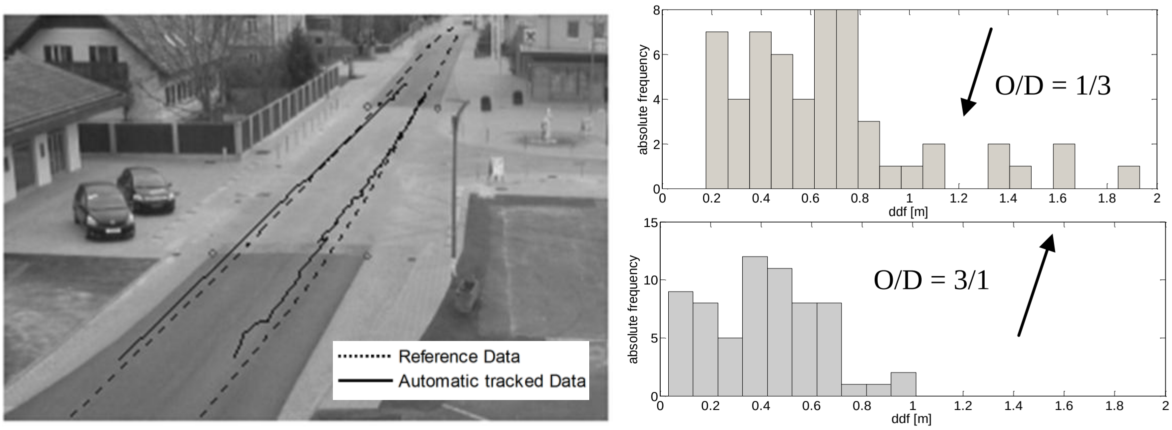

Figure 8.15: LEFT: Mean Trajectories in picture coordinates. RIGHT: histograms of the δ_{dF} in both directions.

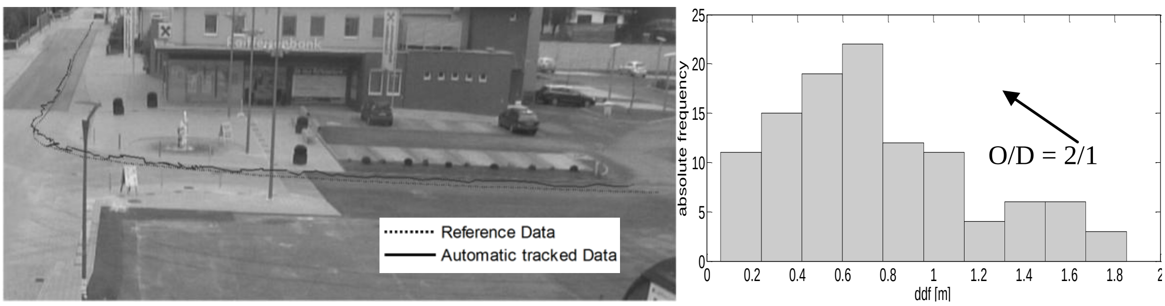

Figure 8.16: LEFT: Sample Trajectory in the right turn, plotted into footage. RIGHT: Histogram of the δ_{dF} of the single turns.

8.4 Demand

Comparable weekdays and daytimes were chosen for the data samples. The figures 8.20, 8.21 and 8.22 show the distribution of extracted trajectories for a given time span.

The minimum sample size was 50 trajectories for each mode. In all further qualitative conclusions, the limited number of trajectories should therefore be considered.

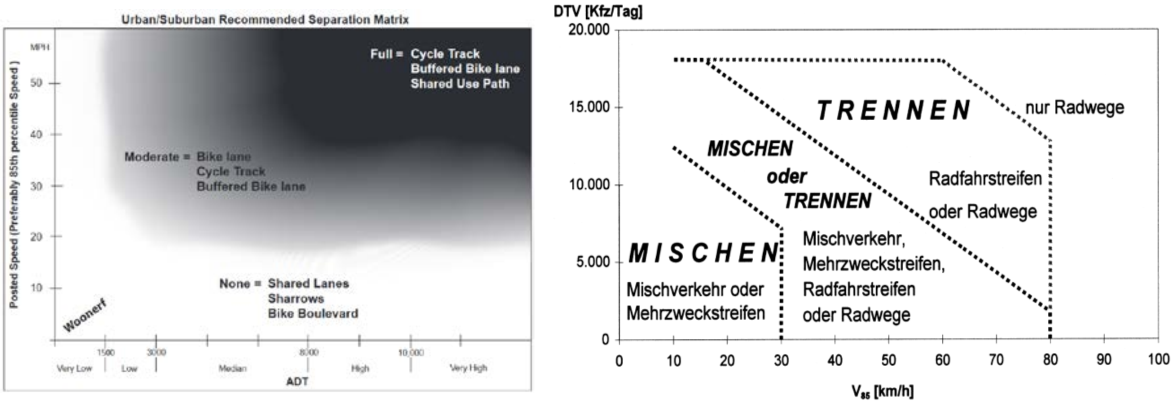

Figure 8.17: Recommended design concept of bicycle traffic in municipalities, according to Oregon Department of Transportation (2011) and the Austrian RVS (Forschungsgesellschaft Strasse, Schiene, Verkehr, 2004).

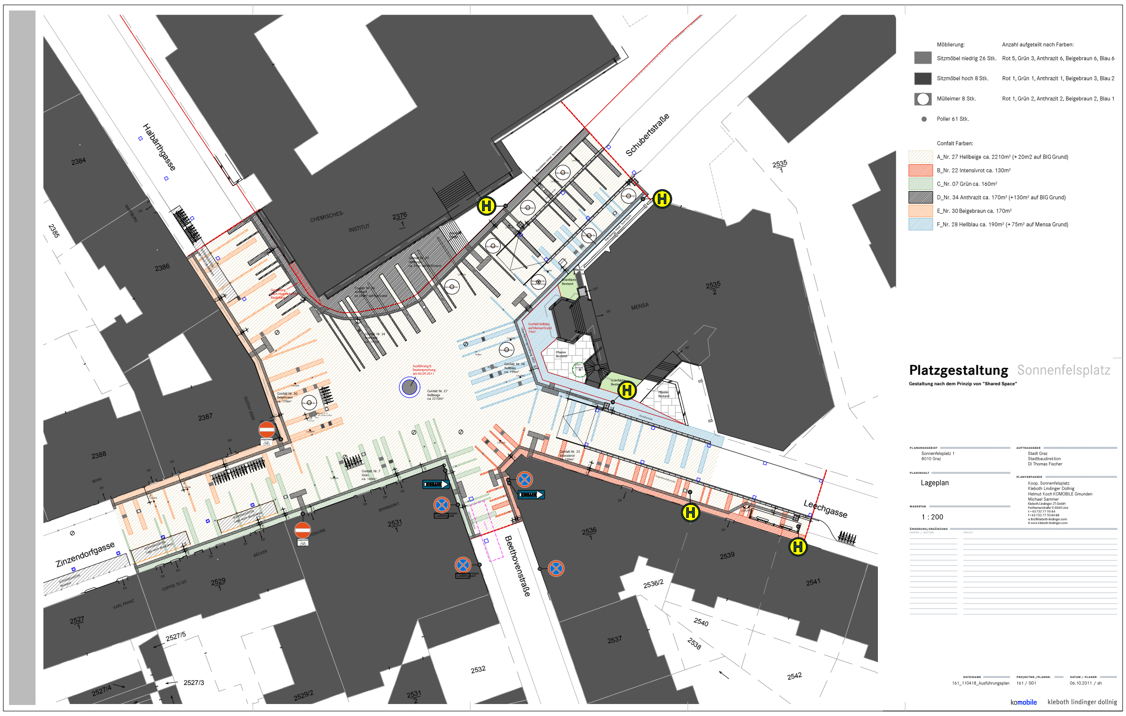

Figure 8.18: Design plan of the shared space scheme at the Sonnenfelsplatz from 2011.

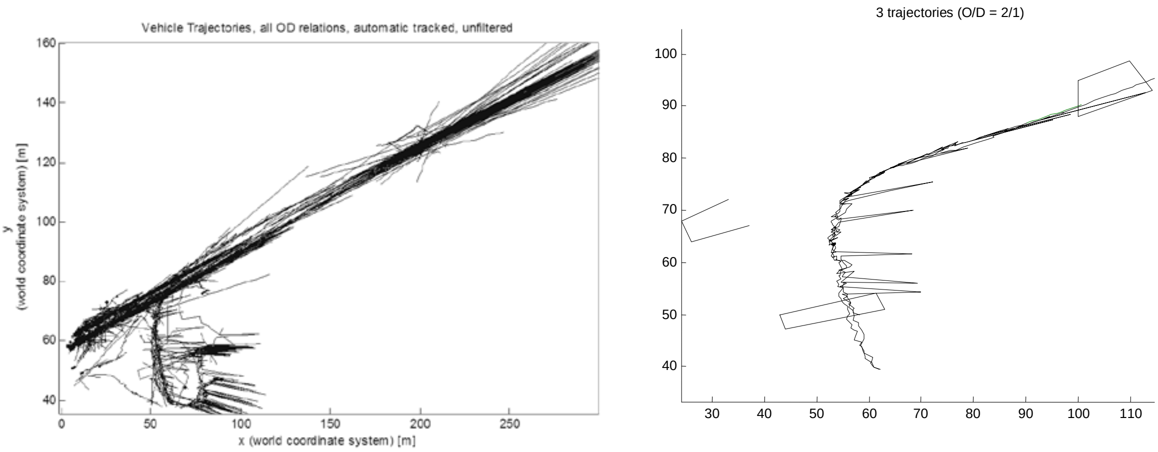

Figure 8.19: Left: Raw Tracking trajectories, Right: OD-filtered (not removing the faulty positions).

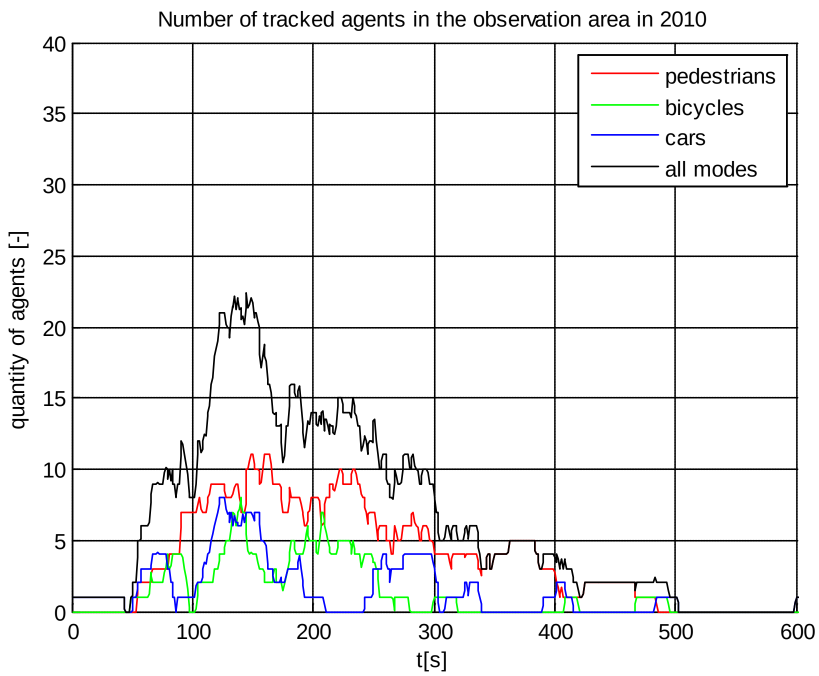

Figure 8.20: Number of simultaneously tracked traffic participants in the observation area of the 2010 data.

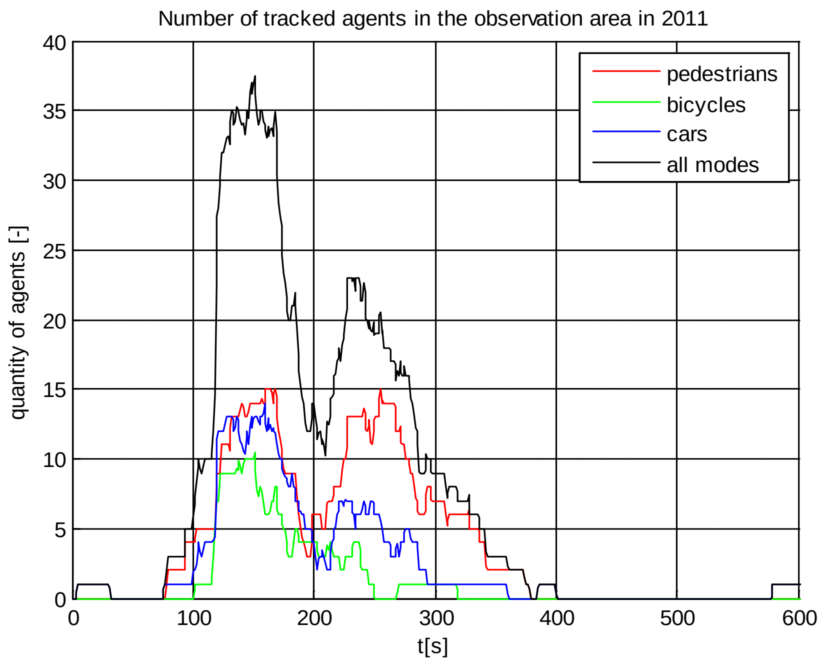

Figure 8.21: Number of simultaneously tracked traffic participants in the observation area of the 2011 data.

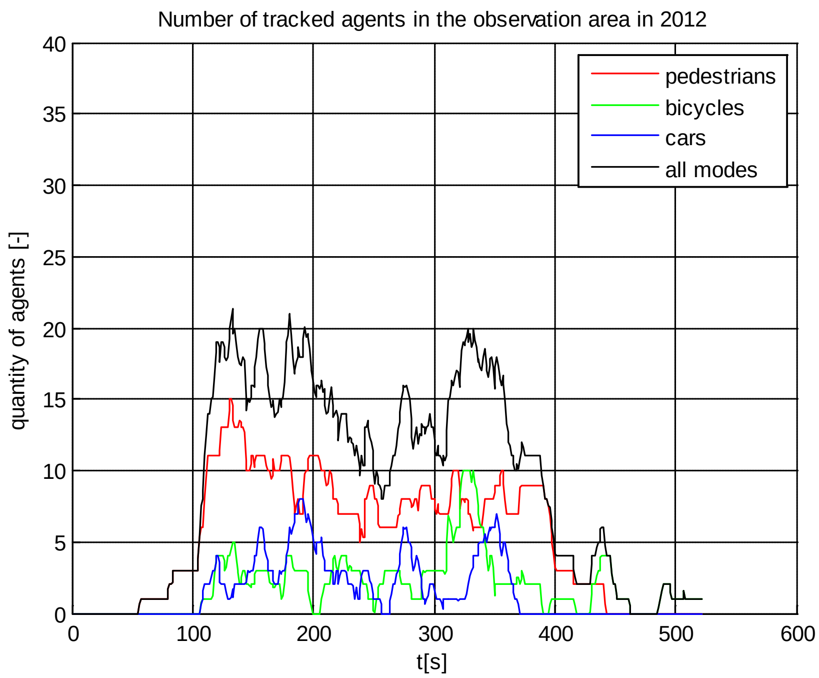

Figure 8.22: Number of simultaneously tracked traffic participants in the observation area of the 2012 data.

Figure 8.23: In 2013, the Sonnenfelsplatz was labeled as a Begegnungszone.

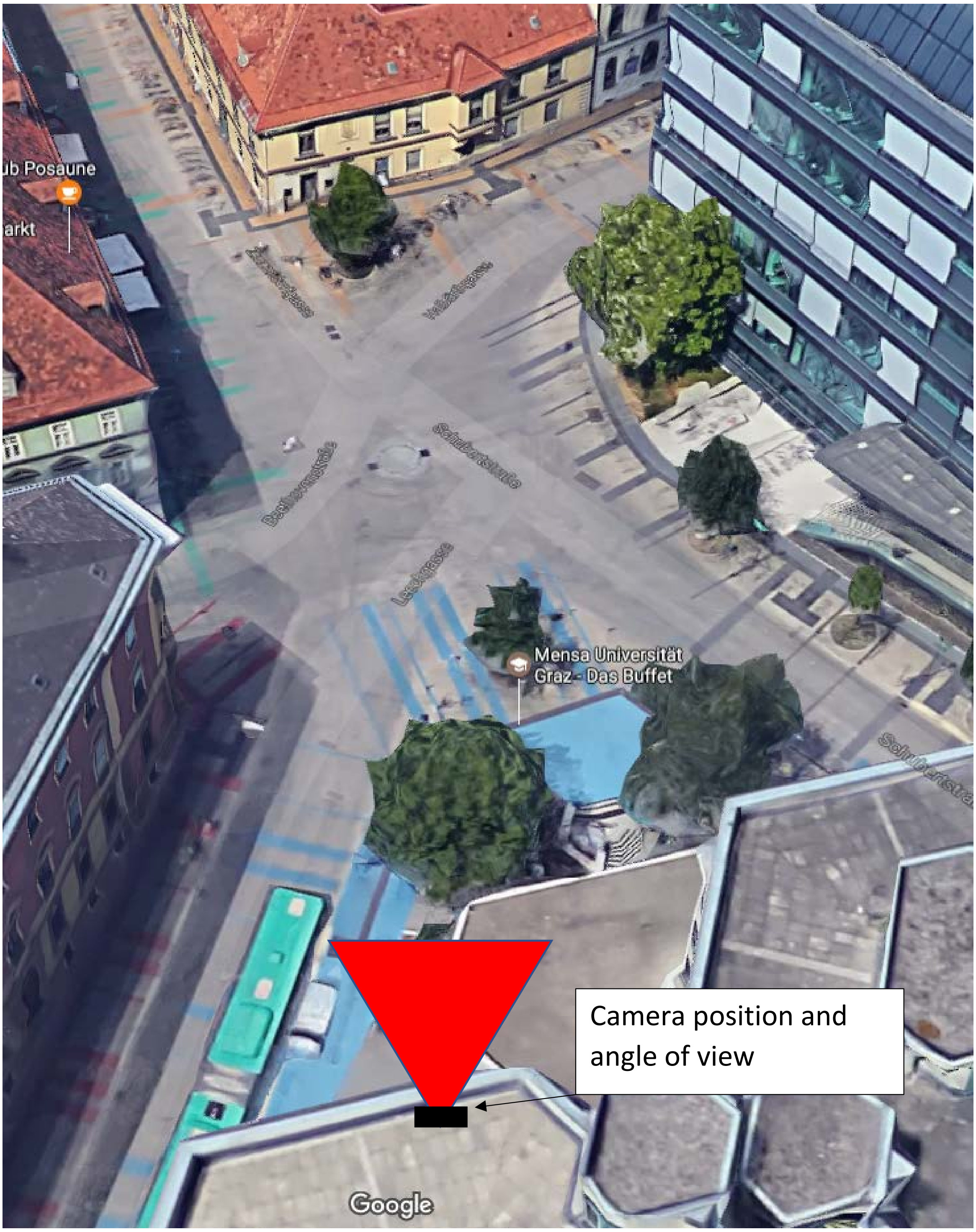

Figure 8.24: Aerial image of Sonnenfelsplatz and camera position plus an illustration of the angle of view. Base map: Google Graphics ©2017.

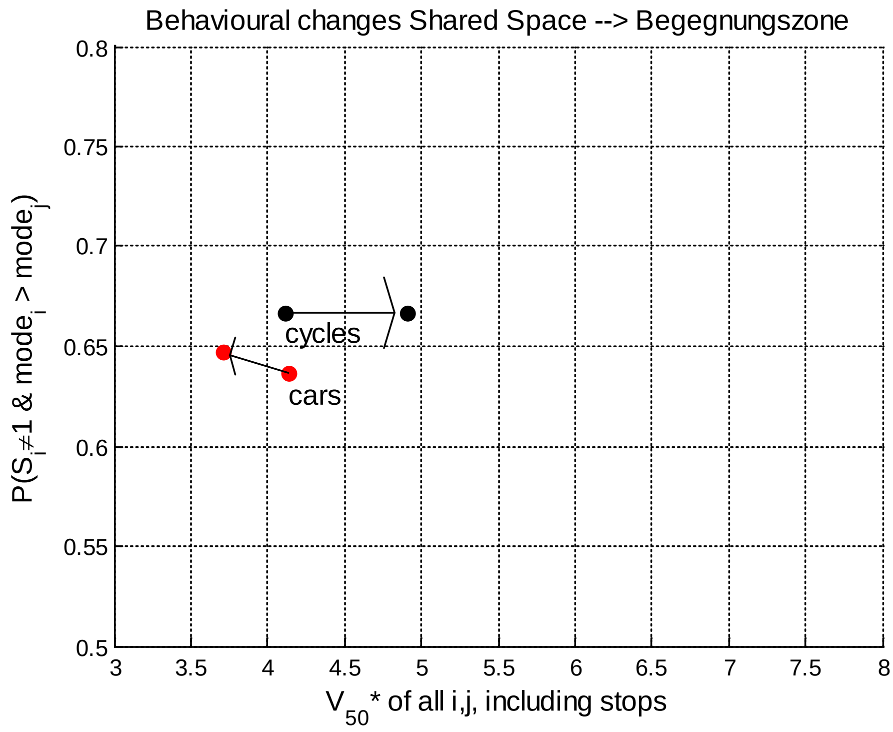

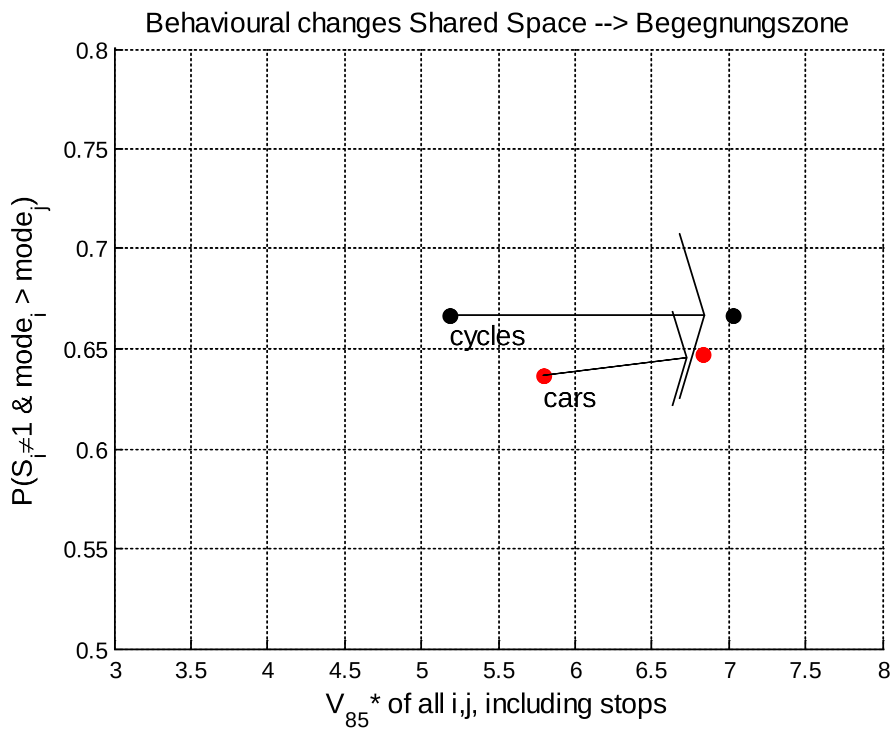

Figure 8.25: Changes in the behavior from shared space to Begegnungszone - indicated by speed and choice of strategy - based on the conflict data sets 2b and 2c. The quiver points at the results gained with data set 2c (Begegnungszone) The x-coordinate represents the 50 % and 85 % percentile of speeds, driven by cars and cyclists respectively. Remark: It's not the V_{xx} of traffic in free flow, usually used in transportation engineering - therefore, the asterisk is used in the symbol (V^*_{xx}). The y-coordinate shows the probability that a road-user (car driver or cyclist) did yield to the conflict partner. To yield means here to stop or avoid left or right.

8.5 Implementation and Results

8.5.1 SF parameter

Extracted from PTV AG (2010).

τ is the relaxation time, which one can relate to a reaction time or inertia, as it couples the difference between the desired speed and direction v_0 and the current speed and direction v to the acceleration a: $a = (v_0 v)/\tau$.

λ governs the amount of anisotropy of the forces from the fact that events and phenomena in the back of a pedestrian do not influence him (psychologically and socially) as much as if they were in his sight. From λ and the angle φ between the current direction of an agent and the source of a force a factor w for all social (i.e. non-physical) forces is calculated that suppresses the force, if $\varphi \neq 0$ and $\lambda < 1$: $w(\lambda) = (\lambda + (1\lambda)(1 + cos(\varphi))/2)$. So, if $\varphi = 0$ one has $w = 1$ and if $\varphi = \pi$ one has $w(\lambda) = \varphi$.

$A_{soc,mean}$, $B_{soc,mean}$, and VD These parameters determine strength (A) and range (B) of the social force between two pedestrians. The social force between two pedestrians is calculated as $F = w(\lambda) Aexp(-d/B)n$. Here $w(\lambda)$ is the factor calculated from λ, which is explained above, d is the distance (body surface to body surface) between two pedestrians and n is the unity vector pointing from the influencing to the influenced pedestrian. Note that if the parameter VD is greater than zero the relative velocities of the pedestrians are considered in addition. In this case the distance d is generalized to and thus replaced by $d- > 0.5sqrt((d + |(d(v_1 v_0)|VD)^2 - |(v_1 v_0)VD^2)$ with VD given in [seconds]. Here v_0 is the velocity of the influenced and v_1 the velocity of the influencing pedestrian and d points from the influencing to the influenced pedestrian with $|d| = d$. (The "influenced pedestrian" is the one for whom the force is calculated.) $A_{phys,border}$ and $B_{phys,border}$
The contact force between a pedestrian and a wall is calculated accordingly as the contact force between two pedestrians. $A_{soc,isotropic}$ and $B_{soc_isotropic}$
These parameters govern a force similar to $A_{soc,mean}$ and $B_{soc,mean}$ with the exception that there is no velocity dependence: $F = Aexp(-d/B)n$. This part of the force suits to adjust the typical distance pedestrians will keep from each other. *react to n*
Only the influences of the n closest pedestrians are considered when the total force for a pedestrian is calculated.

All the following specific global parameters are left to their defaults, the descriptions are taken from (PTV AG, 2010).

Grid size
By this parameter one defines how far at largest pedestrians influence each other. The pedestrians are stored in a grid with cells of size **grid size** x grid size square meters. Each pedestrian only interacts with the pedestrians in the same or adjacent (including over corner) grid cells.

Routing large grid
This parameter defines the topological grid-size; **routing large grid** x **routing large grid**

cells become one cell in the superordinate grid. The required memory depends on this parameter, but the precision of the calculation of distances to destination areas does not. There is no global value that fits best in any case. For small-sized scenarios (in a building, for example) with numerous small obstacles and numerous walkable areas a low value (¡ 10) is recommended. For large areas and big obstacles (e.g. simulation of a district not regarding the details) even 100 or more can be set.

Routing step This is one parameter that governs the calculation of the potential. If it is large, the potential is more precise, but its calculation needs more time. Reasonable values are 2, 3, 4 or 5.

Routing accuracy
This is the second parameter that governs the calculation of the potential. It can take values in [0.0 .. 1.0] and results in more precise potentials, the greater it is.

Routing obstacle dist
During the calculation of the distance potential field, grid cells which are close to walls receive a sort of "extra distance" atop of their true distance. By this, one can achieve that more pedestrians decide to choose a wide corridor instead of a narrow one, if there are two corridors from one and the same source to one and the same destination with identical walking distance. Generally, the pedestrians keep some distance toward walls. With this parameter the distance is set to which nearby walls influence the potential field.

Routing Cell Size
This parameter defines the distances of fixed data points to be set for the calculation of distances to a destination area. The default value is 0.15 m. This default parameter should only be edited if the model included passageways with a width of 50 cm or less since pedestrians will not pass these channels during the simulation. Instead, they will stand still apparently not oriented as soon as an area behind the channel is their next (intermediate) destination area. In this case, the value of the parameter can be reduced to 0.1 m. This change increases the memory requirements and further reductions might cause further problems. Therefore, each project should use the default value until reductions are required for trouble shooting purposes.

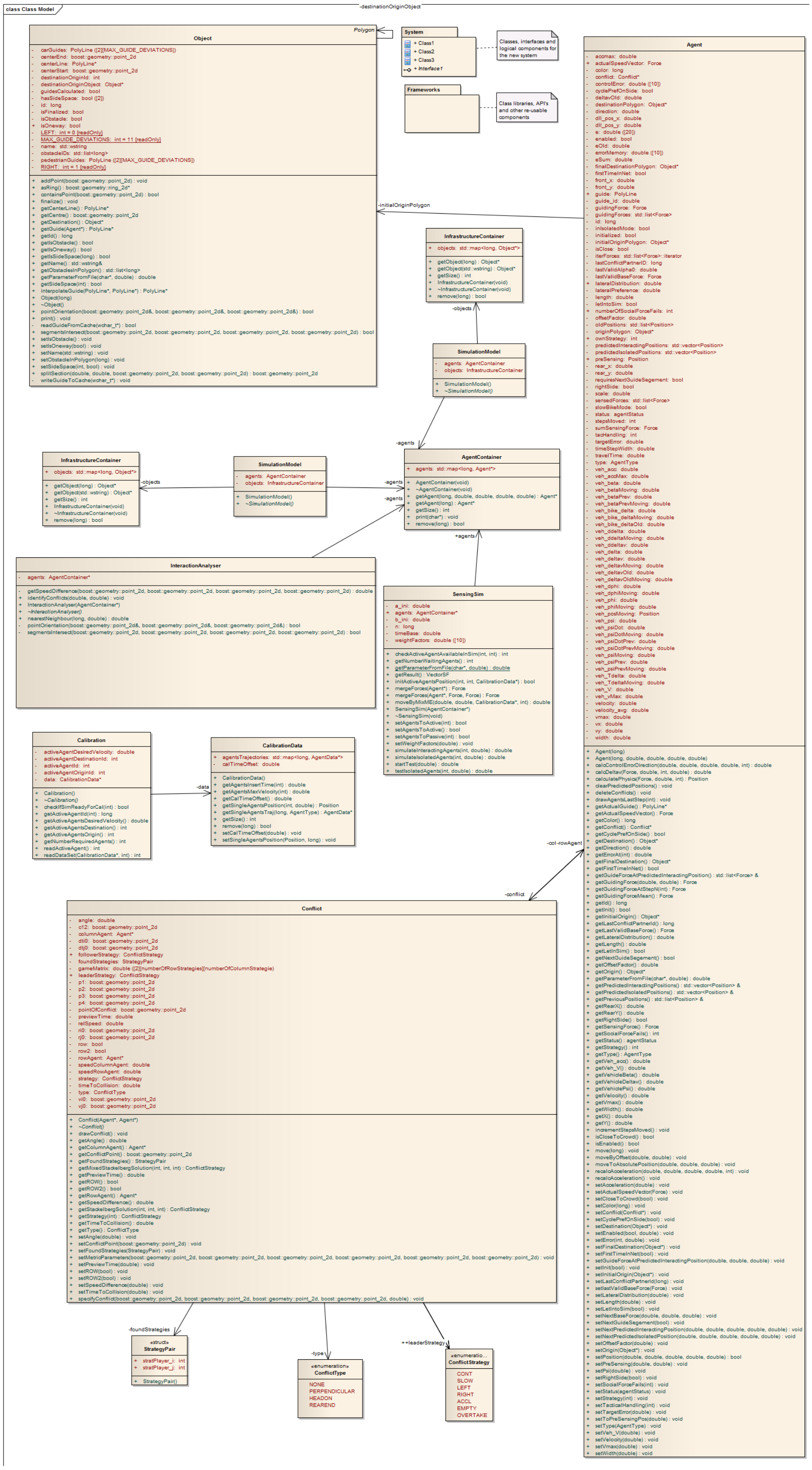

Figure 8.26: Class model of the implementation (Showing only relevant objects). 4 split and zoomed parts are shown in the figures at the next 4 pages.

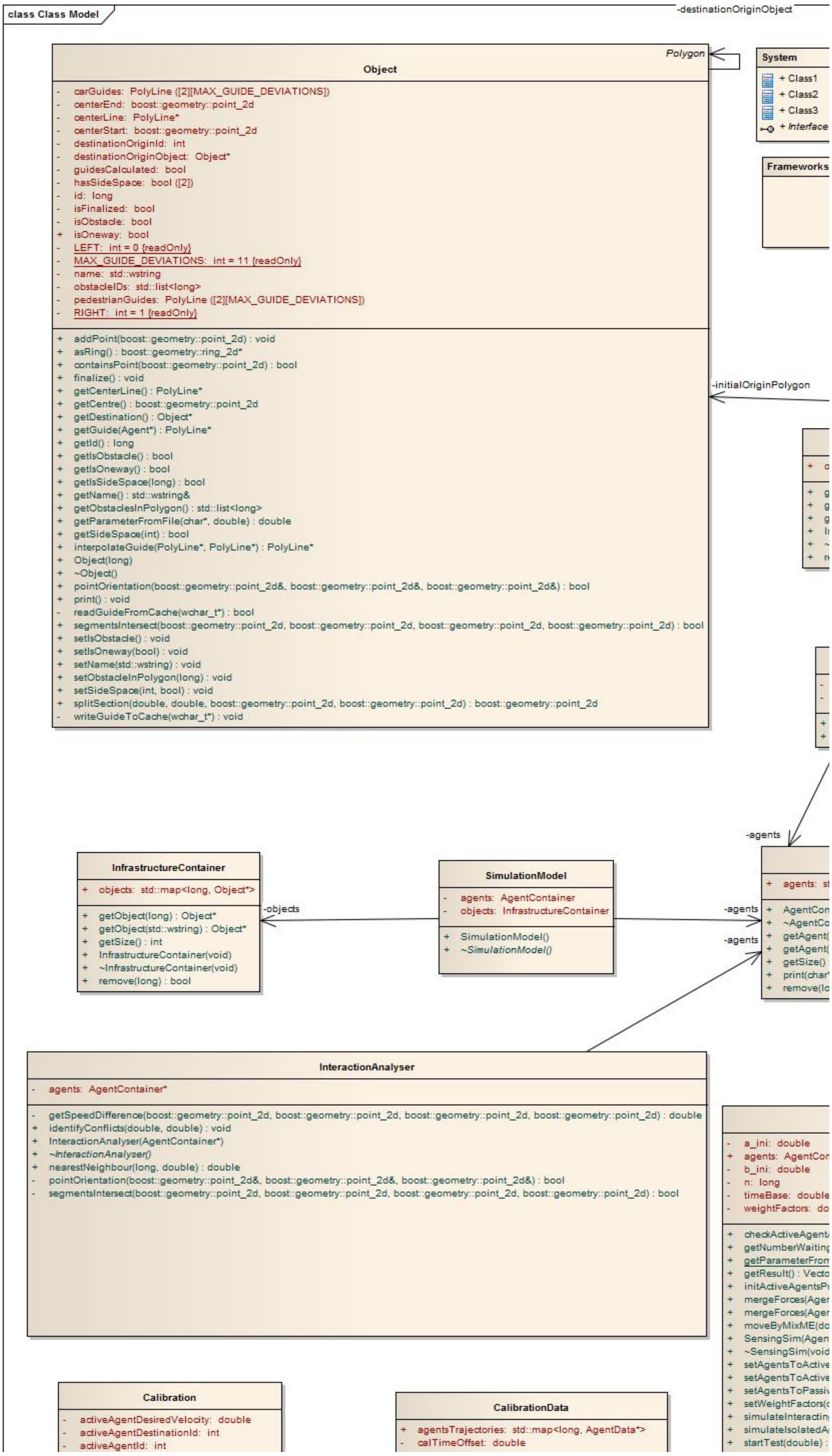

Figure 8.27: Zoomed part 1/4: Class model of the implementation (Top right part of figure 8.26).

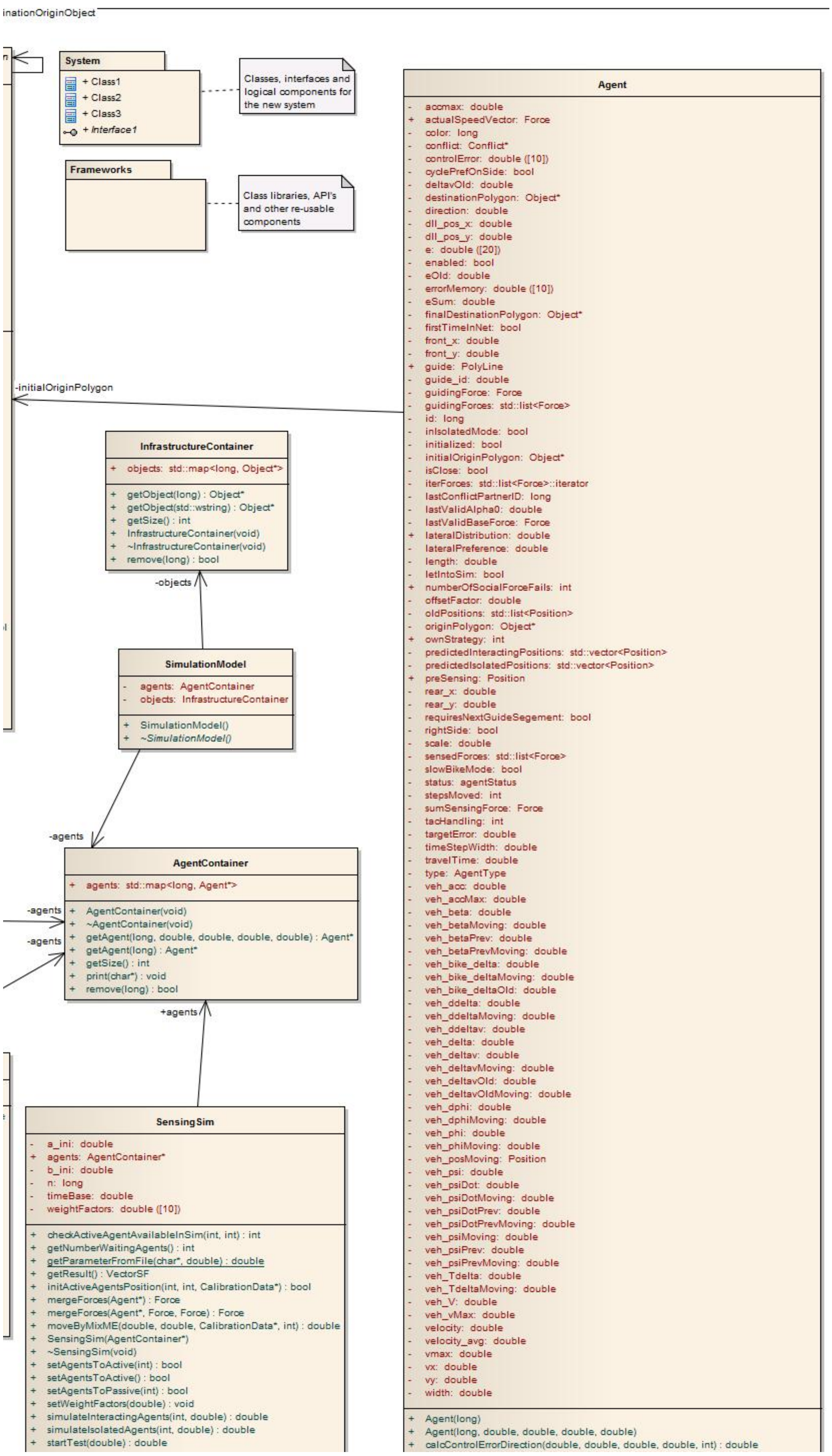

Figure 8.28: Zoomed part 2/4: Class model of the implementation (Top left part of figure 8.26).

Figure 8.29: Zoomed part 3/4: Class model of the implementation (Bottom left part of figure 8.26).

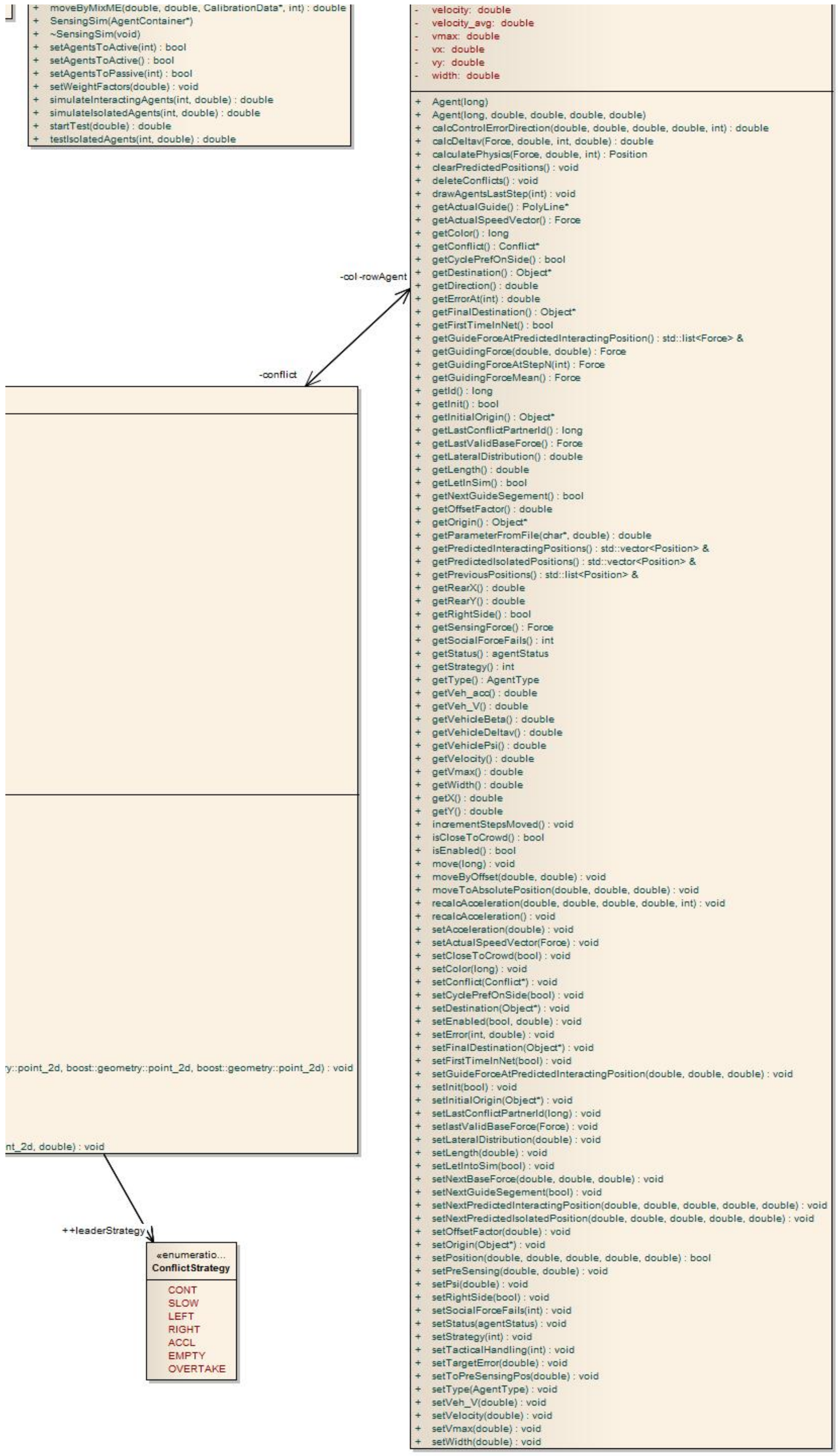

Figure 8.30: Zoomed part 4/4: Class model of the implementation (Bottom right part of figure 8.26).

Parameter	Data Set 1	Data Set 2a	Data Set 2b	Data Set 2c
Date	2010-03-23	2011-10-27	2012-03-20	2016-11-17
Day of the Week	Tuesday	Thursday	Tuesday	Thursday
Time Footage Starts	09:00	09:00	09:00	10:30
Time Footage Ends	14:00	13:30	14:00	12:30
Time between reconstruction [month]	-18.9	0.5	5.4	37
min. Temperature [°C]	6	8	4	1
max. Temperature [°C]	17	9	14	8
mean Wind Speed [km/h]	3	5	4	4
mean rel. Humidity [%]	83	96	81	94
Precipitation [mm/24h]	0.0	2.0	0.0	0.0
Comments	foggy in the very morning	light rain	foggy in the very morning	foggy in the very morning

Figure 8.31: Metadata of the recorded footage at Sonnenfelsplatz, Graz, Austria. At Data Set 2c, the time after reconstruction is referring to the change from shared space to Begegnungszone.

Conflict Nr.	ID 1 (real)	ID 1 (hypo).	ID 2 (real)	ID 2 (hypo.)	Type 1	Type 2	Strategy 1	Strategy 2
1	20	52	19	19	car	bicycle	2	1
2	22	22	24	23	car	bicycle	1	2
3	28	28	27	26	car	bicycle	1	4
4	43	41	44	44	car	bicycle	2	1
5	47	47	45	46	car	bicycle	1	4
6	50	49	51	51	car	bicycle	2	1
7	4	4	6	5	car	bicycle	1	2
8	18	17	19	19	car	bicycle	2	1
9	2	1	3	3	car	bicycle	2	1
10	10	10	9	8	car	bicycle	1	2
11	32	32	34	33	car	car	1	2
12	35	35	36	37	car	car	1	2
13	40	40	39	38	car	car	1	2
14	1	1	3	2	car	car	1	2
15	10	10	12	11	car	car	1	2
16	15	16	14	13	car	bicycle	2	4
17	21	20	23	22	car	car	2	2
18	4	5	7	7	car	car	2	1
19	13	13	12	11	car	car	1	2
20	4	5	6	7	car	car	2	2
21	7	7	9	8	bicycle	bicycle	1	4
22	3	3	1	2	bicycle	bicycle	1	4
23	1	1	2	3	bicycle	bicycle	1	2
24	4	4	5	6	bicycle	bicycle	1	2
25	7	7	9	10	bicycle	bicycle	1	4
26	14	14	12	11	bicycle	bicycle	1	2
27	17	17	15	18	bicycle	bicycle	1	4
28	3	3	1	2	bicycle	bicycle	1	2
29	1	1	2	3	bicycle	bicycle	1	4
30	6	6	4	5	bicycle	bicycle	1	4
31	26	26	24	25	car	bicycle	1	2
32	3	2	1	1	car	pedestrian	2	1
33	4	4	6	5	car	pedestrian	1	4
34	7	8	9	9	bicycle	pedestrian	3	1
35	10	11	12	12	car	pedestrian	2	1
36	13	14	15	15	car	pedestrian	2	1
37	16	17	18	18	car	pedestrian	2	1
38	20	19	24	24	car	pedestrian	2	1
39	22	21	23	23	car	pedestrian	2	1
40	27	26	28	28	bicycle	pedestrian	3	1
41	29	30	31	31	car	pedestrian	2	1
42	33	32	34	35	bicycle	pedestrian	2	2
43	37	36	38	38	car	pedestrian	2	1
44	40	39	41	41	car	pedestrian	2	1
45	43	42	44	44	bicycle	pedestrian	3	1
46	2	1	3	3	bicycle	pedestrian	2	1
47	5	4	6	6	bicycle	pedestrian	3	1
48	7	8	9	9	bicycle	pedestrian	3	1
49	10	11	12	12	bicycle	pedestrian	3	1
50	14	15	13	13	bicycle	pedestrian	3	1
51	18	17	16	16	bicycle	pedestrian	3	1
52	29	29	31	30	car	pedestrian	1	2
53	2	5	1	7	pedestrian	car	2	1
54	9	8	10	11	pedestrian	car	1	2
55	12	15	13	14	pedestrian	car	1	2
56	23	22	24	25	pedestrian	car	2	1
57	30	28	32	33	pedestrian	car	1	2
58	8	5	6	7	pedestrian	car	1	2
59	10	9	11	13	pedestrian	car	1	2
60	10	9	15	14	pedestrian	car	1	2
61	17	19	18	22	pedestrian	car	3	1

Table 8.5: Conflicts 2012 (data sets 2a and 2b). Conflicts Nr. 53-61 are taken in Gleinstaetten.

Conflict Nr.	ID i (real)	ID i (hypo.)	ID j (real)	ID j (hypo.)	Type 1	Type 2	Strategy 1	Strategy 2
1	5	6	3	3	car	bicycle	2	1
2	9	9	7	8	car	bicycle	1	3
3	11	12	10	10	car	pedestrian	2	1
4	13	14	15	15	car	pedestrian	2	1
5	18	18	16	17	car	bicycle	1	4
6	19	21	20	20	bicycle	pedestrian	4	1
7	22	23	19	19	car	bicycle	2	1
8	25	26	24	24	car	bicycle	2	1
9	28	27	29	29	car	pedestrian	2	1
10	30	30	31	32	car	car	1	2
11	33	33	34	35	car	car	1	2
12	38	38	37	36	car	bicycle	1	2
13	40	39	41	41	car	bicycle	2	1
14	44	44	43	42	car	car	1	2
15	44	46	45	45	car	pedestrian	2	1
16	48	47	49	49	bicycle	pedestrian	2	1
17	52	51	15	15	car	pedestrian	2	1
18	53	54	55	55	car	pedestrian	2	1
19	57	59	58	58	car	pedestrian	2	1
20	60	60	62	61	car	pedestrian	1	2
21	65	65	64	63	car	bicycle	1	2
22	65	66	67	67	car	pedestrian	2	1
23	70	70	69	68	car	bicycle	1	2
24	74	72	73	73	car	car	2	1
25	74	72	75	75	car	pedestrian	2	1
26	80	78	76	76	car	bicycle	2	1
27	80	79	81	81	car	pedestrian	2	1
28	84	84	83	82	car	pedestrian	1	2
29	85	86	87	87	bicycle	bicycle	4	1
30	90	88	89	89	bicycle	bicycle	3	1
31	93	92	94	94	car	bicycle	2	1
32	96	95	97	97	bicycle	pedestrian	2	1
33	100	99	98	98	car	bicycle	2	1
34	101	102	103	103	car	pedestrian	2	1
35	101	104	105	105	car	pedestrian	2	1
36	108	109	106	106	car	pedestrian	2	1
37	112	111	110	110	car	bicycle	2	1
38	114	113	115	115	bicycle	pedestrian	2	3
39	116	116	118	117	car	car	1	2
40	121	122	123	123	bicycle	bicycle	4	1
41	126	124	125	125	car	car	2	1
42	128	127	129	129	bicycle	pedestrian	3	1
43	131	130	132	132	car	pedestrian	2	1
44	135	135	134	133	car	pedestrian	1	2
45	137	137	139	138	car	car	1	2
46	140	139	141	141	car	pedestrian	2	1
47	144	143	145	145	car	bicycle	2	1
48	147	146	148	148	car	pedestrian	2	1
49	151	149	150	150	bicycle	pedestrian	2	1
50	154	152	153	153	car	pedestrian	2	1

Table 8.6: Conflicts 2016 (data set 2c).

Shared Space

Si

	C	S	L	R	A
C	0	0	0	0	0
S	1	1	1	1	1
L	1	1	1	1	1
R	0	0	0	0	0
A	0	0	0	0	0

Sj

	C	S	L	R	A
C	1	1	1	1	1
S	1	1	1	1	1
L	1	1	1	1	1
R	1	1	1	1	1
A	1	1	1	1	1

Ni

	C	S	L	R	A
C	1	1	1	1	1
S	1	1	1	1	1
L	1	1	1	1	1
R	1	1	1	1	1
A	1	1	1	1	1

Nj

	C	S	L	R	A
C	0	1	0	1	0
S	1	1	1	1	1
L	0	1	0	1	0
R	0	1	0	1	0
A	0	1	0	1	0

Begegnungszone

Si

	C	S	L	R	A
S	0	0	0	0	0
C	1	1	1	1	1
L	1	1	1	1	1
R	0	0	0	0	0
A	0	0	0	0	0

Sj

	C	S	L	R	A
S	1	1	1	1	1
C	1	1	1	1	1
L	1	1	1	1	1
R	1	1	1	1	1
A	1	1	1	1	1

Ni

	C	S	L	R	A
S	0	1	0	0	0
C	1	1	0	0	0
L	0	1	0	0	0
R	0	1	0	0	0
A	0	1	0	0	0

Nj

	C	S	L	R	A
S	1	1	1	1	1
C	1	1	1	1	1
L	1	1	1	1	1
R	1	1	1	1	1
A	1	1	1	1	1

C…Continue
S…Stop
L…Left
R…Right
A…Accelerate

Figure 8.32: TOP: Example conflict between car and cyclist, it is conflict nr.1 in the data set 2c (see figure 8.6). Matrices S_i, S_j, N_i and N_j within the model definition for shared space and the model definition for Begegnungszonen. Values are rounded (1 and 0.3679 in full notation).

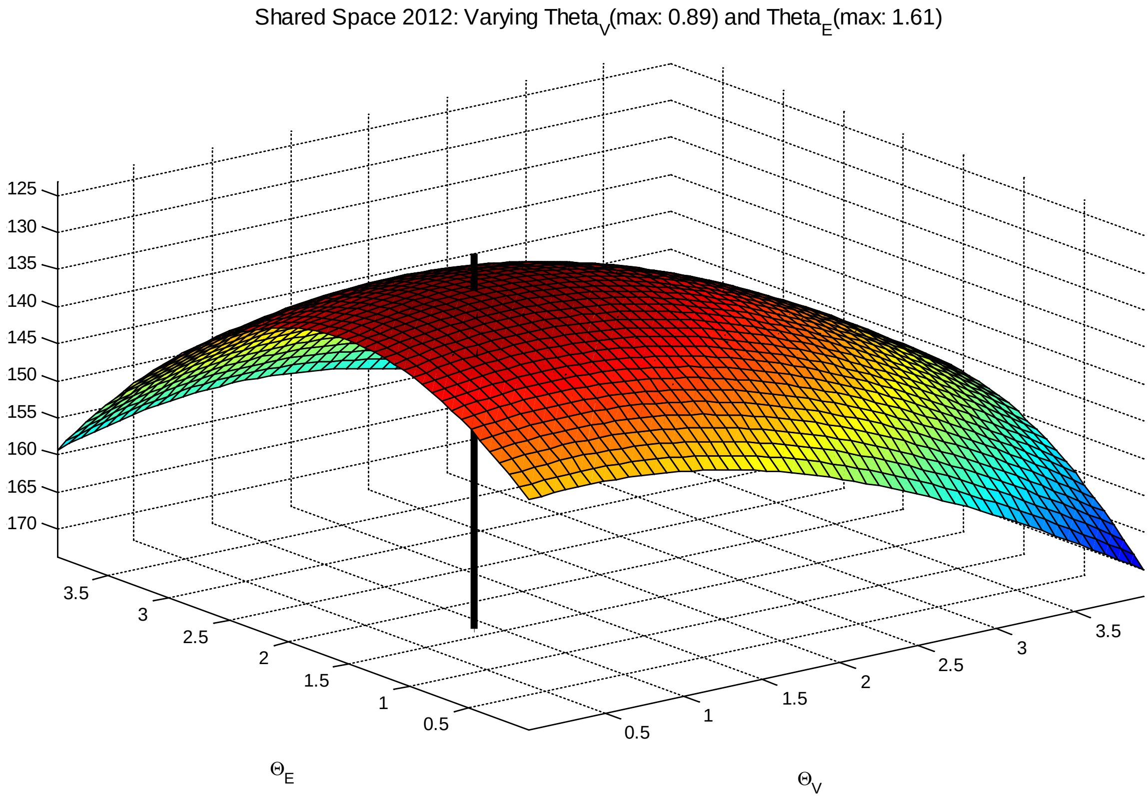

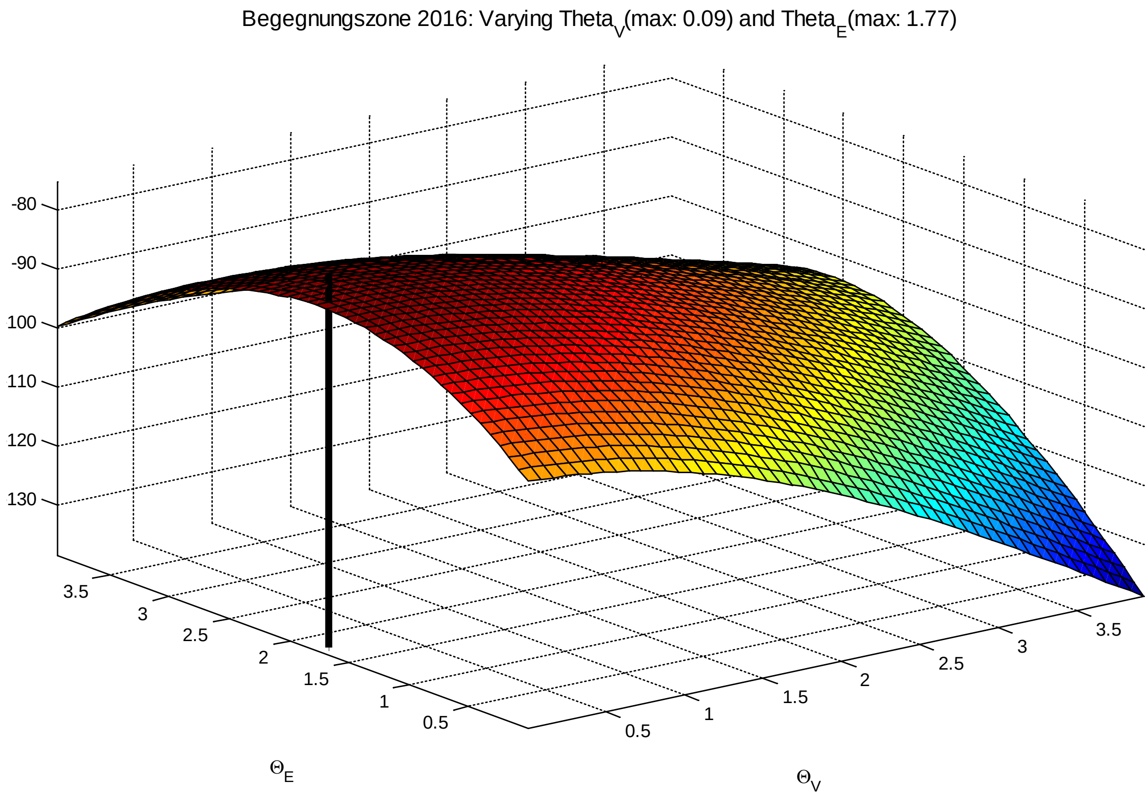

Figure 8.33: Varying Θ_V and Θ_E, leaving the other Θ_x as shown in table 6.2. TOP: Based on the shared space data set 2012 (data set 1b). BOTTOM: Based on the Begegnungszonen data set 2016 (data set 2c).

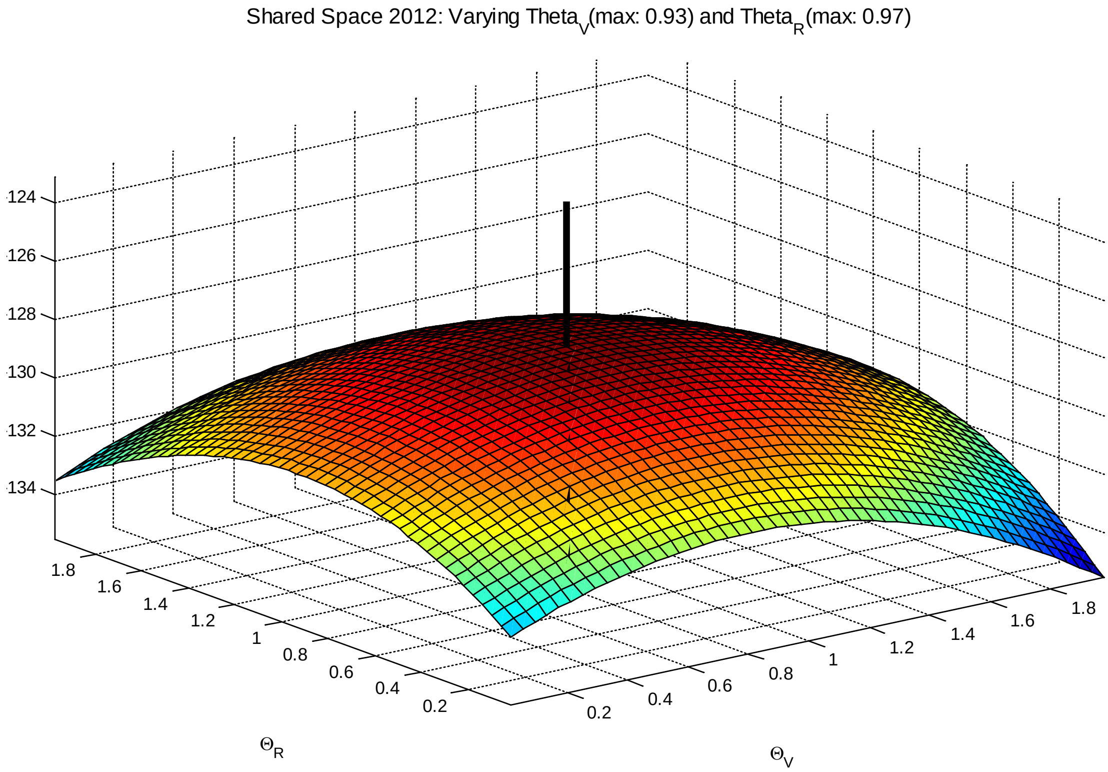

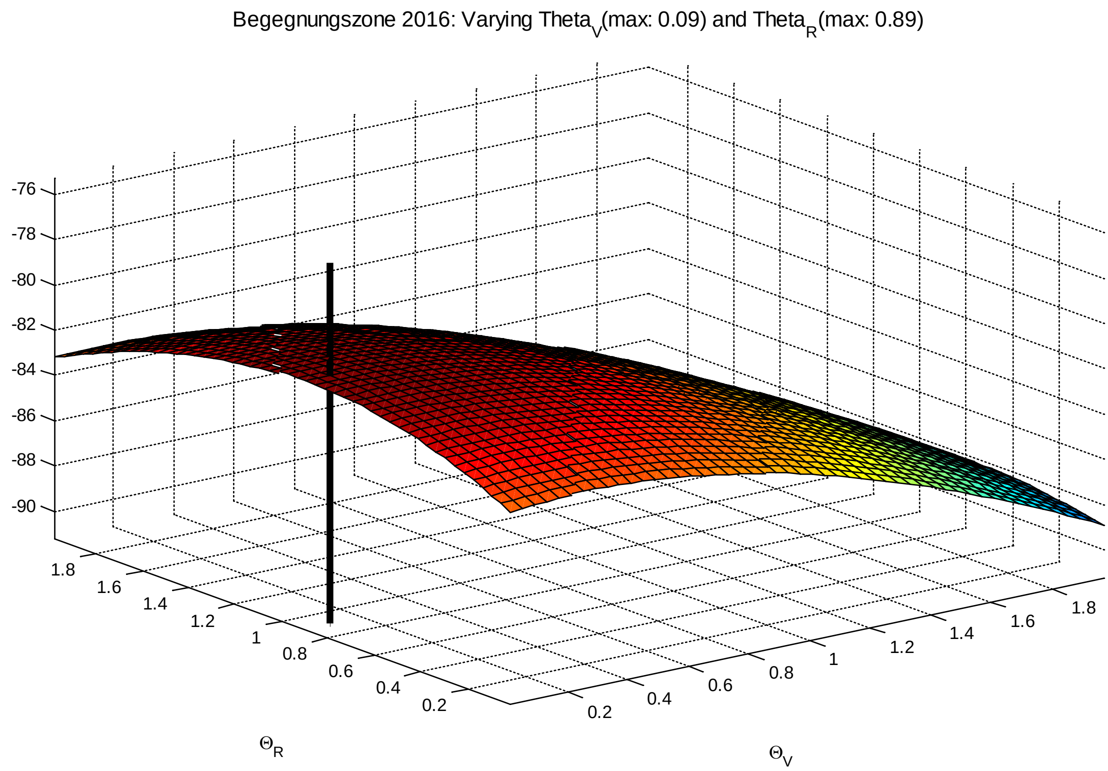

Figure 8.34: Varying Θ_V and Θ_R, leaving the other Θ_x as shown in table 6.2.TOP: Based on the shared space data set 2012 (data set 2b). BOTTOM: Based on the Begegnungszonen data set 2016 (data set 2c).

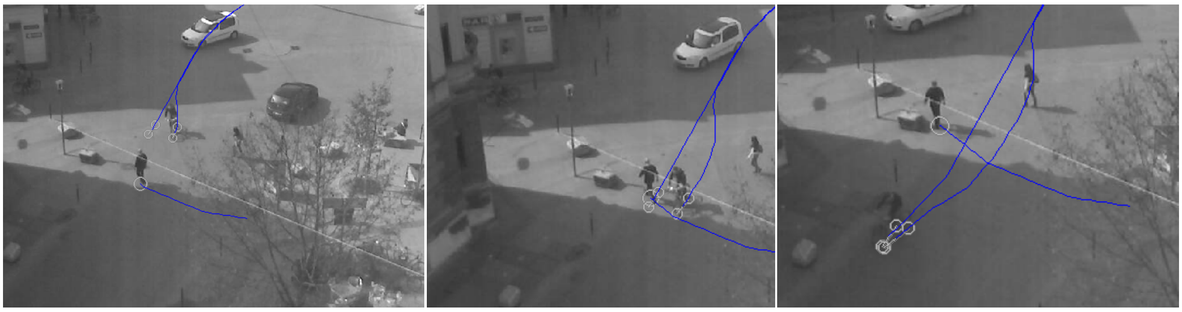

Figure 8.35: A conflict and its real and "no reaction" trajectories at the shared space Sonnenfelsplatz.

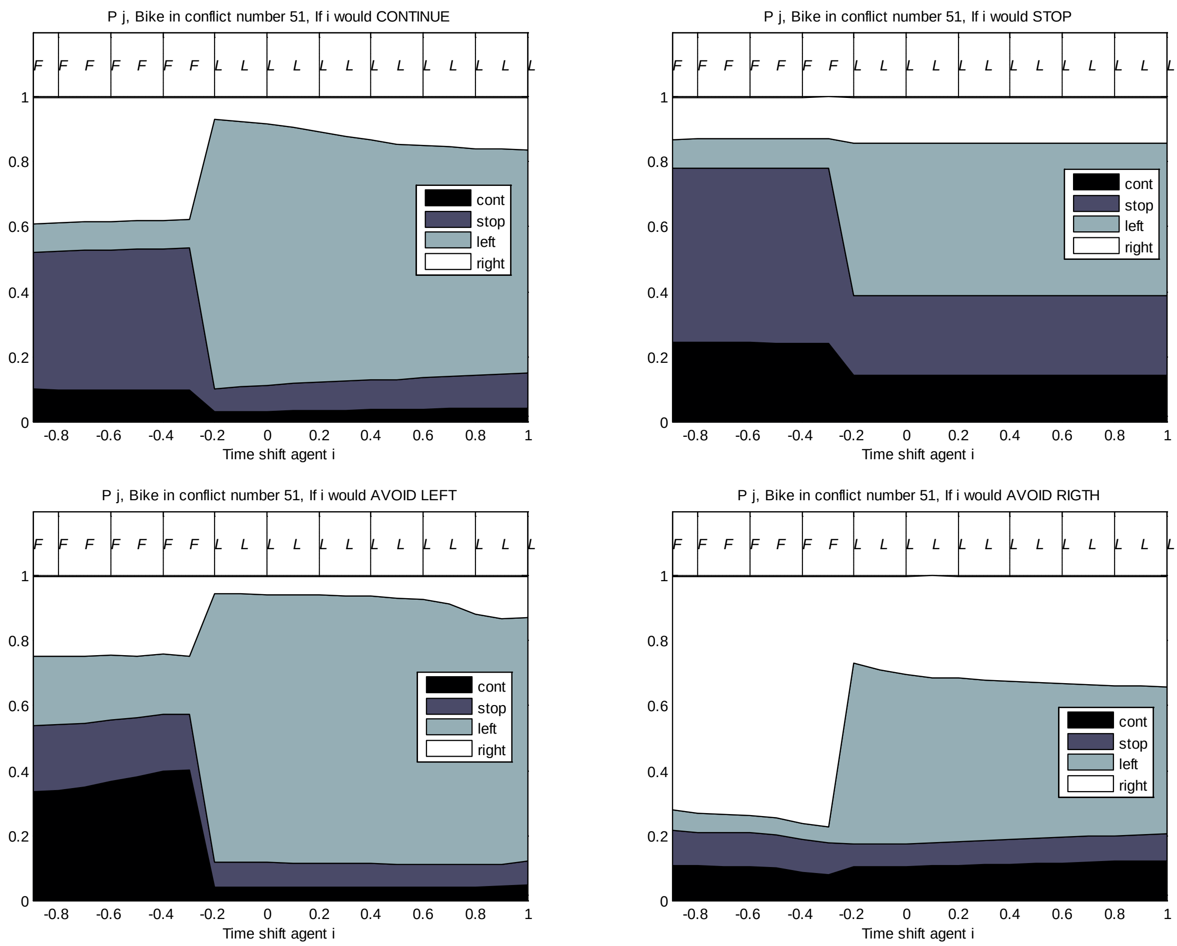

Figure 8.36: P_j in dependency to the time of arrival of agent i. Each figure shows the response to a specific leaders choice S_i.

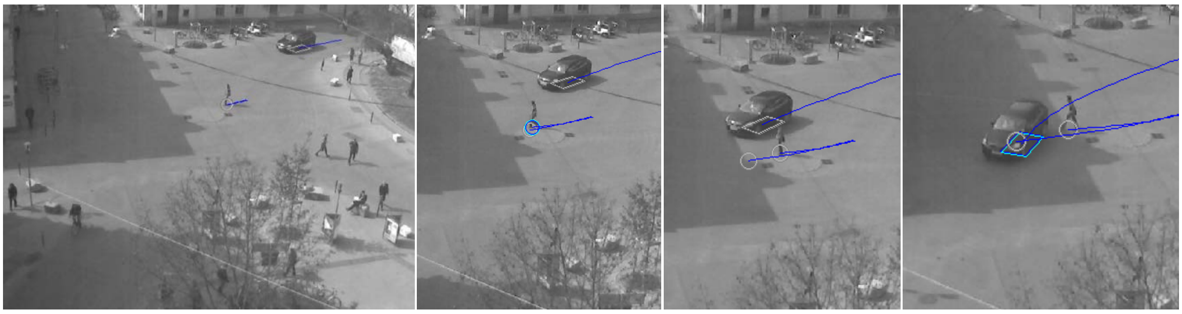

Figure 8.37: A conflict and its real- and hypothetical "no reaction" - trajectories at the shared space Sonnenfelsplatz: A Pedestrian is crossing the square at his shortest central path, priority clearly is at the car drivers side.

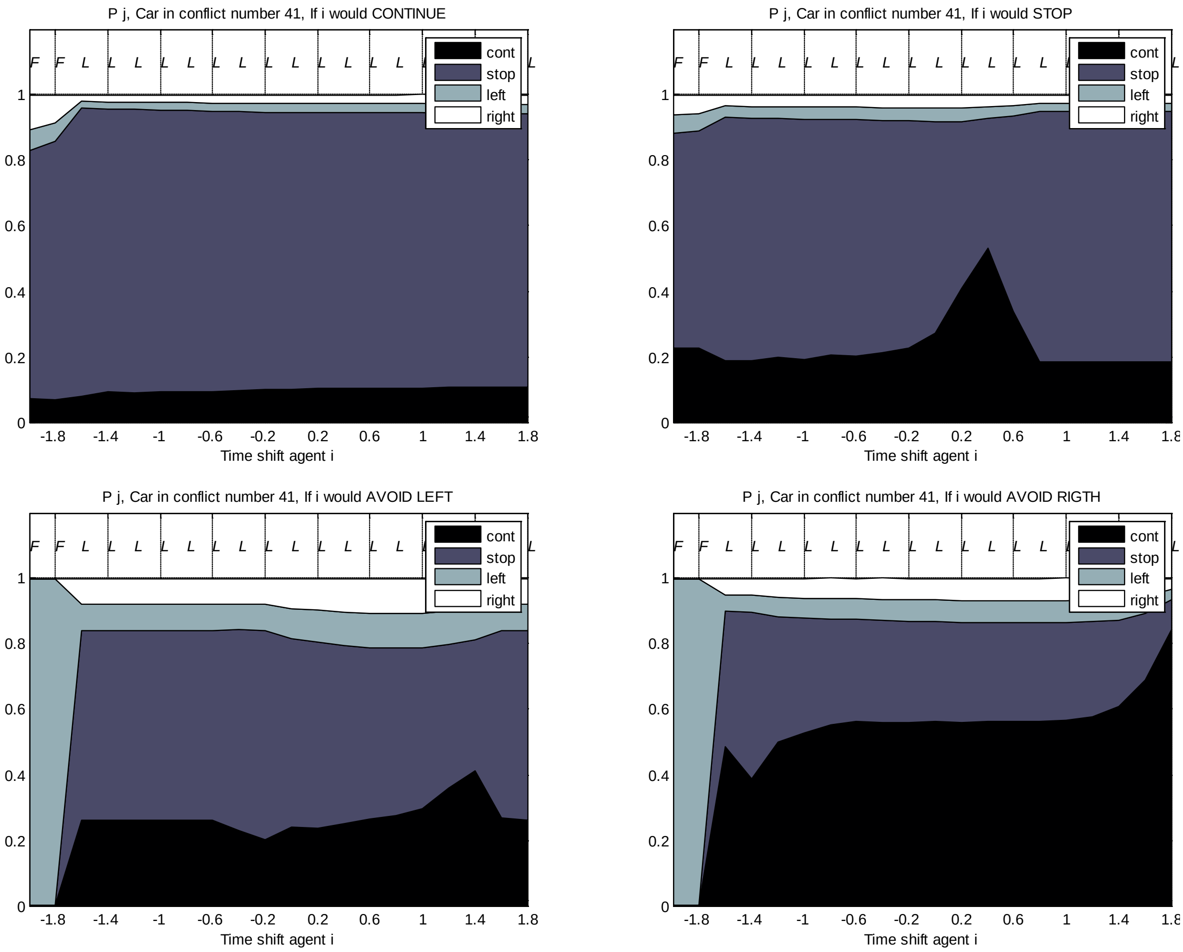

Figure 8.38: P_j in dependency to the time of arrival of agent i. Each figure shows the response to a specific leader's choice S_i.

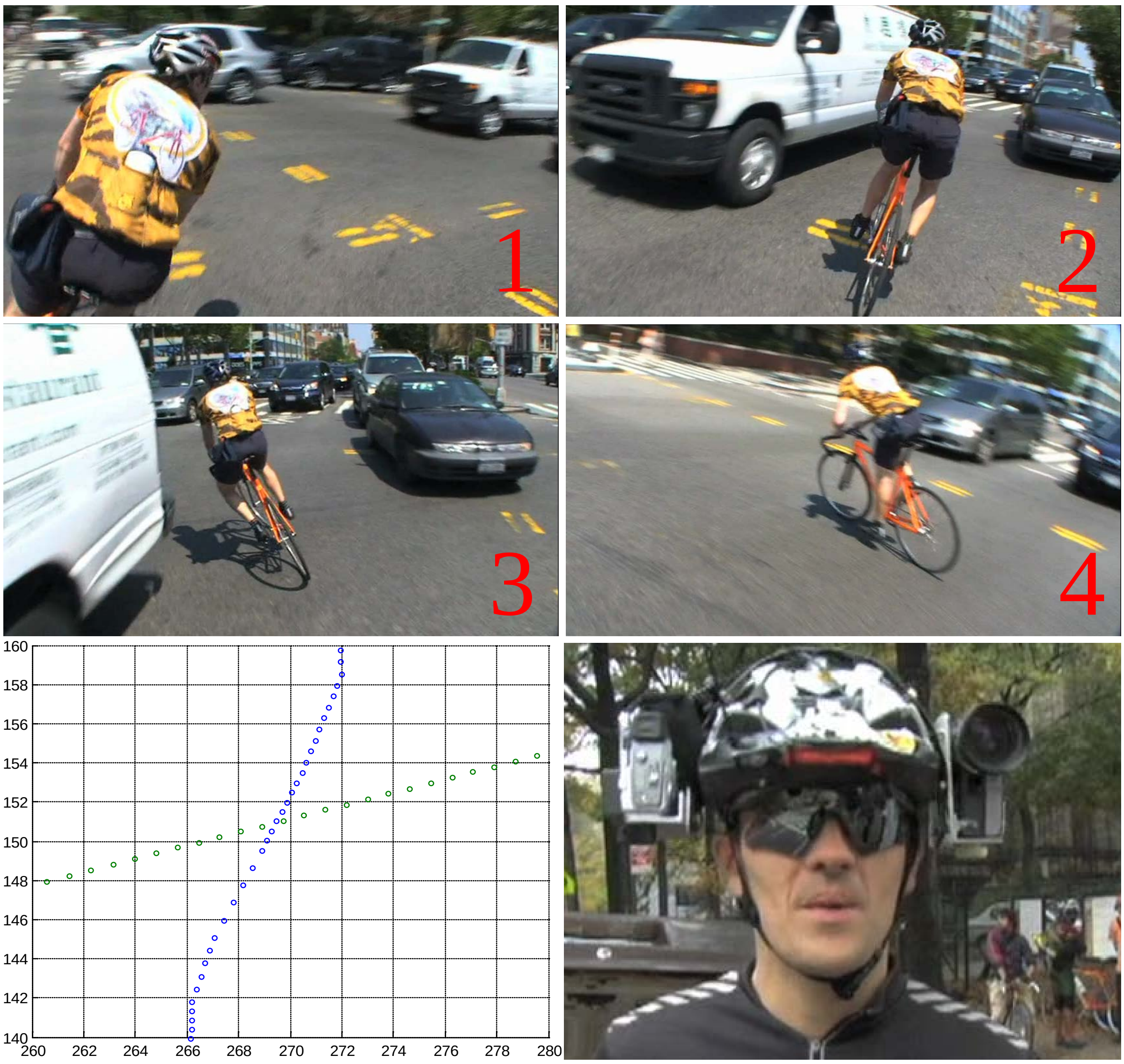

Figure 8.39: Video frames of a cyclist evading a truck by choosing the strategy: RIGHT Zenga (2012).

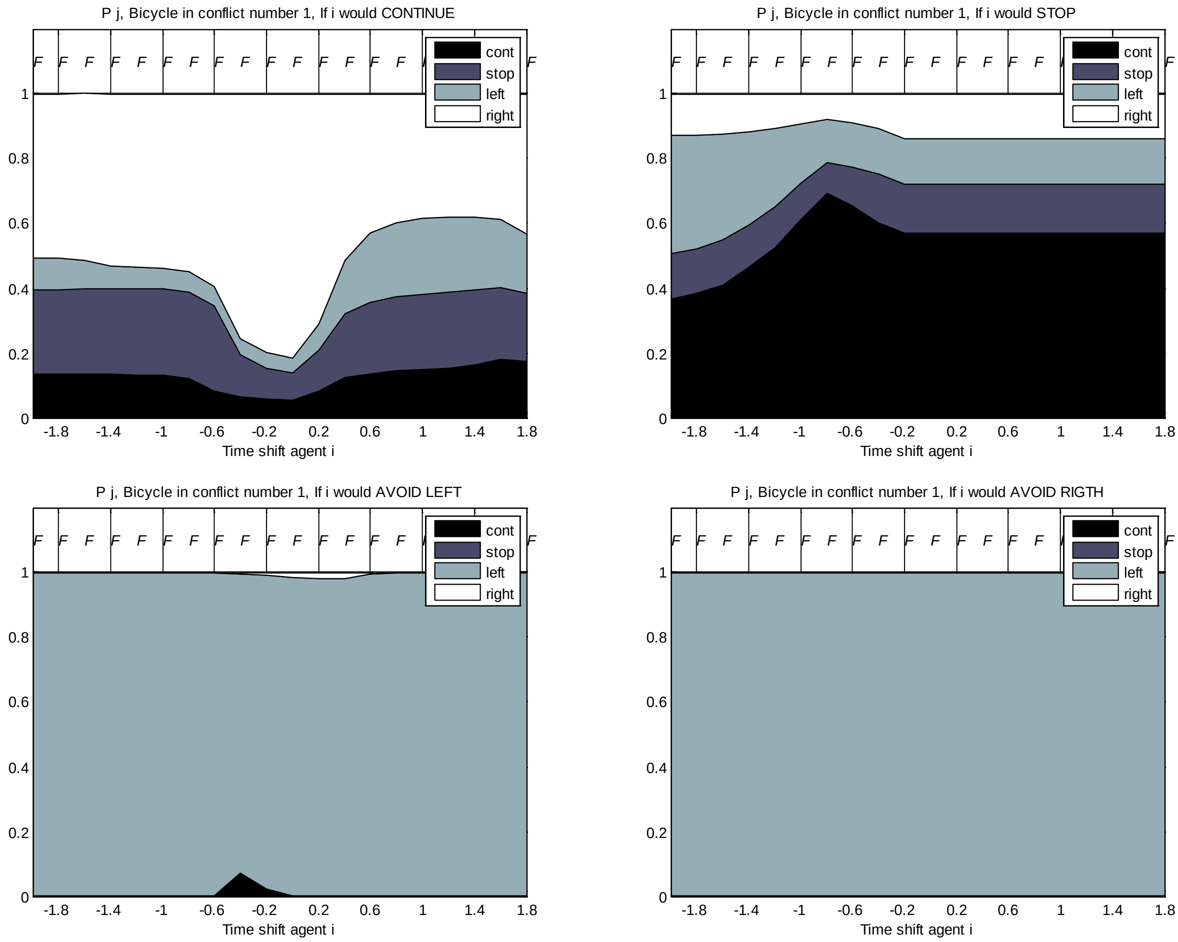

Figure 8.40: P_j in dependency to the time of arrival of agent i. Each figure shows the response to a specific leader's choice S_i.

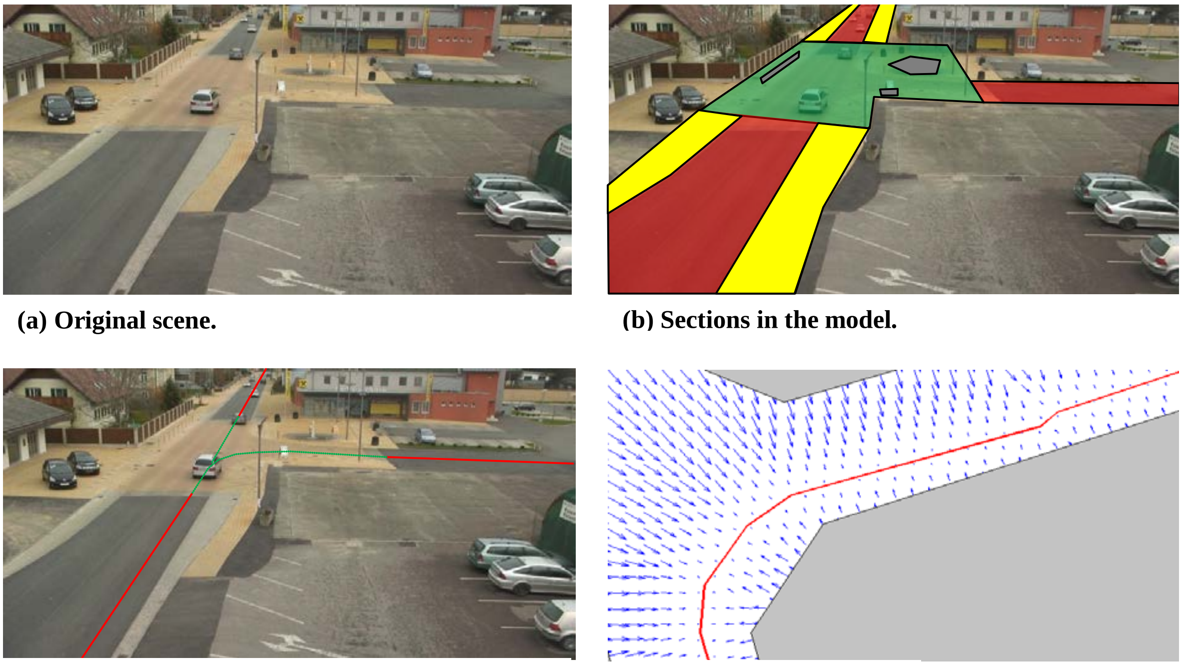

(a) Original scene.

(b) Sections in the model.

(c) Guiding field's maxima.

(d) Force vector field.

Figure 8.41: Obtaining the guiding field for the silver car. The original topology (a) is segmented into sections (b). (c) shows both guiding field's maxima for a car turning right or heading straight (for visualization purposes only). (d) shows the vector field with forces keeping the silver car on its track when turning right (guiding field from (c) transferred to world coordinates) Schönauer et al. (2012b).

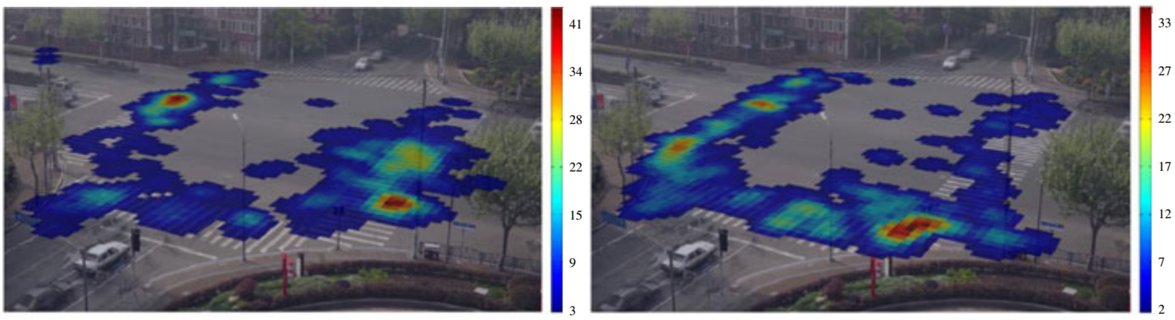

Figure 8.42: Spation conflict distribution at cross-walks at a Shanghai intersection of conventional design , taken from (Tageldin and Sayed, 2016); LEFT: Pedestrian-Vehicle Conflicts; RIGHT: Pedestrian-Bicycle Conflicts

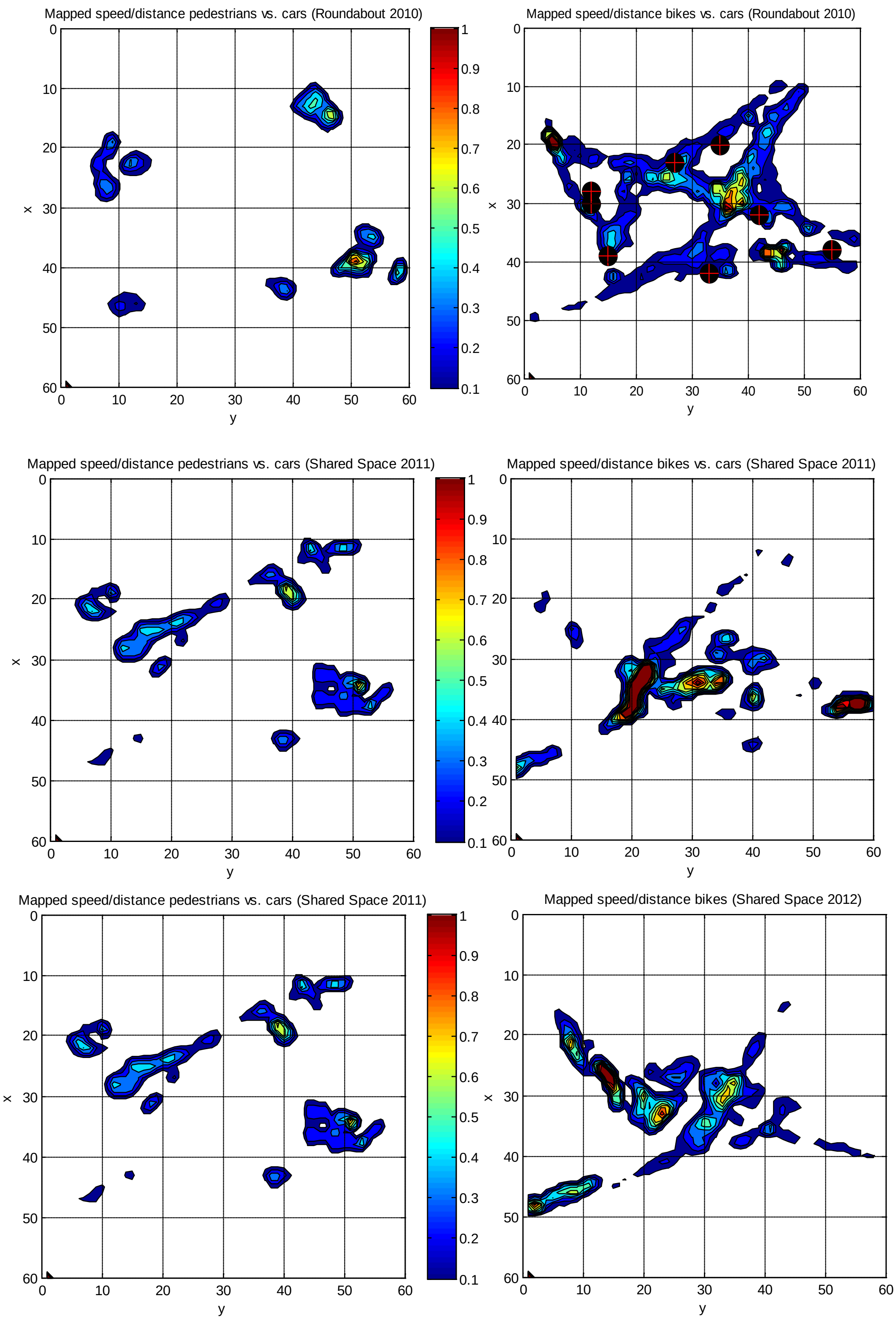

Figure 8.43: Indicator C_{xy} based on cell grid speeds [m/s]. TOP LEFT: Pedestrian/Cars in 2010. TOP RIGHT: Bikes/Cars in 2010 (red markings for accidents during 2006-2008). CENTER LEFT: Pedestrian/Cars in 2011. CENTER RIGHT: Bikes/Cars in 2011. BOTTOM LEFT: Pedestrian/Cars in 2012. BOTTOM RIGHT: Bikes/Cars in 2012.

Bibliography

Abdelfattah, A. M. and Khan, A. (1998). Models for predicting bus delays. *Transportation Research Record: Journal of the Transportation Research Board*, 1623(-1):8–15.

Abdullah, A. S., Hai, K., Osman, N., and Zainon, M. (2006). Vision based automatic steering control using a PID controller unit. *Jurnal Teknologi*, 44(6):97–114.

Ahuja, S., Priest, N., and Vuren, T. (2003). Public transport priority schemes: comparing microsimulation with traditional TRANSYT and LINSIG models. In *Proceedings of the European transport Conference (ETC) 2003, Strasbourg, France*.

Anvari, B. (2014). *A new microscopic model for the simulation of shared space schemes*. PhD thesis, Imperial College London, Faculty of Engineering.

Anvari, B., Bell, M. G., Angeloudis, P., and Ochieng, W. Y. (2014). Long-range collision avoidance for shared space simulation based on social forces. *Transportation Research Procedia*, 2:318–326.

Anvari, B., Bell, M. G., Angeloudis, P., and Ochieng, W. Y. (2016). Calibration and validation of a shared space model: Case study. *Transportation Research Record: Journal of the Transportation Research Board*, (2588):43–52.

Anvari, B., Bell, M. G., Sivakumar, A., and Ochieng, W. Y. (2015). Modelling shared space users via rule-based social force model. *Transportation Research Part C: Emerging Technologies*, 51:83–103.

Arasan, V. (2005). Methodology for Modeling Highly Heterogeneous Traffic Flow. *Journal of Transportation Engineering*, 131(7):544–551.

Arasan, V. and Vedagiri, P. (2008). Bus priority on roads carrying heterogeneous traffic: a study using computer simulation. *European Journal of Transport and Infrastructure Research*, 1:45–64.

Archer, J. (2005). *Indicators for traffic safety assessment and prediction and their application in micro-simulation modelling: A study of urban and suburban intersections*. PhD thesis, KTH, School of Architecture and the Built Environment, Centre for Traffic Research.

Asano, M., Sumalee, A., Kuwahara, M., and Tanaka, S. (2007). Dynamic cell transmission-based pedestrian model with multidirectional flows and strategic route choices. *Transportation Research Record: Journal of the Transportation Research Board*, 2039:42–49.

Astarita, V., Giofré, V., Guido, G., and Vitale, A. (2011). Investigating road safety issues through a microsimulation model. *Procedia-Social and Behavioral Sciences*, 20:226–235.

Åström, K. J., Klein, R. E., and Lennartsson, A. (2005). Bicycle dynamics and control. *Control Systems Magazine*, 25(4):26–47.

Bando, M., Hasebe, K., Nakayama, A., Shibata, A., and Sugiyama, Y. (1995). Dynamical model of traffic congestion and numerical simulation. *Physical Review E*, 51(2):1035–1042.

Barceló, J. (2010). Models, traffic models, simulation, and traffic simulation. In *Fundamentals of Traffic Simulation*, pages 1–62. Springer.

Barceló, J. and Casas, J. (2005). Dynamic network simulation with AIMSUN. In Kitamura, R., Kuwahara, M., Sharda, R., and Voß, S., editors, *Simulation Approaches in Transportation Analysis*, volume 31 of *Operations Research Computer Science Interfaces Series*, pages 57–98. Springer US.

Barceló, J., Casas, J., Ferrer, J. L., and García, D. (1999). Modeling advanced transport telematic applications with microscopic simulators: The case of AIMSUN 2. *Traffic and Mobility, Simulation, Economics, Environment*, pages 205–224.

Barjonet, P. E. (2001). *Traffic Psychology Today*. Springer Science & Business Media.

Bazzan, A. L., Wahle, J., and Klügl, F. (1999). Agents in traffic modelling-from reactive to social behaviour. In *Proceedings of the 23rd Annual German Conference on Artificial Intelligence, Bonn*, volume 99, pages 303–307. Springer.

Bell, M. (2008). Shared surfaces: Travel demand unmanagement. *Proceedings of the 4th International Symposium on Travel Demand Management*.

Ben-Joseph, E. (1995). Changing the residential street scene: Adapting the shared street (Woonerf) concept to the suburban environment. *Journal of the American Planning Association*, 61(4):504–515.

Benner, H., Kretz, T., Lohmiller, J., and Sukennik, P. (2017). Is calibration a straightforward task if detailed trajectory data is available? In *TRB 96th Annual Meeting Compendium of Papers*, Washington.

Beuck, U., Nagel, K., Rieser, M., Strippgen, D., and Balmer, M. (2007). Preliminary Results of a Multiagent Traffic Simulation for Berlin. *Advances in Complex Systems*, 10(289):289–307.

Björklund, G. M. (2005). Driver behaviour in intersections: Formal and informal traffic rules. *Transportation Research Part F: Psychology and Behaviour*, 8(3):239–253.

Bliek, D. (2010). Impacts of shared space design on pedestrian and motorist behaviour. In *Proceedings of the ITE 2010 Annual Meeting and Exhibit*.

Blue, V. and Adler, J. (1999). Cellular automata microsimulation of bidirectional pedestrian flows. *Transportation Research Record: Journal of the Transportation Research Board*, 1678(-1):135–141.

Bode, W. (2009). Verkehrsuntersuchung in der Gemeinde Bohmte unter besonderer Berücksichtigung der Auswirkungen des Shared Space Bereiches [Online]. Retrieved from: www.bohmte.de [Accessed: 2017-07-09].

Bogner, J. and Robatsch, K. (2013). Gemeinschaftsstrasse: ein neues Konzept für alle Verkehrsteilnehmer. *Recht und Finanzen für Gemeinden (RFG)*, 11(1). Manz Verlag Wien.

Bönisch, C. and Kretz, T. (2009). Simulation of pedestrians crossing a street. In *Proceedings of Traffic and Granular Flow 09*, Shanghai. Springer.

Bonnefon, J.-F., Shariff, A., and Rahwan, I. (2016). The social dilemma of autonomous vehicles. *Science*, 352(6293):1573–1576.

Buchanan, C. (1963). *Traffic in Towns: A Study of the Long Term Problems of Traffic in Urban Areas*. Taylor and Francis.

Burstedde, C., Kirchner, A., Klauck, K., Schadschneider, A., and Zittartz, J. (2001). Cellular Automaton Approach to Pedestrian Dynamics - Application . *Pedestrian Evacuation Dynamics 2001*, page pp.87. Retrieved from: https://arxiv.org/pdf/cond-mat/0112119.pdf [Accessed: 2017-07-10].

Butz, M. (2007). Fuss- und Veloverkehr auf gemeinsamen Flächen. *Strasse und Verkehr*, (9):26–29.

Cameron, G. D. B. and Duncan, G. I. D. (1996). PARAMICS - Parallel microscopic simulation of road traffic. *The Journal of Supercomputing*, 10(1):25–53.

Carson, G. and Hickman, R. (2006). Shared space in the Kent Area of Outstanding Natural Beauty (AONB): a new approach to streetscape design. In *Proceedings of the European Transport Conference (ETC)*.

Case, H. W., Hulbert, S. F., Mount, G. E., and Brenner, R. (1953). Effect of a roadside structure on lateral placement of motor vehicles. In *Proceedings of the Thirty-Second Annual Meeting of the Highway Research Board*, volume 32, pages 364–370, Washington.

Champion, A., Mandiau, R., Espié, S., and Kolski, C. (2001). Multi-Agent Road Traffic Simulation: Towards Coordination by Game Theory Based Mechanism. In *Proceedings of the Agents in Traffic and Transportation, Workshop in conjunction with the ITS World Congress*.

Chandler, R. E., Herman, R., and Montroll, E. W. (1958). Traffic Dynamics: Studies in Car Following. *Operations research*, 6(2):165–184.

Childs, C. R., Thomas, C., Sharp, S., and Tyler, N. A. (2010). Can shared surfaces be safely negotiated by blind and partially sighted people? In *Proceedings of the 12th International Conference on Mobility and Transport for Elderly and Disabled Persons (TRANSED)*.

Cloutier, M.-S., Lachapelle, U., d Amours-Ouellet, A.-A., Bergeron, J., Lord, S., and Torres, J. (2017). Outta my way! Individual and environmental correlates of interactions between pedestrians and vehicles during street crossings. *Accident Analysis & Prevention*, 104:36–45.

Cortés, C. E., Fernandez, R., and Burgos, V. (2007). Modeling Passengers, Buses, and Stops in Traffic Microsimulators: MISTRANSIT Approach on PARAMICS Platform. In *Proceedings of the Transportation Research Board 86th Annual Meeting*, number 07-3252, Washington.

Currie, G., Sarvi, M., and Young, B. (2007). A new approach to evaluating on-road public transport priority projects: balancing the demand for limited road-space. *Transportation*, 34(4):413–428.

Daamen, W., Hoogendoorn, S., Campanella, M., and Versluis, D. (2014). Interaction Behavior Between Individual Pedestrians. In *Pedestrian and Evacuation Dynamics 2012*, pages 1305–1313. Springer.

Davis, G. (1998). Method for Estimating Effect of Traffic Volume and Speed on Pedestrian Safety for Residential Streets. *Transportation Research Record*, 1636(1):110–115.

De Jong, L. E. (2013). A simulation model of mixed traffic flow at non-signalised intersections, based on the Shared Space approach. Master thesis, Delft University of Technology, Faculty of Civil Engineering and Geosciences.

Defoort, M. and Murakami, T. (2009). Sliding-Mode Control Scheme for an Intelligent Bicycle. *Industrial Electronics, IEEE Transactions on*, 56(9):3357–3368.

Delpiano, R., Laval, J., Coeymans, J. E., and Herrera, J. C. (2015). The kinematic wave model with finite decelerations: A social force car-following model approximation. *Transportation research part B: methodological*, 71:182–193.

Department for Transport (2011). Shared Space [Online]. Retrieved from www.dft.gov.uk/publications/ltn-01-11/ [Accessed: 2017-07-10].

Dong, W. (2012). Traffic conflict and shared space: A before and after case study on exhibition road. In *Proceedings of the 1st Civil and Environmental Engineering Student Conference*. Imperial College London.

Doniec, A., Espié, S., Mandiau, R., and Piechowiak, S. (2006). Traffic Simulation At Junction: Non-Normative Practices Vs. Deadlock. *Proceedings of the Joint CIB, W78, W102, ICCCBE, ICCC, and DMUCE International Conference on Computing and Decision Making in Civil and Building Engineering, Montreal, Canada*.

Doniec, A., Mandiau, R.and Piechowiak, S., and Espié, S. (2008). A behavioral multi-agent model for road traffic simulation. *Engineering Applications of Artificial Intelligence*, 21(8):1443–1454.

Doniec, A., Piechowiak, S., and Mandiau, R. (2005). A DisCSP Solving Algorithm Based on Sessions. In *Proceedings of the 18th International Florida Artificial Intelligence Research Society Conference on Recent Advances in Artificial Intelligence*, pages 666–670.

Drogoul, A., Vanbergue, D., and Meurisse, T. (2003). Multi-agent Based Simulation: Where Are the Agents? *Multi-agent-based simulation II*, 2581:43–49.

Duncan, A. B. (2016). *Cyclist Path Choices Through Shared Space Intersections in England*. PhD thesis, Portland University, Department of Urban Studies and Planning.

Dutch Ministry of Infrastructure and the Environment (2006). Road Traffic Signs and Regulations in the Netherlands [Online]. Retrieved from: www.government.nl [Accessed: 2017-07-11].

Edquist, J., Rudin-Brown, C. M., and Lenné, M. G. (2012). The effects of on-street parking and road environment visual complexity on travel speed and reaction time. *Accident Analysis & Prevention*, 45:759–765.

Eiter, T. and Mannila, H. (1994). Computing discrete Fréchet distance [Online]. *Technical Report CD-TR 94/64*. Retrieved from: www.kr.tuwien.ac.at/staff/eiter/et-archive/cdtr9464.pdf [Accessed: 2017-07-10].

Engwicht, D. (2005). *Mental Speed Bumps: The smarter way to tame traffic*. Envirobook, Sussex Inlet, Australia.

Evans, L. (1985). Human Behavior Feedback and Traffic Safety. *Human Factors: The Journal of the Human Factors and Ergonomics Society*, 27(5):555–576.

Fellendorf, M. and Vortisch, P. (2001). Validation of the Microscopic Traffic Flow Model VISSIM in Different Real-World Situations. In *Proceedings of the Transportation Research Board 80th Annual Meeting*, Washington.

Fellendorf, M. and Vortisch, P. (2010). Microscopic Traffic Flow Simulator VISSIM. In Barceló, J., editor, *Fundamentals of Traffic Simulation*, pages 63–93. Springer New York.

Firth, K. (2011). Removing Traffic Engineering Control: The Awkward Truth? *Traffic Engineering and Control*, 52(2):73–79.

Fishbein, M. and Ajzen, I. (1975). *Belief, attitude, intention, and behavior: An introduction to theory and research*. Addison-Wesley, Reading.

Flade, A. (1994). *Mobilitätsverhalten*. Psychologie Verlags Union, Weinheim.

Flötteröd, G. and Nagel, K. (2005). Some practical extensions to the cell transmission model. In *Proceedings of the ITSC 2005 8th International IEEE Conference on Intelligent Transportation Systems*, pages 172–177.

Forschungsgesellschaft Strasse, Schiene, Verkehr (2001). RVS 03.02.13, Strassenplanung, Nicht motorisierter Verkehr, Radverkehr.

Forschungsgesellschaft Strasse, Schiene, Verkehr (2004). RVS 03.02.12, Strassenplanung, Nicht motorisierter Verkehr, Fußgängerverkehr.

Fritzsche, H.-T. (1994). A model for traffic simulation. *Traffic Engineering+ Control*, 35(5):317–21.

Füreder, W. and Schwab, D. (2009). *Sicherheitsaspekte Aktionsplan Fussverkehr: Modul Shared Space "Begegnungszonen der besonderen Art" im Überblick, Teil 1*. Bundesministerium für Verkehr, Innovation und Technologie, Wien.

Galiza, R. J., Kim, I., Ferreira, L., and Laufer, J. (2009). Modelling Pedestrian Circulation in Rail Transit Stations Using Micro-Simulation. In *Proceedings of the 32nd Australasian Transport Research Forum (ATRF)*.

Gasser, L. and Huhns, M. N. (1989). *Distributed Artificial Intelligence: Volume 2*. Pitman, London.

Gerlach, J. (2015). Shared space, meeting zones, traffic calming, co-existence-who, how, what, why? *Straßenverkehrstechnik*, 59(5):308–16.

Gerlach, J., Methorst, R., Boenke, D., and Leven, J. (2009). Sense and nonsense about Shared Space - For an objective view of a popular planning concept. *Routes/Roads*, 342:36–45.

Gerlach, J. and Ortlepp, J. (2010). Shared Space, und alles wird gut? - Neue Analysen und Bewertungen / Shared Space, and everything is going to be alright? - New analyses and surveys. *Strassenverkehrstechnik*, 54(1):32–46.

GfL Planungs- und Ingenieursgesellschaft GmbH (2006). Shared Space - Abschlussdokumentation [Online]. Retrieved from: www.bohmte.de [Accessed: 2017-07-09].

Gibson, J. and Crooks, L. (1938). A Theoretical Field-Analysis of Automobile-Driving. *American Journal of Psychology*, 51(3):453–471.

Gipps, P. (1981). A behavioural car-following model for computer simulation. *Transportation Research Part B: Methodological*, 15(2):105–111.

Gipps, P. and Marksjö, B. (1985). A micro-simulation model for pedestrian flows. *Mathematics and Computers in Simulation*, 27(2):95–105.

Gloor, C., Stucki, P., and Nagel, K. (2004). Hybrid techniques for pedestrian simulations. In Sloot, P. M. A., Chopard, B., and Hoekstra, A. G., editors, *In Proceedings of the 6th International Conference on Cellular Automata for Research and Industry, ACRI 2004, Amsterdam, The Netherlands*, pages 581–590. Springer Berlin Heidelberg.

Gräßle, F. and Kretz, T. (2008). An Example of Complex Pedestrian Route Choice. In *Pedestrian and Evacuation Dynamics 2010*, pages 767–771.

Grassmuck, V. (2009). Die Welt als Shared Space. In *Ich, Wir und Die Anderen: Neue Medien zwischen demokratischen und ökonomischen Potenzialen II*, pages 103–123. Heise Verlag, Hannover.

Grundtner, H. (2017). *Die Österreichische Straßenverkehrsordnung*. LexisNexis ARD ORAC, Austria, 37 edition.

Haas, R. and Herberg, H. (1983). Einflüsse von Fahrer- und Straßenmerkmalen auf die Fahrergeschwindigkeit in Ortschaften. In *Forschungsberichte BAST*, volume 83. Bundesanstalt für Straßenwesen, Bereich Unfallforschung, Köln.

Hamilton, W. D. and Axelrod, R. (1981). The evolution of cooperation. *Science*, 211(27):1390–1396.

Hamilton-Baillie, B. (2007). Shared space: Reconciling people, places and traffic. *Built Environment*, 34(2):161–181.

Hamilton-Baillie, B. (2008). Towards shared space. *Urban Design International*, 13(2):130–138.

Hamilton-Baillie, B. and Jones, P. (2005). Improving traffic behaviour and safety through urban design. *Proceedings of the Institution of Civil Engineers. Civil engineering*, 158(5):39–47.

Havik, E. M., Melis-Dankers, B. J. M., Steyvers, F. J. J. M., and Kooijman, A. C. (2012). Accessibility of Shared Space for visually impaired persons: An inventory in the Netherlands. *British Journal of Visual Impairment*, 30(3):132–148.

Havik, E. M., Steyvers, F. J. J. M., Kooijman, A. C., and Melis-Dankers, B. J. M. (2015). Accessibility of shared space for visually impaired persons: A comparative field study. *British Journal of Visual Impairment*, 33(2):96–110.

Heinz, H. (2006). Context-Sensitive Design for Streets in Rural Built-Up Areas. *Transportation Research E-Circular*, (E-C097):3–6.

Heissing, B. and Brandl, H. (2002). *Subjektive Beurteilung des Fahrverhaltens*. Vogel Buchverlag, Würzburg.

Helbing, D. (1998a). *A Mathematical Model for Behavioral Changes by Pair Interactions and Its Relation to Game Theory*, pages 330–348. Springer Berlin Heidelberg.

Helbing, D. (1998b). *From Microscopic to Macroscopic Traffic Models*. Springer Berlin Heidelberg.

Helbing, D. (2001). Traffic and related self-driven many-particle systems. *Reviews of Modern Physics*, 73(4):1067–1141.

Helbing, D., Farkas, I., and Vicsek, T. (2000). Simulating Dynamical Features of Escape Panic. *Nature*, 407:487–490.

Helbing, D. and Mazloumian, A. (2009). Operation regimes and slower-is-faster effect in the control of traffic intersections. *The European Physical Journal B-Condensed Matter and Complex Systems*, 70(2):257–274.

Helbing, D. and Molnár, P. (1995). Social force model for pedestrian dynamics. *Physical Review E*, 51(5):4282–4286.

Helbing, D., Molnár, P., Farkas, I. J., and Bolay, K. (2001). Self-organizing pedestrian movement. *Environment and Planning B: Planning and Design*, 28(3):361–383.

Helbing, D. and Tilch, B. (1998). Generalized force model of traffic dynamics. *Physical Review E*, 58(1):133–138.

Henderson, L. F. (1971). The Statistics of Crowd Fluids. *Nature*, 229:381–383.

Hentschel, P., Floegel, J., and König, P. (2005). *Beck'sche Kurzkommentare, Band 5, Straßenverkehrsrecht*. C. H. Beck, Munich.

Hobson, K. (2008). Reasons to be cheerful: thinking sustainably in a (climate) changing world. *Geography Compass*, 2(1):199–214.

Hong-bo, Q. and Hui-ling, Z. (2009). Bicycle Traffic Organization and Treatment at Signalized Intersection. In *Proceedings of the Second International Conference on Intelligent Computation Technology and Automation*, pages 515–518.

Hoogendoorn, S. P. and Bovy, P. H. L. (2001). State-of-the-art of Vehicular Traffic Flow Modelling. *Proceedings of the Institution of Mechanical Engineers, Part I: Journal of Systems and Control Engineering*, 215(4):283–303.

Hoogendoorn, S. P., Bovy, P. H. L., and Daamen, W. (2001). Microscopic pedestrian wayfinding and dynamics modelling. In Schreckenberg, M. and Sharma, S., editors, *Pedestrian and Evacuation Dynamics*, pages 123–154. Springer, Berlin.

Hoogendoorn, S. P. and Daamen, W. (2006). Free Speed Distributions for Pedestrian Traffic. In *TRB 85th Annual Meeting Compendium of Papers*. Transportation Research Board, Washington.

Huang, W. and Fellendorf, M. (2012). Social Force Model for Vehicle Simulation on Operational Level. In *Proceedings of the 19th ITS World Congress*, Vienna.

Huang, W., Fellendorf, M., and Schönauer, R. (2012). Social Force based Vehicle Model for Two-Dimensional Spaces. In *TRB 91st Annual Meeting Compendium of Papers*. Transportation Research Board, Washington.

Hüttenmoser, M. (2009). Shared space - auf der Strecke bleiben die Kinder. *VERKEHRSZEICHEN - für Mobilität und Umwelt*, 25(1):9–16.

Ismail, K., Sayed, T., and Saunier, N. (2010). Automated Analysis of PedestrianVehicle Conflicts: Context for Before-and-After Studies. *Transportation Research Record: Journal of the Transportation Research Board*, 2198:52–64.

Johansson, A., Helbing, D., and Shukla, P. K. (2007). Specification of the social force pedestrian model by evolutionary adjustment to video tracking data. *Advances in Complex Systems*, 10:271–288.

Kadali, B. R. and Vedagiri, P. (2013). Modelling pedestrian road crossing behaviour under mixed traffic condition. *European transport*, 55(3).

Kaparias, I., Bell, M. G. H., Biagioli, T., Bellezza, L., and Mount, B. (2015). Behavioural analysis of interactions between pedestrians and vehicles in street designs with elements of shared space. *Transportation Research Part F: Traffic Psychology and Behaviour*, 30:115–127.

Kaparias, I., Bell, M. G. H., Dong, W., Sastrawinata, A., Singh, A., Wang, X., and Mount, B. (2013). Analysis of pedestrian-vehicle traffic conflicts in street designs with elements of shared space. *Transportation Research Record: Journal of the Transportation Research Board*, (2393):21–30.

Kaparias, I., Bell, M. G. H., Greensted, J., Cheng, S., Miri, A., Taylor, C., and Mount, B. (2010). Development and Implementation of a Vehicle-Pedestrian Conflict Analysis Method. *Transportation Research Record: Journal of the Transportation Research Board*, 2198(3):75–82.

Kaparias, I., Bell, M. G. H., Miri, A., Chan, C., and Mount, B. (2012). Analysing the perceptions of pedestrians and drivers to shared space. *Transportation research part F: traffic psychology and behaviour*, 15(3):297–310.

Karndacharuk, A., Vasisht, P., and Prasad, M. (2015). Shared Space Evaluation: O 'Connell Street, Auckland. In *Proceedings of the Australasian Transport Research Forum 2015*, Sydney, Australia.

Karndacharuk, A., Wilson, D. J., and Dunn, R. C. M. (2013). An Analysis of Pedestrian Performance in Shared Space Environments. *Transportation Research Record: Journal of the Transportation Research Board*, (2393).

Karndacharuk, A., Wilson, D. J., and Dunn, R. C. M. (2014). A Review of the Evolution of Shared (Street) Space Concepts in Urban Environments. *Transport Reviews*, 34(2):190–220.

Kesting, A., Treiber, M., and Helbing, D. (2010). Enhanced Intelligent Driver Model to Access the Impact of Driving Strategies on Traffic Capacity. *Philosophical Transactions of the Royal Society A: Mathematical, Physical and Engineering Sciences*, 368(1928):4585–4605.

Kettler, D. (2010). Shared Space rechtlich. In Bechtler, C., Hänel, A., Laube, M., Pohl, W., and Schmidt, F., editors, *Shared Space, Beispiele und Argumente für lebendige öffentliche Räume*, pages 177–189. Verein zur Förderung kommunalpolitischer Arbeit, Bielefeld, Germany.

Keuninginstituut and Senza Communicatie (2005). *Shared Space–Room for Everyone [Online]*. Fryslân Province. Retrieved from www.shared-space.org/publicaties [Accessed: 2017-07-11].

King, M. and Wright, L. (2005). Safe Routes to Transit in Developing Cities. In *Proceedings of the 6th International Conference on Walking in the 21st Century, September 22-23*, Zürich, Switzerland.

Kita, H. (1999). A merging-giveway interaction model of cars in a merging section: a game theoretic analysis. *Transportation Research Part A: Policy and Practice*, 33(3-4):305–312.

Kjemtrup, K. and Herrstedt, L. (1992). Speed management and traffic calming in urban areas in Europe: A historical view. *Accident Analysis & Prevention*, 24(1):57–65.

Klebelsberg, D. (1982). *Verkehrspsychologie*. Springer Berlin Heidelberg.

Kleboth Lindinger Dollnig and Komobile Gmunden and Michael Sammer (2009). Sonnenfelsplatz. Innovative civic participation at the first shared space project in Graz [Online]. Retrieved from: www.walk-space.at/infomail/kleboth-koch.pdf [Accessed: 2017-07-11].

Klein, F. and Sommerfeld, A. (1910). Über die Theorie des Kreisels. In *Die technische Anwendung der Kreiseltheorie*, volume 4, pages 762–965. B.G. Teubner, Leipzig.

Knoflacher, H. (1995). *Fußgeher-und Fahrradverkehr: Planungsprinzipien*. Böhlau Verlag Wien.

Knoflacher, H. and Schopf, J. M. (1981). Bestimmung der maßgeblichen Fahrstreifenbreite für Autobahnen, Schnellstraßen und Bundesstraßen, insbesondere im Hinblick auf ihre Führung in Ballungsgebieten. In *Schriftenreihe Straßenforschung*, number 177. Bundesministerium für Bauten und Technik, Vienna.

Krajzewicz, D., Hertkorn, G., Rössel, C., and Wagner, P. (2002). SUMO (Simulation of Urban MObility)-an open-source traffic simulation. In *Proceedings of the 4th Middle East Symposium on Simulation and Modelling*, pages 183–187.

Kramer, U. (2008). *Kraftfahrzeugführung: Modelle-Simulation-Regelung*. Carl Hanser, Munich.

Kraus, H. (2011). Real-Time Capable Vehicle and Driver Model for Traffic Flow Simulationgillet. Master thesis, Graz University of Technology, Institute of Automotive Engineering.

Kretz, T. (2009). Pedestrian Traffic: on the Quickest Path. *Journal of Statistical Mechanics: Theory and Experiment*, (03):pp. 03012.

Lan, L. W. and Chang, C. W. (2005). Inhomogeneous Cellular Automata Modeling for Mixed Traffic with Cars and Motorcycles. *Journal of Advanced Transportation*, 39(3):323–349.

Lee, J., Shalaby, A., Greenough, J., Bowie, M., and Hung, S. (2005). Advanced transit signal priority control with online microsimulation-based transit prediction model. *Transportation Research Record: Journal of the Transportation Research Board*, 1925(-1):185–194.

Lee, T.-C. (2007). *An Agent-Based Model to Simulate Motorcycle Behaviour in Mixed Traffic Flow*. PhD thesis, Imperial College London.

Limebeer, D. J. N. and Sharp, R. S. (2006). Bicycles, motorcycles, and models. *IEEE Control Systems*, 26(5):34–61.

Liu, X.-F., Gao, L.-M., Guang, Z.-W., and Song, Y.-G. (2013). An UAV allocation method for traffic surveillance in sparse road network. *Journal of Highway and Transportation Research and Development (English Edition)*, 7(2):81–87.

Luce, R. D. and Raiffa, H. (2012). *Games and decisions: Introduction and critical survey*. Courier Corporation, North Chelmsford, USA.

Makarem, L. and Gillet, D. (2012). Information sharing among autonomous vehicles crossing an intersection. In *Proceedings on the 2012 IEEE International Conference on Systems, Man, and Cybernetics*, pages 2563–2567.

Mallikarjuna, C. and Rao, K. R. (2009). Cellular Automata Model for Heterogeneous Traffic. *Journal of Advanced Transportation*, 43(3):321–345.

McNichol, T. (2004). Roads gone wild [online]. *Wired Magazine*. Available at: www.wired.com/2004/12/traffic/ [Accessed: 2017-07-11].

Meijaard, J. P., Papadopoulos, J. M., Ruina, A., and Schwab, A. L. (2007). Linearized dynamics equations for the balance and steer of a bicycle: a benchmark and review. In *Proceedings of the Royal Society of London A: Mathematical, Physical and Engineering Sciences*, volume 463, pages 1955–1982.

Melis-Dankers, B. J. M., Havik, E. M., Steyvers, F. J. J. M., Petrie, H., and Kooijman, A. C. (2015). Accessibility of Shared Space by Visually Challenged People. In Kouroupetroglou, G., editor, *Proceedings of the International Conference on Enabling Access for Persons with Visual Impairment, Athens, Greece*, pages 120–126.

Meschik, M. (2008). *Planungshandbuch Radverkehr*. Springer Vienna.

Metron Verkehrsplanung und Ingenieurbüro AG (1999). Kernfahrbahnen - Optimierte Führung des Veloverkehrs an engen Strassenquerschnitten. In *SVI-Forschung*, volume 44. Brugg, Switzerland.

Monderman, H., Clarke, E., and Hamilton-Baillie, B. (2006). Shared space: the alternative approach to calming traffic. *Traffic Engineering & Control*, 47(8):290–292.

Moody, S. and Melia, S. (2014). Shared space: Research, policy and problems. In *Proceedings of the Institution of Civil Engineers-Transport*, volume 167, pages 384–392. ICE, London.

Mosseri, G. M. S., Hall, M. A., and Meyers, J. J. (2004). VISSIM Micro-simulation Modeling of Complex Geometry and Traffic Control: A Case Study of Ocean Parkway, NY. In *Proceedings of the ITE 2004 Annual Meeting and Exhibit*. Institute of Transportation Engineers.

Muhlrad, N. (1993). Traffic Conflict Techniques And Other Forms Of Behavioural Analysis: Application To Safety Diagnoses. In *Proceedings to the 6th International Co-operation on Theories and Concepts in Traffic Safety (ICTCT) workshop Salzburg*, pages 48–64.

Munehiro, K., Takemoto, A., Kasai, S., and Asano, M. (2011). Analysis on Rural Highway Design using Traffic Micro-Simulation in Cold Regions. *Procedia - Social and Behavioral Sciences*, 16:388 – 399. 6th International Symposium on Highway Capacity and Quality of Service, Stockholm, Sweden, 2011.

Näätänen, R. and Summala, H. (1974). A model for the role of motivational factors in drivers' decision-making. *Accident Analysis & Prevention*, 6(34):243–261.

Nagel, K. and Schreckenberg, M. (1992). A cellular automaton model for freeway traffic. *Journal de physique I*, 12(12):2221–2229.

Nash, J. (1951). Non-Cooperative Games. *The Annals of Mathematics*, 54(2):286–295.

Nazla, C. and Williamson, J. (2012). An evaluation of shared space in the Fort Street Area, Auckland, New Zealand [Online]. Retrieved from: www.aucklandcouncil.govt.nz [Accessed: 2017-07-10].

Ngan, V., Sayed, T., and Abdelfatah, A. (2004). Impacts of Various Traffic Parameters on Transit Signal Priority Effectiveness. *Journal of public Transportation*, 7(3):71–93.

Nickel, B. E. (2009). Shared Space und der ÖPNV: Pro und Contra einer neuen Verkehrsplanungside(ologi)e/Shared space and public transport. *DER NAHVERKEHR*, 27(10).

Oketch, T. G. (2001). A Model for Heterogeneous Traffic Flows Including Non-motorized Vehicles. In *Schriftenreihe des Instituts für Verkehrswesen*, volume 59. Universität Karlsruhe.

Oketch, T. G. (2003). Modeled Performance Characteristics of Heterogeneous Traffic Streams Containing Non-Motorized Vehicles. In *Proceedings of the Transportation Research Board 82nd Annual Meeting*, Washington.

O'Neill, B. and Williams, A. (1998). Risk homeostasis hypothesis: a rebuttal. *Injury Prevention*, 4(2):92–93.

Oregon Department of Transportation (2011). Bicycle and Pedestrian Design Guide [Online]. Available at: www.oregon.gov/ODOT/Programs/TDD[Accessed: 2017-07-12].

Österreichische Forschungsgesellschaft Straße-Schiene-Verkehr (2016). Einsatzkriterien für Begegnungszonen ("Application of Encounter Zones"). In *Arbeitspapier*, number 27. Österreichische Forschungsgesellschaft Straße-Schiene-Verkehr.

Österreichisches Statistisches Zentralamt (1997). Ergebnisse des Mikrozensus Juni 1995. In *Beiträge zur österreichischen Statistik*, number 1276.

Papageorgiou, M. (1998). Some remarks on macroscopic traffic flow modelling. *Transportation Research Part A: Policy and Practice*, 32(5):323–329.

Pascucci, F. and Friedrich, B. (2017). Evaluation of traffic quality of shared space streets. In *Proceedings of the Heureka 2017, Stuttgart, Germany*.

Pascucci, F., Rinke, N., Schiermeyer, C., Friedrich, B., and Berkhahn, V. (2015). Modeling of shared space with multi-modal traffic using a multi-layer social force approach. *Transportation Research Procedia*, 10:316–326.

Perkins, S. R. and Harris, J. I. (1967). Criteria for Traffic Conflict Characteristics Signalized Intersections. In *Research publication, Research Laboratories, General Motors Corporation*, number 632.

Pipes, L. A. (1953). An operational analysis of traffic dynamics. *Journal of applied physics*, 24(3):274–281.

Popitz, H., Pohlmann, F., and Essbach, W. (2006). *Soziale Normen*. Suhrkamp Frankfurt/M.

PTV AG (2010). *Benutzerhandbuch Vissim 5.30*. Planung Transport Verkehr AG, Karlsruhe.

Raghava Chari, S. and Badarinath, K. M. (1983). Study of mixed traffic stream parameters through time laps photography. *Highway Research Bulletin, New Delhi*, (20):57–83.

Raksuntorn, W. (2002). *A study to examine bicyclist behavior and to develop a microsimulation for mixed traffic at signalized intersections*. PhD thesis, University of Colorado at Denver.

Ramamayya, T. V. (1988). Highway capacity under mixed traffic conditions. *Traffic Engineering and Control*, 29(5):284–287.

Reid, M., Kocak, N., and Hunt, L. (2009). *DfT Shared Space Project Stage 1 : Appraisal of Shared Space, Report for Department for Transport [Online]*. Retrieved from: www.gov.uk/government/publications/shared-space [Accessed on: 2017-07-13].

Republik Österreich (1960). Straßenverkehrsordnung 1960. In *Bundesgesetzblatt 159*.

Republik Österreich (1999). Datenschutzgesetz 2000. In *Bundesgesetzblatt 165*.

Reuschel, A. (1950). Fahrzeugbewegung in der Kolonne bei gleichförmig beschleunigtem oder verzögertem Leitfahrzeug. *Österreichische Ingenieur- und Architekten–Zeitschrift*, 95:73–77.

Richter, T. and Zierke, B. (2010). Effect of a new Cross-Section design on Low-Volume roads. *Transportation Research Record: Journal of the Transportation Research Board*, 2195(-1):14–19.

Riekert, P. and Schunck, T. E. (1940). Zur Fahrmechanik des gummibereiften Kraftfahrzeugs. *Archive of Applied Mechanics*, 11(3):210–224.

Rinke, N., Schiermeyer, C., Pascucci, F., and Friedrich, B. (2017). A multi-layer social force approach to model interactions in shared spaces using collision prediction. *Transportation Research Procedia*, 25C:1249–1267.

Rudloff, C., Schönauer, R., and Fellendorf, M. (2013). Comparing Calibrated Shared Space Simulation Model with Real-Life Data. In *Proceedings of the 92th Transportation Research Board Annual Meeting*, volume 2390, pages 44–52, Washington.

Saenz, R., Takei, I., and Wang, X. (2007). Mixed Strategy. *International Encyclopedia of the Social Sciences*, pages 290–291.

Salamon, B. (2013). Die 25. StVO-Novelle: ein Überblick. *Zeitschrift für Verkehrsrecht*, 58(6). Manz Verlag Wien.

Samoili, S., Bhaskar, A., Hai Pham, M., and Dumont, A.-G. (2011). Considering weather in simulation traffic. In *Proceedings of the 11th Swiss Transport Research Conference, Monte Verità, Ascona, Switzerland,*.

Schlabbach, K. (1997). Traffic calming in Europe. *ITE Journal*, 67(7):38–40. Institute of Transportation Engineers, Washington.

Schönauer, R., Lipetski, Y., and Schrom-Feiertag, H. (2012a). Vehicle tracking data for calibrating microscopic traffic simulation models. In Röning, J. and Casasent, D. P., editors, *Proceedings of SPIE - The International Society for Optical Engineering, Intelligent Robots and Computer Vision XXIX: Algorithms and Techniques*, volume 8301.

Schönauer, R. and Schrom-Feiertag, H. (2010). Mikrosimulation von Mischverkehr: Konzept MiMiSim und Ausblick auf MixME. In Schrenk, M., Popovich, V. V., and Zeile, P., editors, *15th International Conference on Urban Planning and Regional Development in the Information Society*, pages 1157–1161, Vienna.

Schönauer, R., Stubenschrott, M., Huang, W., Rudloff, C., and Fellendorf, M. (2012b). Modeling Concepts for Mixed Traffic: Steps Toward a Microscopic Simulation Tool for Shared Space Zones. *Transportation Research Record: Journal of the Transportation Research Board*, (2316):114–121.

Schönauer, R., Stubenschrott, M., Schrom-Feiertag, H., and Menśik, K. (2012c). Social and spatial behavior in shared spaces. In Schrenk, M., Popovich, V., and Zeile, P., editors, *Proceedings of the 17th International Conference on Urban Planning and Regional Development in the Information Society GeoMultimedia 2012*, pages 759–766, Schwechat, Austria.

Schopf, J. M. (1985). *Bewegungsabläufe, Dimensionierung und Qualitätsstandards für Fugänger, Radfahrer und Kraftfahrzeugverkehr*. PhD thesis, Technische Universität Wien, Fakultät für Bauingenieurwesen, Wien.

Schweitzer, T. and Fasciati, J. (2008). Unfallgeschehen in Begegnungszonen: Vergleich der Situation vorher und nachher in Burgdorf, Biel, Lyss und Einsiedeln. *Strasse und Verkehr*, 94(9):20–26.

Sen, A. K. (1977). Rational Fools: A Critique of the Behavioral Foundations of Economic Theory. *Philosophy & Public Affairs*, 6(4):317–344. Wiley.

Sharp, A. (1886). *Bicycles & Tricycles: A Classic Treatise on Their Design and Construction*. Dover Publications Inc., Mineola, N.Y.

Sharp, R. S. (2007). Optimal stabilization and path-following controls for a bicycle. *Proceedings of the Institution of Mechanical Engineers, Part C: Journal of Mechanical Engineering Science*, 221(4):415–427.

Simon, P. and Nagel, K. (1998). Simplified cellular automaton model for city traffic. *Physical review. E, Statistical physics, plasmas, fluids, and related interdisciplinary topics*, 58(2):1286–1295.

Sorenson, P. (2017). Shared space in todays world: Quantifying and classifying the range in design. Master thesis, University of Connecticut Graduate School at DigitalCommons@UConn, Available at: digitalcommons.conncoll.edu/ `http://digitalcommons.uconn.edu/gs_theses/1095` [Accessed: 2017-07-23].

Stratil-Sauer, G. (1996). Seitenabstandsverhalten von Radfahrern und Pkw in Wien. Thesis, University of Natural Resources and Life Sciences, Vienna, Institute for Transport Studies.

Streff, F. M. and Geller, E. S. (1988). An experimental test of risk compensation: Between-subject versus within-subject analyses. *Accident Analysis & Prevention*, 20(4):277–287.

Summala, H. (2005). Traffic Psychology Theories: Towards Understanding Driving Behaviour and Safety Factors. In *Proceedings of the International Conference of Traffic and Transport Psychology, Nottingham, England*, pages 383–394.

Summala, H., Pasanen, E., Räsänen, M., and Sievänen, J. (1996). Bicycle accidents and drivers' visual search at left and right turns. *Accident Analysis & Prevention*, 28(2):147–153.

Tageldin, A. and Sayed, T. (2016). Developing evasive action-based indicators for identifying pedestrian conflicts in less organized traffic environments. *Journal of Advanced Transportation*, 50(6):1193–1208.

Teknomo, K. (2002). *Microscopic Pedestrian Flow Characteristics: Development of an Image Processing Data Collection and Simulation Model*. PhD thesis, Tohoku University, Department of Human Social Information Sciences.

Teknomo, K., Takeyama, Y., and Inamura, H. (2001). Microscopic Pedestrian Simulation Model to Evaluate Lane-like Segregation of Pedestrian Crossing. In *Proceedings of Infrastructure Planning Conference, Kouchi, Japan*, volume 24.

Thiemann-Linden, J. (2008). Aktuelle Umsetzung und Einsatzbereiche von Shared Space, Begegnungszonen, Gemeinschaftsstrassen, weiche Fussgängerzonen. *VERKEHRSZEICHEN - für Mobilität und Umwelt*, 24(4).

Thiemann-Linden, J. (2010). Begegnungszonen (zones de recontre) in Frankreich und Belgien. In *Shared Space, Beispiele und Argumente für lebendige öffentliche Räume*, pages 111–117. Verein zur Föderung kommunaler Arbeit - Alternative Kommunalpolitik.

Tonndorf, J. and Vorotovic, V. (2007). Visualisation of Traffic Behaviour Using Microsimulation Computer Simulation Models. *Journal of Maps*, 3(1):135–148.

Topp, H. H. (2010). Shared Space und Begegnungszonen - Erfolgsmodell oder Utopie? / Shared Space and encounter zones - Success model or utopia? *Strassenverkehrstechnik*, 54(10):647–651.

Treiber, M. and Helbing, D. (2002). Realistische Mikrosimulation von Straßenverkehr mit einem einfachen Modell. In Tavangarian, D. and Grützner, R., editors, *Proceedings of the 16th Symposium Simulationstechnik, Rostock, Germany*, page 80.

Vaa, T. (2001). Cognition and Emotion in driver behaviour models: Some critical viewpoints. In *Proceedings of the 14th ICTCT workshop*, pages 48–59.

van Arem, B., de Vos, A., and Vanderschuren, M. J. W. A. (1997). The effect of a special lane for intelligent vehicles on traffic flows - An exploratory study using the microscopic traffic simulation model MIXIC. In *TNO Report, Institute of Infrastructure, Transport and Regional Development*, volume 44. Delft.

Veltkamp, R. C. and Hagedoorn, M. (2000). Shape Similarity Measures, Properties and Constructions. In Laurini, R., editor, *Proceedings of the Advances in Visual Information Systems: 4th International Conference, Lyon, France*, pages 467–476. Springer Berlin Heidelberg.

Volmuller, J. (1976). A driver behaviour model for the design of low-speed roads and streets. In *Proceedings of the Symposium on Geometric Road Design Standards*. Organisation for Economic Co-operation and Development (OECD). Paris.

von Neumann, J. and Morgenstern, O. (1953). *Theory of Games and Economic Behavior*. Princeton University Press.

von Stackelberg, H. (1952). *The Theory of the Market Economy.* Oxford University Press, New York.

Wang, T., Wu, J., and McDonald, M. (2012). A micro-simulation model of pedestrian-vehicle interaction behavior at unsignalized mid-block locations. In *Proceedings of the 15th International IEEE Conference on Intelligent Transportation Systems (ITSC)*, pages 1827–1833.

Wargo, B. W. and Garrick, N. W. (2016). Shared Space: Could Less Formal Streets Be Better for Both Pedestrians and Vehicles? In *Proceedings of the Transportation Research Board 95th Annual Meeting*, number 16-5067. Washington.

Wegener, M. (1996). Reduction of CO2 emissions of transport by reorganisation of urban activities. In Hayashi, Y. and Roy, J., editors, *Transport, Land-Use and the Environment. Transportation Research, Economics and Policy*, volume 6, pages 103–124. Springer, Boston, MA.

Weiss, E. (2012). *The Enlightened Cyclist: Commuter Angst, Dangerous Drivers, and Other Obstacles on the Path to Two-Wheeled Transcendence*. Chronicle Books, San Francisco.

Werner, T. and Helbing, D. (2003). The social Force Pedestrian Model Applied to Real Life Scenarios. In *Pedestrian and Evacuation Dynamics*, volume 3. University of Greenwich, UK.

Whipple, F. J. W. (1899). The stability of the motion of a bicycle. *Quarterly Journal of Pure and Applied Mathematics*, 30(120):312–348.

Widyotriatmo, A. and Hong, K.-S. (2011). Navigation Function-Based Control of Multiple Wheeled Vehicles. *IEEE Transactions on Industrial Electronics*, 58(5):1896 –1906.

Wiedemann, R. (1974). Simulation des Straßenverkehrsflußes. *Schriftenreihe des Instituts für Verkehrswesen der Universität Karlsruhe*, Band 8.

Wilde, G. J. S. (1982). The Theory of Risk Homeostasis: Implications for Safety and Health. *Risk Analysis*, 2(4):209–225.

Xin, W., Hourdos, J., Michalopoulos, P., and Davis, G. (2008). The Less-Than-Perfect Driver: A Model of Collision-Inclusive Car-Following Behavior. *Transportation Research Record: Journal of the Transportation Research Board*, 2088:126–137.

Yannis, G., Golias, J., and Antoniou, C. (2004). Combining traffic simulation and driving simulator analyses for Advanced Cruise Control system impact identification. In *Proceedings of the 83rd Annual Meeting of the Transportation Research Board*, pages 11–14.

Yao, D., Zhang, Y., Li, L., Su, Y., Cheng, S., and Xu, W. (2009). Behavior Modeling and Simulation for Conflicts in Vehicles-bicycles Mixed Flow. *Intelligent Transportation Systems Magazine, IEEE*, 1(2):25–30.

Yi, Z., Houli, D., and Yi, Z. (2007). Modeling Mixed Traffic Flow at Crosswalks in Micro Simulations Using Cellular Automata. *Tsinghua Science & Technology*, 12(2):214–222.

Yokoo, M. (2012). *Distributed Constraint Satisfaction: Foundations of Cooperation in Multi-agent Systems*. Springer Berlin Heidelberg.

Zacharias, J. (1999). The Amsterdam Experiment in Mixing Pedestrians, Trams and Bicycles. *ITE Journal*, 69(8):22–28.

Zenga, B. (2012). Line Of Sight [Movie]. Benny Zenga [Director], Lucas Brunelle [Star & Producer], Alleycat Studios [Production], DVD.

Zhang, L., Kovvali, V., Clark, N., Sallman, D., and Alexiadis, V. (2006). *NG Video User's Manual*. Federal Highway Commision. Publication No. FHWA-HOP-07-009.

Zhang, X. and Chang, G. (2011). A CA-based Model for Simulating Vehicular-Pedestrian Mixed Flows in a Congested Network. In *Proceedings of the Transportation Research Board 90th Annual Meeting*, number 11-3546, pages 116–124.

Zhen-long, L. and De-wang, C. (2003). A stackelberg game approach to ramp metering and variable speed control. In *Proceedings of the 2003 IEEE International Conference on Intelligent Transportation Systems*, volume 2, pages 1060–1063.

Zhen-long, L. and Liquan, F. (2008). Optimal coordination of variable speed control and ramp metering based on stackelberg game. In *Networking, Sensing and Control, 2008. ICNSC 2008. IEEE International Conference on*, pages 666–670.

Zwielich, F., Reker, K., and Flach, J. (2001). Fahrerverhaltensbeobachtungen auf Landstraßen am Beispiel von Baumalleen. Eine Untersuchung mit dem Fahrzeug zur Interaktionsforschung Straßenverkehr. *Berichte der Bundesanstalt für Straßenwesen, Unterreihe Mensch und Sicherheit*, (124). Bremerhaven.

About The Author

The author of this thesis was born on July 4th, 1980 in Melk, Austria. In 1999, he graduated at the secondary technical school in St.Pölten in the program of telecommunication engineering. He worked as system engineer and product manager in the Austrian railway industry until 2003, before he started in the program of "Intelligent Transportation Systems" at the University of Applied Sciences Vienna. In 2007 he enrolled in a doctoral program at the University of Natural Resources and Life Sciences, Vienna. In 2009, he founded the company mobimera Fairkehrstechnologien KG in Vienna as platform to conduct cooperative research on transport technologies including navigation applications, technologies that improves road safety, traffic flow modeling and traffic related emissions. In 2010, he enrolled at the Doctoral School of Civil Engineering at the Graz University of Technology. Parts of this thesis have been made during two funded research projects. From 2010 to 2012 he held a lectureship in the field of environmental factors of transportation at the University of Applied Sciences Vienna. In 2015, railway engineering became again his primary field of business activity and research.